FEBRUARY, 1931

Journal of METALS

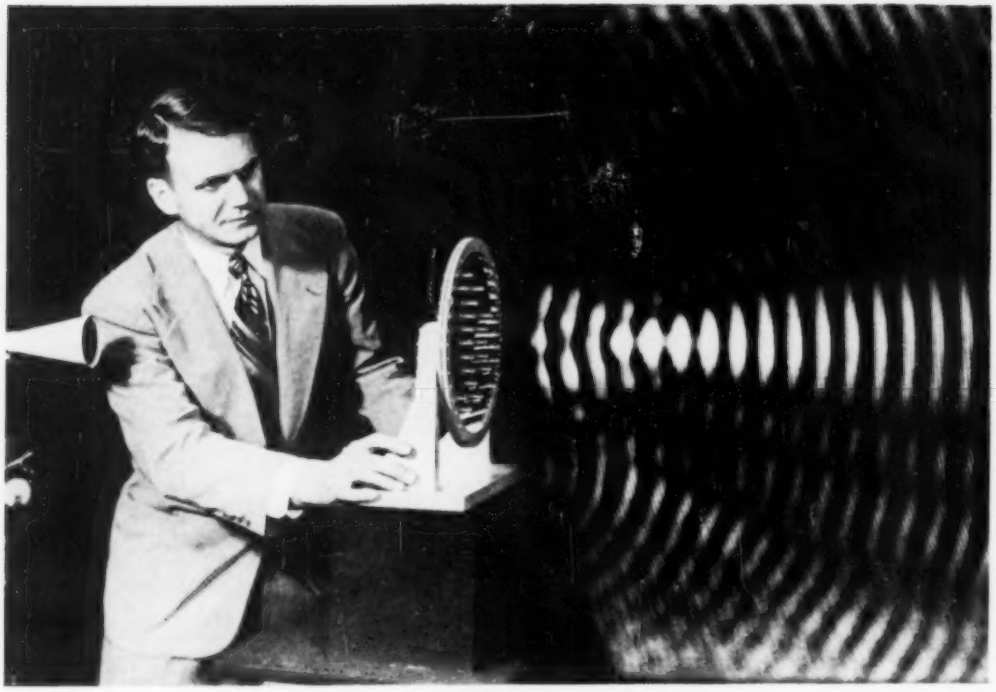

WAVE MAKING

–for better telephone service

Waves from the sound source at left are focused by the lens at center. In front of the lens, a moving arm (not shown) scans the wave field with a tiny microphone and neon lamp. The microphone picks up sound energy and sends it through amplifiers to the lamp. The lamp glows brightly where sound level is high, dims where it is low. This new technique pictures accurately the focusing effect of the lens. Similar lenses efficiently focus microwaves in radio relay transmission.

At Bell Telephone Laboratories, radio scientists devised their latest microwave lens by copying the molecular action of optical lenses in focusing light. The result was a radically new type of lens – the array of metal strips shown in the illustration. Giant metal strip lenses are used in the new microwave link for telephone and television between New York and Chicago.

The scientists went on to discover that the very same type of lens could also focus sound . . . thus help, too, in the study of sound radiation . . . another field of great importance to your telephone system.

The study of the basic laws of waves and vibrations is just another example of research which turns into practical telephone equipment at Bell Telephone Laboratories . . . helping to bring you high value for your telephone dollar.

BELL TELEPHONE LABORATORIES

• WORKING CONTINUALLY TO KEEP YOUR TELEPHONE SERVICE ONE OF TODAY'S GREATEST VALUES

Journal of METALS

VOL. 191, NO. 2 FEBRUARY, 1951

Published to provide a continuing, authoritative, and up-to-date record of technological, engineering, and economic progress in all branches of the metals industry by the

Metals Branch
American Institute of Mining and Metallurgical Engineers, Inc.
29 West 39th Street, New York 18

THOMAS E. LLOYD
Manager of Publications
Editor, Journal of Metals

H. N. UNDERHILL A. S. COHAN
Associate Editors

D. G. GARRETT MARGARET BAGG
Assistant Editors

GRACE PUGSLEY Production Manager

W. J. SEWING Asst. Prod. Mgr.

METALS BRANCH COUNCIL

C. D. King Chairman
E. O. Kirkendall Secretary
M. Gensamer IMD Chairman
C. C. Long EMD Chairman
H. K. Work ISD Chairman
F. N. Rhines J. D. Sullivan
D. S. Eppelsheimer R. J. Lund

TECHNICAL PUBLICATIONS COMMITTEE

F. B. Foley Chairman
E. J. Kennedy, Jr. Secretary

AUXILIARY PUBLICATIONS COMMITTEE CHAIRMEN

F. N. Rhines Institute of Metals Div.
F. M. Washburn Iron & Steel Div.
Philip T. Stroup Extract. Metal Div.

JAMES A. STANGARONE
Advertising Manager

The AIME Publishes:
Journal of Metals
Mining Engineering
Journal of Petroleum Technology

COVER

For laboratory melting of high purity titanium alloys, New York University Metallurgical Laboratory constructed a multiple hearth furnace that will melt up to six button charges. Electrodes are tungsten tipped and water cooled, the furnace has a water cooled copper hearth and Pyrex walls, and melting is done under an argon atmosphere. Alloys with melting temperatures above 4000°F have been melted. Photo courtesy New York University, Watertown Arsenal, and the Air Materiel Command.

FEATURES AND NEWS

Journal of Metals REPORTER	87	Coming Events	73
"Drift of Things"	85	News of Industry	89
Personnel Service	79	Annual Meeting Programs	181
Meet the Authors	74	AIME News	189
New Products	77	Personals	195

TECHNICAL ARTICLES

Gallium—A Byproduct Metal	A. P. Thompson, H. R. Harner	91
Diffusion Phenomena Occurring During Sintering	B. H. Alexander	95
Age Hardening	L. F. Mondolfo	95
New Refractory Hung Arch Reduces Furnace Failures		96
Crusher Plates for Diamonds	R. S. Young	97
Recent Developments in Fluxes for Welding	W. M. Conn	98
Electric Furnace Roof Refractories	T. A. Blackwell	100

TRANSACTIONS

Observations on Rimming Steel Ingots	A. Hultgren, G. Phragmen, S. Wahlfahrt, J. E. Ostberg	101
Vanadium-Oxygen Equilibrium in Liquid Iron	J. Chipman, M. N. Dastur	111
Sintering Practice at Josephtown Smelter	H. K. Najarian, K. F. Peterson, R. E. Lund	116
Aging of Sand-Cast Mg-Al-Zn Alloys	T. E. Leontis, C. E. Nelson	120
Mechanical Properties of Stainless Steel Powder	A. H. Grobe, G. A. Roberts	125
Preparation of Titanium Tetrachloride from Rutile	C. H. Gorski	131
Reverse Leaching of Zinc Calcine	L. P. Davidson, R. K. Carpenter, H. J. Tschirner	134
Metallurgical Reactions of the Fluorides	H. H. Kellogg	137
Cobalt Self-Diffusion: Study of Method of Decrease in Surface Activity	R. C. Ruder, C. E. Birchenall	142
Formation and Behavior of Subboundaries in Silicon Iron Crystals	C. G. Dunn, F. W. Daniels	147
Interface and Marker Movements in Diffusion in Solid Solutions of Metals	L. C. C. da Silva, R. F. Mehl	155
Effect of Ternary Additions on the Age-Hardening of a Copper-Silver Alloy	H. Margolin, W. R. Hibbard, Jr.	174

TECHNICAL NOTES

"Oriented Growth" in Primary Recrystallization	J. J. Becker	115

Published the first day of each month by the American Institute of Mining and Metallurgical Engineers, Inc., 29 West 39th Street, New York 18, N. Y. Telephone: PEnnsylvania 6-9220. Subscription $8 per year for non-AIME members in United States and North, South and Central America; $9, foreign; $6 for AIME members, or $4 in combination with a subscription to "Mining Engineering" or the "Journal of Petroleum Technology". Single copies, 75 cents; special issues, $1.50 . . . The AIME is not responsible for any statement made or opinion expressed in its publications. . . .

Copyright 1951 by the American Institute of Mining and Metallurgical Engineers, Inc. . . . Registered cable address, AIME New York . . . Indexed in Engineering Index, Industrial Arts Index and Chemical Abstracts . . .

Reentered as second-class matter Sept. 21, 1949, at the post office at New York, N. Y., under the Act of March 3, 1879. Additional entry established at Manchester, N. H.

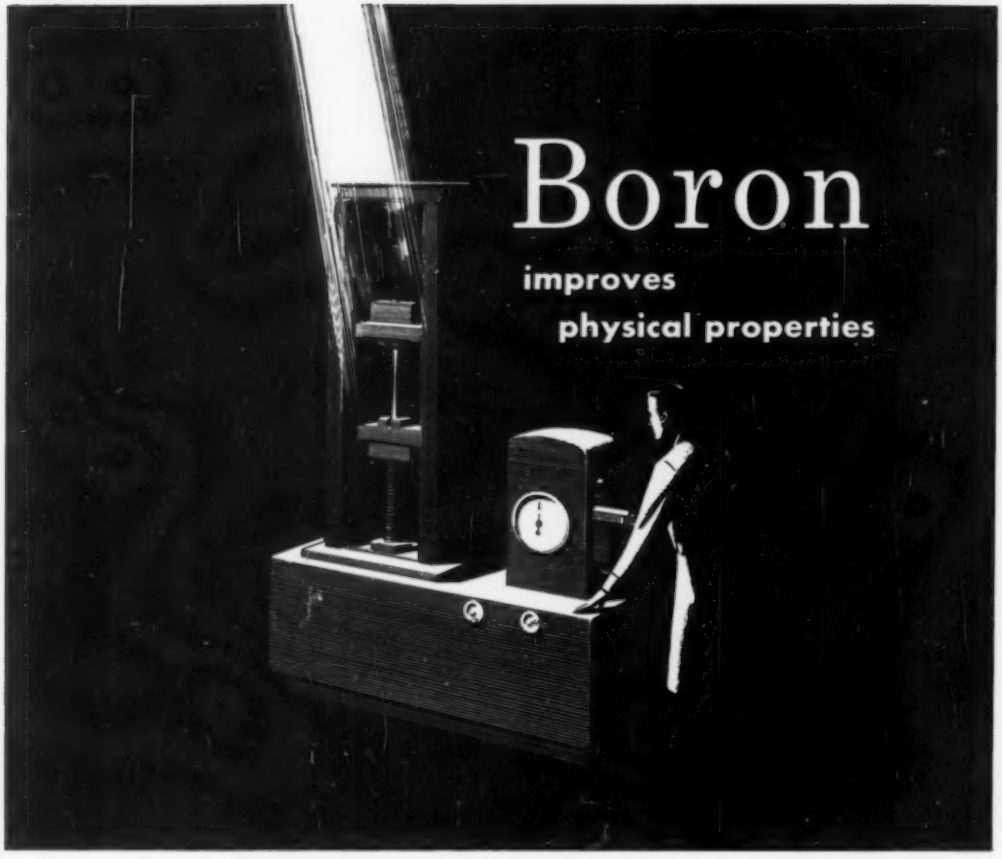

IN wrought steel—cast steel—malleable iron—cast iron—small additions of Ferro-Boron lead to economy and better performance. Boron alloys are useful in deoxidation processes. In the spraying and welding of metals also, Boron has important uses.

Scarcer elements like molybdenum, tungsten, chromium, and nickel can be employed more sparingly if Boron is judiciously added. Very small percentages improve hardenability and strength to a marked degree.

A new patented method developed by the Molybdenum Corporation (U.S. Patent 2509281) incorporates Boron in iron and steel more economically and with more uniform results than could ever before be obtained. Inquiries on any use of Molybdenum, Tungsten, or Boron will receive prompt attention.

AMERICAN Production, American Distribution, American Control, Completely Integrated

Offices: Pittsburgh, New York, Chicago, Cleveland, Detroit, Los Angeles, San Francisco, Seattle

Sales Representatives: American Steel and Supply Co., Chicago; Edgar L. Fink, Detroit; Brumley-Donaldson Co., Los Angeles, San Francisco, Seattle

Subsidiaries: Cleveland-Tungsten, Inc., Cleveland, O.; General Tungsten Manufacturing Co., Inc., Union City, N.J.

Works: Washington, Pa.; York, Pa.

Mines: Questa, New Mexico; Urad, Colorado.

MOLYBDENUM CORPORATION OF AMERICA
Grant Building Pittsburgh, Pa.

MCA

...always quick rapid transfer of heat
...like INTERNATIONAL GRAPHITE ELECTRODES

INTERNATIONAL *Graphite & Electrode* **CORP.**

A SPEER CARBON COMPANY SUBSIDIARY

ST. MARYS, PENNSYLVANIA

experience
skill
service

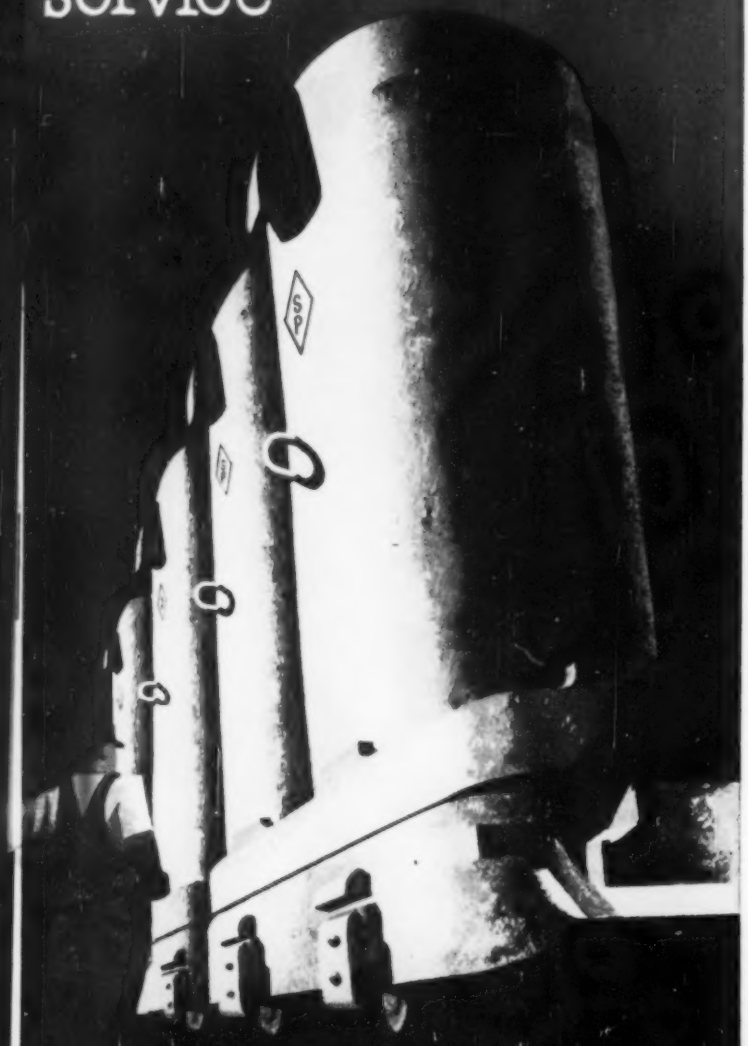

three priceless assets
behind every

SHENANGO·PENN MOLD

SHENANGO-PENN MOLD COMPANY OLIVER BUILDING PITTSBURGH, PENNA.

Short Cuts . . .

Connors Steel Co. Div., H. K. Porter Co., Inc. will increase its steelmaking facilities in Birmingham, Ala., by 40 pct. New equipment will include additional electric furnace capacity, a breakdown mill, a heating furnace, and increased finishing capacity.

Westinghouse Electric Corp. will build $20 million worth of electrical equipment for the Air Force for a wind tunnel to be installed at Arnold Engineering Development Center, Tullahoma, Tenn., for testing full size jet engines, guided missiles, and wing sections and fuselages of aircraft. The Center's research facilities are available to all interested in aircraft development.

Atlantic Steel Co., Atlanta, Ga., will increase its steelmaking capacity 50 pct and double its output of rolled products, as a result of a 3-year expansion program. A 60-ton electric furnace will be installed, as well as a new rolling mill.

National Carbon Div., Union Carbide and Carbon Corp. will further increase capacity for the production of graphite and carbon electrodes at Columbia, Tenn. The largest graphite electrodes ever produced, 35 and 40 in. diam x 110 in. long, can now be made in quantity, and will enable designers to develop electric furnaces with increased power and capacity.

Armour Research Foundation is offering a number of industrial research fellowships to begin in September 1951. Application forms may be obtained from Office of Admissions, Graduate School of Illinois Institute of Technology.

National Steel Corp. plans to increase ingot capacity from 4,500,000 tons to 5,500,000 tons per year by 1952. Further increases will be made by a plant to be constructed on a new site located on deep water of the Delaware River near Camden, N. J. Iron ore will be transported directly in ocean-going carriers from the new Labrador-Quebec iron ore field, in which the company is heavily interested.

Minneapolis-Honeywell Regulator Co. is expanding production and operating facilities with the purchase of the Thomas M. Royal plant in Philadelphia. Present facilities were inadequate to meet the demands of the national mobilization program.

Harbison-Walker Refractories will install a new tunnel kiln at Bessemer, and a completely new plant at Fairfield, Ala., because of the increased need for refractories resulting from the industrial growth of the Birmingham district.

— Coming Events —

Feb. 6, Society for Applied Spectroscopy, 6 pm dinner, Tosca's; 8 pm meeting, Socony-Vacuum Training Center, New York.

Feb. 7, AIME, Chicago Section, Chicago Bar Assn., Chicago.

Feb. 18-22, AIME, annual meeting, Jefferson Hotel; Metals Branch session, Statler Hotel, St. Louis.

Feb. 20-22, American Concrete Institute, annual convention, St. Francis Hotel, San Francisco.

Feb. 21, AIME, Western Section, Open Hearth Committee, Iron and Steel Div., Los Angeles.

Mar. 5-9, ASTM, spring meeting and committee week, Cincinnati.

Mar. 11-14, American Institute of Chemical Engineers, regional meeting, Greenbrier, White Sulphur Springs, Va.

Mar. 13-16, National Assn. of Corrosion Engineers, 1951 conference and exhibition, Hotel Statler, New York.

Mar. 19-23, Conference on Industrial Personnel, Dept. of Industrial Engineering, Columbia University, New York, N. Y.

Mar. 19-23, Western Metal Congress and Exposition, Civic Auditorium and Exposition Hall, Oakland, Calif.

Mar. 21, AIME, Western Section, Open Hearth Committee, Iron and Steel Div., Los Angeles.

Apr. 2-4, AIME, Open Hearth and Blast Furnace, Coke Oven and Raw Materials Conference, Iron and Steel Div., Statler Hotel, Cleveland.

Apr. 2-3, ASME, spring meeting, Atlanta-Biltmore, Atlanta.

Apr. 4-6, Midwest Power Conference, Sherman Hotel, Chicago.

Apr. 13-14, AIME, Institute of Metals Div., New England regional conference, Taft Hotel, New Haven, Conn.

Apr. 16-18, American Society of Lubrication Engineers, Bellevue-Stratford Hotel, Philadelphia.

Apr. 23-26, American Foundrymen's Society, annual convention, Buffalo, N. Y.

Apr. 25-26, Metal Powder Assn., annual meeting, Hotel Cleveland, Cleveland.

Apr. 30-May 4, Materials Handling Exposition, International Amphitheatre, Chicago.

May 7-11, Greater New York Industrial Show, 71st Regiment Armory, New York.

May 9-11, Engineering Institute of Canada, annual meeting, Mount Royal Hotel, Montreal, Canada.

May 13-16, American Institute of Chemical Engineers, regional meeting, Hotel Muehlebach, Kansas City, Mo.

May 23-24, American Society for Quality Control, annual convention, Hotel Cleveland, Cleveland.

June 11-15, ASME, semi-annual meeting, Royal York, Toronto, Canada.

June 18-22, ASTM, annual meeting, Atlantic City, N. J.

Sept. 25-28, ASME, fall meeting, Minneapolis.

Oct. 11-12, AIME, Fuels Conference, Roanoke Hotel, Roanoke, Va.

Oct. 15-17, AIME, Institute of Metals Div., fall meeting, Detroit-Leland Hotel, Detroit.

Oct. 15-19, National Metal Congress & Exposition, Detroit.

Oct. 22-24, Metal and Nonmetallic Mining Convention, Biltmore Hotel, Los Angeles.

Oct. 29-Nov. 3, AIME, fall meeting, Mexico City.

Dec. 6-8, AIME, Electric Furnace Conference, William Penn Hotel, Pittsburgh.

Many years ahead of the field
— the NEW DESK-TYPE METALLOGRAPH

IN SIMPLICITY of operation, speed, and assurance of perfect results—the new AO Metallograph is years ahead. It is sure to encourage better quality and greater uniformity of photomicrographs.

This revolutionary metallograph for routine control work permits you to:

SIT COMFORTABLY AT A SPACIOUS DESK. From start to finish you need not budge from your chair.

FOCUS AUTOMATICALLY AND *ACCURATELY*... while examining specimen through microscope eyepiece.

MEASURE *DIRECTLY* ON GROUND GLASS VIEWING SCREEN. Accurate grain size, case depth, and linear measurements made rapidly with comparison chart.

CHANGE OBJECTIVES RAPIDLY. Revolving turret accommodates four objectives.

TAKE NOTES. Desk provides ample writing and storage space.

USE PHOTOGRAPHIC LAMP FOR EXPOSURES ONLY. Built-in illuminator for visual observations, choice of arc or ribbon filament photographic lamp.

DETERMINE ALL OPTICAL SETTINGS INSTANTLY. No charts or tables needed. Identify by ASTM magnification—50 X to 1500 X.

BUILT-IN PHOTOGRAPHIC EYEPIECES QUICKLY SELECTED. Four eyepieces, especially designed for finest photographic results operate in quick-change slide.

ADJUST ARC LAMP EASILY AND QUICKLY. All adjustments are within easy reach on automatic, motor-driven arc lamp—crater imaged on ground glass window.

USE EITHER MONOCULAR OR BINOCULAR BODIES. Both are available, both function with automatic focusing.

This radically improved metallograph is designed and manufactured with typical American Optical Company precision and quality. The infinity-corrected "Apergon" objectives are designed for maximum image contrast. "Americote" optical surfaces are used throughout. A unique pellicle reflecting unit in the vertical illuminator gives increased light transmission. Husky construction and factory adjustment mean years of trouble-free operation.

Learn more about the new AO Metallograph. For a complete 12-page catalog write Dept. O182.

Manufacturers and designers of precision industrial optical instruments

American Optical

INSTRUMENT DIVISION • BUFFALO 15, NEW YORK

PROFESSIONAL SERVICES

Limited to AIME members, or to companies that have at least one AIME member on their staffs. Rates $40 per year per inch.

ST & CO.
ENGINEERS
METALLURGISTS
CONSULTANTS
Small Jobs Welcomed
SAM TOUR & CO., INC.
Laboratories and offices
44 Trinity Place
New York 6, N. Y.
Testing—Certifying
American Standards
Testing Bureau, Inc.

MAX STERN
Consulting Engineer
Expert for Scrap Recovery and Shipwrecking — Modernization of Plants and Yards for Ferrous and Nonferrous Metal Scrap
150 Broadway New York 7, N. Y.

LEWIS B. LINDEMUTH
Consulting Engineer
140 CEDAR STREET, NEW YORK 6, N. Y.
STEEL PRODUCTION
DESIGN · OPERATION · CONSTRUCTION · METALLURGY

Frank B. Foster, Inc.
INDUSTRIAL PLANTS
ROLLING MILLS
2217 Oliver Building
Pittsburgh 22, Pennsylvania

R. S. DEAN LABORATORIES, INC.
Consulting, Research Development Chemistry, Electrochemistry, & Metallurgy Laboratory Research on a Contract Basis
5810—47TH AVENUE AP-2821
RIVERDALE, MD.

Meet The Authors

A. Paul Thompson (p. 91), director of research of Eagle-Picher Co., Joplin, Mo., received his B.S. degree from Montana State College, and M.S. and Ph.D. degrees from University of Illinois. He has authored numerous papers in the fields of chemistry and metallurgy.

A. P. THOMPSON

H. R. Harner (p. 91), chief chemist and assistant director of research of Eagle-Picher Co., has been associated with that company for all but 3 years since 1924. He studied at Westminster of Missouri for his A.B. degree, and likes fishing, color photography, and wild flowers.

John Chipman (p. 111). See JOURNAL OF METALS, February, 1950.

Minu N. Dastur (p. 111). See JOURNAL OF METALS, October, 1949.

H. R. HARNER

J. J. Becker (p. 115), research associate, General Electric Research Lab, Schenectady, was born in Germany. He studied at Harvard where he was a teaching fellow, and received his S.B., A.M., and Ph.D. degrees.

R. E. Lund (p. 116) is assistant superintendent of sinter leach plants for St. Joseph Lead Co. of Pa., Monaca, Pa. He received his B.S. degree from University of Colorado, and his avocations are hunting and amateur farming.

L. P. Davidson (p. 134) has been general superintendent for the American Zinc Co. of Ill., Monsanto, Ill., for the past 11 years. He was formerly associated with Giesche Co., Poland, and Anaconda Copper Mining Co., and is a graduate of Montana State College.

G. A. ROBERTS

R. K. Carpenter (p. 134), research chemist for American Zinc Co. of Ill., graduated from Missouri School of Mines.

H. J. Tschirner (p. 134) is superintendent of electrolyzing and casting for American Zinc Co. of Ill. Born in Germany, he graduated from Cornell University, and attended Sever Institute of Washington University. He likes wood and metalworking.

C. G. Dunn (p. 147). See JOURNAL OF METALS, October, 1949.

F. W. Daniels (p. 147). See JOURNAL OF METALS, October, 1949.

R. C. RUDER

T. E. Leontis (p. 120). See JOURNAL OF METALS, December, 1949.

A. H. Grobe (p. 125), chief research metallurgist, Vanadium-Alloys Steel Co., Latrobe, Pa., attended Washington and Jefferson, and received his B.S. and D.Sc. degrees from Carnegie Institute of Technology. He likes hunting and golf.

G. A. Roberts (p. 125) is chief metallurgist for Vanadium-Alloys Steel Corp., Latrobe, Pa. He studied at U.S. Naval Academy and Carnegie Institute of Technology, receiving B.Sc., M.Sc. and D.Sc. degrees. He enjoys music, rifle shooting, and photography.

C. H. Gorski (p. 131). See JOURNAL OF METALS, November, 1949.

C. E. NELSON

H. H. Kellogg (p. 137). See JOURNAL OF METALS, June, 1950.

R. C. Ruder (p. 142) is associated with the Pigments Dept., E. I. duPont deNemours & Co. He received his B.S. degree from Penn State, and a D.Sc. degree from Carnegie Institute of Technology. His hobbies are painting, golf, mountain climbing, badminton, and skiing.

Meet The Authors

(*Continued from page 74*)

C. E. Birchenall (p. 142). See JOURNAL OF METALS, January, 1950.

R. F. Mehl (p. 155). See JOURNAL OF METALS, January, 1950.

H. Margolin (p. 174) is a research associate in the Research Div., New York University. A graduate of Yale University with B. Eng., M. Eng., and D. Eng. degrees, he enjoys bridge, and making home movies.

W. R. Hibbard, Jr. (p. 174). See JOURNAL OF METALS, September, 1949.

C. E. Nelson (p. 120) has been associated with Dow Chemical Co. since 1920, and is now technical director of the Magnesium Div. A graduate of Alma College, Mich., this AIME member enjoys fishing and golf, and has previously contributed to the Transactions of the Institute.

W. M. Conn (p. 98) was born in Berlin, and received his B.S. and Dr. Ing. degrees from Technical University Berlin, and Danzig Institute of Technology. He is associated with Rockhurst College, Kansas City, Mo., and was previously with the University of California Extension Div., and a consultant. His free time is spent with the Boy Scouts of America, and Unity Country Club.

H. K. Najarian (p. 116) is general superintendent for the St. Joseph Lead Co. of Pa., where he started in the engineering dept. in 1922. He was born in Marash, Armenia, and studied at Yale University for his B.S. degree. For this serious member of AIME, his job is his hobby.

K. F. Peterson (p. 116) is superintendent of sinter leach plants for St. Joseph Lead Co. of Pa., Monaca, Pa. He has previously held the positions of chemist and research director with the company. An AIME member, he is a graduate of South Dakota School of Mines & Technology. He spends his spare time scouting and gardening.

T. A. Blackwell (p. 100) is assistant to melting superintendent, and general foreman of melt dept. at Atlas Steels, Ltd., Welland, Ont., Canada. Born in Atwood, Ont., Canada, he studied to be a Radio Technician at Radio College of Canada, and was chief inspector for Sparton Radio Co. of Canada before joining Atlas Steels. His hobbies are fishing and reading.

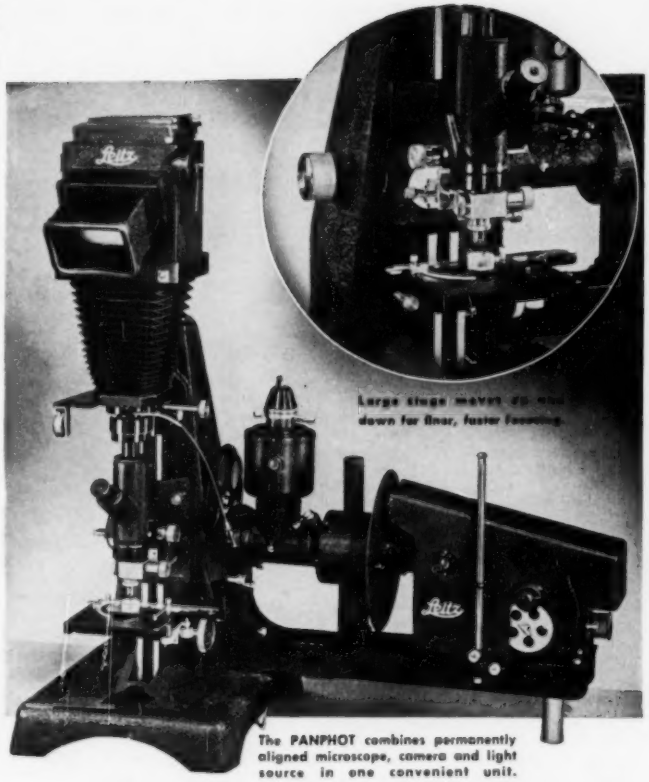

The PANPHOT combines permanently aligned microscope, camera and light source in one convenient unit.

The Leitz Panphot

Universal Camera Microscope

Only the Leitz PANPHOT enables you to switch from microscopic observation to photo-micrography *without moving from your chair*, for it's the only universal camera microscope with operating parts for both functions right at hand. Changeover from one to the other is fast, simple, dependable. Now available to industrial and technical laboratories, the PANPHOT is a perfect combination of research microscope and reflex camera.

The PANPHOT permits the use of transmitted light, reflected light, darkfield illumination and polarized light. The permanently aligned light source provides a filament lamp for observation and an arc light for photo-micrography.

Easy observation of the image to be photographed is provided by a large ground glass in the reflex mirror camera. The camera accommodates 3¼" x 4¼" plates or cut film for black and white or color work.

A full range of accessories is available to equip the PANPHOT for every phase of photo-micrography, photo-macrography and for drawing and projecting micro-images.

Write today for information to Dept. JM

E. LEITZ, Inc., 304 Hudson Street, New York 13, N. Y.

LEITZ MICROSCOPES • SCIENTIFIC INSTRUMENTS
LEICA CAMERAS AND ACCESSORIES

FREYN-DESIGN BLAST FURNACES OF A DECADE

29 The World Around

FURNACE	HEARTH	LOCATION
1	9'-0"	RHODESIA
2	14'-0"	SO. AFRICA
3	16'-1"	SO. AFRICA
4	18'-0"	ENGLAND
5	18'-3"	SCOTLAND
6	18'-3"	SCOTLAND
7	19'-0"	ENGLAND
8	19'-0"	POLAND
9	20'-0"	ENGLAND
10	20'-0"	ENGLAND
11	20'-0"	ENGLAND
12	20'-0"	SCOTLAND
13	21'-0"	U. S. A.
14	21'-6"	WALES
15	21'-6"	SO. AFRICA
16	21'-6"	SO. AFRICA
17	21'-4"	FRANCE
18	21'-4"	FRANCE
19	21'-4"	FRANCE
20	21'-4"	FRANCE
21	22'-6"	ENGLAND
22	25'-0"	U. S. A.
23	25'-0"	U. S. A.
24	25'-0"	U. S. A.
25	25'-0"	U. S. A.
26	25'-9"	WALES
27	25'-9"	WALES
28	26'-6"	U. S. A.
29	26'-6"	U. S. A.

A WORLD-DOMINANT DESIGN

Most of these blast furnaces were designed and constructed under unified responsibility contracts

Many sizes, in many lands, using many ores.

KOPPERS

METALLURGICAL PLANT DESIGN AND CONSTRUCTION

Freyn Engineering

DEPARTMENT OF KOPPERS COMPANY, INC.

109 NORTH WABASH AVENUE · CHICAGO 2, U.S.A. *Associated with* Ashmore, Benson Pease & Co. Ltd., Stockton-on-Tees, ENGLAND; De Lattre & Froment, Paris, FRANCE

New Products

New Products | New Literature | New Services

For Further Information or Literature on any Product, Fill in the Coupon and Send to JOURNAL OF METALS

1—PRECISION REGULATOR: A new regulating device, superior to step regulators in that it provides regulation in infinitesimal steps, is more sensitive and accurate than devices of the Synchro-tie or selsyn type and can produce a voltage proportional to turning a rotor over a range of ±10°, with a sensitivity of 20 sec; produce a torque that is linear with the square of a signal current; and act as an elastic restraint generator, producing a torque proportional to the product of the square of a current and the angular displacement. *Westinghouse Electric Corp.*

2—CATALYTIC EXHAUST: To solve the problem of obnoxious gases from gasoline-powered lift trucks, there has been introduced the OCM Catalytic Exhaust that renders exhaust gases non-poisonous and odorless, eliminating one of the major hazards in gas fork lift truck operations. *Oxy-Catalyst Mfg. Co.*

3—ARGON REGULATOR: For measuring argon flow, a new, direct-reading combination regulator and flowmeter maintains constant inlet pressure and accurate flow. Factory presetting of the second stage of the regulator delivers argon at a constant pressure of 20 psi. With a finger-tip control adjusting valve, it permits accurate, steady flow rates up to 60 cfh. *Linde Air Products Co.*

4—STRAIN RECORDER: A new SR-4 strain amplifier produces both static and rapidly changing SR-4 strain gage measurements of strains, forces, fluid pressures, displacements, vibrations, accelerations, etc., on a strip chart with rectangular coordinates. The unit, The Baldwin-Sanborn recorder produced by *Baldwin Locomotive Works*, is a direct-writing, inkless, vacuum-tube voltmeter consisting of an ac powered strain gage amplifier of the carrier type in which the bridge is excited at 2500 cycles per sec, a D'Arsonval moving coil recording galvanometer, and a paper drive mechanism.

5—HIGH-SPEED GENERATOR: A new GE Tri-Clad high-speed synchronous generator, available in four basic designs, has been announced by *General Electric Co.* The generators have ratings from 1.875 to 50 kva and frequency ratings from 60 to 400 cycles. Three types of 60 cycle units are offered for different categories of voltage regulation and starting requirements.

6—WETTING AGENT: Addition of minute quantities of Hydrodyne, a new multiphase wetting agent, increases efficiency of coolants. For less than ½c per gal, regular coolants give markedly improved heat dissipation, longer tool life and increased machine speeds. Wheels stay cleaner and machine speeds can be stepped up. Uneven wear is avoided by evening cooling over entire surfaces. "Wet" coolant also greatly reduces dust in operator's breathing zone. *Aquadyne Corp.*

7—MERCURY CLEANING: For cleaning mercury in 5-lb lots, new cleaning units work on the same principle as the larger model in reclaiming mercury contaminated by dissolved base metals. The oxifier, powered by an electric motor, violently agitates the mercury for from 2 to 4 hr and provides maximum air contact with the mercury droplets. As base metal contaminations are thoroughly aerated, they oxidize, form skins, and precipitate from the mercury as metallic oxide powders. These can be readily separated from the clean mercury by use of the Bethlehem Type G Filter. *Bethlehem Apparatus Co.*

8—WELDING FLUXES: An expanded line of welding fluxes known as "Lo-Cost Flotectic Fluxes" reduce surface tension and is the least expensive way to better welds. Included in the new flux line is "Flotectic Flux 1100," claimed to be capable of drastically reducing silver solder costs by cutting down on the amount used per weld, as well as speeding up production by insuring rapid flow with maximum capillary action. *Eutectic Welding Alloys Corp.*

9—METAL NAMEPLATE: A self-adhesive metal nameplate with no pre-drilling of holes, screws, rivets or other fastening devices consists of 0.003 in. thick aluminum foil anodized and dyed to government specifications. Backed with a high tensile bonding material, it can be quickly applied to any smooth, cohesive surface on metals, porcelain, bakelite, polysterene, glass, wood, paints or enamels. The product has passed rigid government weathering, salt spray, humidity, abrasion and low and high temperature tests. It is available in brown, red, black, blue, green, and aluminum. *C & H Supply Co.*

10—ADL ELECTROMAGNET: For producing high flux density magnetic fields, the ADL Electromagnet, powerful and versatile, is commercially available. Weighing about two tons it produces the same magnetic fields as other electromagnets weighing 15 to 50 times as much. *Arthur D. Little, Inc.*

11—MOTOR STARTER: For protection of personnel as well as equipment, a new motor starter, the Motor Watchman, has been developed by *Westinghouse Electric Corp.* This class 10-100-S1 starter, rated up to 600-v for 7½ hp polyphase and 5 hp single phase; or 220-v for 1½ hp dc, starts, stops, and provides overload protection for single phase, polyphase, and dc motors. Positive protection is provided by the quick-make, quick-break, over-center toggle mechanism—De-ion arc-quenching—and the bimetallic disk-type thermal overload relay.

12—VACUUM FURNACE: A new furnace, type 29-0410-18, is a standard unit for high temperature and high vacuum or controlled atmospheres. It can be used for heat treating, sintering, annealing, melting, and pouring. The power supply, vacuum pumping system,

Journal of Metals
29 West 39th St.
New York 18, N. Y.

February

Please send me on items indicated
- More Information ☐
- Free Literature ☐
- Price Data ☐

1	2	3	4	5	6	7	8	9	10
11	12	13	14	15	16	17	18	19	20
21	22	23	24	25	26	27	28	29	30
31	32	33	34	35	36	37	38	39	40

Name _____ Title _____
Company _____
Street _____
City and Zone _____ State _____

gages, and controls are enclosed in a metal cabinet. The bell jar is hinged to a vertical base plate, and both sides are accessible. Features include high temperature (up to 2000°C), close temperature control, even heat throughout hot zone, no refractories to outgas. The hot zone of the standard assembly is 5 in. high x 2½ in. diam. The vacuum system is built around the new H-4-P purifying type oil diffusion pump, backed by a 12.5 cfm Kinney mechanical pump. The basic unit is adaptable to pouring operations by the addition of accessory items. *National Research Corp.*

13—PLASTIC TUBING: Cyclon crystal clear flexible plastic tubing, for conducting all types of solutions in industrial, chemical, refining, etc., plants, is a new product of the *Munray Products, Inc., div. of Poly-Cyclo Products Co.* Extruded to a variety of diameters and wall thicknesses, Cyclon tubing can be used interchangeably for pressure and vacuum operations. Highly resistant to chemical attack, permanently stable and non-oxidizing, and not brittle at low temperatures, Cyclon has a variety of applications. Sizes range from 1/64-in. ID to 1½ in. OD, and is available in colors.

14—DRYING OVEN: For baking enamels, lacquer, wrinkle finishes; dehydrating bobbins, coil forms; drying plastic granules and parts after cleaning; and for preheating molds and other such uses, *Grieve-Hendry Co., Inc.*, has developed a new portable industrial electric oven. Uniform temperature throughout is claimed. No stratification is possible, and adjustable damper gives a wide range of constant temperature. The unit CR-1 has single phase 110 v motor, and can be operated on any 110 v outlet. It is 29x24 in. with an inside height of 20½ in. Shelves are removable, and the furnace will heat to 225° in 15 min.

Free Literature

20—PYROMETER: Continuous, accurate temperature measurement of molten iron at the front slagging spout of continuously tapped cupolas can be made through use of an adaptation of the Brown Radiamatic Pyrometer and ElectroniK potentiometer. The system uses a double protecting tube immersed in the flowing metal. *Minneapolis-Honeywell Regulator Co.*

21—pH DATA: A simple explanation of pH and how it is used is contained in a readable booklet, "What Every Executive Should Know about pH." The more technical aspects of pH and its measurements are presented in a comprehensive paper, "The Development of pH Instrumentation." Equipment for virtually every laboratory and industrial requirement is catalogued. *Beckman Instruments, Inc.*

22—MANGANESE STEEL PARTS: TISCO manganese steel parts for crushing and pulverizing equipment, and TIMANG welding rods are described and illustrated in Bulletin 350 offered by the *Taylor-Wharton Iron & Steel Co.*

23—MOISTURE METER: For rapid, accurate moisture content determinations on a wide variety of granular, powdered, or flaked materials, TAG's improved Dielectric Moisture Meter is recommended. Construction and operation data are given in Bulletin 1263 offered by the TAGliabue Instruments Div. of the *Weston Electrical Instrument Corp.*

24—RESEARCH FACILITIES: A staff of nearly 100 persons including chemists, engineers, physicists, assistants, medical and service personnel offer research, development, and engineering services to large and small companies. *Foster D. Snell, Inc.*

25—TANK LINING: Coverage, drying and working times, corrosion resistance, uses, and prices are given in data sheet C-42 for the application of thick protective coatings for tank and duct linings and for protection of equipment and floors. Due to a solids content of 100 pct, fluid and free flowing during applications, coatings can be applied 12 mils (0.012 in.) thick in one application even on vertical surfaces. *Carboline Co.*

26—GRANULATOR: A new oscillating granulator, 43B, is described by *F. J. Stokes Machine Co.* The unit is designed so that leakage of material is practically eliminated. The motor is protected against dust and dirt by mounting it within the granulator housing with only the end exposed for ventilation.

27—FOUNDRY PRACTICE: Foundry practices are described in Booklet No. 100, containing information on fastening cores by nailing, the treatment of "Y" alloy, and alloy structures. *Foundry Services, Inc.*

28—HARD FACING: Applications, precautions and suggestions on the proper procedures of surfacing manganese are given in a 4-p. bulletin on "Hard Surfacing Manganese Steel," saving users thousands of dollars. *Rankin Mfg. Co.*

29—SPECTROMETER: The direct reading Spectrometer, claimed to be the first fully automatic control instrument for the metals industries, is calibrated and adjusted to satisfy the needs of each user. Analysis of as many as 12 elements is read directly and simultaneously from clock dials. The unit, offered by *Baird Associates, Inc.*, is described in Bulletin XXXIV.

30—DATA CARD: A new data card on seamless and welded pipe of carbon, alloy, and stainless steels is offered by *Babcock & Wilcox Tube Co.* Included are ASTM and ASME specifications with grades and analyses for various types of pipe for high temperature and other services.

31—No. 20 STAINLESS: Stainless No. 20, the first commercially rolled stainless steel to offer superior corrosion resistance to hot solutions of sulphuric acid, is described in a new booklet published by *Carpenter Steel Co.* Stainless No. 20 is available in bar, wire, strip, forging billet, tubing, pipe, sheet, and plate form. The steel is especially resistant also to nitric-sulphuric acid mixtures. Tables of physical constants, nominal mechanical properties, and coefficient of expansion are included, and heat treatment, workability, and machining speeds are shown.

32—CHROME PLATING: Of interest to manufacturers of metal products, machinery, machine tools, and equipment is the Model A-20 Chromaster industrial chrome plating unit of *Ward Leonard Electric Co.* This company also announces the establishment of their Industrial Chrome Div., for manufacture of chrome plating units, solutions and processes for industrial hard chrome plating of machine tool accessories, and component parts.

33—ARGON WELDING: "Procedures and Equipment for Argon Metal Arc Welding" is the title of a booklet describing the apparatus for welding with an argon gas shielding the consumable filler metal electrode and the welding area. Features, work range, and photographs are included. *Linde Air Products Co.*

34—HIGH-TEMPERATURE ALLOY GUIDE: Two new cobalt base alloys and technical data on 10 Haynes alloys are contained in a new edition of the book, "Haynes Alloys for High Temperature Service." The 96-p. publication contains a section on each alloy, giving a description of the materials, recommended uses, chemical composition, and physical and mechanical properties in both tabular and graphic form. The new alloys, Nos. 25 and 36, are described in detail. *Haynes Stellite Div., Union Carbide & Carbon Co.*

Personnel Service

THE following employment items are made available to AIME members on a non-profit basis by the Engineering Societies Personnel Service, Inc., operating in cooperation with the Four Founder Societies. Local offices of the Personnel Service are at 8 W. 40th St., **New York 18;** 100 Farnsworth Ave., **Detroit;** 57 Post St., **San Francisco;** 84 E. Randolph St., **Chicago 1.** Applicants should address all mail to the proper key numbers in care of the New York office and include 6c in stamps for forwarding and returning application. The applicant agrees, if placed in a position by means of the Service, to pay the placement fee listed by the Service. AIME members may secure a weekly bulletin of positions available for $3.50 a quarter, $12 a year.

POSITIONS OPEN

Design Engineer with experience in design of metal parts for ammunition and fuses. Salary, $10,000 to $12,000 a year. Location, northern New Jersey. Y4725(a).

Metallurgist, under 30, engineering graduate, with good training in physics of gas in metal reactions. Mechanical aptitude desirable, to serve under plant metallurgist as technical control man for nonferrous casting. Salary, $3000 to $3600 a year. Location, Connecticut. Y4704.

Engineers (a) Metallurgist, ferrous, working knowledge of basic open hearth practice; fundamental knowledge of blooming mill procedure. Thorough knowledge of heat-treatment of carbon and alloy steel to meet variety of specifications, and ability to run heat-treat shop to produce results to meet various specifications. Experienced in chemical analysis of steel in conjunction with open hearth. Ability to perform actual analytical work on steels, nonferrous materials, and ferroalloys. (b) Assistant Metallurgist with same qualifications as above, including some mechanics, electrical engineering and mathematics, but with less responsibility. Salaries open. Location, Pennsylvania. Y4722.

Research and Graduate Assistants research work in physical and chemical metallurgy. Research assistants permitted 1/3 student schedule; graduate assistants, 2/3 student schedule toward advanced degree. Location, East. Y4688.

Engineers (a) Metallurgist, Ph.D. or M.S. degree, research experience, capable of responsible, independent research in physical metallurgy, interested in assuming some directive responsibility. Should have strong theoretical background. (b) Metallurgist with strong background in theoretical aspects of physical metallurgy. Should have at least an M.S. (c) Metallurgist with good theoretical background, and foundry experience. Research experience desired, with an interest in research. Location, Ohio. Y4385D.

Metallurgist with precious metals or nonferrous products experience, to be responsible for analysis and production test of wire and strip materials. Salary $3600 to $4800 a year. Location, Massachusetts. Y4378.

Open Hearth-Bessemer Plant Superintendent, metallurgical engineer, 40 to 50, with 10 years' experience operating open hearth bessemer plants, and knowledge of duplexing. Take charge of steel mill open hearth bessemer plant. Salary, $15,000. Location, India. R7215.

Foundry Research Metallurgist, M.S. desirable, 25 to 35. 2 or more years' experience required foundry metallurgical work, melting, heat rises, etc. Knowledge of modern research techniques. Informed about foundry problems. Will be in charge of research foundry metallurgical problems. Salary, $4500 to $6000. Location, Chicago. R7210.

Manager International Research, I.E., M.E. or Ch. E. Interested in foreign research problems and familiarity with U.S. policies regarding the technological program. Knowledge of research and development project, business and economic fields. Will represent research organization in the expansion of international projects. Salary open. Some foreign traveling. Location, Chicago. R7146.

Engineers (a) Assistant Mill Metallurgist, recent graduate, preferably speaking Spanish, for mill handling 10,000 to 12,000 tons ore a month, producing about 1400 tons copper concentrates. Contract 3 years. Must be single. Salary, $3000 a year plus board and room. (b) Mill Metallurgist, 30 to 45. Flotation experience essential, particularly of copper ores. 3-year contract. Salary, $4200 to $4500 a year plus board and room if single; or plus semi-furnished house, rent free if married. (c) Mill Superintendent, 30 to 45, flotation experience essential, particularly of copper ores. Must speak Spanish. Contract, 3 years. Salary open, board and room furnished free if single; or salary plus a semi-furnished house rent free if married. Location, Peru. Y4753.

Engineers (a) Assistant General Manager, technical and business administration schooling, 40 to 55. 20 years' experience in general operation of iron and steel plants, knowledge of overall management functions. Will be in full charge of steel mill operations under guidance of general manager. Salary, $18,000. (b) Blast Furnace Superintendent, metallurgical engineer, 40 to 50. 10 years' experience in operating blast furnaces for steel mills. Will take charge of blast furnace operations. Salary, $15,000. Location, India. R7214.

MEN AVAILABLE

Metallurgist, M.S., age 30, married, desires research, development or teaching position. Good background in tool-making and die casting, some in research and development work. Presently employed. Preferred location northern U.S. or Canada. M-605.

DO YOU HAVE TROUBLE HANGING ONTO YOUR COPY OF JOURNAL OF METALS?

—

The growing interest in the technical papers published by JOURNAL OF METALS makes it difficult for many subscribers to keep their copies of the magazine. Next time someone wants to borrow your copy, clip out the coupon on the bottom and tell him it only takes $8 to break the habit.

JOURNAL OF METALS can be his for $8 a year, as a non-member subscriber. If he wants to become a member of AIME, which among other things entitles him to a subscription to JOURNAL OF METALS, dues are $20 a year, plus $20 initiation fee.

JOURNAL OF METALS
29 West 39th St.
New York 18, N. Y.

I would like to subscribe to JOURNAL OF METALS.

..... Enclosed find $8 for a one-year subscription.

..... Enter my one-year subscription and bill me.

..... Send me an application for AIME Membership.

Name .....

Title .....

Mailing Address .....

City & State .....

Company .....

if you're interested in doing any of these things with an Electric Furnace,

you need this new book

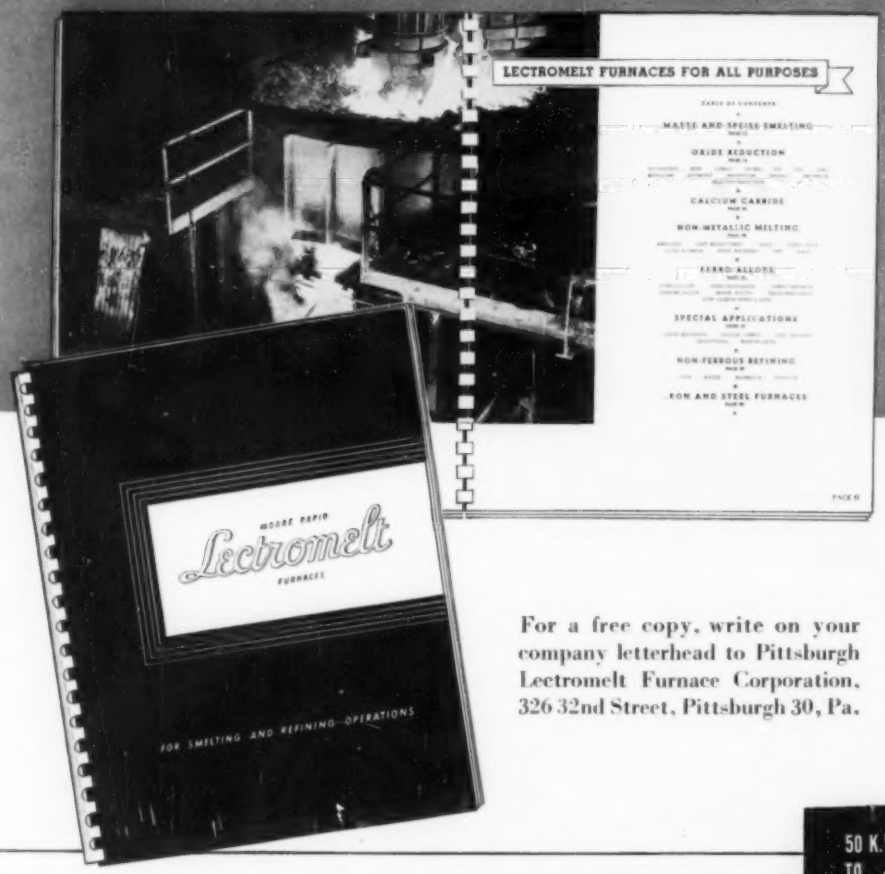

For a free copy, write on your company letterhead to Pittsburgh Lectromelt Furnace Corporation, 326 32nd Street, Pittsburgh 30, Pa.

WHEN YOU MELT... MOORE RAPID *Lectromelt*

Merged for better service to you

Two substantial leaders in service to the metals industry throughout the free world . . . Edgar E. Brosius Company, Inc. and Salem Engineering Company, have now joined hands in order to be of greater service to their customers. The large and capable consulting and industrial furnace designing staff of Salem is now immeasurably strengthened by the mechanical equipment manufacturing capacity of Brosius, whereas, the blast furnace and steel plant machinery designers at Brosius have many brilliant new partners to assist them. So apropos is this merger of talent that you can now call upon new Salem-Brosius, Inc. with complete confidence whether your needs include the smallest of furnaces or the construction of the largest plant projects.

SALEM-BROSIUS, INC., Pittsburgh 15, Pa.

Affiliates: Brosius Division, Pittsburgh 15, Pa.; Salem Engineering Division, Salem, Ohio; Salem Engineering Co., Ltd., Milford nr. Derby, England; Salem Engineering (Canada) Ltd., Toronto, Canada

Advertisement

ELECTROMET *Data Sheet*

A Digest of the Production, Properties, and Uses of Steels and Other Metals

Published by Electro Metallurgical Division, Union Carbide and Carbon Corporation, 30 East 42nd Street, New York 17, N. Y. • In Canada: Electro Metallurgical Company of Canada, Limited, Welland, Ontario

MANGANESE . . .
Deoxidizer and Toughener for Steel

Manganese is one of the most important alloys used in making steel. It is practically indispensable as a deoxidizer and cleanser for improving the hot-working properties of steels. When used as an alloying element, it makes steel stronger and tougher and it is therefore an important constituent of many structural and engineering steels.

Deoxidizes and Cleans Steel

The effectiveness of manganese in deoxidizing steel was first recognized in 1856, when it was used in the Bessemer process of steelmaking to counteract the bad effects of sulphur; in fact, manganese made this process a commercial success. Today, manganese is used as a deoxidizer and cleanser in the production of nearly all grades of open-hearth and electric-furnace steel, as well as high-grade cast iron.

Research work carrried out recently in ELECTROMET'S laboratories at Niagara Falls, New York, has provided new and important information on the value of manganese as a deoxidizer. This work shows that manganese is a more effective deoxidizer than has been previously realized; and that a combination alloy of silicon and manganese is a much stronger deoxidizer than either silicon or manganese by itself. Complete information is given in a report entitled "Solubility of Oxygen in Liquid Iron Containing Silicon and Manganese." If you would like a copy of this report, free of charge, write to the address above.

Improves Hot-Working Properties

By combining readily with sulphur, manganese performs another valuable job, it removes the principal cause of hot-shortness or brittleness—thereby giving steel better rolling and forging properties. In this reaction, the manganese combines with the sulphur to form manganese sulphide, as follows:

$$Mn + FeS = MnS + Fe$$

The manganese sulphide remaining in the steel is a less harmful type of inclusion than the iron sulphide would be, the hot-working properties of the steel are improved.

The weakening and embrittling tendencies of sulphur in cast iron can also be counteracted by the addition of manganese to the cupola charge.

Increases Strength, Toughness, and Wear-Resistance

When used as an alloying element in steel, manganese produces a steel with greater strength and toughness, and there is no serious loss of ductility. Additions of about 13 per cent manganese produce the well-known Hadfield manganese steel. High-manganese steels have exceptional resistance to wear; and consequently they have many applications in engineering jobs. Instead of wearing away quickly under conditions combining severe pressure, shock, and abrasion, these steels actually become harder through use. Thus, they last longer.

Because of the tendency of high-manganese steels to work-harden, they serve industry in important and varied applications. Manganese steel castings, for example, are used for railroad frogs and crossings, rock-crusher parts, steam-shovel dipper teeth, and dredge-bucket lips. The chief applications of manganese steel are in rails used for special service, and light forgings subjected to heavy wear.

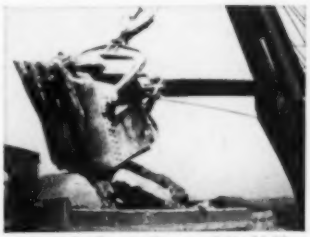

Dipper bucket teeth, cast of Hadfield manganese steel, actually increase in hardness under abrasive wear from gravel and rock in construction work — thus last many times longer than those of ordinary steel.

ELECTROMET Alloys

Manganese is produced by ELECTROMET in forms suitable for practically every use of the iron, steel, and non-ferrous metal industry. Some of the ELECTROMET products are listed below. For a complete description of these alloys, write for a copy of the 100-page booklet, "ELECTROMET Ferro-Alloys and Metals."

The terms "EM" and "Electromet" are registered trade-marks of Union Carbide and Carbon Corporation.

Alloys of Manganese and Their Uses

Standard Ferromanganese	The product most commonly used for adding manganese to steel for the purpose of alloying or deoxidizing and cleansing.
Low-Carbon Ferromanganese	For adding manganese to steels having a low carbon content, such as stainless steels of the 18 per cent chromium, 8 per cent nickel type.
Medium-Carbon Ferromanganese	Commonly used for making manganese steel containing 1.50 to 2.00 per cent manganese, and in the production of Hadfield manganese steel.
Low-Iron Ferromanganese	For applications in the nickel, aluminum, and copper industries where a low-iron alloy is required.
Silicomanganese	Used by the steel industry as a furnace block; as a deoxidizer; and also for manganese additions, particularly in the production of engineering steels containing 0.10 to 0.50 per cent carbon.
Ferromanganese-Silicon Mix	Used as a ladle inoculant for cast iron.
"EM" Silicomanganese Briquets	For adding manganese (with silicon) to cast iron in the cupola.
"EM" Ferromanganese Briquets	For adding manganese (without silicon) to cast iron in the cupola.

PREPARE NOW FOR HIGHER EMERGENCY PRODUCTION

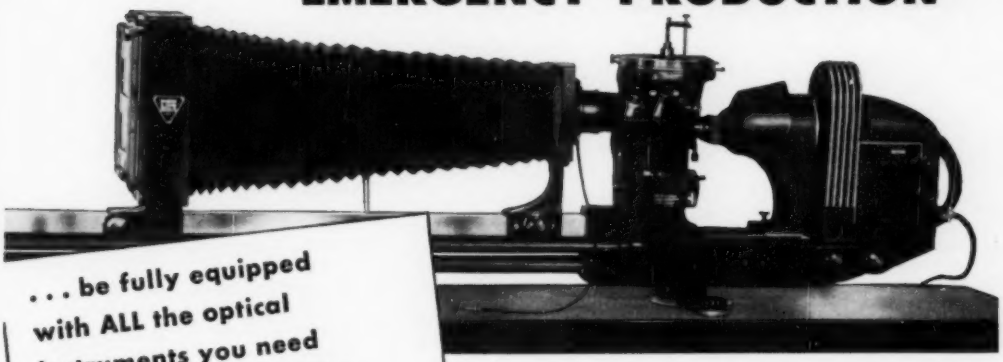

. . . be fully equipped with ALL the optical instruments you need for metallurgy from the complete Bausch & Lomb line

For Ease, Speed and Adaptability in PHOTOMICROGRAPHY

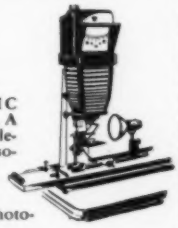

PHOTOMICROGRAPHIC EQUIPMENT MODEL L . . . A compact photomicrographic department! With proper accessories *this one unit* quickly and efficiently meets all your requirements in visual microscopy, high and low power photomicrography, as well as photocopying. Catalog E-210.

For Convenience and Top Image Quality in MICROSCOPY

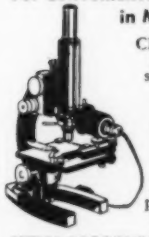

CM METALLURGICAL MICROSCOPE—Large focusing stage, space for convenient manipulation. Used extensively for examination of opaque objects, polished metal specimens and similar materials. Catalog E-223. Tri-Vert Illuminator, available at additional cost, provides bright field, dark field, or polarized light. Catalog D-108.

STEREOSCOPIC *WIDE FIELD* MICROSCOPES—The finest optics ever produced for wide field work! Clear, sharp three-dimensional images . . . invaluable in preparation of polished metal specimens. Study of fractures, porosity, macro-etched specimens and other low power metallurgical studies. Catalog D-15.

For Speed, Accuracy and Convenience in METALLOGRAPHY

RESEARCH METALLOGRAPH—See it . . . photograph it . . . *four* ways! Four different accurate images of the same sample, for more complete identification. Exclusive, patented B&L features permit critical work with bright field, dark field or polarized light . . . with quick, easy change-over. For phase contrast work B&L accessories are simply, speedily attached. The "maximum use" instrument for visual observation and photomicrography. Catalog E-240.

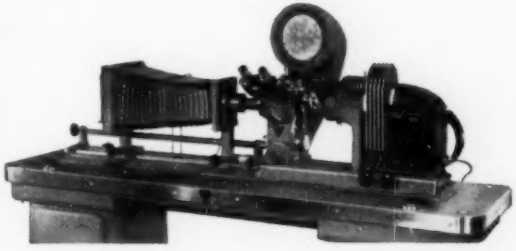

NEW! *BALPHOT* METALLOGRAPH—*All new* design! The economy of limited capacity instruments, with bright field, dark field or polarized light and phase contrast . . . and many other performance advantages of the highest-priced metallographs. Quick-action stage elevating device eliminates coarse adjustment. New *Magna-Viewer* projects bright, magnified screen images . . . ideal for grain size determinations and group viewing. Catalog E-232.

WRITE for complete information to Bausch & Lomb Optical Co., 787-2 St. Paul St., Rochester 2, N. Y.

Bausch & Lomb *Metallurgical* Equipment

"Just what the doctor ordered!"

"We have a new Service Division. It's a separate group in our Sales Department set up to handle service work, such as hearth installations, refractory practice surveys, tests, etc. And the boys in the back room say it's a long step in the right direction.

"This Service Division's a chip off the old block. Just like their comrades in arms in the Sales Department, the Service men are ex-steelmakers. Years ago we found out that steelmakers make good refractory sales and service men. So we've always staffed our Sales Department with men with practical steelmaking experience. They hit the bullseye. And that's why we stick to our guns in hiring new hands for the Service Division.

"Our need for a special Service Division really started back in 1940. Venturing where angels fear to tread, we told the steel industry that our magnesia ramming mix, Ramset, might eliminate a lot of blood, sweat and tears on new hearth installations —in major hot and cold repair work, too.

"Well, the industry said, we're from Missouri. The proof of the puddin' is in the eating. And you gotta show us. So the die was cast and we undertook to supervise Ramset jobs with our limited Sales staff.

WERE WE SWAMPED!

"We were bears for punishment in those days. Pretty soon we found ourselves on the horns of a dilemma. The Sales Department was so busy on service work that they didn't have time to sell. We were robbing Peter to pay Paul. On the one hand we couldn't handle all the service work that needed doing. At the same time our men couldn't be out winning friends and influencing people. In fact, we were between the devil and the deep blue sea. It looked like Basic might soon be a case of out of sight, out of mind, with those customers who weren't getting as much service with a smile as they wanted.

"Naturally we didn't want absence to make the heart grow fonder for somebody else's products. So we took the bull by the horns. Nothing ventured, nothing gained, you know. With the new Division we have arranged to furnish service around the clock. And we aren't sending a boy to do a man's work. We want you to see that it pays to leave the plumbing to the plumbers.

"We saw the light on another point, too. We had the right products and the right men. But something was still missing. Clothes alone don't make the man. Right equipment was necessary to save the day.

MOTHER NECESSITY INVENTS

"Always before, we cut the pattern to fit the cloth—mixing Ramset by hand or in a concrete mixer, moving the tempered Ramset by wheelbarrow to the furnace and compacting the Ramset with backfill tampers. But recognizing that a job worth doing is a job worth doing well, that time is money and that handsome is as handsome does, we decided to get the right tools for the job.

"Seizing time by the forelock, we added an 18-cubic foot mortar-type mixer to our kit. It tempers Ramset rapidly without segregation or balling and permits maintenance of a uniform moisture content.

"A straight line is the shortest distance between two points, so we designed and had built a belt conveyor to match the capacity of the mixer. That eliminates wheelbarrow labor and delivers tempered Ramset from the mixer, OVER charging buggies, into the furnace.

"Realizing also that you can't drive a spike with a tack hammer, we fell to the task of finding a faster, better way of tamping Ramset into place. Even a blind hog turns up an acorn now and then and our rooting uncovered a mechanical tamper that gives Ramset what Paddy gave the drum. The new device has a blow that would fell an ox. It cuts down the manpower previously required, and saves plenty of silver seconds and golden minutes. That's our complete ball of wax—to date.

FIRST COME, FIRST SERVED

"And here's the deal: Since any worker is worthy of his hire, we've hung a 'For rent' sign on this equipment package. It's open for engagements on a bargain basis, calculated to cover amortization, maintenance and delivery to your door by our Service Division truck. Virtue being its own reward, we don't charge anything for the 24-hour supervision of your hearth and major repair jobs by the Service Division.

"To date only one complete package is ready. So renting the equipment is on a first come, first served basis. But it's only the beginning. We expect to have several other expanded equipment packages available soon. When that good day comes there need not be a case of he who hesitates is lost or of haste makes waste.

"Maybe you can't teach an old dog new tricks, but if practice makes perfect, you can be sure the jobs our Service Division undertakes will prove that experience is the best teacher.

"And we're not selling a pig in a poke because blazing a trail isn't a new experience for us. You remember it was our people years ago who paved the way on hearth installation techniques (including the use of forms) now used from the rock-bound coasts of Maine to the sunny shores of California.

"Just remember your success is our happiness. We hope you'll give us a chance to get to the bottom of your trouble.

"Yours for better bottoms,"

OLD BILL BASIC

Basic Refractories Incorporated 843 HANNA BUILDING, CLEVELAND 15, OHIO

Drift of Things . . . . . as followed by **Edward H. Robie**

THOUGH nothing is as important to personal, national, and world well-being as recent international, political, and military developments, we have not lately made any comment on them. We have never been east of Cape Cod, west of the North Pacific coast, north of Saskatoon, or south of Key West, so perhaps our point of view is too circumscribed to be worth offering. However, an excellent guide book to Paris was written by a man who had never been there.

What should the United States do? What should the United States have done? Plainly, those who ran the world before World War II did a sorry job of it. Those who have been running it since that war ended have done even worse, for here we are confronted with a strong possibility of an even more terrible era of devastation and blood-letting. But we have yet to hear any of the world's leaders apologize for their ineptitude. Any evidence of a contrite spirit seems to be missing. Worse still, the voting peoples seem complacent and not moved to demand a change.

Hoover Statement

Of recent public pronouncements by people in the public eye, that of our own Herbert Hoover on Dec. 20 over the Mutual Broadcasting System makes the most sense to us. At 76, Mr. Hoover spoke firmly and clearly and, of course, his background of experience in America, Europe, and the Far East commands the highest respect. Two months before, he had opposed further military or economic aid to Europe until it set up a "united and sufficient" European army, and he urged reorganization of the United Nations without the Soviet Union and its satellites.

In his latest speech he expanded on his former statements. He first surveyed the global military situation, pointing out that the Communists in Europe and Asia have over 300 trained and equipped combat divisions, with more than 30,000 tanks and 10,000 tactical planes, though their long-range air power is limited and their sea power confined to submarines. Some day, he said, "the Communistic empire will go to pieces. But in the meantime they are cannon fodder." Facing the Communists in the Far East are the already defeated Koreans, and perhaps 12 combat divisions in addition. Among our friends, only Formosa and Turkey, in Asia, have any important military strength. Among the European Continental countries, Mr. Hoover estimates something less than 20 combat divisions, with disunity and a feeble will to defend themselves. The British commonwealth has perhaps 30 combat divisions, with a good air force and a superior navy. Here in the U. S. we are planning 30 combat divisions with a gigantic air force and navy.

With this situation, Mr. Hoover can see no hope of defending Asia or continental Europe against the Communist horde by land forces, should the Communists decide to attack, even though the non-Communist countries had the will and means to defend themselves, which they do not have. For the U. S. to undertake to fight the Communist countries in Asia and continental Europe practically single-handed is sheer folly. "That would be the graveyard of millions of American boys and would end in the exhaustion of this Gibraltar of Western civilization. Even were Western Europe armed far beyond any contemplated program, we could never reach Moscow. The Germans failed with a magnificent army of 240 combat divisions and with powerful air and tank forces as contrasted with the 60 divisions now being talked about."

New Frontiers

So Mr. Hoover proposes that we defend Western civilization by arming our air and naval forces to the teeth rather than to send a land army in a futile mission to continental Europe or Asia. Our eastern frontier would be in Britain; our western on Japan, Formosa, and the Philippines, provided they were willing to try to defend themselves with our help. Presumably we would see that Communist aggression was stopped everywhere in the Americas.

Mr. Hoover has been accused of preaching isolationism, but surely the frontiers indicated are sufficiently broad to emphasize our desire to assist other countries. He has been accused of being a defeatist, but he offers a realistic program that has much more hope of success than does a more extended policy of spreading our military and economical policy so thinly that defeat would be practically certain. He has been accused of scuttling the Atlantic Charter and the North Atlantic Treaty, but nothing in those agreements commits the United States to undertake the defense of Europe on a scale far greater than the European countries are willing to assume.

The United States cannot be the omnipresent policeman throughout the troubled non-Communist world. That, thinks Mr. Hoover, is the job of the United Nations. The United States should not have had to provide 90 pct of the military force in Korea. Other United Nations countries at least could have provided men, if not munitions. If they are unwilling to assume their proper share of the burden, the United States must be realistic and pull in its lines a bit. Mr. Hoover suggests four things for the United Nations to do: (1) Declare Communist China an aggressor. (2) Refuse admission of this aggressor to its membership. (3) Demand that each UN member country cease furnishing or transporting supplies of any kind to Communist China that can aid in its military operations. (4) Pass a resolution condemning the infamous lies about the United States.

UN Unity Necessary

We think it is about time that the countries opposed to Russia's policies get together and make the United Nations work. There is still a good chance for this organization to be effective if the Russian shackle on its activities is removed. A UN army, navy, and air corps that will be able to stand off Russia is needed, to which every member nation should contribute. It should operate under codified international law, defining, among other things, what is meant by aggression. No nation should have the right to veto any action that it might consider to be to its disadvantage, and yet this veto power was one of the things that the United States originally insisted on having included in the UN Charter.

The United States should temper its crusade for the institution of our brand of democracy and freedom throughout the world. It works to our general satisfaction but it probably would not function satisfactorily in many other countries—Latin America, for example. It is right that we are aiding even Communist Yugoslavia. If a country minds it own business and does not molest its neighbors, its form of government should be its own affair.

View of Harbor Island Laboratory and Testing Station.

New testing station provides expanded facilities for corrosion studies

During the past 15 years, the Atlantic Ocean at Kure Beach served as a giant test tube for studying attacks of sea water and salt air upon more than 33,000 specimens, including virtually all types of metals and alloys.

Storm damage to the basin, in which the underwater tests were conducted, compelled establishment of a new and protected testing station. Accordingly, some 15 miles north, on Harbor Island, the new Inco Marine Laboratory was built to provide expanded facilities and an even better "Ocean Test Tube."

This new Harbor Island station, along with the atmospheric test racks retained on the shore of Kure Beach, now widen the scope of cooperative enterprise for fighting industry's common enemy — *corrosion*.

The vast amount of valuable data accumulated over the years will continue to be made available to all industry, as well as to government agencies for whom and with whose cooperation much of the research has been undertaken. You are invited to consult us on your corrosion problems.

Lowering piling test specimens into place. Sea water is something more than a mixture of chemicals; its corrosive action over an extended period can be studied properly only by exposure of specimens to attack under natural conditions.

Running water troughs. For studying the action of sea water flowing at moderate velocities, specimens are immersed in the troughs, shown above. The total length of trough used for this purpose now amounts to about 600 feet.

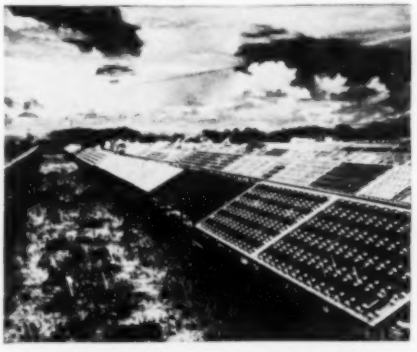

Atmospheric and spray test lot. Shown above is part of the atmospheric test lot at Kure Beach in which over 20,000 specimens have been exposed, some for over nine years. The racks face south, and the specimens, supported on porcelain insulators, are all set at a slope of 30 degrees.

INCO

THE INTERNATIONAL NICKEL COMPANY, INC. 67 WALL STREET NEW YORK 5, N.Y.

Liquid flame-hardening of gear teeth, using a salt bath furnace, provides uniform hardening without any change in dimension and without any scaling or oxidizing of the hardened areas.

A camera mounting device built by the Andrews Air Force Base personnel enables clear and steady motion pictures to be taken from aircraft flying at 600 mph.

A technique that enables observing the same areas of a metal specimen under light and electron microscopes has facilitated use of the latter.

ECA is supplying $583,000 under the Marshall Plan to finance part of the modernization program of Consett Iron Co., Ltd., one of Britain's important steel producers. Most of the money will pay for engineering services for a Morgan-type continuous billet mill, to be built by Davy and United Engineering Co., Ltd.

National Tube Co., will use the French Ugine-Sejournet process of hot extrusion for the production of steel pipe, bars, and special shapes. The extrusion plant, at Gary, Ind., will produce about 3000 tons a year of extruded products, ranging from 0.5 to 4.5 in. diam.

J-35 jet engines are now overhauled at Hamilton Air Force Base instead of shipping them back to an Air Force Depot. This has resulted in a saving of about $150,000 per month and increased the time between overhauls from 50 to 180 hr.

Uranium will be produced from South African gold ores and sold to the United States and the United Kingdom by the Union of South Africa. Uranium content of the ores is low, but in view of the great quantities of ore mined, one of the largest uranium sources is indicated.

Public and privately owned utilities may jointly supply power for the proposed AEC plant near Paducah, Ky., which will produce U-235 by a gaseous diffusion process. Negotiations are in progress with TVA and Electric Energy, Inc., a syndicate of private companies.

USAF cargo planes can unload 5 tons of cargo in 7 sec, using a monorail system developed by the Air Materiel Command. Drop cargo, loaded in 500 lb packages, is swung from an overhead track on trolleys that automatically release their loads when cargo doors are opened. Chutes on packages are opened by a static line as the plane is cleared.

French steel production by October, 1950, was 5 pct ahead of the monthly average of the record year of 1929. Pig iron and rolled steel output remained slightly below the 1929 average. Coal output from the Lorraine basin now exceeds 37,000 per day, as compared with 26,000 tons before the war. New equipment and improved mining methods accounted in part for the increase in Lorraine coal production.

Buehler . . .

. . . OFFERS A COMPLETE LINE OF EQUIPMENT FOR THE Metallurgical Laboratory

Buehler specimen preparation equipment is designed especially for the metallurgist, and is built with a high degree of precision and accuracy for the fast production of the finest quality of metallurgical specimens.

1. No. 1315 Press for the rapid moulding of specimen mounts, either bakelite or transparent plastic. Heating element can be raised and cooling blocks swung into position without releasing pressure on the mold.

2. No. 1211 Wet power grinder with 3/4" hp. ball bearing motor totally enclosed. Has two 12" wheels mounted on metal plates for coarse and medium-grinding.

3. No. 1000 Cut-off machine is a heavy duty cutter for stock up to 3-1/2". Powered with a 3 hp. totally enclosed motor with cut-off wheel, 12" x 3/32" x 1-1/4".

4. 1505-2AB Low Speed Polisher complete with 8" balanced bronze polishing disc. Mounted to 1/4 hp. ball bearing, two speed motor, with right angle gear reduction for 161 and 246 R.P.M. spindle speeds.

5. No. 1700 New Buehler-Waisman Electro Polisher produces scratch-free specimens in a fraction of the time usually required for polishing. Speed with dependable results is obtained with both ferrous and non-ferrous samples. Simple to operate—does not require an expert technician to produce good specimens.

6. No. 1410 Hand Grinder conveniently arranged for two stage grinding with medium and fine emery paper on twin grinding surfaces. A reserve supply of 150 ft. of abrasive paper is contained in rolls and can be quickly drawn into position for use.

7. No. 1400 Emery paper disc grinder. Four grades of abrasive paper are provided for grinding on the four sides of discs, 8" in diameter. Motor 1/3 hp. with two speeds, 575 and 1150 R.P.M.

8. No. 1015 Cut-off machine for table mounting with separate unit recirculating cooling system No. 1016. Motor 1 hp. with capacity for cutting 1" stock.

THE BUEHLER LINE OF SPECIMEN PREPARATION EQUIPMENT INCLUDES . . . CUT-OFF MACHINES • SPECIMEN MOUNT PRESSES • POWER GRINDERS • EMERY PAPER GRINDERS • HAND GRINDERS • BELT SURFACERS • MECHANICAL AND ELECTRO POLISHERS • POLISHING CLOTHS • POLISHING ABRASIVES

Buehler Ltd.
A PARTNERSHIP

METALLURGICAL APPARATUS
165 WEST WACKER DRIVE, CHICAGO 1, ILL.

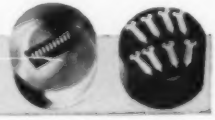

Air Force Purchases Two 50,000-Ton Hydraulic Presses for Making Wing Sections

The Air Force has purchased two hydraulic presses each in excess of 50,000 tons capacity. This culminates an investigation that goes back to the end of the war, when it was discovered that Germany had in operation a 33,000-ton unit. At that time, several press manufacturers including Lake Erie Engineering Co. of Buffalo, Loewy Hydropress Co. of New York, and one or two others submitted designs for hydraulic presses of approximately 60,000 tons capacity. One design, it was reported, was to be constructed at the base of a mountain so it could utilize a lake high up in the mountain as a hydraulic head.

The need for presses of such great capacities hinges on the efforts of the Air Force to produce airplane wing skins in which structural members are an integral part of the skin. Skin milling, a process whereby heavy aluminum plate was machined so that the ribs and skins were integral with each other, was one method devised. The difficulty with this method, however, was that (1) about 80 pct of the aluminum was machined away as scrap, (2) electric power facilities would be strained to produce sufficient aluminum, as well as satisfy other demands, to meet any wartime demand for heavy plate in such quantities, (3) the skin milling machine, a large and heavy unit, is both costly and likewise requires vital materials in its makeup, and (4) machined skins are far more costly than forged skins, in addition to not having the same physical properties.

The two new presses ordered by the Air Forces are to be constructed by Loewy Hydropress Co., New York, and are scheduled for delivery in about 18 months. The 33,000-ton press built by the Germans is now reported in the hands of the Russians.

U. S. Steel To Build New Wholly-Integrated Steel Plant

Fairless Works, a new wholly-integrated steel plant to be built by U. S. Steel Corp. near Morrisville, Pa., is believed to be the largest single expansion project ever undertaken by any steel company. Named in honor of Benjamin F. Fairless, president of U. S. Steel Co., the plant is expected to begin production of finished steel products within 12 months after construction begins in early Spring.

The works will have an initial annual production capacity to produce 289,000 tons of cold rolled sheets, 235,000 tons of hot rolled sheets, 281,000 tons of standard pipe, 285,000 tons of bar products, and 170,000 tons of tin mill products. Some of the principal facilities to be erected will be two blast furnaces with a capacity of 1,200,000 tons of pig iron annually; nine openhearth furnaces with a capacity of 1,800,000 tons of steel annually; an 80-in. hot strip mill and hot strip finishing facilities; finishing facilities for cold rolled sheets and tin plate; a blooming-slabbing mill and auxiliary facilities; a billet mill and auxiliary facilities; and a bar mill with a size range from $\frac{3}{8}$ to 2 in.

It is expected that the new plant will utilize a part of the high grade ore to be mined in Venezuela by Orinoco Mining Co., a U. S. Steel subsidiary. Another subsidiary, National Tube Co., will operate the pipe producing part of Fairless Works.

Engineers Needed at N. R. L.

The Naval Research Laboratory has an immediate need for men to fill existing vacancies in various general fields. In addition to positions listed, the Laboratory is interested in interviewing individuals qualified in the indicated fields. Since the Laboratory requests applicants to give specific "job number" when applying, and the list received by JOURNAL OF METALS contains 46 positions, the Editor will endeavor to supply the necessary information to those requesting it. Please include the division and branch of the field you are interested in.

Civil Service status is not a prerequisite for consideration for these positions, which have ratings of GS-4 to GS-12.

Positions are under the following headings: Chemists, Metallurgy Div. (Crystal Branch); Chemical Engineers, Chemistry Div. (Consultant Branch); Electrical Engineers, Electricity Div. (Airborne, Shipborne Systems Branches); Electronic Scientists, Sound Div. (Sonar Systems, Electronics, Propagation Branches), Radio I (Wave Propagation Res., Vacuum Tube Res., R.F. Res.), Radio II (Antenna Res., Systems Utilization, Radio Techniques, Communications, Search Radar, Countermeasures); Lab Electronic Mechanic, Electricity Div.; Lab General Mechanic, Radio I; Glass Blowers, Optics Div.; Physicists, Electricity Div. (Electromagnetics, Cyrogenics Branches), Mechanics Div., Optics Div. (Applied Optics, Radiometry Branches), Sound Div., Radio I (Absorbent Materials for Radio Wave, R.F. Res.), Nucleonics Div. (Special Research, Accelerators Branches); and Psychologists. Radio III.

Civil Service Positions Open

A limited number of vacancies exist in U. S. Air Force headquarters, Pentagon, Washington, D. C., for mining and metallurgical engineers who also possess photo interpretation experience or potential. Photo intelligence specialists GS-9, $4600 per annum, starting salary through GS-12, $6400 per annum, starting salary. Civil Service grades assigned will depend largely on education and/or equivalent experience in the field of mining engineering and/or metallurgical engineering. Inquiries and requests for required Civil Service application forms should be made to the following: Photo Intelligence Section, Reconnaissance Branch, Directorate of Intelligence, Headquarters, U. S. Air Force, Washington 25, D. C.

Brosius and Salem Engineering Merge

Salem-Brosius Inc. has been formed by the merger of Edgar E. Brosius Co. of Pittsburgh and Salem Engineering Co. of Salem, Ohio. Both companies will continue to use their individual names for business purposes, and no changes are being made in the employment or personnel of either company.

The Brosius Co., formed in 1909, designs and manufactures special machinery for the metal trades industries such as blast furnace accessories, material handling equipment for blast furnaces, and industrial heating and melting furnaces. Salem Engineering, founded in 1934, specializes in the design and construction of industrial furnaces and steel mill equipment. Both companies have conducted business throughout the world. Brosius production facilities will now be available for the fabrication of equipment designed by both companies.

CONFERENCE

April 2 to 4, 1951

The best audience—engineers, superintendents, melters, metallurgists, and executives—of iron, steel, and coke producing companies, will attend a technical meeting to find out what is new in steel, coke, and iron making technology, production methods, and equipment maintenance.

JOURNAL OF METALS will reach every registrant at the meeting in addition to the regular subscribers, carrying the program and advance technical data that will be presented at the meeting.

JOURNAL OF METALS *will carry the only Official Conference Program.*

Reach these men who buy, specify and influence the purchase of your products for these companies. Advertise in the Open Hearth, Blast Furnace, Raw Material, and Coke Oven Conference Special Issue, the April JOURNAL OF METALS.

Write or wire for space reservations now. Plates for advertisements in this issue must be in New York by March 5.

JOURNAL OF METALS

29 West 39th Street • **New York 18, N. Y.**

A Byproduct Metal

by A. P. Thompson and H. R. Harner

GALLIUM, though only recently publicized, is not a newly discovered element. The story of the recognition of its existence and its actual identification and isolation is fascinating. In 1861, Mendeléeff presented his famous paper "The Relation of the Properties to the Atomic Weights of the Elements" before the Russian Chemical Society. Subsequently, he predicted properties of a number of undiscovered elements. Three he designated ekasilicon, ekaboron and ekaaluminum because of their similarity to the elements indicated. These later became known as germanium, scandium, and gallium, respectively, and were discovered during his lifetime. Lothar Meyer's work done contemporaneously in Germany covered much the same ground, but lacked the striking originality and boldness of concept and expression.

Gallium was the first of the three eka elements to be identified and isolated. This was accomplished in 1875 by the French chemist Lecoq de Boisbaudran who named the element in honor of his native country. This was the culmination of a brilliant 15-year study of spectra during the course of which he developed his own law with regard to the periodicity of the lines of similar elements.

Boisbaudran in the early 1860's decided that there was an element missing between aluminum and indium. He predicted its major spectral lines and undertook the search. In 1874, he began the investigation of some zinc blende from the Pyrenees and according to his own words: "Between three and four in the evening of August 27, 1875, I found indications of the probable existence of a new elementary body . . . ".[1] In November 1875 he isolated more than a gram of the metal and within the next 2 or 3 years produced about 75 g.

Similarity between the properties, both chemical and physical, predicted for ekaaluminum by Mendeléeff and those actually found for gallium by Boisbaudran is most striking; for example, a specific gravity of 5.9 g per cc was predicted and 5.94 was found.

As might be expected from its proximity to aluminum, gallium is widely distributed in the earth's crust. It exists in roughly the same quantity as lead, about 15 g per ton of earth.[2] Lead, however, is concentrated at favorable spots while gallium is almost universally disseminated but nowhere in significant commercial concentration. Insofar as the authors are aware, there is no mineral that contains gallium as a major constituent—the nearest exception being germanite, a complex zinc-copper-arsenic-germanium sulphide found in the copper ores of Mansfeld, Germany, and in the Tsumeb copper-lead mine, Southwest Africa. This mineral usually contains from 0.1 to 0.8 pct gallium with one specimen reported to have contained as high as 1.85 pct.

To the extractive metallurgist, the question becomes one of determining where suitable natural or artificial concentrations may be found. The periodic table suggests that gallium might be expected in ores or minerals containing zinc, aluminum, and germanium. Boisbaudran's original work was done on zinc ores and most gallium produced to date has come from such materials.

Gallium is frequently associated with germanium in the comparatively rare mineral germanite and in coals. Unfortunately germanium is rare, and materials containing it must be discounted as a source of gallium. Further, almost any sample of earth or clay, of which of course aluminum is a major constituent, will show a gallium content on

A. P. THOMPSON is Director of Research, and H. R. HARNER is Chief Chemist for The Eagle-Picher Research Laboratories, Joplin, Mo.

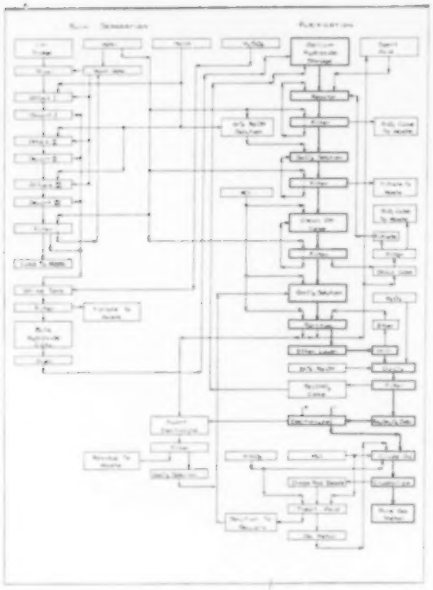

Fig. 1. Process used to recover gallium from lithopone plant residues.

the spectrograph often in the order of 50 g per ton or considerably over the average for the earth's crust. It is also found in bauxite, the source of commercial aluminum and accumulates in the circulating liquors of the Bayer process from which it may be recovered.

In Missouri-Kansas-Oklahoma zinc ore concentrates the metal averages about 0.005 pct or 45 g per ton. It is present in the zinc sulphide mineral itself. Clean sphalerite crystals of four common types were selected and the gallium content estimated spectrographically. The results in pct gallium were: "Black Jack", 0.005; "Rosin Jack", 0.02; "Ruby Jack", 0.01; "Amber Jack", 0.001. The more highly colored sphalerites tend to carry more of the metal. The gangue also was tested spectrographically and contained less than 0.0005 pct gallium, further proving the element to be in the zinc sulphide crystal.

Gallium is closely tied to the Tri-State lead and zinc field of Southwest Missouri, Southeast Kansas, and Northeast Oklahoma. During the early part of the century, W. George Waring, studying the zinc ore of the district, proved the presence of gallium and other rare metals.

The story of gallium in the Tri-State district began in 1915 with the early work of F. G. McCutcheon, now manager of the Eagle-Picher Zinc Smelter at Henryetta, Okla. At that time he was chief chemist of the Bartlesville Zinc Co. of Bartlesville, Okla., producing high grade zinc by redistilling prime western spelter made in large part from Tri-State ore. The leady *heels* or residuum left in the retorts was cast in slabs and stacked outdoors pending shipment to a lead smelter. Following a rain, McCutcheon noticed beads or droplets of metal exuding from the slabs.[3] On analyses these beads proved to be an alloy of about 94 pct gallium and 6 pct indium. The only explanation for the formation of the beads of metal was that the heels were a complex mixture of metals including sodium and calcium. The latter are believed to have reacted with the rain-water to release the beads of rare metal alloy. McCutcheon subjected several slabs to steam and reproduced the phenomena, collecting 300 g of alloy from one 700-lb lot of heels so treated.

Working over a period of years, he developed recovery processes and produced the world's first pound of gallium metal. He then located other Tri-State zinc residues containing gallium and continued its recovery on a small scale as a hobby. By 1944, he had recovered some 6000 g of the metal.

The Eagle-Picher Research group at Joplin meanwhile had become interested in gallium recovery from still a different Tri-State zinc ore residue. The Eagle-Picher lithopone plant at Argo, Ill., was processing 10 tons per day of roasted zinc ore and producing about 1000 lb per day of iron mud leach residue. McCutcheon pooled his knowledge with that of the research dept. and a process shown in Fig. 1 was developed for handling this material. It consisted of a caustic leach that dissolved aluminum and gallium compounds and some silica; precipitation as hydroxides; filtration and dehydration of the cake; hydrochloric acid leach; precipitation as hydroxides; solution of cake in hydrochloric acid; ether partition; electrolysis in caustic electrolyte; and fractional recrystallization of the recovered metal.

The process is complicated, expensive, and to get good recoveries of high purity metal, requires meticulous attention to detail. It must be remembered that gallium is not a noble metal, but in the periodic table is directly below aluminum, an element whose metallurgy has proved most difficult. Since only 0.07 pct gallium is concentrated in the iron mud leach residue, associated with about 10 pct aluminum and 15 pct iron as well as variable amounts of a great many other elements, the difficulty and expense of the separation can easily be realized. Gallium is $2.50 to $7.50 per g depending on the quantity purchased. A new recovery method must be developed for each new gallium raw material. Furthermore, use of strong hydrochloric acid is almost an essential step of any recovery process, introducing a severe materials-of-construction problem, especially on a pilot plant scale.

The chemistry of gallium is comparable to that of aluminum. Therefore, the complicated character of the various chemical and metallurgical steps used in the recovery of the element is not surprising. The chemistry of gallium also bears a marked resemblance to that of the two succeeding elements, indium and thallium. The stability of the compounds of these four elements decreases with increasing atomic weight. As a corollary, the ease of reduction to the metal increases with the atomic weight. All are permanent in air at ordinary temperatures, but when heated develop a protective oxide coating. The normal hydroxides are amphoteric in the case of the first three elements and basic only in the case of thallium. Like aluminum, gallium forms alums.

The usual valence is three. With increasing atomic weight, the tendency to form compounds of lower valence becomes more marked, this property being most noticeable in the case of thallium. Aluminum normally shows no valence other than three while gallium forms a number of divalent and even some monovalent compounds.

Gallium metal is most unusual in its properties. It has one of the longest liquid ranges of any element, melting at 29.75°C (85.5°F) (about 70°C higher than mercury) and boiling at 1983°C (3601°F).[3] There is some difference of opinion on the boiling point, values up to 2100°C and higher being reported. Visual proof of the low melting point is shown in Fig. 2. The boiling points of its congeners, aluminum and indium, are of the same order while that of thallium is about 500°C lower. The vapor pressure of gallium remains quite low at comparatively high temperatures, being only 1 mm at 1315°C (2399°F).

Gallium is one of the few metallic elements that expands on solidifying. The liquid density at 29.8°C is 6.095 g per cc while the solid density at 20°C is 5.907 g per cc, roughly a 3 pct expansion on solidification—almost as great as that of bismuth, 3.3 pct. This property provided an interesting problem in the packaging of the metal for sale. If packaged directly in a glass container as the liquid metal, expansion on solidification breaks the container. On warming a little, the gallium melts, and flowing like mercury, is often lost or contaminated. One supplier packages the liquid metal in rubber bulbs. Eagle-Picher supplies the metal as clean crystals dipped from the melt while cooling, packed in sealed Pliofilm bags. Should the metal accidentally become warm and melt it cannot escape. On resolidifying, the elastic Pliofilm prevents rupture and loss.

Gallium crystallizes in the orthorhombic system, and beautiful specimens are produced. The exact shape of the crystals varies from thin square plates to thick and massive spear points. A typical example is shown in Fig. 3.

As might be expected from its position in the periodic table, gallium is a chemically active metal. The literature contains an imposing list of alloys and solid solutions with other metals.

Since certain suggested uses for gallium are based upon its long liquid range and low vapor pressure at elevated temperatures, the matter of reactivity and of a suitable container is important. The Atomic Energy Commission, which is much interested in the possible use of liquid metals as heat-transfer media, recently has released information on this subject. The section on gallium discusses its properties in this connection quite thoroughly. The introductory paragraphs dealing with materials to handle liquid gallium are most interesting:[4]

"Gallium is more aggressive in its attack on most solid metals at a given temperature than any other molten metal that has been tested. It can be contained successfully at high temperatures only in some of the refractory oxides, quartz, graphite, and such metals as wolfram, and tantalum.

"The mechanism of attack on solid metals by gallium differs widely from one metal to the next, and from one temperature to the next. With tantalum at 600°C (1112°F) for example, the attack occurs chiefly through solution, although at 800°C (1472°F) there is perceptible evidence of diffusion into the solid metal to form a compound. Molybdenum reacts with gallium at these temperatures to form more than one reaction product, one of which is a solid solution. Wolfram, however, is not attacked by gallium at temperatures up to 800°C (1472°F), although it might be expected to behave like molybdenum since compounds of molybdenum and wolfram are isomorphous.

"Although gallium does not readily attack most ceramics, it tends to wet magnesia under certain conditions, but does not wet beryllia or alumina. An anodized coating on aluminum, however, offers no barrier to penetration by gallium even at moderate temperatures."

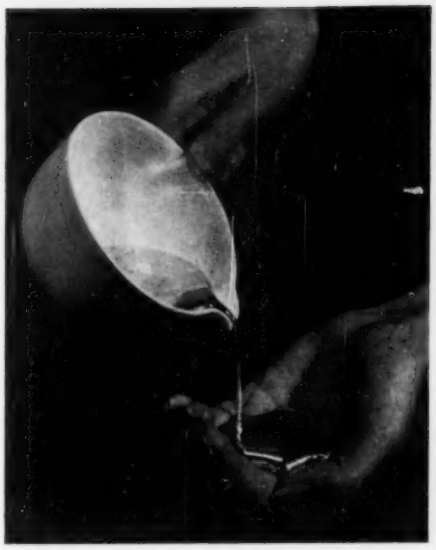

Fig. 2. Molten gallium can be handled with impunity as the melting point is below body temperature.

Important physical properties of gallium are summarized in Table I.

A wide variety of uses has been suggested for gallium, ranging from low melting-point alloys to the treatment of bone cancer.[10] The first use proposed was as fill material in high temperature thermometers. Practical difficulties arose such as the

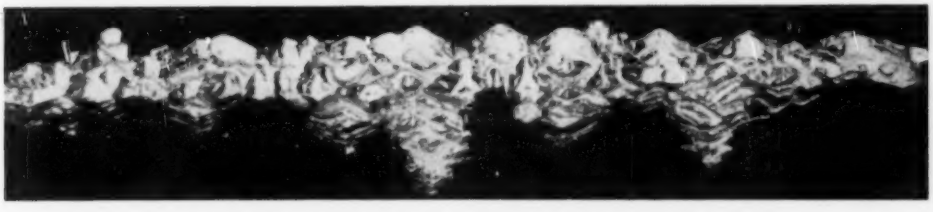

Fig. 3. A crystal over 3 in. long formed by seeding super-cooled gallium with solid gallium.

Table I—Physical Constants of Gallium

Atomic No.	31
Atomic Weight	69.72
Isotope Abundance — Mass No. 69, Pct	61.2
Mass No. 71, Pct	38.8
Crystal Structure	Orthorhombic
Density — 20°C (a), G per cc	5.907
29.65°C (a), G per cc	5.9037
29.8°C (l), G per cc	6.0948
Specific Volume at Melting Point, (Solid)	0.1694
(Liquid)	0.1641
Melting Point	(85.5°F) 29.75°C
Boiling Point	(3601°F) 1983°C
Latent Heat of Fusion — G-cal per g	19.16
Btu per lb	34.5
Latent Heat of Vaporization, G-cal per g	1014
Heat of Combustion (2 Ga + 3 O = Ga_2O_3), Kcal	259
Vapor Pressure — 1315°C (2399°F), Mm of Hg	1.0
1726°C (3139°F), Mm of Hg	100
1983°C (3601°F), Mm of Hg	760
Specific Heat — solid, 16° to 24.2°C, Cal per g	0.0926
liquid, 21° to 130°C, Cal per g	0.0977
Linear Thermal Coefficient of Expansion — 0° to 30°C, Cm per cm	1.8×10^{-5}
Volume Resistivity at 20°C, Microhm-cm	56.8
Volume Conductivity at 20°C, (Copper-100 Pct), Pct	3.04
Volume Resistivity of Liquid at 46.1°C, Microhm-cm	28.4
Magnetic Susceptibility at 18°C, Cgs units	0.24×10^{-6}
Reflectivity — 4360 A, Pct	75.6
5890 A, Pct	71.3
Electrochemical Equivalents — Ga^{+++}, Mg per coulomb	0.24083
G per amp-hr	0.86698
Lb per 1000 amp-hr	1.91137
Viscosity — 77°C, Dyne-sec per sq cm	0.01612
1100°C, Dyne-sec per sq cm	0.00578

lack of availability of quartz glass tubing in the required bores and OD sizes. It is understood that some thermometers have been produced but the cost has been exceedingly high and the results far from satisfactory.

The use of gallium as a backing material for optical mirrors has been suggested, as it reflects a high percentage of the incident light.[5] For certain purposes in atomic and astrophysical spectrum research work the gallium lamp has proved quite useful. The Bureau of Standards reported satisfactory service from quartz vacuum lamps using Ga-Zn and Ga-Cd mixtures to replace mercury.

The Atomic Energy Commission has investigated gallium as a possible heat-exchange medium.[6] Its favorable thermal characteristics, particularly the long liquid range and low vapor pressure, encourage consideration of its use in extracting heat from a high level, since any atomic energy power plant must use temperatures considerably above those of conventional steam-power plants if even a small part of the potential energy is to be utilized. However, gallium's considerable reactivity as expressed in terms of attack on possible container materials thus far has delayed its application in this field.

The addition of a small percentage of gallium oxide to relatively high grade uranium-base material in the form of the oxide, and subsequent fractional distillation in the dc arc, has made it possible to determine 33 volatile impurity elements at concentrations as low as a fraction of a part per million.[7] This procedure is said to have been employed by the Manhattan Project for control and inspection in the production of high-purity uranium metal, oxides, and salts.

One principal use of gallium reported by the Germans is in organic synthesis.[8] Its chloride salts act as catalysts in the Friedel-Crafts reaction. In some cases a smaller amount of catalyst is required than when other chloride salts are used; in other cases a higher yield is obtained or the reaction time is shortened.

Low-melting point alloys are formed by gallium with indium, tin, and aluminum,[9] and may find use in fire alarm systems. The addition of 2 to 4 pct gallium improves the mechanical properties of aluminum. Gallium increases the hardness of aluminum ternary alloys. An iron alloy containing 3 pct gallium and 14 pct nickel resembles beryllium and titanium steels in hardenability. The addition of 4.5 pct gallium will harden magnesium on heat treating. Gallium also may find a place in electrical contact alloys.

Prior to 1932 gallium was available only in small quantities for laboratory research purposes at about $250 per g. In 1932 the Chemical Manufacturers' Assn. of Leopoldshall (Germany) began to recover gallium from the residue from the Mansfeld copper schists. By 1937, the annual production had risen to about 50 kg and the price had dropped to about $2.50 per g.[5] Directly prior to World War II, German production was about 300 lb per year.[6]

During the period 1943 to 1945, the Anaconda Copper Mining Co. in connection with its recovery of indium, produced several thousand grams of gallium but have reported no output since then.[10] The price is said to have been about $3 per g. In 1946, The Eagle-Picher Co. was the only producer. In 1947, Aluminum Co. of America entered the field[11] and in 1948 the Saratoga Laboratories, Inc., started production.[6] In 1948 the price for 99.9 pct gallium metal was $2.50 to $5.00 per g or $1135 to $2270 per lb, and U. S. production was estimated to have been about 200 lb.[11] Actual shipments probably did not exceed 100 lb. Since 1946, a license has been required for the export of the metal.

References

[1] Mary Elvira Weeks: *The Discovery of the Elements* (1934). 217. Easton, Pa. Mack Printing Co.

[2] L. H. Ahrens: Occurrence of the Elements. *South African Journal of Science*, XLI, 152-160 (1945).

[3] F. G. McCutcheon: Private communication.

W. F. Hildebrand and J. A. Scherrer: Recovery of Gallium from Spelter in the United States. *Journal of Ind. & Eng. Chem.*, **8**, 225 (1916).

[4] Richard N. Lyon et al: *Liquid Metals Handbook* (1950). U. S. Government Printing Office.

[5] Erich Einecke: *Das Gallium* (1937). 127. Verlag von Leopold Voss.

[6] U. S. Bureau of Mines: *Minerals Yearbook* (1948). p. 1331-1332.

[7] Bourdon F. Scribner and Harold R. Mullin: Carrier-Distillation Method for the Spectrographic Analysis and its Application to the Analysis of Uranium-Base Materials. *Journal of Research of the National Bureau of Standards*, **37**, 379-339 (1946).

[8] Ulich, H., and G. Heyne: *Z. Electrochem.* **41**, 509-14 (1935) [CA, 29: 7768-9].

Ulich, H.: *Die Chemie* 55, 37-8 (1942) [CA, 37: 2521-6].

Ulich, H., A. Keutmann and A. Geierhaas: *Z. Electrochem.* **49**, 292-6 (1943) [CA, 37: 6650-7].

Ulich, H.: *Oel u. Kohle in Gemeinschaft mit Brennstoff-Chem.* 39, 523-7 (1943). [CA, 38: 958-4].

[9] Argonne National Laboratory Report: ANL-4109. *Properties of Gallium* (1948), 1-10.

[10] Horace C. Dudley: *The Biological Significance of Radiogallium* (Ga^{72}), (1949). Naval Medical Research Institute, National Naval Medical Center, Bethesda, Md. Project NM o11 013.

[11] U. S. Bureau of Mines: *Minerals Yearbook* (1947), p. 1258.

Diffusion Phenomena Occurring During Sintering

by Ben H. Alexander

THE process of sintering of copper was previously investigated by measuring the change in size and shape of the interstices between fine wires that were closely wound on a spool. These studies are being extended to compacts made from two dissimilar metals. The compacts are made by winding wires of the two metals on a spool at the same time. In such compacts, all possible junctions (A-A, B-B, and A-B) are present although the junctions of dissimilar metals (A-B) are present in the greatest number. The systems being studied are: Ag-Cu, Cu-Ni, Ag-Au, Cu-Fe, Cu-Zn, Ag-Ni, Cu-W, Ag-Zn, and Au-Ni. They were chosen to give a wide range of mutual solubilities and consequently greatly differing amounts of diffusion upon sintering.

After heating the specimens for various periods of time at high temperatures, the progress of sintering and of homogenization are being studied, and dimensional and geometric changes resulting from diffusion are measured.

BEN H. ALEXANDER is Section Head in the Metallurgy Dept., Sylvania Electric Products Inc., Bayside, L. I.

It has been found that although a perfectly uniform bond or *neck* is formed between two wires of the same metal, this is not true when the adjacent wires are dissimilar. In the latter case the bond appears to form by the preferential movement of one kind of atom, with the result that the bond or neck is asymmetric, i.e., it is wider on one side than the other. An overall increase in volume of the compacts accompanies this peculiar bond formation, the expansion being greater, the more asymmetric the bond. An attempt is being made to correlate the volume changes, which are considerable in some cases (15 to 20 pct), with the extent of diffusion or homogenization. The present type of specimen should make this correlation easier than with the more familiar *Kirkendall* specimen where the volume changes are greatly restricted.

It has further been found that the rate at which a bond or neck forms between two unlike metals is about equal to the faster of the rates of bond formation between the metals in like pairs.

Age Hardening

by L. F. Mondolfo

AGE hardening in several alloy systems is being investigated at present by hardness and electrolytic potential measurements. X-ray diffraction and resistivity measurements are to be started in the near future. The alloys investigated so far are: AlCu, 4 pct Cu; AlAg, 25 pct Ag; AlCuMg, 4 pct Cu, 1.7 pct Mg; AlZnMg, 6 pct Zn, 2 pct Mg; MgAl, 9 pct Al; and CuBe, 2 pct Be. Other alloys are in preparation.

The results indicate the following tentative conclusions: There are at least two types of age hardening, depending on the complexity of the transformation required to form the lattice of the precipitate from the lattice of the solid solution. A simple transformation, as for example a body centered cubic precipitate forming from a face centered cubic solution, takes place in one step, and only one peak of hardness results. With more complex transformations, at least one intermediate lattice is formed and at least two peaks of hardness result. The first hardening results from the transformation from solid solution to intermediate lattice, and the second hardening from the intermediate lattice to stable precipitate, if there is only one intermediate lattice formed.

Hardening does not result from actual precipitation but from the straining of the lattice caused by segregation and atomic movement prior to the formation of the new phase. Completion of the transformation, by causing a more stable condition, results in softening.

L. F. MONDOLFO is Associate Professor, Dept. of Metallurgical Engineering, Illinois Institute of Technology, Technology Center, Chicago.

New Refractory Hung Arch

Reduces Furnace Failures

EVERY steel mill operator must get more and more production out of existing equipment. When a furnace is down for repairs, operations are curtailed with no possibility of recovering lost production. One of the primary causes of furnace shutdowns is suspended arch failures. Suspended arch failures are not entirely caused by expansion of the refractories themselves. The method of arch suspension failing to localize refractory expansion results in mechanical spalling.

To minimize arch failures, the arch must be sufficiently flexible in movement to overcome possible heating and twisting of steel supports, and casting warpage, and to absorb and localize refractory expansion. To minimize replacement time, and, because of the ever-increasing shortage of experienced masons, repairs must be made with the fewest number of men and manhours.

Several years ago, the George P. Reintjes Co., Kansas City, Mo., started to sell arches to the steel industry. Considerable time was spent studying arch requirements of open hearth, soaking pit, and many other types of steel mill furnaces. As a result, Reintjes developed a refractory pendulum hung suspended arch which incorporated all of the desirable features which the steel mill engineers and operators wanted.

This arch was so flexible that it could be attached to the existing steel framework of most any furnace with practically no structural changes even though the framework was warped or twisted to such an extent that it could no longer support the arch for which it was originally designed.

On one of the first installations, this double hung arch was put to a crucial test. The pit cover was dropped off the jacks as it was being lowered into position. In dropping, the frame was twisted, leaving one corner 4 in. lower than the opposite corner, yet not a single refractory or casting was damaged in any way. The pit was under fire within two days after the accident. For the four pit covers, each having approximately 250 sq ft of arch, the total erection mason labor required per pit was less than 20 hr. The erection of the arch is shown in Fig. 1, which also shows how the U-bolts supporting the tubing extend through the lower flange of the overhead beams. If the beams become warped or sag in service, the arch can be re-aligned simply by turning a nut. The secret of the low erection cost lies not only in the pendulum hung action, but also because the horizontal "S" locks the tiles in position, requiring no straight edges or bracing to align the arch.

Tests were conducted to determine the strengths of the upper and lower tiles. The breaking point for the lower and upper tiles, both 3 in. wide, was 675 lb, the equivalent of 2700 lb per lineal ft of arch. In some tests, the breaking point per unit was over 900 lb.

Fig. 1. When a tile is dropped in place, it is automatically aligned.

Crusher Plates

For Diamonds

by R. S. Young

A LARGE proportion of the world's output of industrial diamonds is sold to users in the form of crushed boart. The term *boart* is applied to the dull gray, green, or yellow diamonds found in many fields. Frequently they have an opaque coating and sometimes have twin structures, slip planes, or corrugated skin. The dark color and inclusions in these diamonds make them unsuitable for gem purposes, and their imperfect and weak crystal structure usually renders them unfit for wire drawing dies, wheel dressers, and lathe tools. Boart, the lowest-priced category of industrial diamonds, is chiefly employed in drill bits and grinding wheels, where its unique hardness and abrasion resistance have resulted in widespread use.

Boart is received at the sorting offices of the distributing organization serving the leading industrial diamond producers in sizes ranging from 1 to 40 mm diam. It is crushed to pass through a Tyler No. 7 mesh sieve, which has an opening about 2.8 mm. A laboratory-type jaw crusher, similar to those used for ore samples, and a roll crusher, are employed. Since the object in crushing is to leave the diamond particles in the largest size possible, below 7 mesh, jaw crushing is the major operation. The use of the roll crusher, with hardened steel rolls, may be considered a secondary procedure applicable only to those diamonds whose shape has allowed them to pass through the jaw crusher without sufficient reduction.

The jaw crusher plates have to withstand the impact and abrasion of diamond. The usual type of unalloyed white cast iron jaw plates wore away so rapidly that they had to be replaced after crushing only 50,000 carats in some cases. In addition, the quantity of abraded iron that had to be separated with a magnet from the diamond powder made this operation tedious. Manganese steel jaw plates, having about 13 pct manganese, gave a vastly increased life, crushing about 900,000 carats before replacement was required. Manganese steel, however, is nonmagetic and since the small quantity of abraded steel could not be removed from the boart with a magnet, allowance had to be made for this by giving the purchaser a slightly higher caratage than ordered.

About a year ago, on the recommendation of the Diamond Research Laboratory, the abrasion-resistant nickel-chromium white cast iron known as Ni-Hard was employed for these jaw plates. The Type I or regular type of Ni-Hard with the following nominal composition was employed: 3.25 pct C, 0.50 pct Si, 0.50 pct Mn, 0.1 pct S, 0.3 pct P, 4.25 pct Ni, and 1.75 pct Cr. The Ni-Hard plates were chill cast, and were stress relieved by drawing at 400°F for 4 hr.

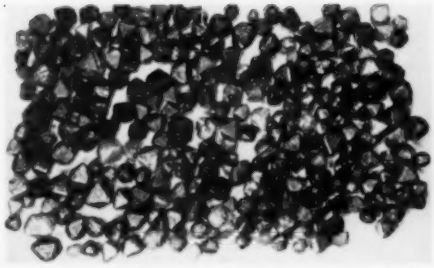

Crown jewels of industry—Industrial diamonds that must be crushed for grinding wheels, drill bits, and other diamond tools.

The results have been satisfactory. Life has been slightly better than that of manganese steel, the Ni-Hard plates crushing about 1,000,000 carats before replacement is necessary. Since Ni-Hard is less expensive than manganese steel, the replacement cost is considerably lower. A far greater advantage, however, is that the small quantity of abraded Ni-Hard can be removed from the boart by magnetic separation.

This is the severest condition of operation in the world for jaw crusher plates. The terrific impact and abrasive forces encountered in diamond crushing may be visualized when it is recalled that the quantity of 1,000,000 carats crushed in the life of such an abrasion-resistant material as a Ni-Hard jaw plate is only about 440 lb. This weight would represent, for the ordinary type of mine or smelter product, 100 to 150 samples.

R. S. YOUNG is Director of Research at Diamond Research Laboratory, Industrial Distributors (1946) Ltd., Johannesburg, South Africa.

Recent Developments In

Fluxes for Welding

by William M. Conn

PLATES to be joined by automatic submerged arc welding are clamped together or tacked along the seam to be welded. The welding zone is blanketed by granular flux. A bare wire electrode is inserted into the flux and an arc struck between the electrode and the plates. The electrode is automatically or manually moved along the seam to be welded. Metal from the electrode is deposited due to the heat of the electric arc, which also fuses the plates sufficiently to secure, upon cooling, a strong bond between the plates.

Desirable properties of a flux to be used in arc welding were summarized by several writers.[1] The most important considerations according to research and development work during the past decade are:

1—Flux, and slag formed from it, should shield the weld metal during the entire range of liquidization and solidification, preventing the oxidation and nitration of the metal in liquid and semi-liquid form.

2—The ignition and re-ignition of the electric arc should be facilitated and the arc should be stabilized.

3—Sputtering of metallic particles should be avoided.

4—The depletion of the metal because of the heat of the electric arc should be compensated for by replacing ingredients lost.

5—Alloying metals, such as manganese, titanium, molybdenum, and vanadium can be supplied through the flux if desired.

6—Viscosity, surface tension, and wettability of metal and flux while in molten condition should be controlled.

7—Gas developed from the molten metal and impurities because of oil, mill scale, rust, etc. on the plates should be taken up or should pass through the slag, making it possible to weld rusty or wet plates.

8—The flux and slag should rise quickly to the surface of the molten pool avoiding nonmetallic inclusions in the weld.

9—No fumes should be developed during welding which may annoy or endanger the operator.

10—The slag forming a continuous blanket over the freshly deposited weld metal should prevent rapid cooling.

11—The slag should be easily removable or automatically peel off the weld after cooling.

Three principal groups of flux have been developed for submerged-arc welding. They are based on the use of raw (natural) clay, glass, and mullite (aluminum silicate, $Al_2Si_2O_{13}$). Many additional suggestions may be found in the patent literature, but few results have been made known so far.

The basic patent for production of fluxes using ground raw clay with addition of chemicals was issued to Robinoff, Paine and Quillen.[2] The composition of the flux was not specified in detail, the only requirement being that it should contain iron oxide. The flux is placed on the seam and a bare electrode is projected through the flux. An arc is started under the flux, and welding takes place below the deep bed of flux. The composition of such a flux is mentioned by Jones, Kennedy and Rotermund[3] and presented in Table I. The most important ingredients are raw clay, lime, and ferromanganese. They are mixed and used with no additional processing. Large amounts of gas and vapor are given off in welding when the intense heat of the electric arc acts on the raw materials, such as on the clay which contains both physically and chemically bound water. The ingredients have the tendency to separate or settle because of the difference in specific weights.

The most widely used flux, made of granulated glass, basically is described in the patents of Jones, Kennedy and Rotermund and the Linde Air Products Co.[4] The flux is processed by heating to complete chemical reactions between the components before using it on the welding machine. A typical composition of this type of flux is shown in Table I. The most important ingredients are silica sand and compounds

DR. WILLIAM M. CONN is associated with Rockhurst College, Kansas City, Mo.

of calcium and magnesium, for example, lime and magnesite. In processing, they form a calcium-magnesium metasilicate. The flux ingredients are mixed and heated to the melting point, in order to obtain a homogeneous product and avoid the difficulty of separation. Melting is carried out in a glass tank furnace using gas or oil for attaining the high temperatures required. Various types of electric arc furnaces also are being used in melting. The fusing temperature ranges from 2400° to 2700°F; and melting time is 5 to 6 hr.

After melting and refining, the melt is cooled quickly by pouring it from the furnace on a cold surface. A glass is formed upon rapid cooling, which is ground and screened to the desired size. About 6 pct of a fluorine containing material such as fluorspar, is added to the batch before or after its removal from the furnace.

The use of natural or synthetic mullite as a basic material for welding fluxes is disclosed in the patent of Cohn.[4] The composition of a typical flux containing mullite is presented in Table I. The principal source of raw material is clay which is changed into mullite by heating. Suitable clays are found in many parts of the United States and abroad. Upon heating, the structure of clay changes and all materials that might produce vapor and gas during welding are removed. New compounds are formed, the most important one being mullite, which contains 72 pct alumina and 28 pct silica, melting at about 3320°F. The formation of mullite is desirable because of its hardness, low coefficient of thermal expansion, and high resistance to slag attack and abrasion. The entire batch of materials that will form the flux is heated to the desired temperature, or the clay is heated separately to produce mullite.

The clay (or clay plus mullite) is mixed with the ingredients shown in Table I. By adjusting the composition of the flux it may be adapted readily to the particular purpose for which it is to be used. For instance, an increase in the amount of manganese in the batch will result in a lower firing temperature for the flux and in a lower melting point for part of the flux, making it possible to weld at higher speed. On the other hand, a high melting point is often advantageous for heavy plate welding. If the same flux is to be used for both heavy and light plate, an intermediate composition is preferable.

Two methods are used in preparing ceramic flux, the dry method and the wet method. In the dry method, the ingredients are mixed and, if necessary, ground. The batch is then removed from the mixer or mixer-grinder and placed into containers made of clay, such as saggers used in firing various ceramic products. The saggers with the batch are placed into a ceramic kiln which may be of the down-draft type or a tunnel kiln. The firing temperature of the flux of Table I is 1900°F, and the total time for heating the flux, maintaining it at a high temperature, and cooling it amounts to about five days. The firing temperature is high enough to remove volatile components and to obtain the formation of mullite. The firing temperature is, however, far below the melting range of mullite. Firing of flux and other ceramic products depends both on temperature and time. Heating the material to a high temperature for a short period of time will produce the same result as heating the material to a lower temperature for a longer period of time. After cooling, the fired flux is ground, screened, and shipped.

In the wet method of preparing ceramic flux, water is added to the batch after mixing and grinding. The batch contains only a small amount of fluorine containing material, which acts as a mineralizer in the formation of mullite. The batch passes through a wet pan and an extrusion machine, from which a column emerges which is cut into bricks or slabs. The bricks are dried and fired similar to the saggers in the dry method, and then crushed and screened. The remainder of fluorine containing material is preferably added after crushing the flux.

Table I. Composition of Fluxes Used in Submerged-Arc Welding

Component	Raw Clay Flux, Pct	Glass Flux, Pct	Mullite Flux, Pct
SiO_2	55.6	49.5	22.7
Al_2O_3	20.9	3.9	58.1
CaO	5.5	33.4	4.5
MgO	—	10.4	5.2
MnO	8.5	—	4.8
Fe_2O_3	9.5	0.1	0.8
TiO_2	—	—	1.4
F_2	—	2.7	2.5

The methods of manufacturing ceramic flux are quite similar to standard methods used in the production of many ceramic products including brick, fire brick, pottery and terracotta. The raw materials of the flux are quite inexpensive, since clay is the main ingredient of the flux. The raw materials cost approximately 1.15c per lb for an Eastern or Middle Western plant, to which must be added 1.05c per lb for processing, amortization and license fees, computed on a conservative basis. Companies using large amounts of flux for welding steel should find it economically desirable to produce flux at their own plant or in a ceramic plant in their vicinity.

The flux consisting of raw clay and chemicals is used very little today. Advantages of the ceramic flux in comparison to the glass flux are: Ceramic flux permits the use of higher voltages in welding; the linear footage of welding per pound of flux is increased because of its lower density; the composition of the slag and its low viscosity in a molten condition permit the passage of large amounts of gas and vapor, thus making it possible to weld, without further preparation, steel that is rusty or moist.

Acknowledgment

Acknowledgment is made to the Pacific Flux Co., El Cerrito, Cal. for permission to publish this paper, based on research and development work extending over many years, and to the assistants, industrial firms, and Government agencies that helped in various phases of this work. Special mention must be made of L. W. Delhi, under whose leadership and guidance all modern fluxes in the field of submerged arc welding have come into being.

Bibliography

[1] P. Schimpke and H. A. Horn: *Praktisches Handbuch der Gesamten Schweisstechnik*, Vol. II, 2nd ed., Springer, Berlin, 1935. W. Spraragen and G. E. Claussen: Coatings and Fluxes in the Welding of Steel. *Journal American Welding Society Suppl.* **18**, 153-165, 1939. W. M. Cohn: Review of Fluxes Used for Automatic Arc Welding. *Welding Engineer* **25**, 17-19, 1940.

[2] B. S. Robinoff, S. E. Paine and W. E. Quillen: *U. S. Patent* 1,782,316; 1930.

[3] L. T. Jones, H. E. Kennedy and M. A. Rotermund: *U. S. Patent* 2,043,960; 1936. Linde Air Products Co.: *German Patent* 744,155; 1944.

[4] W. M. Cohn: *U. S. Patent* 2,258,675; 1941.

Electric Furnace Roof Refractories

by T. A. Blackwell

SINCE the electric arc furnace supplanted the old crucible process for tool steel production, furnace construction and design has gone through many changes, until today the majority of these furnaces are 3-phase circular furnaces with capacities ranging from 1 ton to 100 tons.

Any refractory used in roof construction is to confine heat, but also it must withstand stresses, slagging, thermal shock, and disintegration. Therefore, roofs have been made up of many different types, shapes, and sizes of refractories. Throughout all these trials, regular silica brick was the most popular and economical refractory for general roof applications. With latest advances in steelmaking, such as the use of oxygen and the attainment of very high temperatures, considerable experimental work is being done with the more refractory types of brick, such as sillimanite.

A number of years ago when Atlas was operating only 5 ton and 10 ton furnaces, block shape silica brick was used for roof construction. Since installing the 35 and 50 ton furnaces, all roofs have been constructed with 9 in. or 12 in. straights, side arches, and wedges. The regular use of the block shape brick was discontinued after the installation of the larger furnaces, primarily because of the spalling on the larger sizes.

At the present time all roofs are constructed in the same manner for all furnace sizes. First, an expansion strip of corrugated paper $\frac{1}{8}$ in. thick is placed next to the water-cooled ring. Then two courses of Hi-Duty fire brick are installed, and the balance is made up of 9 in. silica straights, side arches, and wedges, with a $13\frac{1}{2}$ in. brick for the electrode rings. A transverse expansion allowance of 1/16 in. per ft and a circumferential expansion of $\frac{1}{8}$ in. per ft have been found to be most desirable for continuous furnace operation. This expansion allowance is made by using combustion expansion strips of corrugated paper. This corrugated paper is placed transversely at every tenth brick and circumferentially between every third course. All bricks except those at the expansion joints are laid after dipping in a silica cement.

The brick forming the first course next to the electrode ring brick are laid with a buttered joint using the same silica cement. No expansion joints are made in the center section. Around the $13\frac{1}{2}$ in. brick at the electrode opening, a circular steel band approximately $1\frac{1}{2}$ in. wide x $\frac{1}{4}$ in. thick is used. When tightened slightly by bolts the band forms a clamp to provide added support to the electrode ring brick. Before using these circular steel bands, trouble was encountered with complete rings dropping into the furnace. This was believed to be caused by the water-cooled electrode coolers sliding back and forth on top of these ring brick when furnace was being tilted. During this time, full average life on the rest of the roof was being obtained, but sometimes it was necessary to install one or two sets of rings. Since using these steel bands, the problem of rings dropping into the furnace has been eliminated, but more spalling of the ring brick on the hot face has been encountered. This, it is felt, is caused by the clamp forcing the brick slightly apart at the hot face. Therefore, while this problem is not nearly as serious, it is necessary sometimes to install an extra ring during the life of the roof because of this spalling. After the roofs are built, they are placed on a drying floor, which consists of a low temperature electrical heating element installed in the floor at roof center. Another drying floor consisting of steam pipes laid under steel plates is also available.

With present construction, using 9 in. silica brick and using the ring clamps, roof life is believed quite good. At the present time, life is 80 heats on the 50-ton furnaces, 70 heats on the 35-ton furnaces, and 50 heats on the 10-ton furnace. This difference in average roof life on the various size furnaces can be explained mainly by the different grades of steel melted and melting methods used. All the tonnage grades with short refining periods are melted in the 50 ton furnaces; grades such as bearing steels, high carbon-high alloy tool steels; some stainless grades are melted in the 35 ton furnaces; and all stainless and valve steels are melted in the 10 ton furnace. Another reason for the lower life on the 10 ton furnace roofs is that this furnace is a top-charge furnace, with sharp temperature gradients.

In 1944 and 1945, two mullite roofs were installed on the 10 ton furnace, used for melting stainless, high speed, and regular tool steels. Roof life was 59 and 82 heats with these roofs.

In 1946, while running with intermittent operation on this same furnace, the mullite roof was tried with this method of operation. Four roofs were tried and life was 63, 84, 71, and 48 heats. This last roof with only 48 heats suffered an accident.

The average life of the first five roofs (disregarding the last 48-heat roof) was 72 heats. This was only $2\frac{1}{2}$ times better than with the silica roof, and consequently further use was discontinued.

Regarding the use of mullite roofs the following observations were made: 1—Each roof failed because it burned out above the tap hole. 2—Spalling was negligible, i.e., there was practically no spalling visible. 3—The roofs did not appear subject to thermal shock. 4—There was no dripping of the roof, i.e., no icicles formed. 5—Roof changes are saved, but with intermittent operation, roof changes were no problem. 6—It must be considered that furnace roofs are subject to accidents and this is a definite disadvantage with mullite roofs where so much extra cost is involved.

Sufficient super-duty silica brick has been received to try four or five complete roofs, using exactly the same size and shape brick and the same method of construction. The first roof has been just built, so that no figures are yet available. If this is not found economical, it is proposed to try the main roof constructed of the regular silica brick with only the electrode ring brick being of the super-duty type. When these experiments are completed, rammed monolithic center sections and roofs will be tried.

T. A. BLACKWELL is associated with Atlas Steels, Ltd., Welland, Ont., Canada. This article was presented at the Electric Furnace Steel Conference, Pittsburgh, Dec. 7 to 9, 1950.

Observations on Rimming Steel Ingots

by A. Hultgren, G. Phragmen, S. Wohlfahrt and J. E. Ostberg

Detailed study was made of a number of rimming ingots, both low and high carbon, and especially upon effects of superimposed air pressure. Requirement to suppress core bubbles is between 10 and 15 atm; at 6.5 atm freezing was in semikilled manner and at 3 atm, steel was of rising type. Probable mechanism of freezing under various conditions is discussed.

AN earlier paper[1] reported an investigation made by a committee for studying rimming steel ingots appointed by Jernkontorets in Stockholm. The present paper is the outcome of some further work done by the same committee.

Since the characteristics of ordinary rimming steel are connected closely with the amount of gas liberated during freezing and since this amount of gas is governed by the pressure, it was considered of interest to ascertain in what manner and to what extent definite pressures applied to the top of the liquid steel in the mold would affect the solidification process and the consequent structure of a rimming steel of ordinary composition.

The experiments were made at the Domnarfvets Steel Works. The steel was made according to normal practice in a 4-ton Rennerfelt electric furnace. Ferromanganese was added in the furnace; no aluminum was added, with one exception. Analyses of the four heats are given in Table I.

The top-poured ingots measured about 12 in. sq x 48 in. and weighed about 1300 lb. One or two ingots of each heat were allowed to solidify under pressure, using a special device for admitting compressed air to the upper closed part of the mold, as shown in Fig. 1. A heavy plate sealed with asbestos was bolted to the top of the mold. The plate had a tapered aperture for pouring. Immediately after pouring the hole was closed by a wedged plug, and compressed air was admitted through a hole in the plug. Because of some delay in applying the plug, full pressure was not reached immediately. The pressure was adjusted to the desired value as indicated by a manometer. In order that the interior of the ingot might have the benefit of the pressure, the freezing of the top crust was delayed by a refractory lining applied to the top part of the mold, Fig. 1. Ingots were also cast from each heat without applied pressure, and with and without refractory lining at the top.

Axial sections of ingots were cut either of the whole ingot or of some part of it of special interest; sections were polished and usually etched.[1]

To facilitate description of structures the following terms may be used for different types of ingots solidified under gas evolution:

1. *Box-hat* or *boot-leg* ingot: Abundant gas evolution during casting and during rimming; no rim holes.

2. *Normal rimming* ingot: Lively gas evolution during rimming; usually rim holes in lowest part of

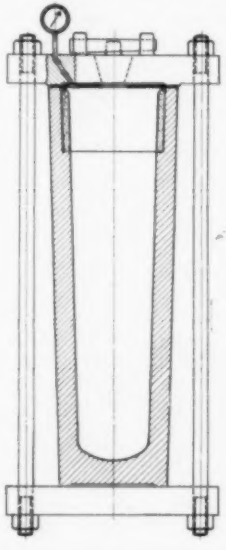

Fig. 1—This test mold shows the arrangement for freezing under pressure. To insure the benefit of pressure to the interior of the ingot, freezing of the top crust is delayed by a refractory lining at the top of the mold.

A. HULTGREN, Member AIME, is Professor of Metallography, K. Tekniska Hogskolan, Valhallavagen, Stockholm, Sweden; G. PHRAGMEN, deceased, was Director, Metallographic Institute; S. WOHLFAHRT is Managing Director, Domnarfvet Steel Works, Domnarvet; and J. E. OSTBERG is Metallurgist, Surahammar Steel Works, Surahammar.

Discussion of this paper, TP 3008C, may be sent (2 copies) to AIME by April 1, 1951. Manuscript received Sept. 26, 1950. St. Louis Meeting, February 1951.

This paper is a somewhat revised translation of a report that appeared in Swedish in "Jernkontorets Annaler" (1950).

This page of Metals Transactions AIME is a continuation from p. 64. The missing pages appeared in Journal of Metals.

Corrections: January 1951 issue Transactions: Vol. 189 should read Vol. 191. Index 1950 Transactions, Vol. 186 should read Vol. 188.

Fig. 2 (below)—Section of Ingot 7521-5. Without lines and no pressure.

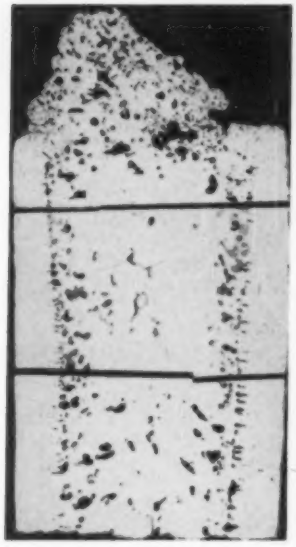

Fig. 3 (right)—Sections of Ingot 7521-3. With lines and no pressure.

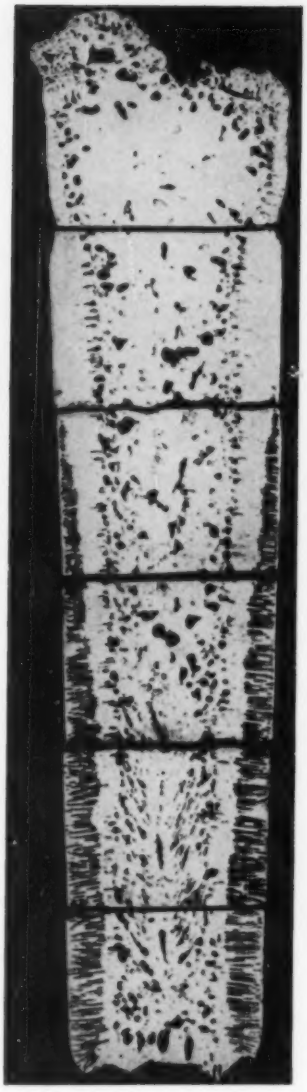

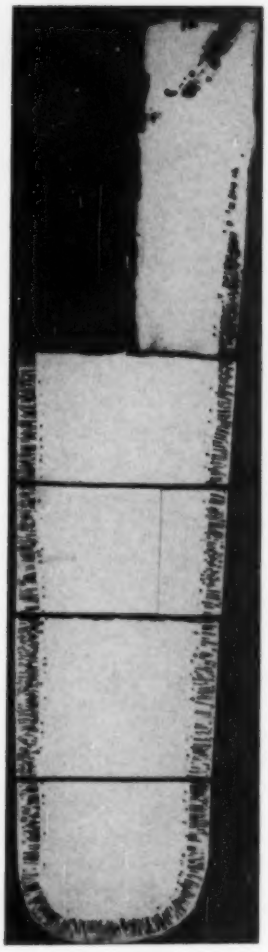

Fig. 4—Distribution of blowholes in Ingot 7521-4. Applied pressure upon completion of casting was 15 atm.

ingot, the volume of which roughly balances shrinkage during solidification of rim zone, with the result that the top surface retains about the same level during rimming.

3. *Rising* ingot: Moderate gas evolution during rimming period causing rim holes to form along more than half the ingot, their total volume exceeding shrinkage in this period and thus causing the top surface to rise continuously.

4. *Semikilled* ingot: Slight gas evolution; the gas evolved remains wholly or largely as blowholes, usually oblong and located in upper half of ingot, where ferrostatic pressure is low enough for gas

Table I. Composition of Test Heats

Heat	Composition, Pct				
	C		Mn	P	S
	Killed Sample	Unkilled Sample			
J 7338	0.06		0.32	0.009	0.024
J 7521	0.12		0.48	0.013	0.027
J 7646	0.08		0.33	0.008	0.015
J 7699	0.07	0.10	0.24	0.010	0.028

Fig. 5 (left)—Etched section of top of Ingot 7521-4, not heat treated.

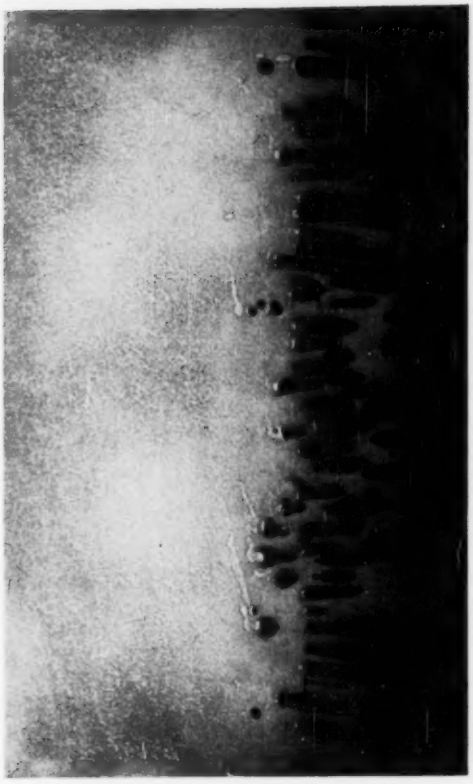

Fig. 6 (right)—Etched section of a heat-treated section of the middle portion of Ingot 7521-4.

liberation; when blowhole volume balances shrinkage no pipe cavity is formed.

Results

Heat J 7521: Ingot 7521-5, No pressure applied, no refractory lining, Fig. 2: Only the top 18 in. was sectioned. Rim holes are absent, which is normal. Rim channels are present after passing into small blowholes at the inner end. There is a large *cauliflower* or *nigger head* at the top.

Heat J 7521: Ingot 7521-3, No pressure applied, refractory top lining, Fig. 3: The structure indicates that the mold was filled to about 4 in. beyond the beginning of the lining. During rimming the level of the steel rose about 4 in. Later, liquid metal penetrated the top crust, forming a cauliflower.

Rim holes terminate only 10 in. below the lining; their length decreasing continuously from the bottom end upward. The inner part of the rim zone bordering on the intermediate blowholes is almost solid, like the uppermost part. The rising top level and the larger total rim-hole volume are obviously connected.

The core contains many blowholes, their volume being related to the volume of liquid steel that escaped through the top crust. In the lower third of the core, the core holes form pointed V patterns, to be explained as follows: After this part had reached a late stage of solidification and had developed numerous large blowholes, solidification proceeded further toward the top under pressure, causing the still deformable bottom aggregate to give way, its blowholes being compressed.

A few large vertical blowholes are also seen along the axis in the lower part. Their volume equals the sum of the shrinkage and the compression of the surrounding blowholes during the final freezing period. These central blowholes seem not to have been compressed, probably because the stiff metal aggregate at this late stage resists the higher pressure from above.

The gas pressure of a freezing steel is a function of the composition of the mother liquor from which gas is evolved. The cause of the vertical pressure gradient postulated probably was the fact that, through sedimentation of suspended crystals, the lower portion of the core at a given temperature during freezing contained less mother liquor than the upper portion and, in consequence, its final degree of segregation was less.

The fact that this ingot rose during rimming indicates that less gas was evolved in unit time than in ingot 7521-5 during this period, possibly because of retardation of freezing by the top lining.

Heat J 7521: Ingot 7521-4, applied pressure, 15 atm: Full pressure was reached 1 min-22 sec after the end of casting. Fig. 4 shows the distribution of blowholes and Fig. 5 the etched section of half the top portion, by oversight not annealed.* A columnar structure is faintly visible in the etched surface. This is not the primary structure but the austenite structure formed during cooling. (The true primary structure of a section taken about half height is seen in

* Usually, in order to obliterate the traces of secondary (γ transformation) structure, the sections were heat treated by heating to about 1000°C, water quenching, and tempering several hours at 700°C.

Fig. 7—Section of the top of Ingot 7521-2, not heat treated. Columnar secondary structure was observable in the original. Applied pressure was 10 atm.

Fig. 6; this section was heat treated.) In Fig. 5 is seen a lower set of wide rim holes beginning near the surface and ending about 1 in. beneath it.

These rim-holes had begun to form before pressure was applied and afterwards continued to grow until the total pressure reached was sufficient to suppress gas evolution. Farther upward a short set of blowholes appears beginning about 0.6 in. beneath the surface. The solid 0.6 in. surface layer is of the type common in the upper part of rimmed ingots; it indicates ample gas evolution. With the exception of the blowholes described, the ingot section is solid up to the funnel-shaped porous region at the top, Figs. 4 and 5, probably formed by the top crust, as shrinkage proceeded, being forced downward like a cork in a bottle.

The primary structure displayed in Fig. 6 enables a detailed study of the mode of freezing. The rim holes show the well-known alternate constrictions and expansions. Their inner end is flattened and terminated by a "segregation button." Each blowhole temporarily reached farther inward and, owing to the rising pressure, a portion of a partly frozen mass was pressed into it and some mother liquor was squeezed out, forming the button.

In a zone farther inward, occasional extensions of rim holes occur as well as separate rounded blowholes, without visible connection with the rim holes. The latter also are flattened at their inner ends and have a button segregate. In addition, a steeply sloping string of segregate is often attached to such a blowhole. The latter blowholes probably formed under rising pressure in the following way: During the rimming period a great many gas bubbles detach and rise. By the resulting rapid upward movement of the liquid metal, the mother liquor at the solidification front is largely removed and mixed with the main mass of the liquid. In other words, the liquid metal into which the crystals grow is relatively little segregated. As the pressure rises, gas evolution stops, hence movement of the liquid also. During subsequent freezing in quiet liquid two simultaneous changes occur: (1) pressure rises continuously, and (2) the mother liquor at the front is rapidly enriched in alloying elements, including carbon and oxygen. Gas evolution is suppressed by 1 and promoted by 2. When the effect of 1 predominates the growth of the rim holes is stopped; their inner ends are compressed; and depressions form in the solidification front opposite the blowholes. If, however, 2 overtakes 1, owing to the slow rise of pressure, new blowholes appear, preferably in the depressions where enrichment is greater. If such blowholes are openly spaced and if they expand faster inward than the front grows, their inner ends lack support; hence they detach themselves and rise. Since, at this stage, the surrounding mass probably contains crystals, the bubble will rise slowly, displacing crystals which do not close up behind the bubble. The mother liquor in the wake of the rising bubble forms string segregate. Such steep string segregates were observed earlier in steel ingots insufficiently killed. Their absence in ordinary rimming-steel ingots is probably caused by the fact that

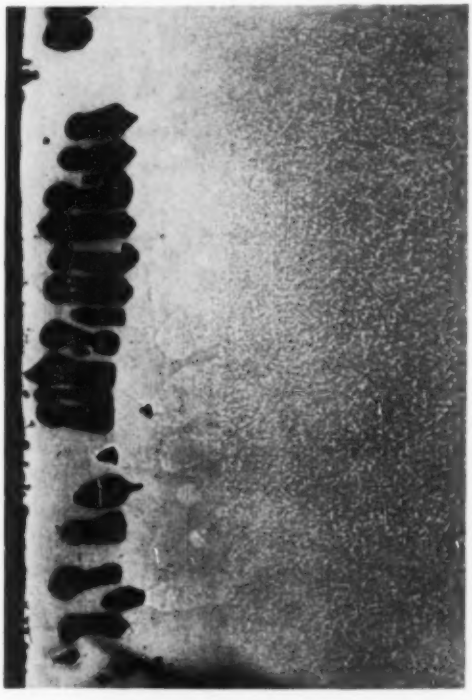

Fig. 8—Reverse side of section shown in Fig. 7 in the annealed condition.

rimming and movement in the liquid goes on to the stage at which the moving mass is sluggish enough to prevent the bubbles from rising.

Heat J 7521: Ingot 7521-2, applied pressure, 10 atm: Full pressure was reached 2 min-3 sec after casting was finished.

Fig. 7 shows the columnar secondary structure of the ingot top, not heat treated. The rim holes end 14 in. below the top insulation, consequently this ingot showed, like ingot 7521-4, greater rising tendency during rimming than ingot 7521-3, solidified without applied pressure in a mold with refractory top lining. Presumably the cap applied to the mold to some extent obstructed the reaction of the steel with the oxygen of the air, thus restricting gas evolution during rimming.

The central top area is more porous than in ingot 7521-4 (15 atm), a natural consequence of the lower applied pressure (10 atm); otherwise the interior of this ingot also is solid.

The rim holes end at a depth of about 0.6 in. beneath the ingot surface. Fig. 8 (annealed, back of section shown in Fig. 7) shows a fine dendritic primary structure extending to about 1 in. from the surface. The inner ends of the rim holes are flat or have a blunt shape. In the intermediate region farther inward are outlined extensions of the holes which have been filled and also freshly formed blowholes largely filled with a mass of coarser primary structure with continuous transition into the core structure. Up to about 3.5 in. from the surface, the core shows random dendritic patches; farther in the structure it is wholly globular. The dendritic intermediate zone indicates a scarcity of crystal nuclei in the liquid at the stage at which the rising pressure stopped gas evolution. The fact that the rim holes of this ingot are shorter than those of ingot 7521-4 is unexpected in view of the longer time for reaching full pressure.

Heat J 7699: Ingot 7699-A, applied pressure, 6.5 atm: Full pressure was reached after 57 sec.

Fig. 9 shows the blowhole distribution in the ingot. The external zone up to about 0.8 in., is free from blowholes but contains numerous rim channels; hence, there was more gas evolution in the early stage of freezing than in heat 7521. Inside this external zone, an intermediate zone extending to about 2 in. from the surface, shows numerous narrow blowholes, often interrupted. These were formed under rising pressure. The lower part of the core is practically solid but in the upper part are seen long narrow blowholes converging toward the center of freezing, typical of a semikilled steel ingot. In the middle portion along the axis, a set of fine cores is seen.

Freezing probably proceeded as follows: When the pressure was applied the top level sank about 8 in. The pressure was, however, insufficient for complete suppression of gas evolution. On continued freezing, therefore, the blowholes formed caused the top level to rise about 3.5 in. in 2 to 3 min. After full pressure was attained the top surface was frozen over, as judged from the thickness of the crust. At this moment the core material probably consisted of a great quantity of crystals and little mother liquor. For this reason the final stage of freezing was associated with a small amount of shrinkage and, in consequence, only small cores and few blowholes were formed. In the bottom portion, radial as well as vertical blowholes occur. The latter type of holes was seen also in ingot 7646-4 (below).

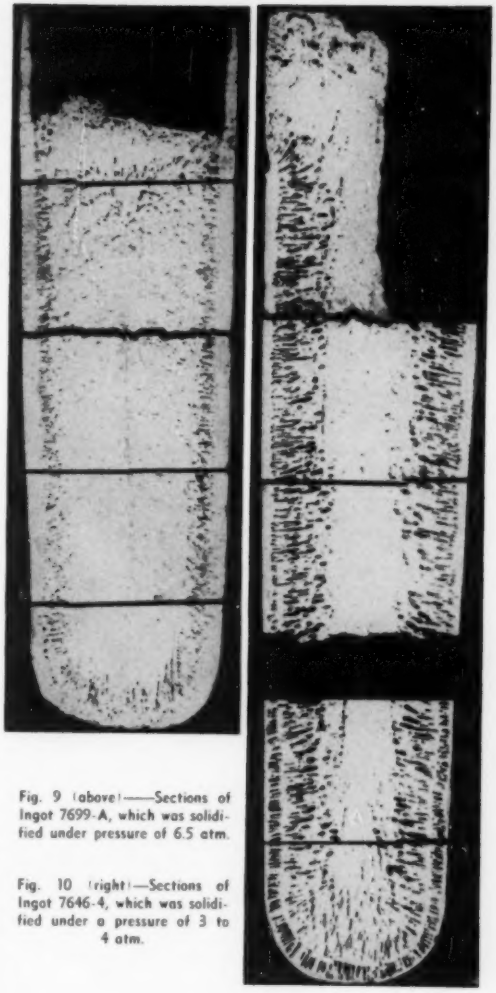

Fig. 9 (above)——Sections of Ingot 7699-A, which was solidified under pressure of 6.5 atm.

Fig. 10 (right)—Sections of Ingot 7646-4, which was solidified under a pressure of 3 to 4 atm.

Heat J 7646: Ingot 7646-4, applied pressure varying between 3 and 4 atm: About 2 oz per ton of aluminum was added to the ladle. Full pressure was reached 50 sec after end of casting.

Fig. 10 shows the blowhole distributions in the ingot. Freezing probably occurred as follows: Before pressure was applied, rim holes formed in the lower part of the ingot (blowhole zone I) reaching a maximum depth of 1 in. near the bottom. From the bottom toward half height the length of the rim holes gradually decreased to zero, their outer boundary moving inward and their inner boundary moving outward; the upper half of the rim zone is correspondingly nearly solid.

In the lower third of the ingot, blowhole zone I is succeeded by a solid intermediate zone about 0.4 in. thick, indicating that the sum of applied and ferrostatic pressures in this portion was sufficient for suppression of gas evolution at this degree of segregation.

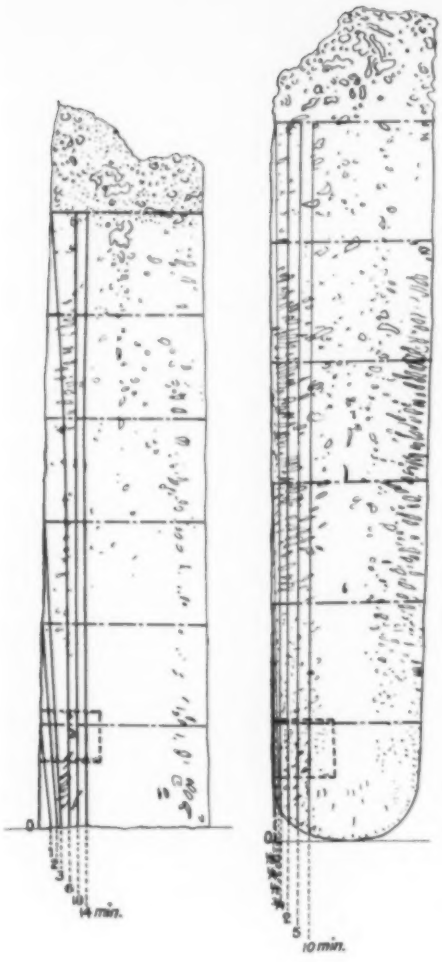

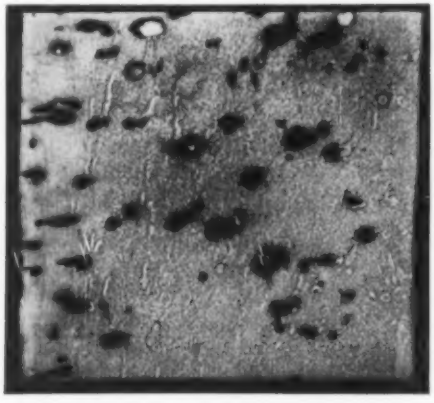

Fig. 11 (top left)—Blowhole distribution in high-carbon ingots, bottom and top poured, respectively, computed freezing-front positions are shown also.
a—left. b—right.

Fig. 12 (bottom left)—Section of the top-poured ingot at location indicated in Fig. 11b.

Proceeding inward, the next zone is characterized by numerous long blowholes in a direction deviating somewhat in an upward direction from the perpendicular to the surface (blowhole zone II). It is assumed that, through segregation, the mother liquor has passed the composition corresponding to gas saturation at the established total pressure. These blowholes are not regarded, therefore, as rim holes. In the upper half of the ingot the solid rim zone is followed directly by blowhole zone II. This zone is followed by a solid core of about one third the ingot width. At the boundary the blowholes are often flattened or bent upwards. Along the axis and in the top part some porosity may be seen.

The great volume of the blowholes in zone II has its counterpart in a top portion formed by rising during this stage of freezing, to the extent of 6.3 in. beyond the original level before the cap stopped it. The moment of capping then corresponds to cessation of blowhole formation.

In the bottom portion, and occasionally in upper portions also, roughly vertical, long blowholes and rows of such holes are found, mostly in zone II, but a few in the core also. Probably there has been enough gas evolution for the inner ends of some of the perpendicular blowholes to detach themselves ahead of the actual freezing front and to rise slowly, their movement being retarded by the sluggish consistency of the aggregate. In other words, the perpendicular growth of a blowhole indicates that it is adequately supported by the surrounding solidified steel. The fact that the rising gas bubbles were retained as blowholes and did not move to the top is, of course, a sign of a sluggish mass. The comparative solidity of the core region also results from the small amount of mother liquor in the aggregate when rising was checked.

Reviewing the results reported above for rimming steel solidified at different pressures, it is seen that under the conditions of the experiments, an applied pressure of 15 atm was sufficient to prevent all gas liberation as bubbles in the core of the ingot, while 10 atm was not quite sufficient. Disregarding the shielding effect of the top crust in later stages of freezing, the final composition of the mother liquor in these ingots seems to correspond to an applied pressure of 10 to 15 atm. It is of course possible that some supersaturation is required before gas is liberated, in which case the equilibrium pressure was still higher. Rimming steel subjected to such pressures behaves, of course, like a killed steel during freezing. At an applied pressure of 6.5 atm, the steel froze like a semikilled steel, and at 3 atm like a rising steel.

Rimming Steel with High Carbon Content

Since rimming steel with about 0.40 pct C is used to some extent in Sweden, three ingots of such material were examined, two made at Degerfors and one at the Surahammar works.

Ingots Made in Degerfors: One top and one bottom poured ingot were available from different basic open-hearth heats; compositions are given in Table II. The compositions were similar, with the exception of phosphorus which was considerably higher in the first ingot. Casting time was about 45 sec for the

Table II. Composition of High-Carbon Ingots

Heat	Composition, Pct					Casting Method
	C	Si	Mn	P	S	
M 3110	0.40		0.58	0.061	0.039	top-poured
M 3090	0.37		0.58	0.014	0.037	bottom-poured

top-poured, and about 6 min for the bottom-poured ingot.

Blowhole distribution in both ingots is shown in Fig. 11, which also gives freezing front positions for a series of intervals after casting commenced. These positions were calculated from the formula $D = 0.87\sqrt{t}$, where D is thickness in in., and t time in min. The top-poured ingot has more blowholes in the rim zone than has the bottom-poured one. Both show cauliflower tops.

Fig. 12 shows the primary structure of a selected part of the section of the top-poured ingot, its position being indicated in Fig. 11. Corresponding freezing front lines are plotted in Fig. 13. The skin portion (zone I), about 0.15 in. thick, shows numerous "blowhole seats" too small to be visible in reproduction. Next inward is zone II, extending to a depth of about 0.6 in., showing dendritic structure and containing some large blowholes but no blowhole seats. The next zone, III, also contains blowholes but has a globular primary structure. A reconstruction of the freezing sequence would be as follows: Zone I obviously is solid as a result of strong gas evolution, most bubbles being scrubbed off, leaving blowhole seats. Zone II formed under limited gas evolution—rising type—and zone III formed under increasing gas evolution with most of the gas moving away. Upward passage of the bubbles was retarded by projections in the freezing front and suspended small crystals. In this way the marked steep string segregates were formed. Blowhole segregates formed on compression of blowholes with each new gas bubble forming at a higher pressure than a preceding one nearer the surface.

The successive formation of three distinct zones can be explained if the variation in ferrostatic pressure during the rapid casting is considered. While zone I froze, the pressure was low and gas evolved freely. As the steel level rose and pressure with it, less and less gas was liberated (zone II). After casting was finished, and under the following period of stationary ferrostatic pressure, gas evolution increased as segregation mounted. This explanation appears to agree with the position of the freezing front lines plotted in Fig. 13.

Most of the oblong blowholes in the rim zone of this ingot, consequently, are believed to be of the kind typical of rising steel. In the top fifth of the ingot—below the top part that has risen—there are only a few blowholes in the rim zone, probably owing to a lower ferrostatic pressure and hence greater gas evolution.

A similar selected part of the bottom-cast ingot is shown in Figs. 14 and 15. Here also three zones may be distinguished. On account of the slow casting—6 min—zone I, with numerous blowhole seats, disturbed dendritic structure, and few blowholes indicating strong gas evolution, is about 1 in. thick. Its inner boundary may be calculated to correspond with a moment 2½ min after casting commenced and with a steel level almost half way up. Zone II extends to about 2.5 in. from the surface corresponding to 8 min after zero casting time. During this period, the ferrostatic pressure was sufficient to

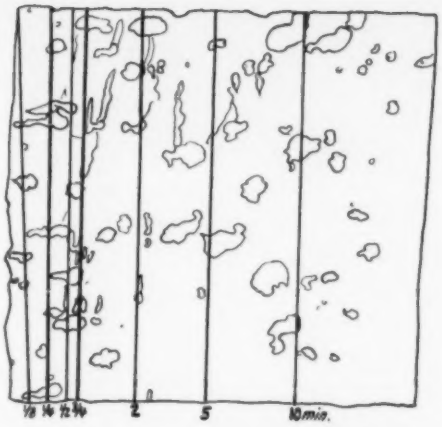

Fig. 13—Freezing-front lines for section shown in Fig. 12.

Fig. 14—Section of the bottom-poured ingot at location indicated in Fig. 11a.

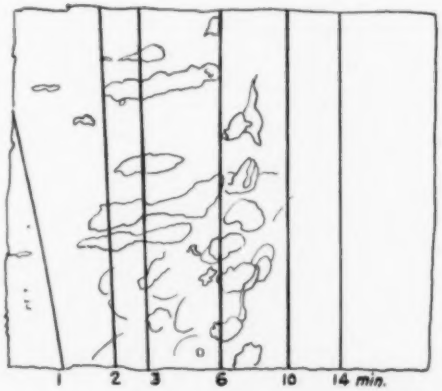

Fig. 15—Freezing front lines for section shown in Fig. 14.

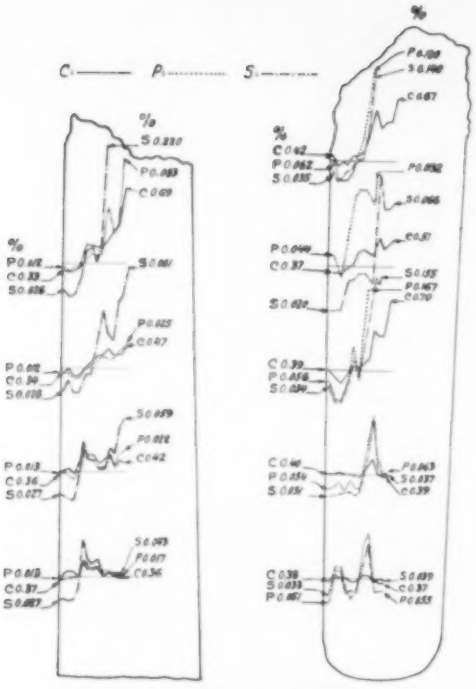

Fig. 16—Carbon, phosphorus, and sulphur variation in the high-carbon ingots.

check gas evolution, to such an extent that part of the gas remained as large blowholes and part came off, leaving large blowhole seats. Reasoning similar to that given for the top-cast ingot applies to zone III. During this period, when the top crust was not yet strong enough, liquid penetrated it and formed a top part above the crust. A considerable volume of blowholes must have formed simultaneously to account for this phenomenon. These holes were later largely compressed when new blowholes formed in the core. In this way the inner boundary of zone III was moved outward.

Analyses of drilled samples taken from different levels in the two ingots are given in Fig. 16. The low values found in the outer part of the rim zone are evidence of strong gas evolution and movement. In the top-cast ingot, the phosphorus and sulphur contents at the lower levels show a maximum within zone II, in agreement with the postulated checked gas evolution; otherwise, the distribution of elements is similar in the two ingots. As a result of sedimentation segregation, the core shows low values in the bottom portion, and high values in the top portion. Certain peaks within the core are probably due to blowhole segregates.

Ingots Made in Surahammar: One 12 in. top-cast ingot made in the acid open-hearth furnace was examined. It contained: 0.38 pct C, 0.03 pct Si, 0.46 pct Mn, 0.34 pct P, and 0.018 pct S. Ferromanganese was added in the furnace, but no aluminum. Casting lasted less than 1 min. Gas evolution was uniform and top level did not change during rimming. Eight to ten minutes after casting the ingot was capped. The rim was then 4 in. wide.

Fig. 17 shows the blowhole distribution. Some large rim holes appear in the lower half of the ingot and in its top portion. In the region where rim holes are absent there are intermediate blowholes. The core is solid, except for a few large blowholes around and at the freezing center in the top.

The primary structure of a section from half height is seen in Fig. 18. Surface zone I, about 1 in. thick, corresponding with a time of formation of 1.3 min, contains few blowholes and has a disturbed finely dendritic structure with occasional blowhole seats. Obviously it froze under fairly strong gas evolution. Next is solid zone II, with globular structure and with blowhole seats here and there. It is terminated at a depth of about 2.5 in. by some intermediate blowholes. This depth seems to correspond to the moment of capping. The transition to the core zone with its globular structure is otherwise smooth.

This ingot is somewhat more solid than the two already described of a similar composition, indicating good rimming action. Possibly the casting temperature was low, whereby freezing was accelerated

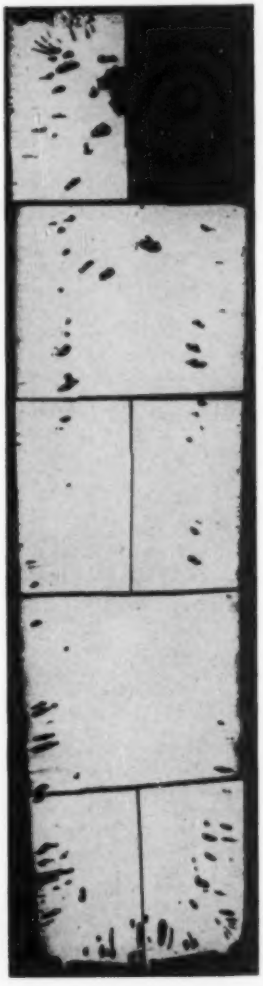

Fig. 17 (right) — Blowhole distribution in a high-carbon acid open-hearth ingot.

and the amount of gas liberated per unit time was greater. Why rim holes formed in the upper part where gas evolution and movement during rimming should have been strong is not clear.

The high-carbon rimming steel ingots examined differ in some respects from rimming steel ingots with 0.055 to 0.21 pct C examined earlier.[1] Increasing carbon content increases the development by etching of primary dendritic structure in the surface zone. Further, there is, in the high-carbon ingots, a tendency for a globular structure to develop fairly early during the formation of the rim zone. Gas bubbles appear to detach themselves less easily and, during rising, are more often detained than in lower carbon ingots. To some extent, the lesser amount of gas set free may be responsible. On the other hand, the widening of the freezing range caused by the higher carbon content may be of importance. The degree of segregation with respect to the distribution of phosphorus, sulphur, etc., between solid and liquid probably increases with the carbon content; thus, the marked contrast in the etched structure is explained. Further, the depth of the freezing zone during growth of the rim zone is increased for the same reason; in other words, the freezing front is less smooth, with the effect on the bubbles referred to. The uneven front should also tend to retard the movement of the liquid.

Globular primary structure indicates the presence of numerous small crystals in the liquid. Possibly protruding points of the crystals growing from the wall are to some extent broken off by the moving liquid. The main cause of the globular structure, however, is believed to be connected with the stronger segregation in the liquid steel ahead of the freezing front and the consequent retardation of the growth of the rim zone. The temperature of this segregated liquid corresponds to its liquidus and is therefore lower than the liquidus for the main melt immediately inside it which is only slightly contaminated by mother liquor. Thus the latter will be subjected to turbulence below its liquidus temperature; in other words, the conditions for precipitation of numerous crystals and formation of a globular, nondendritic structure are realized. High contents of other elements lowering the freezing point may be assumed to have a similar effect.

The Degerfors steel showed a rising tendency. As ingot M3090 shows, slow casting is likely to counteract this tendency and to produce a fairly thick solid surface zone otherwise typical of normal rimming steel. As stated, the Surahammar ingot had a fairly solid surface zone, despite rapid casting. It may be concluded therefore that a carbon content of 0.40 pct does not preclude good rimming.

Large Inclusions in Rimming Steel Ingot

In rimming steel ingots large round or rounded nonmetallic inclusions are commonly present. Although their matrix is transparent they usually contain particles of opaque (Fe, Mn)O and MnS or FeS. The matrix, obviously, is a silicate poor in silica. Such inclusions may be seen with a binocular microscope at a magnification of 20 to 30 diam. Their color may be yellowish, brownish, or gray. Some ingots from the earlier investigation[1] were examined in this way; all inclusions above 0.05 mm being measured and counted, and their distribution in the ingot section determined. The results are given in Tables III and IV.

The results may be summarized as follows:

Fig. 18—Structure of a half-height section of the ingot shown in Fig. 17.

1. The core contains *a greater amount of large inclusions* than the rim zone.
2. In the rim zone, the amount possibly increases towards the bottom.
3. In the core there is a definite such tendency.
4. The amount is not necessarily governed by the carbon content of the steel.

The fact that there are more large inclusions in the core than in the rim zone, although the former, for the carbon contents in question, has a lower oxygen content, probably results from its coarser primary structure in the sense of more open spacing of the small scale segregates. The number of inclusions of the same kind smaller than 0.05 mm would accordingly be less in the core. The accumulation of large inclusions in the lower portion of the core is probably connected with the sedimentation of the metal crystals, a well-known feature in killed-steel ingots also.

Extent of Continuity in Rim Channels

In an ingot of normal rimming steel, at least the upper half, the rim zone is free from rim holes; however this portion probably always contains long narrow, roughly horizontal pores; so-called rim channels. These, like the rim holes, are assumed to be remnants of gas bubbles evolved at the freezing front during rimming. The movement of the liquid metal in the upper part of the ingot being very rapid, only small portions of the bubbles manage to remain as holes.[1] It appeared to be of interest to establish the extent of continuity existing within each channel.

This was done by cutting sections from a 2-ton

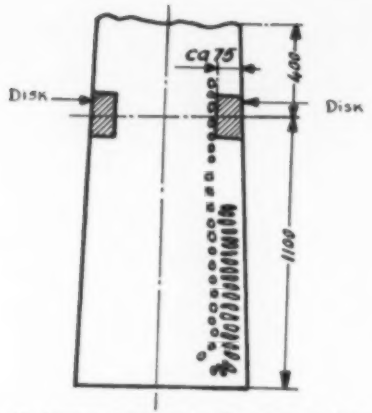

Fig. 19—Location of test samples. Dimensions are in mm.

ingot made at Domnarfvet, containing 0.08 pct C, 0.20 pct Mn, 0.017 pct P, and 0.029 pct S; their locations are shown in Fig. 19. The outer surface was machined to a depth of 0.28 in., corresponding to several times the depth ordinarily lost by burning during heating. The samples were prepared further by installation of a threaded cap, as shown in Fig. 20. Tests were conducted by filling the top depression with water, then putting the space between cap and sample under 8-atm air pressure. Metal was then bored out and the test repeated until the test piece was no longer pressure tight. Boring was done from outside in, in one instance, and inside out in the other. In the first instance, the sample remained pressure tight for a distance from the outside surface of 1¼ in., whereas in boring from the inside surface, a depth of 2⅞ in. was reached before there was leakage. It may be concluded, therefore, that the rim channels were discontinuous to a depth of 1¼ in. from the surface, whereas there was continuity from this depth to the intermediate blowhole zone. Similar results were obtained on samples from a 0.25 pct C ingot.

Table III. Inclusion Distribution in Bottom-Cast Ingots Made at Kallinge

Sample No.	Average Distance from Bottom, In.	Ingot A, 0.08 Pct C, Vol Pct x 10^5		Ingot B, 0.09 Pct C, Vol Pct x 10^5	
		Rim Zone	Core	Rim Zone	Core
11	34.5	1.1	1.3	0.6	1.8
10	31.5	0.5	1.0	0.3	1.8
5	14.7	1.3	1.0	1.7	1.4
4	11.1	0.7	2.8	3.4	5.1
3	7.9	1.4	9.0	2.0	4.4
2	4.75	1.4	8.0	2.2	8.9
1	1.6	0.9	8.5	0.7	7.7
Avg		1.0	4.1	1.4	3.8

Table IV. Inclusion Distribution in Top-Cast Ingots Made at Nykroppa

Sample No.	Average Distance from Bottom, In.	Ingot F1, 0.14 Pct C, Vol Pct x 10^5		Ingot F3, 0.11 Pct C, Vol Pct x 10^5		Ingot K1, 0.21 Pct C, Vol Pct x 10^5	
		Rim Zone	Core	Rim Zone	Core	Rim Zone	Core
	50.0	0.3	1.1	0.5	0.3		
8	44.0	0.5	0.5	0.2	0.8	4.9	0.9
7	38.0	0.8	1.2	0.5	0.9	1.9	2.5
6	32.5	1.8	2.5	0.3	0.8	1.1	4.7
5	26.6	2.1	0.8	0.5	3.0	1.5	6.8
4	20.6	2.9	1.5	0.5	2.2	1.0	8.6
3	14.7	1.5	2.5	2.7	3.9	1.7	11.8
2	9.1	1.1	4.6	0.4	7.9	1.6	14.3
1	3.0	0.4	4.0	3.3	24.2	1.2	10.9
Avg		1.3	1.8	1.0	4.9	2.5	7.2

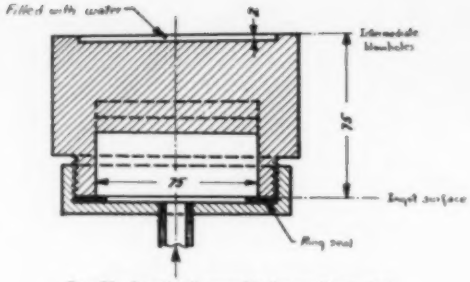

Fig. 20—Details of assembly for continuity test.

Summary

1. When rimming steel is allowed to solidify under pressure the evolution of gas during solidification is reduced, the more the higher the pressure. Accordingly, blowhole distribution and primary structure are governed by the pressure. When the pressure exceeds a certain minimum, no gas evolution takes place and the structure shows the characteristics of a killed steel.

2. On experimenting with a steel with 0.12 pct C (determined on unkilled sample) and 0.48 pct Mn, an additional air pressure of 10 to 15 atm was sufficient for preventing all gas evolution during solidification. Under an additional pressure of 6.5 atm (0.07 pct C, 0.24 pct Mn) a semikilled ingot was obtained and under 3 to 4 atm (0.08 pct C, 0.33 pct Mn) a rising ingot.

3. The application of a lid, with a casting orifice, appeared to reduce gas evolution during rimming somewhat. Hence the steel may rise during this period. A similar effect probably was produced by a refractory lining at the top of the mold.

4. Rimming steel with about 0.40 pct C differs from such steel of lower carbon contents in that a good rimming action seems more difficult to produce, although not impossible. The inner part of the rim zone tends to develop a globular freezing structure. On slow casting, the outer part of that zone contains fewer blowholes than on rapid casting.

5. Large nonmetallic inclusions in rimming steel ingots with 0.08 to 0.21 pct C appear in larger amount in the core than in the rimming zone and in larger amount in the lower than in the upper part of the core.

6. Rim channels in rimming steel ingots in two cases were found to show continuity from a depth beneath the ingot surface of about 30 mm to the intermediate blowholes but not outside of the 30 mm depth.

The experiments with rimming steel ingots solidified under pressure and the tests to establish the extent of continuity were made at the Domnarfvet Steel Works, the ingots of high-carbon content were made at the Degerfors and the Surahammar steel works. The investigations of structure and inclusions were carried out at the Royal Institute of Technology, Stockholm. For valuable assistance with the latter tasks the authors are indebted to Raymond Nordstrom.

Until his untimely death in 1944, G. Phragmén was very active in the investigations. Behind the results reported stands the whole committee, which since 1940 has included H. Gillo and M. Wiberg.

References

[1] A. Hultgren and G. Phragmén: Solidification of Rimming-steel Ingots. *Trans.* AIME (1939) **135**, p. 133.

Vanadium-Oxygen Equilibrium in Liquid Iron

by John Chipman and Minu N. Dastur

This paper presents equilibrium data on the reaction of water vapor with vanadium dissolved in liquid iron at 1600°C. The thermodynamic behavior of vanadium and oxygen when present together in the melt is discussed. A deoxidation diagram is presented which shows the concentrations and activities of vanadium and oxygen in equilibrium with V_2O_3 or FeV_2O_4.

STUDIES of the chemical behavior of oxygen dissolved in pure liquid iron[1-3] have served to determine with a fair degree of accuracy the thermodynamic properties of this binary solution. The practical problems of steelmaking, however, involve not the simple binary but ternary and more complex solutions. Only a beginning has been made toward understanding the behavior of such systems. The silicon-manganese-oxygen relationship was studied long ago by Körber and Oelsen[4] and more recently by Hilty and Crafts.[5] The carbon-oxygen reaction was investigated by Vacher and Hamilton[6] and by Marshall and Chipman.[7] A number of deoxidizing reactions have been studied empirically[8-10] with the object of determining the appropriate "deoxidation constants."

The work of Chen and Chipman[11] afforded a clear-cut view of the effect of the alloy element, chromium, on the thermodynamic activity of oxygen in liquid ternary solutions. These investigators determined the oxygen content of experimental melts which had been brought into equilibrium with a controlled atmosphere of hydrogen and water vapor and were able to show that the presence of chromium decreases the activity coefficient of oxygen. They determined also the conditions under which the two deoxidation products, Cr_2O_3 and $FeCr_2O_4$, were formed and showed that the activity of residual oxygen is considerably less than its percentage.

It was the object of this investigation to apply a similar method to the study of molten alloys of iron, vanadium, and oxygen. Vanadium was once considered a moderately potent deoxidizer, but this is now known to be erroneous, in the light of its behavior in steelmaking practice. Its reaction with oxygen retains a certain amount of practical interest in that a high percentage of one element places a limit on the amount of the other that can be retained. As a deoxidizer it will be shown that vanadium lies between chromium and silicon.

Experimental Method

The apparatus was that used by the authors[3] in their study of the equilibrium in the reaction:

$$H_2(g) + \underline{O} = H_2O(g); K_1 = \frac{p_{H_2O}}{p_{H_2} \cdot a_O} \qquad [1]$$

Crucibles of Norton alundum or of pure alumina were used. The latter were made in this laboratory and were of high strength and low porosity. Under conditions of use they imparted no significant amount of aluminum (less than 0.01 pct) to the bath. Temperature measurements were made with the optical equipment and calibration chart of Dastur and Gokcen.[12]

The charge was made up of calculated amounts of ferrovanadium (20 pct V) and clean electrolytic iron totaling approximately 70 g. The first few heats were made in alumina crucibles with an insufficient amount of vanadium so that no oxide of vanadium would be precipitated under the particular gas composition. All the heats were made at 1600°C under a high preheat and with four parts of argon to one part of hydrogen in the gas mixture to prevent thermal diffusion. The rate of gas flow was maintained constant at 250 to 300 ml per min of hydrogen. The time for each heat was three quarters of an hour after the melt had melted and attained the required temperature (1600°C).

The water-vapor content of the entrant gas mixture was gradually raised in succeeding heats, keeping the vanadium content of the melt constant. This was controlled by manipulation of saturator temperature. A point was reached when for a given $H_2O:H_2$ ratio some of the dissolved vanadium was oxidized and appeared as a thin, bright oxide film on top of the melt. By raising the temperature of the melt it was possible to dissolve the oxide film which reappeared as soon as it was cooled down to 1600°C. The temperature readings taken on the oxide film were consistently higher by 80° to 85°C as observed by the optical pyrometer. The heat was allowed to come to equilibrium under a partial covering of this oxide film.

At the end of the run the power and preheater were shut off and the crucible containing the melt was lowered down into the cooler region in the furnace. This method of quenching proved quite

JOHN CHIPMAN, Member AIME, is Professor of Metallurgy, Massachusetts Institute of Technology, Cambridge, Mass. MINU N. DASTUR, formerly Graduate Student and Research Assistant, Massachusetts Institute of Technology, is now associated with H. A. Brassert & Co., New York.

Discussion of this paper, TP 3006C, may be sent (2 copies) to AIME by April 1, 1951. Manuscript, Oct. 16, 1950. St. Louis Meeting, February 1951.

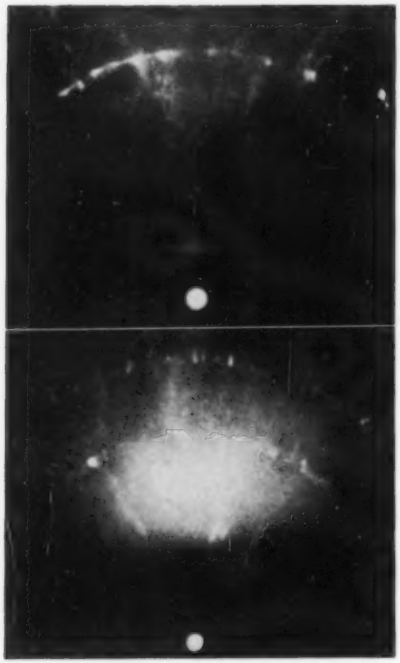

Fig. 1—X-ray diffraction photograms of oxide crusts.
a (above)—Heat No. 143 containing 0.90 pct V.
b (below)—Heat No. 118 containing 0.10 pct V.

effective, the solidification time never exceeding 10 sec.

Results

Altogether 30 heats were made, of which 12 were unsaturated vanadium-iron alloy melts and 3 were discarded due to failure of some part of the apparatus or the breaking of a crucible. The equilibrium runs for saturated vanadium-iron melts are marked with an asterisk in Table I.

Identification of Oxide Phases

The oxide films formed on the surfaces of five typical ingots were examined by X-ray methods. The amount of film material was insufficient for use as a powder sample. Films were too thin to register a pattern by the back-reflection method. The forward-reflection Hull method was therefore employed using a pinhole camera. The X-ray beam from a chromium target was made to graze the specimen at a very acute angle so as to enable it to traverse as great a thickness of the oxide layer as possible.

The results for two ingots of high- and low-vanadium content are shown in Fig. 1 where the differences in pattern are clearly evident. Measurements of the observed patterns recorded in Table II agreed as well as could be expected for this method with the known patterns of V_2O_3 and FeV_2O_4. The former was found on ingots containing more than 0.35 pct V. The latter, which is the spinel identified by Mathewson, Spire, and Samans,[14] was found on two ingots of 0.10 pct V.

Identification of the very small nonmetallic inclusions found in the ingots by microscopic examination was considerably less certain than the X-ray identification of the oxide films. Inclusions in low-vanadium ingots were of duplex structure containing wüstite and a dark phase, presumably the spinel. At higher vanadium levels wüstite disappeared and one or sometimes two dark phases were visible. In view of the inconclusive nature of this evidence, the identification rests solely upon the X-ray evidence.

Activity of Oxygen

It has been shown[3] that the value of K_1 (eq 1) for pure iron-oxygen alloys at 1600°C is 3.95. In this case the activity of oxygen, a_o, is equal to its percentage by weight in the melt.[1] In the presence of vanadium the activity is found to be somewhat diminished; it becomes necessary, therefore, to in-

Table I. Fe-V-O Equilibrium Data at 1600°C

Heat No.	Crucible Used	V Charged, Pct	$\frac{P_{H_2O}}{P_{H_2 corr.}}$	V Analysis, Pct	Oxygen Analysis, Pct		Condition of Ingot
					Data	Chosen Value	
69	Alundum	0.44	0.0354	0.41	0.0132, 0.0132	0.0132	Fair
70	Alundum	0.44	0.0442	0.41	0.0151, 0.0162	0.0156	Sound
71	Alundum	0.44	0.0584	0.38	0.0196, 0.0190	0.0193	Fair
72	Alundum	0.44	0.0790	0.38	0.0274, 0.0279	0.0276	Sound
73*	Alundum	0.44	0.1050	0.31	0.0289, 0.298	0.0293	Porous
74	Alundum	0.19	0.0363	0.134	0.0109, 0.0113	0.0111	Sound
75	Alundum	0.19	0.0643	0.130	0.0186, 0.0186	0.0186	Porous
76	Alundum	0.19	0.0839	0.125	0.0221, 0.0225	0.0223	Sound
77	Alundum	0.19	0.1049	0.128	0.0302, 0.0304	0.0303	Sound
78	Alundum	0.19	0.1390	0.120	0.0373, 0.0381	0.0377	Sound
95	Alundum	0.93	0.0294	0.83	0.0133	0.0133	Fair
96	Alundum	0.93	0.0419	0.83	0.0178, 0.0194	0.0186	Sound
98*	Alundum	0.93	0.0530	0.80	0.0227, 0.0231	0.0229	Sound
107*	Pure Al_2O_3	0.93	0.0606	0.75	0.0221, 0.0234	0.0227	Sound
108*	Pure Al_2O_3	0.19	0.228	0.080	0.0640, 0.0626	0.0633	Sound
109*	Pure Al_2O_3	0.19	0.2780	0.053	0.0733, 0.0750	0.0742	Sound
111*	Alundum	1.58	0.0352	1.16	0.0214, 0.0228	0.0221	Porous
112*	Alundum	1.58	0.0389	1.31	0.0231, 0.0182	0.0207	Porous
113*	Pure Al_2O_3	0.13	0.1210	0.032	0.0835, 0.0874	0.0854	Sound
114*	Pure Al_2O_3	0.32	0.2086	0.098	0.0514, 0.0496	0.0505	Sound
115*	Pure Al_2O_3	0.66	0.0985	0.365	0.0328, 0.0309	0.0319	Fair
116*	Pure Al_2O_3	0.79	0.0689	0.536	0.0249, 0.0247	0.0248	Fair
117*	Pure Al_2O_3	0.53	0.1048	0.358	0.0324, 0.0329	0.0326	Sound
118*	Pure Al_2O_3	0.26	0.2048	0.099	0.0529, 0.0512	0.0521	Sound
119*	Pure Al_2O_3	1.56	0.0312	1.35	0.0181, 0.0178	0.0180	Sound
120*	Pure Al_2O_3	0.47	0.1132	0.259	0.0325, 0.0349	0.0337	Sound
121*	Pure Al_2O_3	0.37	0.1670	0.150	0.0413, 0.0415	0.0414	Sound

* Iron-vanadium alloys saturated with oxygen.

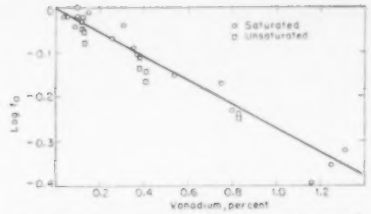

Fig. 2 (above)—Effect of vanadium on the activity coefficient of oxygen, f_o.

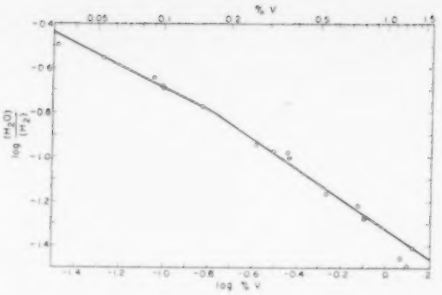

Fig. 3 (right)—Equilibrium in the reaction of water vapor with vanadium in liquid iron at 1600°C. Above the break, the oxide is V_2O_3; below the break, FeO·V_2O_3.

troduce an activity coefficient, f_o, defined by the equation:

$$f_O = a_O / \%\,O$$

The equilibrium constant of eq 1 becomes:

$$K_1 = \frac{p_{H_2O}}{p_{H_2} \cdot f_O \cdot \%\,O} \qquad [1a]$$

Using the value $K_1 = 3.95$, values of f_o are readily obtained for each heat of Table I. These are shown in Fig. 2 where the logarithm of f_o is plotted against the percentage of vanadium. The straight line represents adequately both saturated and unsaturated heats. The effect of vanadium on the activity coefficient of oxygen is considerably larger than that reported for chromium.[11]

Reaction of Vanadium with Water Vapor

If we assume that either of two solid phases occurred in the films found on the saturated heats, and that these have compositions corresponding to the structures indicated by X-ray diffraction, the equations for the two equilibria may be written:

$$V_2O_3(s) + 3H_2(g) = 2V + 3H_2O(g);\ K_2 = a^2_V \left(\frac{p_{H_2O}}{p_{H_2}}\right)^3 \qquad [2]$$

$$FeV_2O_4(s) + 4H_2(g) = 2V + 4H_2O(g);\ K_3 = a^2_V \left(\frac{p_{H_2O}}{p_{H_2}}\right)^4 \qquad [3]$$

It may be assumed that the solution is dilute enough to conform to Henry's law and hence that the activity of vanadium may, by definition, be placed equal to its percentage by weight.

The data on all saturated heats are plotted in Fig. 3. A logarithmic scale is used and two lines are drawn having slopes of 3:2 and 4:2 corresponding to the requirements of eqs 2 and 3, respectively. These two lines fit the data fairly well except for some deviation at the highest vanadium level. This deviation may be attributed to departure from Henry's law or possibly to the appearance of a third (lower) oxide phase, but there is no evidence of either and it may be regarded as the result of experimental inaccuracy. The two lines intersect at 0.17 pct V at which composition the two oxide phases coexist in equilibrium with the melt at 1600°C.

The equilibrium constants and free energies of reactions 2 and 3 corresponding to the two lines of Fig. 3 are, at 1600°C:

$$K_2 = 1.1 \times 10^{-4};\ \Delta F^\circ_2 = +34{,}000 \text{ cal} \qquad [2a]$$

$$K_3 = 1.7 \times 10^{-5};\ \Delta F^\circ_3 = +40{,}800 \text{ cal} \qquad [3a]$$

The free-energy change in the deoxidation of steel by vanadium is obtained by combining these two equations with eq 1 of the previous paper which is:

$$H_2(g) + \underline{O} = H_2O(g);\ \Delta F^\circ = -32{,}250 + 14.50T \qquad [4]$$
$$\text{at } 1600°C \quad \Delta F^\circ = -5100 \text{ cal}$$

This yields the following values for the two free-energy changes at 1600°C:

$$2\underline{V} + 3\underline{O} = V_2O_3(s);\ \Delta F^\circ = -49{,}300 \text{ cal} \qquad [5]$$

$$Fe(l) + 2\underline{V} + 4\underline{O} = FeV_2O_4(s);\ \Delta F^\circ = -61{,}200 \text{ cal} \qquad [6]$$

The experimental data are insufficient to express the free energy as a function of temperature. Approximate equations covering this relationship will be derived in a later section.

Comparison with Low-Temperature Data

The free energy of V_2O_3 is obtained from its heat of formation at 25°C which, according to Siemonsen and Ulich,[14] is −296 kcal, and entropy values given by Kelley.[15] The heat capacities of V and V_2O_3 in the range 25° to 1600°C are taken respectively from Jaeger and Veenstra[16] and Cook.[17] The result, for

Table II. X-Ray Diffraction Patterns of Oxide Films

Vanadium Content, Pct										Theoretical Pattern		
0.90		0.54		0.36		0.10		0.10				
d	Intensity	*d*	Intensity	*d*	Intensity	*d*	Intensity	*d*	Intensity	Due to	*d*	Intensity
3.65	M	3.68	S	3.67	S					V_2O_3*	3.65	M
2.95	VW			2.98	VVW	2.99	S	2.99	M	FeV_2O_4†	2.994	M
2.70	VS	2.72	VS	2.72	VS					V_2O_3	2.70	S
						2.53	S	2.54	S	FeV_2O_4	2.552	VS
2.48	W	2.48	VW							V_2O_3	2.47	M
2.21	VW									V_2O_3	2.18	W

Notes: S = strong; M = medium; W = weak; V = very. *ASTM data card No. 3655. †Ref. 13.

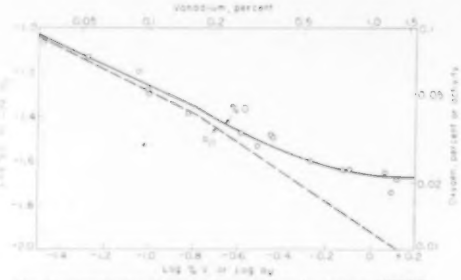

Fig. 4—Deoxidation diagram for vanadium in steel at 1600°C. Lower line shows oxygen activity; upper line, oxygen percentage in equilibrium with solid V_2O_3 or FeV_2O_4.

a temperature range of 1400° to 1700°C, may be expressed in the simple form:

$$2V(s) + 3/2O_2(g) = V_2O_3(s);\ \Delta F^\circ = -287{,}500 + 54.3T \quad [7]$$

For comparison with our experimentally determined free energy we must subtract from this the free energy of solution of 3/2 mol of oxygen in liquid iron. From our previous paper[5] this is:

$$3/2\ O_2(g) = 3\underline{O};\ \Delta F^\circ = -83{,}800 - 1.71T \quad [8]$$

$$\Delta F^\circ \text{ (at } 1600^\circ) = -87{,}000 \text{ cal}$$

The result is:

$$2V(s) + 3\underline{O} = V_2O_3(s);\ \Delta F^\circ = -203{,}700 + 56.0T \quad [9]$$

$$\Delta F^\circ \text{ (at } 1600^\circ) = -98{,}800 \text{ cal}$$

The next step in the computation requires the free energy of solution of solid vanadium in the dilute solution corresponding to the experimental range. This information is lacking altogether. Instead of assuming that the solution is ideal, the comparison of calculated and observed free energies will be completed by computing the deviation of the solution from Raoult's law. For this purpose eq 5 is subtracted from 9 to obtain:

$$V(s) = \underline{V};\ \Delta F^\circ \text{ (at } 1600^\circ C) = -24{,}700 \text{ cal} \quad [10]$$

Now if vanadium formed an ideal solution in iron, this free-energy change could be computed by well-known methods which are adequately discussed in "Basic Open Hearth Steelmaking."[10] The heat of fusion of vanadium has not been measured but, since temperatures not far below its melting point are the concern here, the error introduced by this uncertainty is entirely negligible. Taking the entropy of fusion as 2.1 cal per degree mol, the free-energy change for eq 10 is computed as −16,700 cal. The discrepancy of 8000 cal is greater than the probable errors of the subsidiary data, although earlier values for the heat of formation of V_2O_3 differed by 34,000 cal from that used here. It will be assumed that the 8000 cal represents the actual deviation from Raoult's law of the ideal solution.

The activity coefficient of vanadium in the dilute solution, defined here as the ratio of its activity to its mol fraction, is computed by equating the deviation —8000 cal to $RT\ln\gamma^\circ$ from which:

$$\gamma^\circ = 0.12 \quad [11]$$

To apply this to temperatures other than 1600°, the deviation from Raoult's law will be attributed to a heat of solution of vanadium in iron, i.e., it will be assumed that the solution is "regular" and that the deviation is not in the entropy. The resultant equation is:

$$V(s) = \underline{V};\ \Delta F^\circ = -3900 - 11.1T \quad [12]$$

It should be stressed that eqs 10, 11, and 12 are approximations which depend upon thermochemical data of unproved accuracy. An error of 5 kcal in the heat of formation of V_2O_3 would correspond to a factor of 2 in the value of γ°. It seems safe to conclude that the vanadium-iron solution exhibits negative deviation from Raoult's law and that γ° is probably less than 0.25.

Effect of Temperature on Equilibria

Since all the experimental data were obtained at 1600°C, the effect of temperature can be learned only through calculations. The foregoing equations provide the basis for a very reasonable approximation. Combination of eqs 9 and 12 gives:

$$V_2O_3 = 2\underline{V} + 3\underline{O};\ \Delta F^\circ = +195{,}900 - 78.2T \quad [13]$$

$$\log K = -42{,}800/T + 17.10$$

Available data are insufficient for a similar calculation of the equilibrium involving the spinel.

Deoxidation with Vanadium

Although vanadium is not used as a deoxidizer in practice, its behavior in the deoxidation reaction illustrates a principle which is applicable to all such reactions. It has been shown that the activity coefficient of oxygen is strongly decreased by the presence of vanadium. The deoxidation constant corresponding to equilibrium in eq 13 must be expressed in terms of the activities of vanadium and oxygen, thus:

$$K = a^2_{\underline{V}} \cdot a^3_{\underline{O}} = [f_V \cdot \%\ V]^2\,[f_O \cdot \%\ O]^3 \quad [13a]$$

Values of K at 1500°, 1600° and 1700°C are 1.0×10^{-4}, 1.8×10^{-4} and 2.6×10^{-4}.

In Fig. 4 the lower line represents the activity of oxygen corresponding to any concentration of vanadium for metal in equilibrium with V_2O_3 at 1600°C. Since the oxygen concentration is small its effect on the activity of vanadium is considered negligible.

The upper line of Fig. 4 shows the experimentally determined oxygen content of the same metal. The two portions of each curve intersecting at 0.17 pct V correspond to equilibrium with V_2O_3 above and FeV_2O_4 below the intersection.

This deoxidation diagram proves to be somewhat more complex than its earlier prototypes. At the same time it contains a greater amount of information. It displays the two-fold effect of a deoxidizing element in reducing not only the solubility of oxygen in the melt but also the activity of that oxygen which remains. The question of whether, in a given case, the upper or the lower line is used must depend upon the information desired, that is, how much oxygen is in solution in the metal or how that oxygen behaves.

Summary

An experimental study has been made in which molten iron-vanadium alloys containing 0.03 to 1.3 pct V were brought into equilibrium with controlled atmospheres of water vapor and hydrogen at 1600°C. When the gas mixture is sufficiently oxidizing, an oxide film forms on the metal surface. This was identified as V_2O_3 on melts containing 0.36 pct or more, and as the spinel FeV_2O_4 on melts containing 0.10 pct V.

From the oxygen content of the melts and the

known value of $K_1 = p_{H_2O}/(p_{H_2} \cdot a_O)$ in pure iron, the activity of oxygen in the alloy was obtained. Vanadium decreases the activity coefficient of oxygen, the logarithm of the latter being proportional to the concentration of vanadium.

A deoxidation diagram is presented in which two lines show respectively the percentage and the activity of oxygen in the alloy. Each line shows a change in slope at approximately 0.17 pct V. Above this concentration the solid phase is V_2O_3 and below it is FeV_2O_4.

Acknowledgment

This paper represents a part of a program of research on the physical chemistry of steelmaking sponsored by the Office of Naval Research under contract No. N5ori-07816, Task Order XVI, NR-031-186.

References

[1] M. G. Fontana and J. Chipman: *Trans.* ASM (1936) **24**, p. 313.

[2] J. Chipman and K. L. Fetters: *Trans.* ASM (1941) **29**, p. 953.

[3] M. N. Dastur and J. Chipman: *Trans.* AIME (1949) **185**, p. 441; JOURNAL OF METALS (Aug. 1949) TP 2661C.

[4] F. Körber and W. Oelsen: *Mitt.* Kaiser-Wilhelm-Inst. für Eisenfor. (1933) **15**, p. 271.

[5] D. C. Hilty and W. Crafts: *Trans.* AIME (1950) **188**, p. 425; JOURNAL OF METALS (Feb. 1950) TP 2806E.

[6] H. C. Vacher and E. H. Hamilton: *Trans.* AIME (1931) **95**, p. 124.

[7] S. Marshall and J. Chipman: *Trans.* ASM (1942) **30**, p. 695.

[8] H. Wentrup and G. Hieber: *Archiv für das Eisenhüttenwesen* (1939) **13**, p. 15.

[9] D. C. Hilty and W. Crafts: *Trans.* AIME (1950) **188**, p. 414; JOURNAL OF METALS (Feb. 1950) TP 2805C.

[10] G. Derge: *Trans.* AIME (1946) **167**, p. 93; METALS TECHNOLOGY (Aug. 1946) TP 2004C.

[11] H. M. Chen and J. Chipman: *Trans.* ASM (1947) **38**, p. 70.

[12] M. N. Dastur and N. A. Gokcen: *Trans.* AIME (1949) **185**, p. 665; JOURNAL OF METALS (Oct. 1949) TP 2693C.

[13] C. H. Mathewson, E. Spire and C. H. Samans: *Trans.* A.S.S.T. (1932) **20**, p. 357.

[14] H. Siemonsen and H. Ulich: *Ztsch. Electrochemie* (1940) **46**, p. 141.

[15] K. K. Kelley: U. S. Bureau Mines *Bulletin* No. 434.

[16] F. M. Jaeger and W. A. Veenstra: *Recueil des Travaux Chimiques* (1934) **53**, p. 677.

[17] O. A. Cook: *Journal* Amer. Chem. Soc. (1947) **69**, p. 331.

[18] Basic Open Health Steelmaking. AIME 1st Ed. p. 480; 2nd Ed. chapter 16.

Technical Note

"Oriented Growth" in Primary Recrystallization

by Joseph J. Becker

RECENTLY the "oriented growth" hypothesis of recrystallization textures has been receiving considerable attention. According to this view, "whenever a new generation of grains is growing in a highly oriented matrix . . . one may assume . . . that from among available nuclei of a great variety of orientations those with suitable orientation relationship with respect to the matrix have by far the highest rate of growth (oriented growth) and will, therefore, predominate."[1] This statement includes primary recrystallization of single crystals and of polycrystalline materials showing strong deformation textures as particular cases. While the phenomenon of oriented growth undoubtedly does operate, and may be of importance in coarsening or secondary recrystallization, the writer feels that its extension to primary recrystallization is a different matter. Several aspects of this phenomenon may be pointed out which are difficult to rationalize on the basis of oriented growth.

In recrystallizing deformed single crystals of alpha brass, Maddin, Mathewson, and Hibbard[2] found that the twin composition planes of the recrystallized grains were parallel to the three operative slip planes they observed, and not to the fourth octahedral plane. The writer's current work seems to indicate further that when only one or two slip systems can be seen to operate, the recrystallized grains are aligned only with those slip planes actually observed. This behavior could hardly be accounted for by oriented growth, because on the latter basis the recrystallized texture of a deformed single crystal should certainly have the same symmetry as the crystal itself. Growth rates could not be expected to distinguish between crystallographically equivalent directions, unless the presence of a visible slip system vastly increases the growth rate in the appropriate direction. This seems unlikely.

These relationships were observed by the writer only when considerable care had been exercised before annealing to etch away the effects of cutting out the centers of tensile specimens with a jeweler's saw and to etch off the ends of compression specimens. When these precautions were not taken, nucleation inevitably appeared to occur at the saw cuts or at the ends, and the resulting orientations never showed a [111] rotation but appeared quite random. The provision of many nuclei of many orientations did not enhance the correlation, but destroyed it.

Recrystallization textures are sometimes strongly dependent on annealing temperature, which would imply that the anisotropy of growth rates is a suddenly varying function of temperature. This might be regarded as unlikely.

Recrystallization textures can be strongly dependent on the degree of deformation. If textures are to be explained by selective growth from among nuclei of all orientations, it is difficult to see how the recrystallization process could have any dependence whatever on the manner or degree of deformation.

It is felt that the above points should be considered before the oriented growth hypothesis is applied to primary recrystallization, with the necessary complete divorce of the mechanism of recrystallization from the details of the deformation process.

JOSEPH J. BECKER, Junior Member AIME, is with the Research Lab., General Electric Co., Schenectady, N. Y.

TN 52E. Manuscript received Oct. 2, 1950.

References

[1] P. A. Beck and H. Hu: Reply to discussion of their paper on Recrystallization Texture and Coarsening Texture in High Purity Aluminum. *Trans.* AIME, **188**, 1057; JOURNAL OF METALS (Aug. 1950) TP 2908E.

[2] R. Maddin, C. H. Mathewson, and W. R. Hibbard, Jr.: The Origin of Annealing Twins in Brass. *Trans.* AIME, **185**, 655; JOURNAL OF METALS (Sept. 1949) TP 2676E.

Sintering Practice At Josephtown Smelter

by H. K. Najarian, Karl F. Peterson, and Robert E. Lund

PRIMARY products of the Josephtown smelter are zinc metal of various grades, lead-free zinc oxide pigments, cadmium metal, and sulphuric acid. Zinc concentrates of domestic and foreign origin are blended and desulphurized at the roaster plant. The equipment includes five, 12-hearth Herreshoff roasters and two modified Trail-type suspension roasters. The sulphur dioxide containing gases from the roasting operation are diverted to a four-unit contact acid plant for the manufacture of sulphuric acid. The roasted calcines are agglomerated by sintering on Dwight-Lloyd-type sintering machines; the sinter is crushed and sized within required limits; and the sized sinter is smelted in vertical shaft-type electrothermic furnaces. Of the 13 electrothermic furnaces of various sizes now in operation, four are designed to produce American process zinc oxide of various specifications; and the remaining nine furnaces are equipped with vacuum-type condensers and produce zinc metal. Papers describing the general smelting practice at Josephtown have been published by AIME.

Since both High Grade zinc metal and lead-free zinc oxide pigments are produced direct from the electrothermic furnaces without need for subsequent refining, the elimination of impurities such as lead and cadmium has to be accomplished during roasting and sintering operations.

To effect the producing of both High Grade and Prime Western zinc products, the roasting and sintering operations are on two separate circuits. A High Grade circuit produces finished sized sinter low in lead, cadmium, etc., for the High Grade furnaces; and the Prime Western circuit produces finished sinter destined for the furnaces producing Prime Western metal.

Sintering at the Josephtown smelter differs in many important respects from the sintering practice in smelters operating horizontal retort zinc furnaces. Requirements of the electrothermic smelting furnaces define the physical characteristics of the sinter, while the chemical composition of the sinter is controlled according to the grade of metal and oxide to be made as final products. Three principal objectives in the sintering process at Josephtown smelter are:

1. To transform the zinc calcine from the roasting operations into a hard, yet porous agglomerate that will not crumble in the smelting furnace.

N. K. NAJARIAN and KARL F. PETERSON, Members AIME, and ROBERT E. LUND, Junior Member AIME, are General Smelter Superintendent, and Superintendent and Assistant Superintendent, respectively, of Sinter and Leaching Plants, St. Joseph Lead Co., Monaca, Pa.

Discussion on this paper, TP 3011D, may be sent (2 copies) to AIME by April 1, 1951. Manuscript, Oct. 16, 1950. St. Louis Meeting, February 1951.

2. Crushing and sizing of the sinter to obtain a proper screen analysis which is normally —¾ in. down to +¼ in. particle size.

3. To eliminate, particularly in the High Grade circuit, as much of the impurities such as sulphur, lead, and cadmium as possible.

The sintering plant as originally built in 1930 was equipped with three standard 42 in. x 44 ft Dwight-Lloyd sintering machines. Each machine was equipped with a 15x60 in. sintering corporation fan driven by 150 hp, 900 rpm synchronous motor through a magnetic clutch and capable of delivering 30,000 cfm of air at 15 in. of water and 150°F. Each sintering machine was driven by 7½ hp dc motor with controllers for varying the speed of the machine from 8 to 32 in. per min. The pallets were cast iron and the grates of the herringbone type. The charge was mixed in a 4 ft diam x 8 ft Stehli pugmill and transported by belt conveyor, elevator and tripper conveyor to a small bin over each machine.

Shortly after the start of operations the following changes were found necessary:

1. The herringbone grates which plugged very quickly and were difficult to keep clean were replaced by straight, narrow cast-iron grate bars running at right angles to the travel of the pallets. These grate bars are held in place by a center bar extending across the pallet on the 24 in. dimension and by removable retaining plates which form the sides of the pallets.

2. Mechanical grate knockers were developed in conjunction with new grate bars for continuously and automatically cleaning the grates.

3. As the cast-iron pallets cracked, they were replaced with cast-steel pallets.

In 1938, the capacity of the sinter plant was increased with the installation of two 42 in. x 22 ft machines which were brought from the company's Herculaneum lead smelter. With a circulating load of some 250 to 300 pct, production of finished sinter on the 42 in. x 44 ft machines at this time amounted to about three tons of sized sinter per machine hour.

In 1945, one of the 42 in. x 22 ft machines was replaced by a 60 in. x 44 ft machine of our own design.

In 1948, as part of the plant-wide expansion program, the sinter plant not only was expanded but also divided into two separate plants; namely, Prime Western and High Grade circuits. The sinter destined for furnaces producing Prime Western zinc metal is made in a new plant comprising two 60 in. x 44 ft Dwight-Lloyd-type sintering machines, each having a 45,000 cfm Sturtevant fan at 18 in. water static pressure and served by an 8 ft diam x 12 ft long rotary charge pelletizer and auxiliary crushing and sizing equipment. The sinter destined for furnaces producing High Grade zinc metal and zinc oxide pigments is produced in the old sinter plant which was expanded to accommodate four of the 60 in. x 44 ft sintering machines, replacing the old sintering units. In the High Grade sinter circuit, two units of the 60 in. x 44 ft machines are used as preliminary soft sinter machines; and the remaining two units of the 60 in. x 44 ft machines are used to make finished hard sinter.

Purification Theory

Partial elimination of lead and cadmium in the sintering of zinc ores is common knowledge. However, by some manipulation and by taking advantage of the double circuit, it is possible to make zinc sinter which is nearly free of contaminators. Lead

and cadmium, both being more easily reduced with carbon than zinc and being quite volatile in the sulphide form, are driven ahead of the intensely hot burning zone in the sinter cake. On the soft sinter machines, the charge is quite refractory; therefore little slagging takes place during the burning of the charge. The top part of the bed is more nearly free of impurities than the bottom due to condensation of lead and cadmium compounds at the grate area.

It is important to have an open fast-burning charge and a high fusion point charge in order to get good elimination. Equally as important is a charge with the proper amount of fuel and moisture. Our experience has shown 4 to 4.6 pct coke is necessary with a calcine sulphur of from 1 to 3 pct.

To produce a sinter of requisite hardness, it is necessary to add to the charge enough silica sand to obtain 8 to 9 pct SiO_2 in the finished sized sinter. However, addition of this silica to the sinter mix inhibits the elimination of lead and cadmium during sintering. Therefore the low-lead calcines brought in to this High Grade sinter circuit from the roaster plant are given a preliminary soft sintering without the addition of silica sand. This results in the elimination of 80 pct of the lead and some 90 pct of the cadmium and sulphur.

The product of the soft sintering step is resintered with the addition of silica sand and some intermediate products to produce the finished, hard sized sinter required for the High Grade furnaces.

Prime Western Sintering Circuit

The feed for the Prime Western sintering circuit comprises very fine suspension roaster calcines, —3/16 in. residues from the Prime Western furnaces, and dust collected in the Dracco collector from sinter, coke, residue, and furnace plants.

A typical charge going to the Prime Western machines is, in pounds per minute: calcine, 250; Dracco dust, 200; residue fines, 100; coke (—8 mesh), 50; sand (about 30 mesh), 8; and circulating return sinter, 1000.

All of these charge components are stored in steel storage feeder bins of adequate capacity. From the storage bins, calcines and Dracco dust are fed by screw feeders and the remaining components are fed by belt-type feeders on to a collecting screw conveyor which delivers it to an elevator discharging directly into a rotating pelletizer. The mixed charge contains about 4.4 pct coke fuel, part of which comes in through the Dracco dust and the residue fines. The residue fines in the charge are that portion of the reclaimed high-zinc furnace residues which passes through a 3/16 in. screen opening. The charge material is mixed quite thoroughly while the material is being conveyed through the screw conveyors and the elevator to the pelletizer. This unit is 8 ft in diam and 12 in. long. It rolls on two large steel tires and is driven by a 15 hp motor directly connected to a speed reducer, which is in turn connected to an 18 T-8 in. F spur gear driving the ring gear that encircles the drum. The discharge end is completely enclosed and vented to a sinter machine wind box.

In the pelletizer, the charge is moistened with water or dilute zinc sulphate solution by means of a pipe spray so designed that the solution is sprayed on the material during its entire passage through the pelletizer. The wetting solution is a byproduct of the leaching operations plus run-off water from Cottrell conditioning chambers. It has been found that a small amount of zinc sulphate in the spray water in the pelletizer promotes adherence of fine particles to the larger granular particles, resulting in more or less rounded pellets of various sizes. This, experience shows, makes an ideal feed for sintering.

The mix in the pelletizer tends to stick and build up on the inside of the pelletizing drum. A ribbon screw, rotating independently of the pelletizer and contacting the inside periphery of the pelletizer drum near the horizontal center line, continuously cleans the inside of the drum. The drum rotates at about 17 rpm and the cleaner screw at about 80 rpm, both in the same direction.

The pelletized feed is discharged onto a rotating table where two plows split the feed and transfer it to belt conveyors which in turn carry it to the feed end of the sintering machines. The charge drops onto the grates through a rubber-covered swing spout which distributes the charge across the grates in an even fashion, allowing the coarser particles to roll onto the bare surface of the grates. The sintering machine speeds are maintained so that the charge is kept as low as possible behind the spreader plate so as to maintain a fluffy charge. The density at this point is about 130 lb per cu ft.

The charge is ignited by a gas-fired muffle using byproduct CO from the zinc condensers as fuel. Sintering machine speeds vary between 12 and 16 in. per min depending on rapidity of burning. The draft on the wind boxes will average 13 in. of water, varying from as low as 9 in. to as high as 18 in. depending on the condition of the charge. A dense, poorly pelletized charge will be slow burning and have a high wind-box draft. The operator changes the charge as conditions dictate. If for some reason the charge becomes tight and will not burn as rapidly as mix is being fed onto the machines, the condition soon is aggravated by unburned mix appearing in the return sinter. To remedy this, the operator cuts the volume of new charge in the mix; that is, calcine, residue fines, and Dracco dust so that the machine can be run more slowly and allow more time for burning. Proper moisture in the mix is very important to good charge preparation. Our experience has been that 9½ to 11 pct moisture, depending somewhat on the fineness of the material and the ratio of fines to coarse, gives good results. The charge is approximately 97 pct —¼ in. and 35 pct —200 mesh. Charge thickness on grates is carried at approximately 11 in.

A 35 to 40 pct —200 mesh material in the mix has been found to be essential for obtaining a good pelletized charge. Our experience has shown that a pelletized charge comprising rounded granules permits freer passage of gases through the sinter bed and is far superior to a charge of angular particles of various sizes with fines filling the interstices.

The sinter cake as discharged from the machines usually shows a small red hot zone in the lower part of the bed. The cake is broken into some one half dozen pieces as it drops 8 ft onto a 36 in. wide pan conveyor. The pan conveyor carries the sinter to a 24x42 in. toothed slugger rolls which crushes the chunks to —3 in. Sizing is accomplished by first screening the product of the rolls over a rotating trommel having ¾ in. openings. The oversize from the trommel is crushed again in a smooth-faced 36 in. diam x 16 in. face rolls set ⅝ to ¾ in. apart. Roll product is returned to the trommel and a large circulating load is maintained in order that a minimum of fines is produced. The —¼ in. return sinter is separated by screening through a trommel having

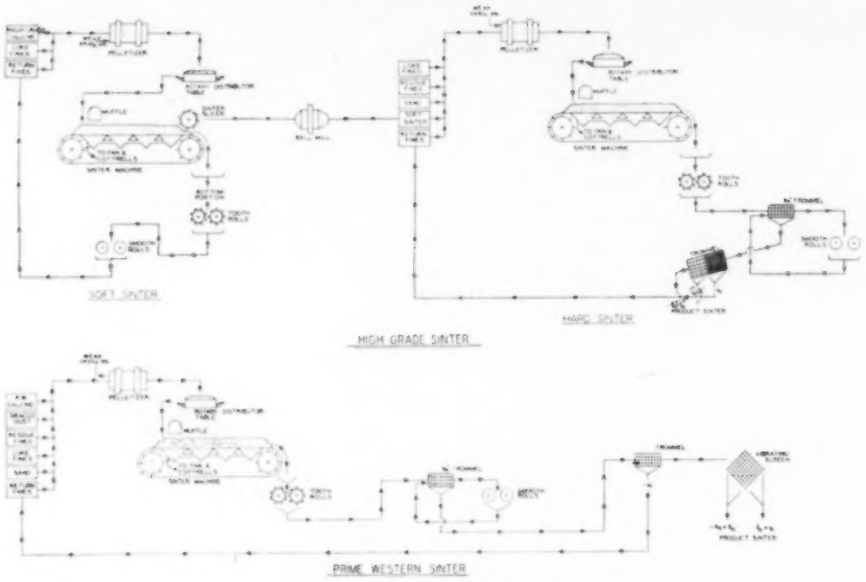

Fig. 1—Sinter circuits of Zinc Smelter Division.

$\frac{1}{4}$x$\frac{3}{4}$ in. slotted openings. The oversize of this screen is again screened over a 7/16 in. screen to make two finished products which are blended to give a uniform sinter size.

The sizing of the sinter feed to the furnaces is very important for proper charge distribution in the furnaces. A typical screen analysis of this sized sinter is as follows: —$\frac{3}{4}$ +$\frac{1}{2}$ particle size, 35 pct; —$\frac{1}{2}$ +$\frac{3}{8}$, 20; —$\frac{3}{8}$ +$\frac{1}{4}$, 32; and —$\frac{1}{4}$, 8. A typical chemical composition is: Zn, 55.0 pct; Pb, 0.65; S, 0.2; Cd, 0.01; Fe, 10.0; SiO_2, 8.7; and MgO and CaO, 1.2.

High Grade Sintering Circuit

Sintering in the High Grade circuit is in two separate steps. Low-lead calcine from the roasting plant is sintered first without the addition of silica sand to the charge. The resulting product is a soft, easily crushed sinter of high purity. The lead content is 0.005 pct or less, the cadmium content is 0.001 pct or less, and the sulphur content is 0.1 pct. The top half of the soft sinter cake containing the least amount of impurities is removed by means of a rotary slicer, mixed with silica sand, residues from furnaces using High Grade sinter, coke and return fines and sintered a second time to produce the hard, sized sinter which constitutes the feed to the High Grade metal and oxide furnaces.

Of four units of 60 in. x 44 ft Dwight-Lloyd sintering machines in the High Grade circuit, two are used for the soft sintering step and the other two for the hard sintering step.

Soft and Hard Sintering

A typical charge mix for soft sintering is: low-lead calcines (about 0.05 pct Pb), 400 lb per min; return sinter (crushed), 1000 lb per min; and coke (—8 mesh), 65 lb per min.

An 8 ft x 72 in. Allis Chalmers ball mill is being installed to grind the calcines to insure enough fines (35 to 40 pct —200 mesh) for proper pelletization of the mix. The return sinter is the bottom portion of the sinter cake crushed to —$\frac{1}{2}$ in.

The portion of the cake left on the pallet after removing the top is discharged onto a 36-in. pan conveyor which carries it to the 24x42 in. slugger rolls. The product of the slugger rolls, all —1 in., is transferred by means of a 24-in. pan conveyor to a 20 in. diam x 20 in. face smooth rolls set at $\frac{5}{8}$-in. opening. The crushed product is conveyed by an elevator and 24-in. pan conveyor to the soft sinter "return fines" bin to be recirculated over the soft sinter machines.

As in the Prime Western sintering circuit, the constituents of the hard sinter mix are fed from respective storage bins by constant volume feeders. This mix is transported to a 6x12 ft rotary drum pelletizer which discharges the pelletized mix onto a rotating table feeder and thence to two sinter machines.

Sinter Slicers

The slicers on the discharge ends of the soft sinter machines are in the form of a double drum inside of which is a 16 in. screw flight. The outside drum contains cutters tangent to the drum and extending out to be approximately 4 in. from the circumference of the drum. Four of these knives are placed about the circumference of the drum 90° apart and extending the full length of 4 ft 6 in. The cutters are rotated at 20 rpm by means of a 15 hp motorized reducer. Power is transmitted by means of a chain and sprockets. As the drum rotates, it cuts off approximately ½ in. of charge as deep in the bed as is desired and drops the cuttings into a slot in the inner drum where the screw conveys it to the end and discharges into a chute on one side of the sinter machine. This is the product of these machines. That part which is not taken off by the slicer after burning is crushed to —½ in. and recirculated.

The product of the sinter slicer which cuts the top 1/3 to ½ of the soft sinter cake is granular, largely

—¼ in., and contains the least percentage of contaminators such as lead and cadmium. An 8 ft x 72 in. wind-swept Hardinge mill is being installed to grind this material so as to provide some 35 to 40 pct —200 mesh material, the product necessary for good pelletizing of the sinter mix. This ground product, high zinc residues from the High Grade furnaces, coke, silica sand, and return fines, constitute the charge for the High Grade sinter circuit.

A typical charge to High Grade hard sinter circuit sinter machines in pounds per minute is: ground soft sinter, 450; High Grade residue fines, 180; return sinter fines, 1000; silica sand, 10; and coke, 62.

Feeding the various mix constituents, conveying, pelletizing and sintering, crushing and screening are essentially a duplicate of the Prime Western sintering circuit. The product of this plant is a sized hard sinter and is used on all furnaces producing High Grade metal and oxide pigments.

Sizing is carried on in the same manner and with the same standards as were previously mentioned in the discussion of the Prime Western circuit.

Typical chemical analysis of the High Grade sinter is: Zn, 56 pct; Pb, 0.004; S, 0.1; Cd, 0.003; Fe, 10; SiO_2, 8.7; and CaO and MgO, 1.2.

Dust Collector

A very important part of the sintering plant is the Dracco dust collector. The unit is made up of 56 individual compartments each containing 80 tapered woolen bags. The bags measure 113 in. long, 6 in. in diam on the top end and 8 in. in diam on the bottom end. Filter rate is from 3.7 to 5.2 cu ft per min per sq ft of bag area. The pressure drop across the bags is from 4 to 5 in. of water. This baghouse takes care of the major part of the dust produced at material transfer points in the sintering, residue, and furnace plants. Suction is supplied by a 12 ft diam Buffalo fan directly connected to a two-speed motor. At low speed, the fan is capable of delivering 200,000 cfm at 8 in. water static pressure and uses a 400 hp, 514 rpm motor. At high speed, the fan rotates at 600 rpm, is driven by a 600 hp motor and will deliver 275,000 cfm at 9½ in. water static pressure. The fan is operated at high speed during the day shift while the furnace plant operations require additional dust removal capacity. Approximately 85,000 cfm is allocated to the sintering plant for dust removal. Approximately 80 tons of dusts are collected each 24 hr and returned to the Prime Western sinter circuit through this baghouse unit.

Cottrells

An integral appendage to the sintering plant is the Cottrell installation for recovery of fume from the sintering machine gases. Sintering machine gases are discharged from the machine fans into large spray conditioning chambers for humidification prior to entering the Cottrells. Three separate Cottrell precipitators serve the sintering plant. Two precipitators, each rated at 100,000 cfm, receive gases from the hard sinter and soft sinter machines of the High Grade circuit. A precipitator of 150,000 cfm rating was installed to serve the Prime Western circuit with anticipation of expansion to include a third Dwight-Lloyd machine.

Cottrell precipitators were installed by Research Corp. and are of the rod-curtain type. Shell construction is of concrete with a 1-in. ceramic lining. Each precipitator comprises four sections, two in series and two in parallel. Each section in the 100,000 cfm precipitators consists of 21 ducts while the 150,000 cfm precipitator sections contain 27 ducts. Rated gas velocity is approximately 4 fps with a total treatment time of 5 sec. Gas flow is horizontal. High voltage supply for ionization of the gases in each Cottrell is furnished by three transformers of 75,000 v, 25 kva rating with associated mechanical rectifiers.

Proper conditioning of the gases entering the Cottrells is essential for efficient collection. In general terms, the absolute humidity of the gases is maintained as high and the dry bulb temperature as low as physical conditions of the collected dust and corrosion limitations permit. Gases entering the conditioning chambers are cooled to a dry bulb temperature of 130° to 135°F before entering the Cottrells. Absolute humidity is 9 to 11 pct by volume with corresponding relative humidity in the range of 70 pct. Operators maintain optimum precipitator voltage and corona current by transformer tap and rheostat adjustments. All three rectifiers of each Cottrell are operated continuously, one is connected to both inlet sections, and one each to outlet sections. Care is given to cleaning Cottrell electrode members and to proper gas distribution. Precipitators are inspected daily to insure effective rapper operation and clean gas distributing plates.

Dust collected by the Cottrells averages approximately 2 pct of the calcine and soft sinter feed to the sintering machines. This dust is collected in large hoppers under the precipitating chamber. There are two hoppers to each half of the precipitator, each equipped with a 9-in. screw conveyor which feeds into a long, 12-in. collect conveyor. The dust is conveyed to a tank where it is slurried with acid plant scrubber effluent and pumped to the leaching plant for further treatment. Recovery of metallic compounds from the flue gases averages 90 to 95 pct with corresponding exit dust loadings from the Cottrells of about 0.01 grains per cu ft.

A typical analysis of the collected fume from the Prime Western machines is: Zn, 30 pct; Cd, 7; Pb, 9; total S, 10; sulphide S, 5; and Cl, 1.

The conditioning chambers associated with each Cottrell are of acid-proof brick construction and built in two separate units. Each unit averages 27 ft high, is 50 ft deep, and 15 ft wide on the 150,000 cfm Cottrell, 12 ft wide on the 100,000 cfm Cottrells. Average gas velocity is about 3 fps with settling time for suspended solids and water droplets of 17 sec.

Gases entering the conditioning chambers at about 200°F are cooled and humidified by means of high-pressure water sprays to the afore-mentioned conditions. A portion of the run-off water from the conditioning chambers is recirculated after settling of solids in a 30 ft sq settling basin. Warm water makeup is added to enhance vaporization in the conditioning chambers. Bleed-off water, which contains some soluble zinc, is used in the sinter mix.

Water to the conditioner sprays is pressured by a four-stage centrifugal pump operating at 500 psi pressure. High pressure was found desirable in order to obtain effective water vaporization with a reasonable number of sprays.

The material settled in the conditioning chambers, which closely resembles sinter in chemical composition, is cleaned out periodically, allowed to dry by stockpiling a short while, and fed back into the Prime Western sinter mix circuit through a screw feeder. This material represents roughly 1 pct of the calcine and soft sinter feed to the sinter charge.

The Aging of Sand-Cast Mg-Al-Zn Alloys

by T. E. Leontis and C. E. Nelson

THE properties and casting characteristics of sand-cast Mg-Al-Zn alloys, used commercially in this country and abroad, have been discussed in a number of articles during the past few years.[1-6] In addition, broad surveys of many compositions in the magnesium corner of the Mg-Al-Zn diagram between 0 and 12 pct Al and 0 and 6 pct Zn have been presented by Busk and Marande[7] and by Fox.[8] The purpose of this paper is to furnish a comprehensive survey of the changes in tensile properties, microstructure, and dimensional stability of two magnesium alloys, AZ92A and AZ63A,* as a function of aging time and temperature after solution heat treatment.

Rates of precipitation in Mg-Al-Zn alloys are slow enough so that a substantially homogeneous, supersaturated solid solution can be maintained even when these alloys are air-cooled from the heat-treating temperature. Consequently, even though it has been demonstrated[9, 10] that significantly higher strengths can be developed in some alloys in the aged condition by quenching rather than air cooling from the heat-treating temperature, general practice is to air-cool magnesium alloys. All the work discussed in this paper is based, therefore, on aging studies performed on material air-cooled from the heat-treating temperature. This investigation was intended to be a study of commercially practical aging cycles; the tensile properties were determined, therefore, up to aging times of 25-hr duration.

The alloys used in this investigation were prepared in the laboratory by remelting commercial ingots of the appropriate composition according to the procedures described in a previous paper[11] as the "crucible method." All melts were given the standard superheating treatment in order to insure the maintenance of a uniform grain size of 0.003 to 0.004 in. Standard test bars, $6\frac{1}{2}$ in. long with a $2\frac{1}{2}$ in. long reduced section having a diameter of $\frac{1}{2}$ in., were cast from these melts in green-sand molds using a four-bar pattern.

The alloys were heat treated according to the following schedules:

AZ92A alloy: 500° to 780°F in 2 hr + 780°F (24 hr)

AZ63A alloy: 500° to 740°F in 2 hr + 740°F (16 hr)

In commercial practice,[12] AZ92A alloy is heat treated at 770°F for 18 hr and AZ63A alloy is heat treated at 730°F for 10 hr. The slightly higher temperatures and longer periods of heat treatment were used in order to obtain as homogeneous a solid solution as possible and thus to minimize inconsistencies in the data after aging. The preheat is the same as used commercially and is necessary for preventing liquation in segregated areas of nonequilibrium eutectic commonly found in cast Mg-Al-Zn alloys. All heat treatments were performed in circulating air furnaces electrically heated and controlled to ±5°F. The atmosphere of the furnace was rendered protective by the maintenance of a concentration of 0.5 to 1.0 pct sulphur dioxide. Aging treatments were performed either in the same furnaces but without

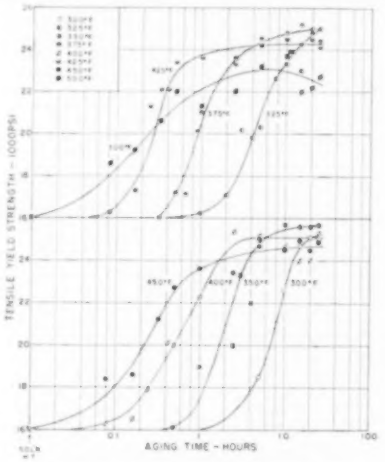

Fig. 1—Tensile yield strength of AZ92A alloy. Temperature legend applies to Figs. 1 to 8.

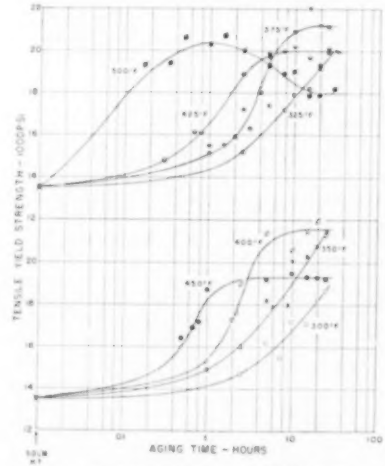

Fig. 2—Tensile yield strength of AZ63A alloy.

* ASTM designation for magnesium alloys:
AZ92A = Mg + 9Al + 2Zn + 0.2Mn
AZ63A = Mg + 6Al + 3Zn + 0.1Mn

T. E. LEONTIS and C. E. NELSON, Members AIME, are Associated with The Dow Chemical Co., Midland, Mich.

Discussion of this paper, TP 3015 E, may be sent (2 copies) to AIME by April 1, 1951. Manuscript, Oct. 9, 1950; revision Dec. 13, 1950. St. Louis Meeting, February 1951.

the use of sulphur dioxide, or in electrically heated oil baths controlled to ±1°F.

The tensile properties were determined on the cast-to-size test bars without machining the surface. Most of the property values are the average of eight determinations, one bar being taken from each of eight separately cast batches of each alloy. Yield strength values are based on 0.2 pct offset; elongations are over a 2-in. gage length.

The dimensional changes accompanying aging were determined on the same type of cast bars. After solution heat treatment, the shoulders of the bars were machined to a diameter of 0.675 in. and the ends were faced parallel to a length of 5.7 ± 0.05 in. and polished to a fineness of 1/0 grit emery paper. All measurements of length were made with a dial gage mounted on a specially constructed fixture. The smallest division on the gage was 0.0001 in. All measurements were made in a constant-temperature room after the bars had been allowed to stand in the room for at least 1 hr. The actual temperature at the time of measuring was recorded and all length readings were reduced to equivalent lengths at 80°F.

Tensile Properties and Hardness

The tensile yield strength, elongation, and hardness of AZ92A and AZ63A alloys are presented as a function of aging time for a series of aging temperatures in Figs. 1 to 6, inclusive.

The tensile strengths have not been plotted in the same way because of the slight change that takes place in this property upon aging. Tensile strength values for selected aging times at all aging temperatures are given in Table I. The tensile strength of AZ92A does not deviate significantly from the value of 40,000 psi in the solution heat-treated state. The same is true for AZ63A alloy except after extended aging times at the higher aging temperatures.

The aging curves in Figs. 1 to 6 show that these magnesium alloys exhibit a considerable degree of age hardening as measured by the increase in yield strength and hardness and the decrease in ductility with increasing aging time. The curves follow the general S-curve trends observed in all age-hardening alloy systems. Rate of increase in strength and hardness increases with increasing aging temperature and the maximum property decreases with increasing temperature.

The higher alloy content of AZ92A alloy produces a greater rate of aging in this alloy than that exhibited by AZ63A alloy. Also, significantly higher strength and somewhat lower ductility are developed in AZ92A alloy. Although aging of AZ63A alloy at 300° and 350°F has not been extended in this study to sufficiently long times to produce maximum strength at these temperatures, previous work in our laboratory has shown that yield strengths not significantly greater than those obtained at 375° and 400°F are produced by aging at the lower temperatures for as long as one month.

Growth

The growth of the two alloys under consideration was determined over a wide range of aging temperatures. The results are depicted in the form of growth vs. time curves in Figs. 7 and 8; the data on these graphs were obtained on material originally in the solution heat-treated condition. All the curves have the shape characteristics of reactions following a process of nucleation and growth.

As in the case of the property changes accompanying aging, AZ92A alloy exhibits a greater amount and faster rate of growth than AZ63A alloy. Neither

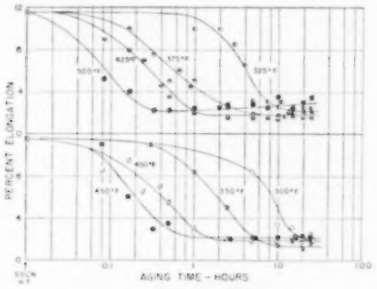

Fig. 3—Elongation of AZ92A alloy.

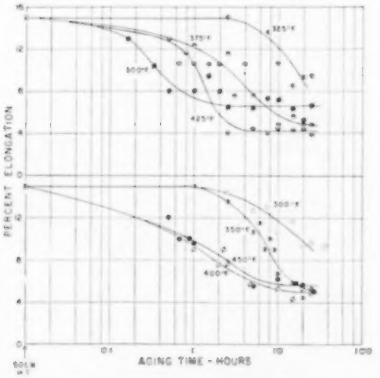

Fig. 4—Elongation of AZ63A alloy.

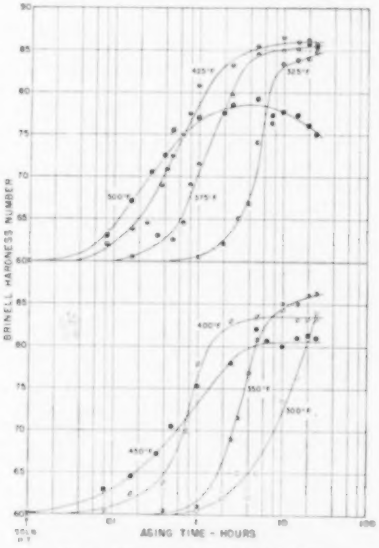

Fig. 5—Brinell hardness of AZ92A alloy.

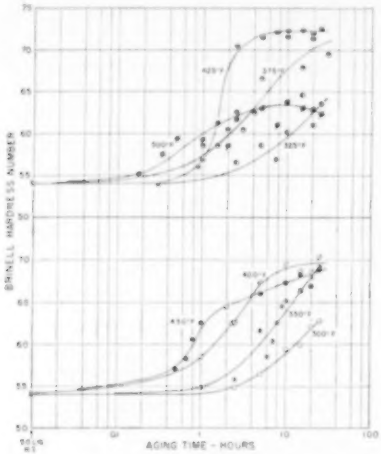

Fig. 6 (left)—Brinell hardness of AZ63A alloy.

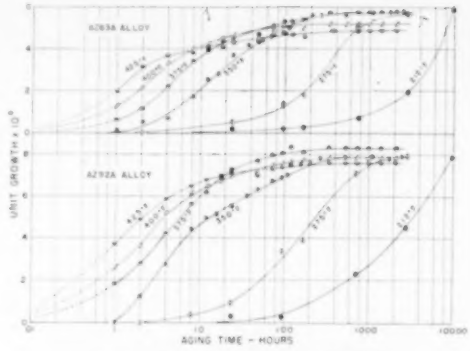

Fig. 7 (above)—Growth of AZ63A and AZ92A alloys.

AZ92A nor AZ63A attains maximum growth at 212°F in 10,000 hr of aging. A few growth measurements have been performed on material in the as-cast condition. The results of these tests, tabulated in Table II, indicate a substantial amount of aluminum and zinc are retained in solid solution when these alloys cool from the freezing temperature. Unfortunately, these measurements have not been carried to sufficiently long aging times to arrive at equilibrium values. Nevertheless, they do indicate that growth is encountered in as-cast material. Fig. 9 shows the variation in the amount of growth with temperature. The marked decrease in growth of both alloys at temperatures above 425°F is closely associated with the rapid increase in solubility of aluminum and zinc in magnesium at these temperatures. These curves also show that the present commercial aging treatment of 5 hr at 425°F is a good selection. This aging cycle contributes nearly maximum strength properties (Figs. 1 and 2) as well as high dimensional stability in as short an aging time as can be obtained. Furthermore, there is considerable advantage in practice in having one aging treatment for both alloys.

Another important consideration in castings is the relief of residual stresses that may be present in the as-cast state or that may arise from cooling after heat treatment. It has been determined by Found and Pittsley[10] that the magnitude of residual stresses in magnesium-alloy castings is considerably lower than that generally encountered in other alloys. The work of these investigators also shows that stresses arising in AZ63A and AZ92A alloys in cooling from the heat-treating temperature are essentially eliminated by the aging treatment recommended in the present paper.

The time required to attain a certain percentage of the maximum possible growth at each temperature is a measure of the rate of precipitation at that temperature. A linear relation should exist between the logarithm of this time quantity and the reciprocal of the absolute temperature. Such a plot is shown in Fig. 10. Deviations from the linear relationship are exhibited by both alloys at the higher temperatures. The marked increase in the solid solubility of the alloying elements in magnesium at temperatures greater than 450°F decreases the driving force of the precipitation reaction at these temperatures. The effect is naturally more pronounced in the alloy of lower total alloy content.

Microstructure

In Figs. 11 and 12 are shown selected microstructures of AZ92A and AZ63A alloys after various degrees of aging. The structures of the alloys in the

Table I. Tensile Strength as a Function of Aging Temperature and Time

Aging Temp, °F	Tensile Strength (1000 psi) for Indicated Aging Time, Hr						
	½	2½	5	10	15	20	25
AZ92A Alloy							
300			42.6	40.6	44.3	43.1	42.6
325	40.6	42.6	41.7	42.6	43.1	43.7	43.8
350	42.0	41.3	43.2	42.4	42.7	41.4	43.2
375	42.8	42.0	42.7	40.4	40.5	41.2	42.0
400	40.4	44.0	41.5	41.6	42.3	41.2	42.1
425		40.7	39.2	40.0	39.7	39.3	40.0
450	37.8	41.6	41.0	39.9	40.9	39.5	39.9
500	37.8	41.4	40.9	41.6	38.0	39.1	39.3
AZ63A Alloy							
300			41.6	39.9	40.1	41.1	40.2	41.4
325			41.5	41.5	41.4	41.7	41.0	42.9
350	42.2	42.8	42.9	40.1	41.1	40.1	37.4
375	42.4	44.5	40.9	39.8	39.5	39.3	38.5
400	41.4	43.8	38.2	39.6	37.0	38.7	39.5
425	41.3	39.1	39.3	40.2	39.6	39.1	38.7
450	43.3	39.6	37.7	38.4	38.4	37.9	37.6
500		39.8	38.4	37.3	37.4	35.8	37.2

Table II. Growth Upon Aging Alloys in the As-Cast Condition

Alloy	Aging Temp, °F	Unit Growth, Aging Time, Hr			
		24	96	168	720
AZ92A	275	0.00008	0.00014	0.00014	0.00034
	350	0.00022	0.00029	0.00031	0.00034
AZ63A	275	0.00001	0.00014	0.00012	0.00025
	350	0.00013	0.00025	0.00025	0.00026

Table III. Increase in Tensile Strength and Ductility

	As-Cast				Solution Heat Treated			
		1000 Psi				1000 Psi		
	E, Pct	TYS	TS	Brinell Hardness No.	E, Pct	TYS	TS	Brinell Hardness No.
AZ92A	1.6	15.7	25.0	62	11.6	16.0	41.5	60
AZ63A	7.0	14.0	30.9	57	15.0	13.5	40.6	54

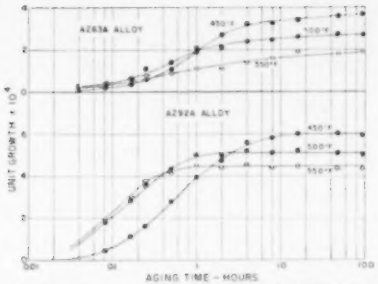

Fig. 8 (above)—Growth of AZ63A and AZ92A alloys. These data supplement those in Fig. 7.

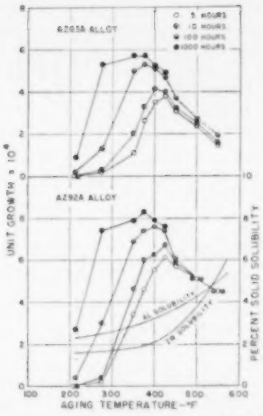

Fig. 9 (right)—Growth vs. temperature.

solution heat-treated condition is not shown inasmuch as they have appeared in the previous publications.[10, 16] This solution treatment dissolves the $Mg_{17}Al_{12}$ compound in the magnesium phase but leaves small particles of Mn and Mg_2Si undissolved. Solution heat treatment produces an increase in tensile strength and ductility as shown in Table III.

The structures shown in the accompanying figures illustrate that there are two distinct types of precipitate in the aged condition of Mg-Al-Zn alloys. One is the discontinuous type which forms at the grain boundaries and resembles pearlite in appearance. The other is the continuous type which appears within the grains and forms a Widmanstätten pattern.

In the temperature range investigated, the first precipitate to form is the pearlitic type along the grain boundaries. As aging proceeds, a finely divided precipitate appears within the grains, usually beginning at the center of each grain and proceeding outward to the grain-boundary precipitate. The discontinuous precipitate consists of alternate plates of $Mg_{17}Al_{12}$ and Mg solid solution. The higher the temperature, the greater is the lamellar spacing of the pearlitic precipitate. At a magnification of 250X, the lamellae are not resolved in either alloy aged at temperatures below 425°F. In the micrographs presented here, the true nature of this pearlitic precipitate can be seen only in AZ63A alloy aged at 500°F (Fig. 12*f*). In structures produced in AZ92A alloy by aging at temperatures above 425°F, it is difficult to distinguish the two types of precipitate (Fig. 11*f*).

The more rapid rate of aging of AZ92A alloy is again demonstrated by the micrographs. As an example, comparison of Figs. 11*b* with 12*a* shows that after the same aging treatment, AZ92A alloy has considerably more precipitate than AZ63A. Similar comparisons can be made for other aging treatments.

Table IV. Typical Properties of Fully Aged AZ92A and AZ63A

	E, Pct	1000 Psi TYS	1000 Psi TS	BHN
AZ92A	2	23	40	84
AZ63A	5	19	40	73

Table V. Maximum Possible Growth of AZ92A and AZ63A

	Maximum Possible Unit Growth	
	Solution Heat Treated	Heat Treated + Aged
AZ92A	0.00083	0.00022
AZ63A	0.00059	0.00021

Summary

The aging studies on two commercial Mg-Al-Zn alloys, AZ63A and AZ92A, reported in this paper show that a wide variation in the properties can be attained by selection of aging temperature and time. Properties typical of these two alloys in the fully aged condition are given in Table IV.

Although both AZ63A and AZ92A alloys exhibit a measurable amount of growth when aged after solution heat treatment, suitable aging treatments render these alloys dimensionally stable to subsequent exposure at temperatures prevailing in engine applications. The figures in Table V indicate the maximum possible growth that can be expected in AZ63A and AZ92A alloys in the heat-treated and in

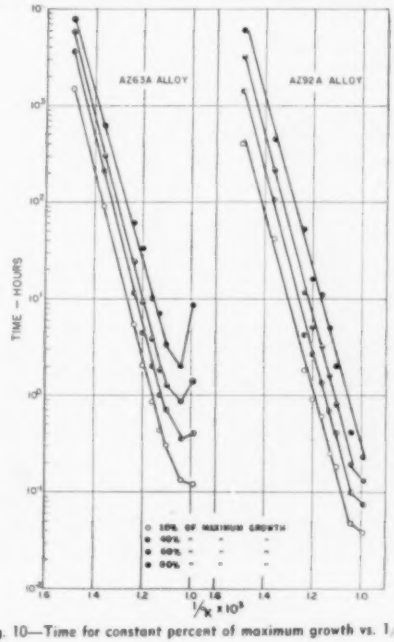

Fig. 10—Time for constant percent of maximum growth vs. 1/T.

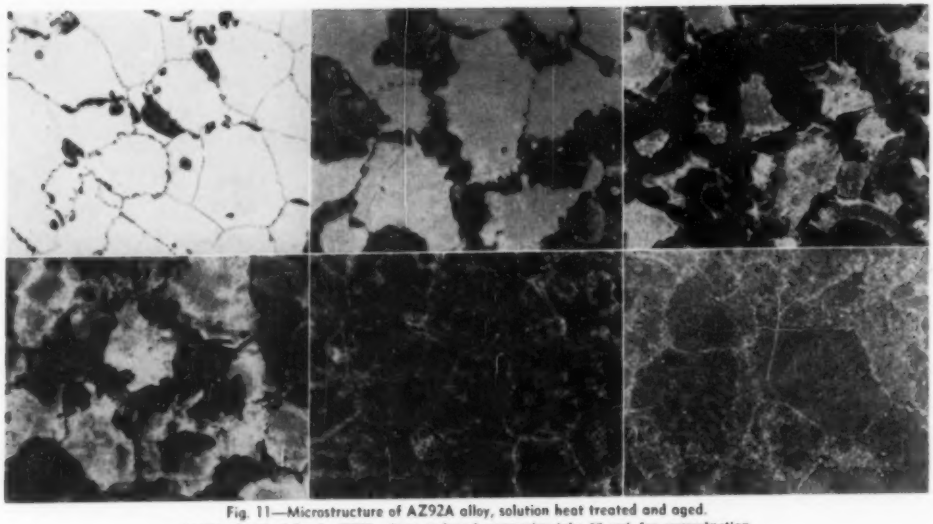

Fig. 11—Microstructure of AZ92A alloy, solution heat treated and aged.

Acetic glycol etchant. X250. Area reduced approximately 30 pct for reproduction.
a (upper left)—Aged at 300°F, 5 hr. *b* (upper center)—Aged at 300°F, 25 hr.
c (upper right)—Aged at 350°F, 15 hr. *d* (lower left)—Aged at 375°F, 15 hr.
e (lower center)—Aged at 425°F, 5 hr. *f* (lower right)—Aged at 500°F, 5 hr.

the heat-treated and aged condition. The satisfactory performance of these alloys in engine parts during the past years indicates that remaining possible growth after aging is of little consequence.

References

[1] A. Beck: The Technology of Magnesium and Its Alloys. (1940) London. F. A. Hughes and Co., Ltd.

[2] H. Vosskühler: *Metallwirtshaft* (1938) **17**, p. 935.

[3] P. A. Fischer: *Magnesium Review and Abstracts* (1944) **4**, p. 65.

[4] J. D. Hanawalt, C. E. Nelson, and R. S. Busk: *Trans.* AFA (1945) **53**, p. 77.

[5] F. A. Fox: *Metal Industry* (London) (1944) **64**, pp. 101, 114, 133.

[6] L. W. Eastwood, J. A. Davis, and J. DeHaven: *Trans.* AFA (1945) **53**, p. 114.

[7] R. S. Busk and R. F. Marande: *Trans.* AIME (1946) **166**, p. 346; METALS TECHNOLOGY (June 1946) TP 2009E.

[8] F. A. Fox: *Journal* Inst. of Metals (1945) **71**, p. 415.

[9] A. E. Flanigan, I. I. Cornet, R. Hultgren, J. T. Lapsley, and J. E. Dorn: *Trans.* AIME (1948) **175**, p. 524; METALS TECHNOLOGY (Sept. 1947) TP 2282E.

[10] R. S. Busk and R. E. Anderson: *Trans.* AIME (1945) **161**, p. 278.

[11] C. E. Nelson: *Trans.* AIME (1944) **159**, p. 392.

[12] C. E. Nelson: *Light Metal Age* (1944) **2**, p. 17.

[13] G. H. Found and R. Pittsley: *Proc.* Soc. Expt. Stress Analysis (1950) **8**, Part I.

[14] P. F. George: *Trans.* AFS (1949) **57**, p. 133.

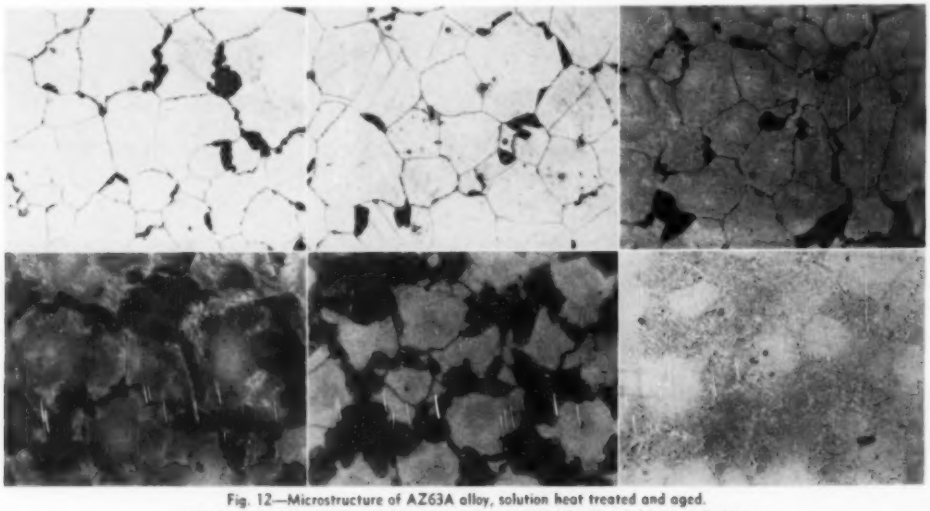

Fig. 12—Microstructure of AZ63A alloy, solution heat treated and aged.

Acetic glycol etchant. X250. Area reduced approximately 30 pct for reproduction.
a (upper left)—Aged at 300°F, 25 hr. *b* (upper center)—Aged at 350°F, 5 hr.
c (upper right)—Aged at 350°F, 15 hr. *d* (lower left)—Aged at 375°F, 15 hr.
e (lower center)—Aged at 425°F, 5 hr. *f* (lower right)—Aged at 500°F, 5 hr.

Mechanical Properties of Stainless Steel Powder

by

Arthur H. Grobe

and

George A. Roberts

Tensile, hardness and density properties are presented for a new 18-8 stainless steel powder for the —50, —100, and —140 mesh cuts and also for a prepared blend containing 62 pct —325 mesh powder. The data were obtained for sintering temperatures of 2100° to 2350°F and for compacting pressures of 30 to 50 tons per sq in.

A NEED has existed for a stainless steel powder of uniform composition from particle to particle, which could be readily molded and sintered, and which would yield moderate to high strength and ductility when processed into parts by standard powder metallurgy techniques. The literature reveals that previously available powders have been lacking in one or several of these desirable characteristics. Originally attempts to produce stainless steel powder by blending and diffusing elemental metal powders were unsuccessful.[1] A truly alloyed stainless steel powder reported by Dale in 1947 yielded reasonable mechanical properties but required an exceptionally high sintering temperature of 2400°F in pure dry hydrogen.[1] A later development reported in 1950 by Stern provided a stainless type powder of excellent molding properties[2] but this powder likewise required sintering at temperatures over 2350°F and did not yield properties as high as those previously reported. The powder was not truly alloyed prior to sintering.

A prealloyed stainless steel powder has been developed that is readily moldable at 30 to 50 tons per sq in., can be sintered at low temperatures (2100° to 2300°F), and which yields compacts with both high strength and ductility. The powder is prepared by the liquid disintegration method,[3] direct from molten metal. Early attempts to make 18 pct Cr, 8 pct Ni stainless steel powder by this method did not produce a usable powder for pressing and sintering because of a preponderance of spherical particles with relatively high, surface oxide content. It was learned that silicon additions to iron alloys, powdered by this process, gave bright powder of low-oxide content and such additions were made to 18-8 stainless with similar results. An attendant change in particle shape occurred reducing the number of spheroids materially. The optimum composition which has been studied and is reported here contains approximately 2.5 pct Si. Silicon additions to stainless steel of the 18-8 type improve the resistance to high-temperature oxidation and promote the formation of ferrite. Corrosion resistance is, however, controlled by chromium content and even though ferrite may exist the corrosion resistance is not generally impaired.[4]

ARTHUR H. GROBE and GEORGE A. ROBERTS are associated with the Metallurgical Dept., Vanadium-Alloys Steel Co., Latrobe, Pa.

Discussion of this paper, TP 3007 E, may be sent (2 copies) to AIME by April 1, 1951. Manuscript, Oct. 17, 1950. St. Louis Meeting, February 1951.

Experimental Procedure

A detailed study of the 18-8, 2.5 pct Si powder has been made in accordance with the following outline:

1. Four blends
   a. — 50 mesh
   b. —100 mesh

c. —140 mesh
d. —100 mesh special mixture with 62 pct —325 mesh

2. Properties of powder blends
   a. Apparent density
   b. Flow rate
   c. Compression ratio
3. Pressing and sintering

   Density, shrinkage and mechanical properties
   a. All blends sintered (sintering time 45 min)
      1) Pressures—30, 40, 50 tons per sq in.
      2) Temperatures—2100°, 2200°, 2300°F
   b. All blends sintered—coined*—resintered (both sintering times 45 min)
      1) Pressures—30, 40, 50 tons per sq in.
      2) Temperatures—2100°, 2200°, 2300°F
   c. —100 mesh blend sintered (sintering temperature 2250°F)
      1) Pressure—30, 40, 50 tons per sq in.
      2) Times of sintering—15, 45, 90, 180, 300 min
   d. —100 mesh blend sintered—coined (sintering temperatures 2250°F)
      1) Pressures—30, 40, 50 tons per sq in.
      2) Times of sintering—15, 45, 90, 180, 300 min
   e. —100 mesh blend sintered—coined—resintered (sintering temperature 2250°F)
      1) Pressures—30, 40, 50 tons per sq in.
      2) Times of sintering—15, 45, 90, 130, 300 min
4. Properties of wrought material of same composition

Apparent density was determined using the Hall flowmeter with the 25 cc cup. Flow rate was determined in accordance with Metal Powder Association Standard 3-45T. Compression ratio is calculated as the ratio of the green to the apparent density.

Density of pressed and sintered compacts was measured on specimens ½ in. in diam and weighing 12 g. Tensile bars were made in a split die producing a square-ended specimen 4 in. x ¼ in. thick. The width at each end was ⅜ in. with a reduced center section ¼ in. wide to provide a gage length of 1 in. All compacts were pressed in a die lubricated with calcium stearate dissolved in carbon tetrachloride. Coining was performed in the same dies, and accordingly some difficulty was encountered in completely coining samples which had exhibited large amounts of shrinkage during the initial sintering.

Sintering was conducted in a tube furnace with a hydrogen atmosphere. Tank hydrogen was deoxidized with platinized alumina and dried in an Electrodryer. Samples reached the sintering temperature in 15 to 20 min and all sintering times reported are times at temperature. Cooling was accomplished in the same atmosphere in the water-cooled end of the tube, where the samples were held for 30 min.

All samples were measured and weighed before and after each treatment. Shrinkage is recorded as the change in length of the 4-in. tensile specimens. Rockwell F hardness, tensile strength, and elongation values were determined for all treatments on the tensile samples.

A 30-lb induction heat was produced of the same

* All coining pressures the same as original pressing pressure.

Table I. Apparent Density, Flow Rate, Compression Ratios and Sieve Analyses of the Four Blends

Properties		Blends			
		—50 Mesh	—100 Mesh	—140 Mesh	—100 Mesh with 62% —325
Apparent density, g per cc		2.94	2.87	2.83	2.94
Flow rate, seconds		31.6	28.0	26.5	25.0
Compression ratio, tons per sq in.	30	1.79	1.79	1.77	1.74
	40	1.91	1.91	1.94	1.86
	50	2.01	2.01	2.04	1.96
Sieve analyses, pct	+50	2.1			
	—50 +100	35.6	1.9		
	—100 +140	17.5	24.4	1.3	5
	—140 +200	13.8	23.5	28.6	10
	—200 +270	11.1	13.9	25.1	8
	—270 +325	5.5	14.6	18.1	15
	—325	14.4	21.7	26.9	62

Table II. Properties of the —50 Mesh Powder

Compacting and Coining Pressure, Tons per sq in.	Sintering* Temp., °F	Tensile Strength, Psi	Elongation, Pct in 1 in.	Hardness, Rockwell F	Green Density, g per cc	Density After First Sinter, g per cc	Coined Density, g per cc	Density After Final Sinter, g per cc	Shrinkage† During First Sinter, Pct	Shrinkage† During Second Sinter, Pct
30-0	2100	9,500	2‡	27.4					0.4	
30-30	2100	24,500	6‡	64.7	5.26	5.27	5.80	5.80	0.4	0.1
40-0	2100	15,500	2	52.1					0.4	
40-40	2100	33,000	8	76.3	5.63	5.65	6.24	6.25	0.3	0.1
50-0	2100	13,000	2	68.8					0.3	
50-50	2100	42,000	8	78.9	5.88	5.90	6.58	6.58	0.3	0.1
30-0	2200	15,000	4‡	39.4					0.5	
30-30	2200	37,000	12	68.9	5.23	5.35	5.87	5.94	0.5	0.3
40-0	2200	20,500	5	59.5					0.5	
40-40	2200	45,500	16	82.0	5.57	5.67	6.31	6.36	0.4	0.2
50-0	2200	28,000	8	69.0					0.5	
50-50	2200	60,500	22	85.5	5.82	5.91	*6.56	6.60	0.5	0.3
30-0	2300	27,500	8‡	51.4					1.2	
30-30	2300	46,500	13	82.9	5.30	5.55	5.83	6.04	1.2	1.2
40-0	2300	31,000	9	65.2					1.0	
40-40	2300	70,000	25	88.0	5.68	5.90	6.23	6.40	1.0	1.1
50-0	2300	32,500	8	74.3					1.0	
50-50	2300	80,000	27	91.8	6.01	6.24	6.55	6.81	1.1	0.9

* Sintering time was 45 min at temperature.
† Shrinkage was measured on the 4 in. length of the tensile specimen.
‡ Specimen broke beyond gage marks.

Table III. Properties of —100 Mesh Powder

Compacting and Coining Pressure, Tons per sq in.	Sintering* Temp., °F	Tensile Strength, Psi	Elongation, Pct in 1 in.	Hardness, Rockwell F	Green Density, g per cc	Density After First Sinter, g per cc	Coined Density, g per cc	Density After Final Sinter, g per cc	Shrinkage† During First Sinter, Pct	Shrinkage† During Second Sinter, Pct
30-0	2100	15,000	4	43.0					0.5	
30-30	2100	31,000	10‡	57.3	5.13	5.20	5.68	5.68	0.6	0.1
40-0	2100	20,000	3‡	48.8					0.5	
40-40	2100	44,500	15‡	76.3	5.50	5.58	6.08	6.10	0.5	0.1
50-0	2100	26,000	6	66.0					0.5	
50-50	2100	49,000	17	81.2	5.79	5.86	6.43	6.43	0.5	0.1
30-0	2200	20,500	10	48.4					0.8	
30-30	2200	40,500	13	64.3	5.15	5.30	5.71	5.84	0.8	0.7
40-0	2200	25,500	8	54.7					0.6	
40-40	2200	54,000	20	78.7	5.48	5.59	6.14	6.23	0.7	0.4
50-0	2200	29,500	9‡	61.1					0.6	
50-50	2200	63,500	22	86.2	5.76	5.88	6.44	6.53	0.6	0.4
30-0	2300	32,500	13	56.8					2.0	
30-30	2300	52,000	15	78.5	5.12	5.39	5.76	6.16	2.2	1.8
40-0	2300	41,500	15	73.8					1.9	
40-40	2300	74,500	26	85.2	5.44	5.90	6.13	6.49	2.0	1.7
50-0	2300	49,000	17	76.7					1.7	
50-50	2300	87,000	32	91.0	5.75	6.19	6.43	6.79	1.8	1.5
40-40	2350	78,000	28	97.2	5.47	6.15			3.1	1.6
50-50	2350	78,500	26‡	103.4	5.71	6.31			2.4	1.4

* Sintering time was 45 min at temperature.
† Shrinkage was measured on the 4 in. length of the tensile specimen.
‡ Specimen broke beyond gage marks.

composition and forged from a 3-in. ingot to a ⅞ in. sq bar. Tensile specimens were machined of the same size and design as those employed for the powder compacts.

Experimental Results

The powder employed was of the following composition: C, 0.09 pct; Si, 2.42; Mn, 0.63; S, 0.007; P, 0.019; Cr, 17.48; and Ni, 8.02.

All of the blends tested molded very well. For commercial applications the —50 mesh powder would yield best moldability at 40 to 50 tons. Standard —100 mesh powder is equivalent to this at 40 tons, while the finer powders have commercially satisfactory green strength at 30 tons.

The basic powder properties and the sieve analyses of the four blends are shown in Table I. This is fundamentally a free flowing powder in all blends with an apparent density of approximately 2.9 g per cc.

Tables II to V, inclusive, present the complete property information for the four blends or cuts studied when pressed at 30 to 50 tons per sq in. and sintered for 45 min at 2100° to 2300°F. In the first column the figures "30-0", for example, indicate pressing and sintering only, while "30-30" indicates pressing-sintering-coining and resintering.

There is a general tendency for the tensile strength and elongation to increase slightly as the particle size decreases. This is especially pronounced at low densities. On the other hand, shrinkage increases greatly as the average particle size becomes finer.

Table IV. Properties of —140 Mesh Powder

Compacting and Coining Pressure, Tons per sq in.	Sintering* Temp., °F	Tensile Strength, Psi	Elongation, Pct in 1 in.	Hardness, Rockwell F	Green Density, g per cc	Density After First Sinter, g per cc	Coined Density, g per cc	Density After Final Sinter, g per cc	Shrinkage† During First Sinter, Pct	Shrinkage† During Second Sinter, Pct
30-0	2100	17,000	3‡	38.0					0.6	
30-30	2100	31,000	12	66.7	5.10	5.19	5.63	5.64	0.6	0.2
40-0	2100	21,000	4‡	61.0					0.5	
40-40	2100	39,000	13	73.2	5.51	5.59	6.14	6.15	0.5	0.1
50-0	2100	27,000	6‡	66.9					0.5	
50-50	2100	50,500	17	84.9	5.77	5.87	6.43	6.44	0.5	0.1
30-0	2200	21,000	10	38.8					0.8	
30-30	2200	40,000	15	68.3	5.11	5.29	5.61	5.79	0.8	0.6
40-0	2200	26,000	6	61.7					0.8	
40-40	2200	52,000	18	78.2	5.49	5.64	6.13	6.24	0.9	0.5
50-0	2200	33,500	10‡	70.2					0.7	
50-50	2200	60,000	21	85.7	5.78	5.92	6.43	6.54	0.7	0.3
30-0	2300	38,500	14	63.8					2.8	
30-30	2300	59,500	20	83.0	5.08	5.73	5.86	6.29	2.8	1.8
40-0	2300	42,000	14	67.2					2.1	
40-40	2300	70,000	24	89.8	5.50	6.06	6.27	6.69	2.1	1.7
50-0	2300	50,500	17	80.4					2.0	
50-50	2300	80,500	27	94.8	5.78	6.32	6.56	6.91	2.1	1.5
40-40	2350	84,500	30	103.3	5.45	6.28			3.8	1.8
50-50	2350	86,000	31	107.1	5.73	6.48			2.9	1.6

* Sintering time was 45 min at temperature.
† Shrinkage was measured on the 4 in. length of the tensile specimen.
‡ Specimen broke beyond gage marks.

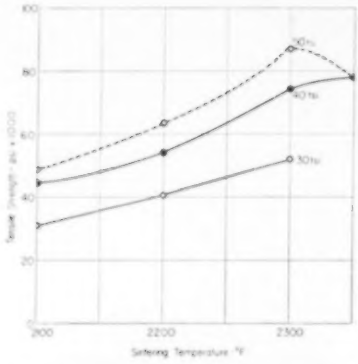

Fig. 1—Tensile strength vs. sintering temperature for —100 mesh powder.

Sintered, coined, and resintered. Each sintering 15 min at temperature. Pressed and coined at pressures shown.

For commercial applications a shrinkage of 1 to 1.4 pct is practical, and accordingly —50 mesh powder could be sintered at 2300°F for 45 min while the very finest powder tested should be sintered at 2200°F if shrinkage is the prime consideration.

The detailed study made of the —100 mesh powder sintered at 2250°F was predicated on the shrinkage consideration which indicated this temperature as optimum for the powder. Data shown in Table VI record all properties obtained by varying the sintering time from 15 to 300 min and the pressing and coining pressures from 30 to 50 tons per sq in. In this instance tensile tests were made on bars sintered and coined with no subsequent resintering in addition to the usual conditions in which sintering was the final operation. It is to be particularly noted that while the tensile strength is increased by coining, the elongation is reduced markedly. Nevertheless, elongations still remain at a relatively high level for powder parts. One factor not recorded in these data is the great increase in yield strength that is a natural result of the coining operation and is of engineering importance.

Selected information from the tables has been assembled into graph form in Fig. 1 to show the trends of properties as a function of the major commercial variables for the standard —100 mesh powder.

The tensile strength of —100 mesh powder increases approximately 100 pct as the sintering temperature is increased from 2100° to 2300°F. A consistent but smaller improvement results from increasing the pressure from 30 to 50 tons per sq in. These results apply to single pressing and sintering. Fig. 1 refers to these same variables but after coining and resintering. The properties after the treatment at 2100°F are equal to those of single sintering at 2300°F. Values of tensile strength over 80,000 psi are obtained at 2300°F with a pressing and coining pressure of 50 tons per sq in.

The increase in strength by lengthening the sintering time beyond 1 hr is slight, but the increase from 15 to 45 min is significant. The increased tensile strength as a result of coining without resintering is apparent.

The tabular shrinkage data are not as consistent as would be obtained commercially, since each specimen in this entire series of tests was individually pressed and sintered, thus increasing the difficulty of obtaining precise control.

From the tabular data it is apparent that the tensile strength and elongation increase simultaneously and in a regular manner except for those samples on which the final operation was coining. In Fig. 2 the validity of this relationship is established. Open circles are plotted for each and every tensile specimen broken, regardless of screen size, pressing, or sintering conditions. The curve is a straight line until tensile strengths of 85,000 psi are reached, when the elongation increases at a more rapid rate. This is caused by the close approach of the tensile strength to that of the wrought material, whereas the elongation is still considerably lower than that of the wrought material. Coined samples show a lower elongation and a poorer correlation than sintered samples (see solid circles in Fig. 2).

Table V. Properties of —100 Mesh Powder with 62 Pct —325 Mesh

Compacting and Coining Pressure, Tons per sq in.	Sintering* Temp., °F	Tensile Strength, Psi	Elongation, Pct in 1 in.	Hardness, Rockwell, F	Green Density, g per cc	Density After First Sinter, g per cc	Coined Density, g per cc	Density After Final Sinter, g per cc	Shrinkage† During First Sinter, Pct	Shrinkage† During Second Sinter, Pct
30-0	2100	20,000	7	46.1					0.8	
30-30	2100	33,500	13	67.7	5.13	5.25	5.69	5.72	0.8	0.3
40-0	2100	26,000	9	60.0					0.8	
40-40	2100	44,000	16	78.3	5.47	5.60	6.07	6.10	0.8	0.2
50-0	2100	31,500	7‡	72.5					0.7	
50-50	2100	50,000	14	84.5	5.74	5.85	6.38	6.40	0.7	0.2
30-0	2200	24,000	10	53.5					1.3	
30-30	2200	42,000	15	68.7	5.14	5.46	5.72	6.00	1.3	0.8
40-0	2200	30,000	10	61.8					1.1	
40-40	2200	53,000	18	82.1	5.45	5.73	6.06	6.30	1.1	0.7
50-0	2200	38,500	12	70.1					1.0	
50-50	2200	60,000	18	84.5	5.77	6.04	6.37	6.57	1.0	0.4
30-0	2300	43,500	14‡	70.4					3.8	
30-30	2300	71,000	23	87.7	5.09	6.14	6.19	6.67	3.9	2.5
40-0	2300	50,500	17‡	74.9					2.9	
40-40	2300	82,500	29	90.7	5.49	6.50	6.57	7.05	3.0	2.0
50-0	2300	63,500	23	84.0					2.9	
50-50	2300	89,500	39	94.9	5.75	6.66	6.74	7.23	3.0	1.7
40-40	2350	84,500	27	104.3	5.40	6.40			3.6	2.2
50-50	2350	92,000	38	107.3	5.76	6.80			4.3	1.2

* Sintering time was 45 min at temperature.
† Shrinkage was measured on the 4 in. length of the tensile specimen.
‡ Specimen broke beyond gage marks.

Microstructural examination of these sintered stainless steel compacts reveals that at 2200°F and higher sintering temperatures ferrite is forming at grain boundaries. The amount of ferrite increases as the sintering temperature is raised as is shown in Figs. 3 and 4. This ferrite is the result of the high silicon content of the powder and the reduced carbon after sintering (the latter results from the decarburizing action of the hydrogen gas and of the small amount of oxide present). A small amount of ferrite is present for the short sintering treatment at 2200°F, Fig. 3, and with longer sintering times at higher temperatures this phase becomes almost continuous, Fig. 4. A few samples sintered at 2350°F show approximately 15 to 20 pct of ferrite as a continuous phase.

Because of the high strengths obtained on these powder compacts of stainless steel and the lack of data on a wrought material of similar analysis, a lot of stainless steel of the following composition was produced from a small ingot: C, 0.09 pct; Si, 2.65; Mn, 0.71; S, 0.006; P, 0.022; Cr, 17.74; and Ni, 8.32; density, 7.73 g per cc.

The tensile properties obtained are charted in Table VII. It is apparent that the high values of tensile strength obtained for these stainless steel

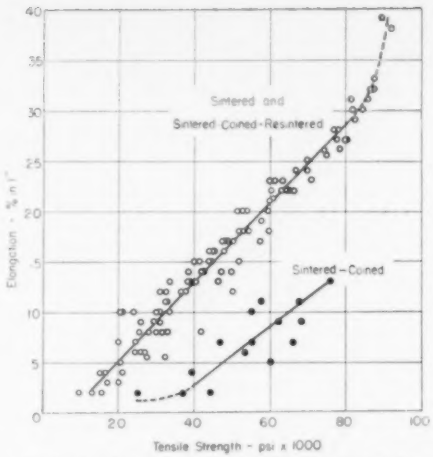

Fig. 2—Correlation of elongation and tensile strength for tensile specimens of all powders for all conditions.
Solid circles, —100 mesh powder sintered at 2250°F in the as-coined condition.

Table VI. Properties of —100 Mesh Powder at 2250°F

Compacting and Coining Pressure, Tons per sq in.	Sintering and Resintering Times, Min	Tensile Strength, Psi	Elongation, Pct in 1 in.	Hardness, Rockwell F	Green Density, g per cc	Density After First Sinter, g per cc	Coined Density, g per cc	Density After Final Sinter, g per cc	Shrinkage* During First Sinter, Pct	Shrinkage* During Second Sinter, Pct
30-0	15-0	16,500	4†	36.8					0.5	
30-30	15-0	25,000	2†	81.5					0.5	
30-30	15-15	32,500	11	72.1	5.10	5.18	5.72	5.76	0.7	0.4
40-0	15-0	24,500	7	62.5					0.6	
40-40	15-0	37,000	2	91.8					0.6	
40-40	15-15	48,000	16	67.7	5.55	5.61	6.18	6.21	0.7	0.3
50-0	15-0	30,000	8	70.9					0.6	
50-50	15-0	44,500	2	99.2					0.6	
50-50	15-15	61,000	21	86.1	5.79	5.87	6.46	6.48	0.7	0.5
30-0	45-0	33,500	11	67.6					2.2	
30-30	45-0	39,500	4†	77.9					2.1	
30-30	45-45	47,500	17†	79.4	5.16	5.37	5.86	5.90	1.8	1.2
40-0	45-0	40,000	15†	69.6					1.6	
40-40	45-0	53,500	6	92.1					1.9	
40-40	45-45	65,000	22	87.1	5.55	5.72	6.15	6.28	1.6	1.4
50-0	45-0	47,500	14†	75.7					1.6	
50-50	45-0	60,500	5	99.2					1.6	
50-50	45-45	77,000	28	92.5	5.85	6.00	6.46	6.61	1.5	1.3
30-0	90-0	38,500	13	68.5					3.2	
30-30	90-0	47,000	7	83.9					3.2	
30-30	90-90	58,000	19†	80.8	5.10	5.49	5.73	6.03	3.1	1.4
40-0	90-0	51,500	20	74.6					2.8	
40-40	90-0	55,500	7	92.6					2.3	
40-40	90-90	66,500	22†	88.9	5.54	5.90	6.17	6.47	2.3	1.3
50-0	90-0	57,500	17	87.8					2.8	
50-50	90-0	68,500	9	98.0					2.8	
50-50	90-90	82,000	30	94.4	5.77	6.12	6.43	6.71	2.5	1.1
30-0	180-0	45,000	16	69.2					3.9	
30-30	180-0	55,500	10	86.9					3.9	
30-30	180-180	60,000	23	81.5	5.09	5.77	5.90	6.22	3.0	1.1
40-0	180-0	53,000	20	81.8					2.7	
40-40	180-0	62,500	9	95.9					3.0	
40-40	180-180	75,000	28	84.9	5.48	6.14	6.31	6.65	3.0	1.2
50-0	180-0	54,500	18†	71.9					2.4	
50-50	180-0	66,500	7†	100.8					2.3	
50-50	180-180	87,500	33	95.3	5.80	6.35	6.55	6.81	2.6	1.2
30-0	300-0	48,500	17†	74.8					3.9	
30-30	300-0	58,000	11	81.4					4.1	
30-30	300-300	67,000	24	79.9	5.22	6.01	6.09	6.34	4.1	1.2
40-0	300-0	61,500	23	83.7					3.8	
40-40	300-0	68,000	11	98.1					3.6	
40-40	300-300	81,500	31	94.0	5.57	6.51	6.55	6.85	3.2	1.5
50-0	300-0	64,500	22†	85.5					3.0	
50-50	300-0	76,500	13	99.7					3.1	
50-50	300-300	87,500	32†	97.1	5.87	6.69	6.81	7.06	3.0	1.2

*Shrinkage was measured on the 4 in. length of the tensile specimen. † Specimen broke beyond gage marks.

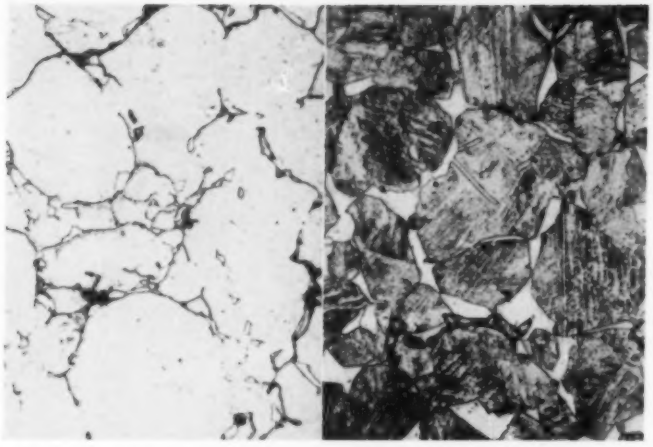

Fig. 3 (left)—Structure of tensile specimen prepared from —100 mesh powder pressed at 30 tons per sq in. and sintered 45 min at 2200°F.
Etchant, Marble's reagent. X500. Reduced approximately 50 pct for reproduction.

Fig. 4 (right)—Structure of tensile specimen prepared from —100 mesh powder pressed at 50 tons per sq in.
Sintered 45 min at 2300°F. Coined at 50 tons per sq in. and resintered 45 min at 2300°F. Etchant, Marble's reagent. Samples taken near tensile fracture showing effect of deformation on matrix structure. X500. Reduced approximately 50 pct for reproduction.

powder compacts by normal powder metallurgy techniques approach those of the wrought material. Ductility is, as expected, relatively lower and could only be increased by increasing the density through extra cold coining and sintering or hot coining operations.

The tensile samples of wrought material had visible amounts of ferrite only at the surfaces which were decarburized during the hydrogen treatment. This is probably responsible for the slight drop in tensile strength as the treating temperature was raised and confirms the supposition that the ferrite in the compacts from the stainless steel powder is partly the result of decarburization throughout the slightly porous compact.

The carbon content of the compacts decreased to at least 0.05 pct at 2100°F and to 0.00 to 0.02 pct at 2300°F. This loss of carbon is accompanied by a weight loss due to the reduction of oxides which under even the most severe conditions of sintering times and temperatures did not exceed 0.35 pct.

Conclusions

1. A prealloyed 18-8 stainless steel powder has been developed that is readily moldable, can be sintered at temperatures as low as 2100°F in a hydrogen atmosphere, and yields compacts with higher strengths and ductility than heretofore possible by standard powder metallurgy techniques.

Table VII. Tensile Properties Obtained

Treatment*	Tensile Strength, psi	Elongation in 1 in., Pct
45 min at 2100°F	105,000	74
45 min at 2200°F	102,000	72
45 min at 2250°F	99,000	72
45 min at 2300°F	99,500	68
15 min at 2100°F†	108,500	74

* All samples cooled in water cooled zone of tube furnace as per powder samples except starred item which was water quenched.

2. The powder containing 2.50 pct Si is free flowing with an apparent density of 2.9 g per cc and a maximum weight loss in hydrogen of 0.35 pct.

3. Optimum pressing and sintering conditions vary with the screen analysis, the finer powders being capable of handling at slightly lower pressures and temperatures. For —100 mesh standard powder pressing at 40 tons per sq in. and sintering for 45 min at 2250°F gives a tensile strength of 40,000 psi and an elongation of 15 pct. Coining at 40 tons and resintering at 2250°F for 45 min provides a tensile strength of 65,000 psi and an elongation of 22 pct.

4. The highest properties realized for the —100 mesh powder were 87,000 psi tensile strength with 32 pct elongation. For a special blend of fine powder these values were 92,000 psi and 38 pct, respectively. These strength properties approach those for wrought material of the same composition.

5. Tensile strength and elongation show a straight-line relationship for this powder, regardless of screen analysis or pressing and sintering conditions. Coining, not followed by resintering, however, lowers elongation while raising tensile strength.

6. Silicon promotes the formation of small quantities of ferrite at high sintering temperatures, especially as the hydrogen atmosphere reduces the carbon content of the compacts to below 0.02 pct.

Acknowledgment

The assistance of Lester M. Gibson in the work of specimen preparation and testing is gratefully acknowledged.

References

[1] John D. Dale: Stainless Steel Powder. *Proc.* Metal Powder Assn. (1947) III, p. 4.
[2] G. Stern: A New Type of Stainless Powder. *Proc.* Metal Powder Assn. (1950) VI, p. 49.
[3] U. S. Patent 2,384,892.
[4] H. W. Gillett: Present Knowledge of Low-Carbon 18-8. Symposium on Evaluation Tests for Stainless Steel. Amer. Soc. for Testing Materials. Special Technical Publication 93 (1941) 41 pp.

Preparation of Titanium Tetrachloride from Rutile

by C. H. Gorski

A method for preparing titanium tetrachloride is described which consists of reducing rutile with coke and chlorinating the reduced product at 200° to 500°C. The crude distillate is purified by treatment with copper powder and distillation. Recoveries, exceeding 90 pct of the titanium in the rutile, were obtained.

IN recent years considerable interest in metallic titanium has been aroused because of its outstanding physical and chemical properties. The present commercial processes for preparing titanium are modifications of the Kroll[1] process and consist essentially of the reduction of titanium tetrachloride with magnesium in an inert atmosphere to produce metallic titanium with magnesium chloride as a byproduct.

At present,[2] commercial titanium tetrachloride costs $0.32 a pound, which makes the price of the included titanium $1.28 a pound. As the titanium tetrachloride must be purified further before processing into metal, its ultimate cost obviously will be higher. Consequently, one of the prime requisites for the production of lower cost titanium metal is a source of low-cost titanium tetrachloride.

Recently, Knickerbocker, Gorski, Kenworthy, and Starliper[3] described a method for preparing titanium tetrachloride from low-grade Arkansas rutile by smelting the rutile with pyrite and coke to form a titanium matte and then chlorinating the titanium matte to prepare a crude titanium tetrachloride. This process had several inherent advantages. Low-grade rutile concentrates were utilized, the chlorination temperature was relatively low (approximately 200°C), and the reaction was strongly exothermic. However, this process had several disadvantages, chief of them being the rather low recoveries of titanium tetrachloride (65 to 81 pct) and the difficulty in purifying the crude titanium tetrachloride obtained.

Because of the high-titanium and low-iron contents of rutile as compared to ilmenite, rutile should be of greater potential value as a source of titanium tetrachloride than ilmenite. Rutile, however, is not chlorinated directly in commercial practice, because reaction temperatures above 700°C are required, at which point chlorine attacks most of the common materials of construction. The process now in use consists of converting the titanium in rutile to the cyanonitride by high-temperature reduction in an electric furnace, and then chlorinating this compound. The disadvantages of this process are the difficulty of producing the cyanonitride, the use of high-grade rutile concentrates in the charge, and the presence of several percent of silicon tetrachloride in the finished product. It would be of considerable interest to develop a new process for the preparation of titanium tetrachloride from rutile by chlorination at 200° to 500°C.

Process Development

Several investigators[4-7] have studied the reduction of titanium dioxide with carbon in an effort to prepare titanium monoxide. Invariably, the titanium monoxide formed in this manner was not pure, as it contained titanium carbide and one or more of the lower oxides of titanium. As these lower oxides of titanium are more reactive chemically than rutile, and as it is known that titanium carbide may be chlorinated readily, a study was made of the chlorination of carbon-reduced rutile. A sample of rutile concentrates from Hot Spring County, Ark., containing 76.19 pct TiO_2, 5.65 pct Fe_2O_3, 4.18 pct SiO_2, and 2.88 pct Al_2O_3, was used for this investigation.

The experimental procedure consisted of making an intimate mixture of —100-mesh rutile and petroleum coke, adding water and molasses as a binder to form a paste, charging into a graphite crucible that was covered, except for a vent to allow the

C. H. GORSKI, Member AIME, is Metallurgist, U. S. Bureau of Mines, Rolla, Mo.

Discussion on this paper, TP 2995D, may be sent (2 copies) to AIME by April 1, 1951. Manuscript, Sept. 18, 1950. St. Louis Meeting, February 1951.

Papers by authors of staff of U. S. Bureau of Mines not subject to copyright.

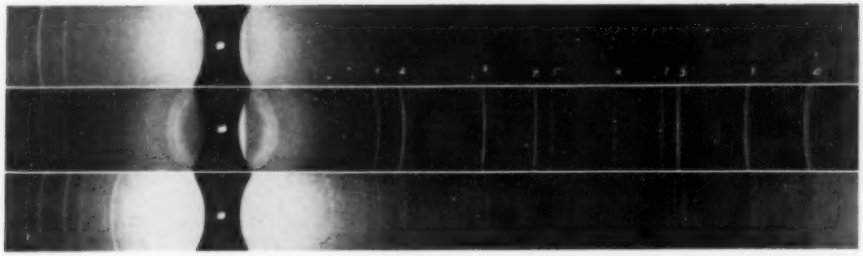

Fig. 1 (top)—Rutile reduced at 1400°C with coke.

Fig. 2 (center)—Titanium carbide.

Fig. 3 (bottom)—Rutile reduced at 1200°C with coke.

escape of gases, and heating with a 3.0 kva high-frequency induction furnace. The charge was held at the reaction temperature (1050° to 1400°C) for 30 min and permitted to cool in the absence of air. After cooling, the charge, which was in the form of a sinter, was ground to —100-mesh, mixed with 30 pct of its weight of —100-mesh petroleum coke, and chlorinated. (The petroleum coke had the following chemical analysis: 79.0 pct fixed carbon, 13.8 pct volatile combustible matter, 6.5 pct ash, and 0.72 pct moisture.) Chlorination was effected in a quartz tube heated by a tube furnace held in a vertical position. The chlorine flowed up through the charge, and the reaction product, which consisted essentially of titanium tetrachloride with minor amounts of ferric chloride, was passed through the top end of the quartz tube, condensed in an air condenser, and collected in a 500-ml wide-mouthed Erlenmeyer flask. The exit gas was bubbled through a flask containing concentrated hydrochloric acid to keep air from entering the system in case the chlorine flow was halted temporarily. The crude titanium tetrachloride was purified by one of several methods described later.

Effect of Experimental Variables

Several series of runs were made to study the effect of varying the amount of petroleum coke and reaction temperature on the reduction of rutile and subsequent chlorination of the reduced product.

In the first series of experiments, each charge consisted of 250 g of rutile concentrates, 37 g of petroleum coke, 14 g of molasses, and 33 g of water. Sufficient coke was used so that its fixed carbon content was approximately equal to the stoichiometric amount of carbon necessary to reduce the titanium dioxide content of the rutile concentrates to titanium monoxide. The samples were heated for 30 min at 1100° to 1400°C. The chemical analyses of these reduced products are shown in Table I. The amounts of titanium and combined carbon in the samples decreased as the reduction temperature was lowered.

Chlorination of the reaction products at 500°C showed titanium recoveries of 98 pct or more could be obtained from the samples furnaced at 1300° and 1400°C. The samples furnaced at 1100° to 1200°C gave titanium recoveries of approximately 90 pct.

In another series of experiments the temperature was held constant at 1400°C, the amount of rutile was 250 g, the amount of petroleum coke used was increased from 37 g in stages to 66.6 g, and the molasses was similarly increased from 14.0 to 15.8 g. Chlorination of these samples at 500°C gave titanium recoveries of 95 to 99 pct. Increasing the amount of coke in the induction furnace charges had no marked effect upon the recovery of titanium by chlorination at 500°C. When the amount of coke was increased, however, it was possible to lower the chlorination temperature to as low as 200°C and recover more than 90 pct of the titanium.

An overall summary of several runs, showing the chemical analyses of the chlorination residues, the chlorination conditions, the conditions under which the rutile was reduced, and the titanium recoveries obtained, is shown in Table II. In these runs each sample was chlorinated until there was no further reaction, as indicated by the absence of vapor passing through the condenser.

More than 95 pct titanium could be recovered consistently when rutile was reduced at 1200° to 1400°C with an excess of petroleum coke and then chlorinated at 500°C. When the reduction temperature was less than 1050°C, the titanium recovery was lowered considerably.

Further experimental work showed that the reduced rutile could be chlorinated at temperatures as low as 136° to 144°C, approximately the normal boiling point of titanium tetrachloride, with a recovery of 84.6 pct of the titanium in the rutile.

Purification of Titanium Tetrachloride

The product obtained by the chlorination of reduced rutile consisted primarily of titanium tetrachloride and ferric chloride with minor amounts of sulphur chloride and other unidentified compounds. Simple distillation of this crude product gave a titanium tetrachloride containing 0.27 pct iron and 0.09 pct sulphur. This product obviously is not pure enough for use in preparing titanium metal.

Several schemes of purification were tried in an

Table I. Chemical Analyses of Reduced Rutiles

Run No.	Reduction Temp. °C	Analysis, Pct			
		Ti	Fe	C (comb.)	C (free)
1	1,400	52.0	5.8	2.8	2.2
2	1,300	51.5	4.5	2.4	1.4
3	1,200	49.8	4.4	2.1	3.8
4	1,100	48.7	4.7	1.7	4.2

effort to prepare titanium tetrachloride at least as pure as titanium tetrachloride currently sold as a reagent of cp grade. These consisted of treatment of single-distilled titanium tetrachloride with hydrogen sulphide followed by distillation, treatment of single-distilled titanium tetrachloride with calcium hydride[5] followed by distillation, direct treatment of crude titanium tetrachloride with copper powder followed by distillation, and treatment of single-distilled titanium tetrachloride with copper powder followed by distillation.

The most effective method of purification consisted of agitating the single-distilled titanium tetrachloride with 2 pct of its weight of copper powder for 1 hr at 100°C and again distilling. A water-white distillate was obtained that was spectrographically equal to or better than cp titanium tetrachloride in every respect. The titanium recovery in this step should be 95 pct or better.

Hydrogen sulphide gave promising results as a purification agent. Further research probably would show it to be as effective as the copper-powder treatment. Calcium hydride was ineffective as a purification agent. The titanium tetrachloride prepared by the hydride addition was considerably higher in vanadium than cp titanium tetrachloride.

The method of analyzing titanium tetrachloride has been outlined by Stoddard and Pietz[6] and consisted of hydrolyzing the titanium tetrachloride and running a spectrographic analysis of the product of hydrolysis. A sample of titanium tetrachloride, currently sold as a reagent of cp grade, was run in the same manner and was compared with each of the titanium tetrachloride samples prepared in the laboratory.

A chemical analysis of cp titanium tetrachloride showed 0.006 pct iron and 0.008 pct silicon. The pure titanium tetrachloride made by treatment with copper followed by distillation was water-white and by spectrographic analysis contained equal or smaller amounts of impurities than the commercial cp product. The cp titanium tetrachloride was straw-colored. This discoloration was caused partly by the presence of vanadium compounds and partly by chlorine dissolved in the liquid.

X-Ray Analysis

Several X-ray diffraction patterns were made of some of the samples of reduced rutile in an effort to identify the major constituents. The data were obtained with a 143.2 mm diam Debye-Sherrer camera. The sample was mounted on a fine-drawn pyrex fiber with collodion and rotated in an X-ray beam passing through a 0.030-in. diam collimator for a 3-hr exposure.

The X-ray diffraction patterns for titanium carbide and titanium monoxide are very similar, and it was impossible to differentiate between these compounds by X-ray analysis. The samples reduced at 1300° to 1400°C were essentially mixtures of titanium carbide and titanium monoxide, whereas those reduced at 1100° to 1200°C contained minor amounts of titanium suboxide (Ti_3O_5) in addition to titanium carbide and monoxide. Diffraction patterns of rutile and of titanium carbide are shown in Figs. 1 to 3.

Table II. Overall Summary of Chlorination Runs

Run No.	Reduction Conditions	Chlorination Conditions	Residue Analysis, Pct			Titanium Chloride Recovery, Pct
			Ti	Fe	C Total	
10	1300°C with 13 pct excess of coke*	7 hr at 500°C	2.0	0.9	59.1	98.3
11	1200°C with 75 pct excess of coke	5 hr and 20 min at 200°C	8.1		48.8	91.1
12	1400°C with 11.2 pct excess of coke	5 hr at 500°C	1.6	2.8	38.7	98.2
13	1000°C with 13 pct excess of coke	3 hr at 500°C	15.2		43.2	79.0
14	1200°C with 13 pct excess of coke	7 hr and 20 min at 500°C	4.0	1.7	49.5	96.3

* Excess of coke means the excess above that necessary to reduce the titanium dioxide content of the rutile to titanium monoxide. In these calculations it was assumed that only the fixed carbon content of the coke took part in the reaction.

Summary

A relatively simple method of preparing titanium tetrachloride has been developed. This process consists in reducing the rutile with coke at 1100° to 1400°C to form a reduction product identified as a mixture of titanium suboxides and minor amounts of titanium carbide. This reduced product is then chlorinated at 200° to 500°C to form a crude titanium tetrachloride, which may be purified by distillation and treating the singly distilled product with copper powder and redistilling. The product thus obtained was equal to or greater in purity than titanium tetrachloride currently sold as a reagent of cp purity. In this manner 90 pct or more of the titanium in the rutile has been recovered.

The chief advantage of this method of preparing titanium tetrachloride is the low chlorination temperatures (200° to 500°C). The product is substantially free from silicon compounds, thus making the purification simpler than the purification of commercial, technical grade titanium tetrachloride, which usually contains several percent of silicon tetrachloride.

Acknowledgments

Acknowledgment is made to the many associates in the Metallurgical Branch who assisted in this work, particularly to J. P. Dowdy, who made many of the chemical determinations, and Fred Hoertel for the X-ray diffraction patterns of many of the samples of reduced rutile.

References

[1] W. J. Kroll: The Production of Ductile Titanium. *Trans.* Electrochemical Society (1940) **78**, 35-47.

[2] *Oil, Paint and Drug Reporter*, Nov. 13, 1950.

[3] R. G. Knickerbocker, C. H. Gorski, H. Kenworthy, and A. G. Starliper: Titanium Investigations: Research and Development Work on the Preparation of Titanium Chloride and Oxide from Titanium Mattes. *Trans.* AIME, **185**, 785-791; JOURNAL OF METALS (Nov. 1949) TP 2706D.

[4] A. Laugier: Ann. Chim. Phys. (1814) **89**, (1) 306, 317.

[5] P. Berthier: Ann. Chim. Phys. (1843) **7**, (3) 84.

[6] H. Moissan: Compt. Rend. (1895) **120**, 290.

[7] W. Dawihl and K. Schröter: Production and Properties of Titanium Monoxide. *Ztsch. für Anorg. und Allgem. Chem.* (1937) **233**, 178-183.

[8] D. G. Nicholson: Purification of Titanium Halides by Treatment with Metal Hydrides and Distillation. U. S. Pat. 2,457,917. (Jan. 4, 1949).

[9] C. Kerby Stoddard and E. Pietz: Pilot Plant Distillation and Purification of Titanium Tetrachloride. U.S. Bureau of Mines. *Rept. of Investigations* 4153 (Dec. 1947) p. 6.

Reverse Leaching of Zinc Calcine

by L. P. Davidson, R. K. Carpenter, and H. J. Tschirner

THE electrolytic zinc plant of the American Zinc Co. of Illinois, at Monsanto, was expanded in 1943 to a capacity of 100 tons of slab zinc daily. This capacity was not attained because of inability of the leaching plant to deliver an adequate amount of solution for electrolysis. Changing the leaching method so that the acid was added to the roasted zinc material reversed the usual procedure and made it possible to attain the desired capacity. The conditions which prevented satisfactory work before this change and the difficulties which arose in reversing the usual leaching procedure are described.

The "reverse" leach operation as now practiced is carried out as follows: All the calcine to be leached is fed continuously to a slurry mixing tank. About one third of the acid to be used is fed to the tank with the calcine. The slurry is discharged continuously to a Dorr duplex classifier in closed circuit with a Hardinge mill. The classifier overflow is pumped to any of six leaching tanks where the leach is completed.

A finished leach is discharged through Allen-Sherman-Hoff pumps to Dorr thickeners, from which the overflow goes to the zinc dust purification and the underflow to vacuum filters.

This change in leaching procedure from the usual one of adding calcine to a large amount of acid made it possible to provide an adequate amount of purified solution to the electrolyzing division and at the same time filter and dry all the residue produced. Operating savings in reagents and better metallurgical recoveries were also important benefits.

The original flowsheet of the leaching plant provided leaching, sedimentation of the insoluble residue, and purification of the neutral zinc sulphate solution with zinc dust. The thickened residue was filtered and washed. The purification cake of excess zinc dust, precipitated copper and cadmium, and any insoluble residue was filtered off on plate-and-frame duplex classifier.

Settlement in the thickeners was inadequate and the suspended solids in the thickener overflow gave rise to filtration difficulties after the zinc dust purification. Further, the filtration and washing of the leach residue was poor, and it became necessary to pump a large amount of unwashed or poorly washed residue to storage ponds outside the plant building.

Two causes of the poor settling and filtration were determined: Soluble silica and ferrous iron in the calcine treated. The latter was a result of poor roasting and with more experience ceased to be a major problem. The silica was a normal constituent of the feed and the working out of the problem became a matter of controlling its solubility.

The obvious method to render the silica insoluble was by intensive roasting. This, however, met with total failure as such roasting resulted in silicates, probably zinc, soluble in the 13 pct acid used for leaching. Attempts were made to coagulate the fine gelatinous slime with addition agents. Glue, lime, starch, beef-blood serum and others were tried without success. All the suggested tried-and-tested means of operating the thickeners gave no consistently good results. Variations in leaching time, in addition of calcine to the leaching tanks, "conditioning" of the pulp by prolonged agitation, immediate discharge of the leach upon completion to avoid breaking up flocs were all tried and given up as ineffective.

Byron Marquis, of Singmaster and Breyer, worked with the plant staff on a beaker scale until a leaching procedure was developed which gave consistent results and a promise of overcoming the difficulties which had plagued the plant operation. It was suggested that the difference in solubility of silicates and zinc oxide in sulphuric acid could be made use of in a leaching method where the acidity was controlled carefully. Such control is possible when acid is added to a slurry of calcine. This process reverses the normal procedure of adding calcine to a vessel of acid, hence the term "reverse leach" was applied.

In this way, the overall acid concentration can be kept very low. In the tests made, it did not exceed 0.05 g per liter free sulphuric acid.

Numerous advantages were realized when no silicates were taken into solution and later precipitated as a bulky gel. The gel had made reasonable thickening and filtration of the leach pulp and practical drying of the residue impossible. When the gel was eliminated, thickening rates were increased as much as five times. The volume of residue after thickening represented about 10 pct of the total leach pulp and had been as high as 95 pct when the gel was present. The thickened pulp was filterable and the filtered cake was dried readily after washing.

The zinc extraction from the calcine was slightly lower. This was more than compensated for by the increase in zinc recovered in solution from zinc which had been trapped in the gelatinous residue. The amount of copper recovered was lower. However, the amounts of other impurities, such as arsenic, antimony, and germanium, taken into solution were lower. This was particularly true of antimony. Since the inception of reverse leaching, no concentrates have failed to yield solutions free of antimony even when present in the calcine to the extent of 0.2 to 0.3 pct.

Oxidation of ferrous iron is a problem of reverse leaching. Ferrous hydrate does not precipitate at pH 5.3 to 5.4 where a leach is finished. The usual oxida-

L. P. DAVIDSON, Member AIME, is General Superintendent, R. K. CARPENTER is Research Engineer, and H. J. TSCHIRNER, Junior Member AIME, is Superintendent of Electrolyzing and Casting, American Zinc Co. of Illinois, Monsanto, Ill.

Discussion of this paper, TP 3001 D, may be sent (2 copies) to AIME by April 1, 1951. Manuscript, Sept. 1, 1950; revised, Nov. 28, 1950. St. Louis Meeting, February 1951.

tion to the ferric state with manganese dioxide is not possible because of the low concentration or absence of free sulphuric acid. An excess of calcine will precipitate the ferrous iron but this method wastes calcine, results in a very viscous pulp which tends to cake in pumps and pipe lines, and places an undue load on the thickener mechanisms. Soluble copper will catalyze the oxidation of ferrous iron to the ferric state when air is passed through the pulp. A low-pressure air line was introduced into each leaching tank and the soluble copper normally present in the solution was sufficient for oxidation.

The question arose as to the solution of zinc oxide in sulphuric acid at concentrations of 0.05 g per liter. Tests showed that when stoichiometric quantities of zinc oxide and 200 g per liter sulphuric acid were reverse leached, 98 pct of the zinc oxide was dissolved. After 15 min the pH was 2.5. An additional 2 pct zinc oxide raised the pH to 5.8, the maximum which could be attained, even with 100 pct excess.

After the leaching technique had been developed, complete cyclic electrolyzing tests were made with solutions from various calcines. When these results proved satisfactory, pilot-plant work was started to determine equipment for this process on plant scale.

A slurry of zinc oxide and zinc sulphate solution will cement and "set up." This slurry could not be made in the leaching tanks because of this tendency and because zinc extraction from the large cemented lumps is low. The preparation of the slurry, of necessity, had to be carried out in equipment outside the leach tanks. Standard classifying, grinding and pumping equipment was found to be adequate. Many trials were made before a satisfactory mixing vessel was developed.

Development of Equipment

The reverse leach flowsheet, as illustrated in Fig. 1, was installed in the plant in the summer of 1944. A Merrick Feed-O-Weight was chosen to weigh and feed the calcine to the mixing equipment. With this, the collection and feeding of the calcine from the 12 storage bins became automatic. A 6-in. horizontal screw feeder was provided in the pyramidal bottom of each bin. The screw is totally encased except that portion in the bin which operates in a semicircular trough. Each is motor driven through a Reeves variable speed control. Two 10-in. collection screws, each conveying the calcine from six bin feeders, discharge into the scale hopper of the Feed-O-Weight. Operation of the conveyors is intermittent and controlled by Bindicators on the scale hopper. This system permits the selection and blending of calcines to make up a uniform plant feed since the rate of withdrawal from any bin can be controlled.

The blended calcine was fed into the slurry mixer along with purified solution assaying 135 g per liter zinc. It was imperative to agitate this pulp continuously and guard against temperatures over 45°C, because such a slurry on standing or heating quickly formed a zinc oxy-sulphate cement.

The slurry mixer was a three volume-ton, top discharge tank provided with a 22 in. duplex turbo mixer driven by a 5 hp motor geared to 350 rpm. The impeller was 6 in. from the tank bottom. The overflowing slurry was laundered to a standard Dorr duplex classifier.

The oversize material from the classifier was ground in a 4½ ft x 16 in. conical Hardinge ball mill in closed circuit with the classifier. Classifier overflow was piped to a 125 gpm Allen-Sherman-Hoff

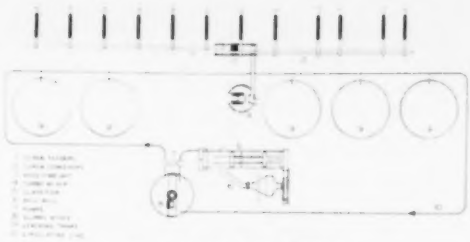

Fig. 1—Reverse leach flowsheet.

Packless rubber-lined pump and pumped through a 4-in. line to a 25 volume-ton Dorr slurry mixer used as a surge tank. A 4-in. circulating line was provided between the surge and leaching tanks.

The slurry was leached in 40 volume-ton, cone bottom, mechanically agitated tanks. These tanks, 14 ft deep x 10 ft in diam, are constructed of lead-lined steel with a 4-in. acid-proof brick inner-lining. A 1-in. copper line introduces compressed air beneath the center of the agitator shaft. These tanks discharge into a 5-in. copper manifold leading to two 500 gpm Allen-Sherman-Hoff Packless pumps, discharging in turn into three 50-ft Dorr thickeners in parallel.

The thickener overflow was laundered to the zinc dust purification tanks. The underflow was filtered and washed on Moore filters. The residue then was repulped with water and refiltered on three Eimco filters. The dewatered cake was dried in a rotary drier and shipped.

Within 24 hr of operation, all the slurry piping, except vertical sections, cemented shut. The cementing occurred first in valves, tees, and short nipples and progressed from there. The air agitating outlets in the surge tank cemented shut. This was the first difficulty encountered.

The surge tank was discarded. The circulating line was replaced by open wooden launders. The slurry pump was coupled as closely as possible to the overflow from the classifier with a 4-in. flanged rubber coupling. A vertical 4-in. copper line was installed to conduct slurry from the pump to the highest point in the launder distributing system.

In mixing the calcine and zinc sulphate solution more difficulties arose. A crust of cemented slurry soon formed at the top of the turbo-mixer. This cementation was not eliminated by relocating or providing an additional impeller. The mixer was replaced by a mixing launder in which neutral zinc sulphate solution entered through a perforated bottom and was met by the calcine from the top. Subsequently, calcine was dropped into an inclined launder onto a stream of solution. The operation was fairly satisfactory but extremely dusty. Frequent cleaning of the pipe and launders was necessary.

This method was used in the plant until it was found that the slurry could be made satisfactorily by mixing an excess of calcine with spent electrolyte. Replacing the zinc sulphate solution with spent electrolyte made possible the use of a large, vented, bottom-discharge mixing tank, which discharged the slurry continuously through an air lift into the classifier. Mild steel plate and rakes were satisfactory in the classifier with the zinc sulphate-calcine slurry. The use of spent electrolyte introduced soluble copper and resulted in severe corrosion. Stain-

less steel rakes were installed first and eventually all exposed parts of the classifier and other equipment were replaced with stainless steel.

Early in 1950, the launder system was replaced by a stainless steel distribution box with rubber hose lines from the box to the individual leaching tanks.

Now the slurry is made in a stainless steel tank where the calcine is mixed with the acid and discharged through the air lift to the classifier. The feeding of the calcine, spent electrolyte, and iron solution is controlled and proportioned automatically. Adequate suction is provided by a small fume scrubber so that the operation is dust and vapor free. About one third of the leaching takes place in this tank. The cementing problem is minimized by the increase in the solution: solid ratio and the reduction in the amount of free zinc oxide present for cement formation.

Thickener underflow was filtered originally on Moore filters. It was found that these filters were unsatisfactory for the new pulp, because the consistency was such that heavier particles settled out in the filter tanks. This had not been the case when the voluminous silica gel was present. Air agitation was not successful in keeping heavier particles in suspension. The cake picked up on the Moore filter dewatered so fast that it was impossible to transfer it to the wash tank before the cake cracked badly. Further, once cracked, portions of the heavy cake, especially around the bottom of the leaves, fell off. Both of these conditions made satisfactory washing impossible.

Therefore, the thickened pulp was pumped directly to the Eimco filters. Filtration was satisfactory but washing was not. A cake in excess of ½ in. was necessary for proper discharge. The water-soluble zinc in such a cake was not removed during the washing time available. Residues high in water-soluble zinc were difficult to dry.

An unforeseen condition of the thickened reverse-leach pulp led to a change in the thickener operation. When this pulp has aged more than 48 hr, it becomes extremely viscous and difficult to filter, and there is a retention of zinc sulphate. The filtrate from an aged pulp will contain less zinc than the solution in which it has thickened. The difference is as much as 60 g per liter zinc. It can be recovered by washing the filter cake with water. The first displacement and as high as the first three displacements of liquor in the filter cake, depending on the time the pulp has aged, will contain more zinc than the original filtrate. An aged pulp requires a large amount of water and much time to wash the filter cake free of zinc sulphate, or in other words, more filter capacity for the same amount of solids.

In making the changes outlined to overcome the difficulties encountered, a very satisfactory and workable process has been developed.

Operations

Calcine, as-received, is fed at a uniform rate from the storage bins into the mixing tank. Return electrolyte is added to maintain a slurry density of about 1.5 sp gr. This density permits classification at 100 mesh. Oversize material is ground in the ball mill and returned to the classifier. A typical screen analysis of the ground slurry is given in Table I. Grinding to smaller particle size does not increase the zinc extraction materially.

Slurry containing 4.5 to 5 tons of equivalent calcine is fed to one of six leaching tanks which will

Table I. Screen Analysis of Ground Slurry

Mesh	Pct
35	Nil
65	1
100	3
150	6
200	10
—200	80

contain a "heel" of return electrolyte just covering the agitator. This is neutralized so rapidly that little or no silica is taken into solution. Slurry addition is timed, 30 min per tank, since the weighing device is set to deliver the calcine for one leach in that time.

Acid containing from 0.5 to 1.0 g per liter iron as ferric sulphate is added to the slurry until a test of the pulp at the top of the tank shows acid to methyl-orange indicator. The acid addition is stopped until the test shows neutral or basic to methyl-orange. Then, more acid is added until a positive test again occurs. This is repeated until the acidity persists for about 3 min, which is the point of maximum zinc extraction, and the leach would be complete except for the presence of ferric sulphate. Precipitation of ferric hydroxide occurs here with the release of some free sulphuric acid which must be neutralized. A small amount of slurry is added. Completeness of iron precipitation is checked with ammonium thiocyanate test papers. Small amounts of ferrous iron are oxidized by compressed air introduced beneath the agitators and dispersed through the leach. The copper required for this reaction originates from the calcine. Ferrous iron occurs only in those calcines which have not been roasted thoroughly.

While satisfactory washing could be attained using a cotton twill filter cover, blinding of the cloth and decreasing filtration rate with time required frequent changes of the cover. In 1948, a nylon filter cover was used for the first time with excellent results. This is a specially woven cloth with tightly twisted yarn in which filtering is only through the fabric openings. The only blinding comes from precipitation of gypsum and this has been largely overcome by the use of low-pressure steam instead of air for the blow-off.

Summed up, the operating difficulties which called for correction because of inability to attain the rated capacity of the plant were:

1. Difficult and slow filtration of the purified solution.
2. Absence of clear overflow from the thickener.
3. Inability to filter and wash residue.
4. Inability to dry residue.
5. Wasteful impounding of residue.
6. Wasteful consumption of sulphuric acid, manganese dioxide, and calcine.

The introduction of "reverse" leaching has made it possible to:

1. Provide an adequate amount of purified solution.
2. Have 8 to 10 ft of clear solution in the secondary thickeners.
3. Filter and wash effectively the entire residue output.
4. Dry all the residue filtered.
5. Stop the impounding of unwashed residue.
6. Cut the consumption of sulphuric acid, manganese dioxide, and calcine.

Metallurgical Reactions of Fluorides

by Herbert H. Kellogg

Graphs representing the standard free-energy of formation as a function of temperature for 21 fluorides are presented, along with estimated values for the standard free-energy of formation of 20 additional fluorides. A few of the many possible uses of these data in metallurgical calculations are discussed, including the fluorination of oxides, sulphides, and chlorides, and the reduction of metal fluorides.

RECENT papers which have presented free-energy data for oxides, sulphides, chlorides, carbonates, sulphates, and silicates in the form of free energy vs. temperature plots,[1-5] have found important uses in teaching and metallurgical development work. This method of presentation of thermodynamic data serves to make available in readily usable form thermodynamic constants which are scattered throughout the literature, and to show by graphical means the stability relations which exist between the compounds of a given type. It is certainly desirable to have these free-energy-temperature diagrams for as many types of compounds as are of present or potential use in metallurgical processes. Thus, even though there are but few uses of metallic fluorides in extractive metallurgy today, the potential uses of fluorine processes are of great importance and serve as the principal justification of this paper.

Recent developments in the production of fluorocarbons have resulted in vastly improved methods for the production and handling of fluorine and corrosive fluorides, with consequent reduction in costs.[6,7] The extractive metallurgist should no longer overlook possible fluorine processes when development of a new process for a relatively high unit-price metal is being considered.

In a previous paper[5] the author outlined in some detail the importance and use of free-energy data in metallurgical calculations and also discussed the properties of a standard free-energy vs. temperature diagram. The same method of presentation is adopted in this paper, and the reader is referred to the earlier work for explanations of the use of free-energy data.

Thermodynamic Data

This paper presents standard free-energy vs. temperature diagrams, Figs. 1 and 2, for those fluorides for which the major thermodynamic constants are known. In the calculations of the standard free-energy of formation (ΔG°), values of the enthalpy of formation at 298°K (ΔH°_f) were taken from "Selected Values of Thermodynamic Constants";[8] most of the values of standard entropy at 298°K (S°_{298}) were taken from "Selected Values",[8] but in a few cases the values given by Kelley[9] were preferred; data for the phase changes came from "Selected Values" and several of Kelley's publications;[9-12] and most of the specific-heat data were taken from Kelley.[10] The appendix gives a detailed list of the sources of the data.

As explained in an earlier paper,[5] the accuracy of some of the standard free-energy relationships is not high. An error of ±1 kcal at 1000°C is expected in most of the curves of Figs. 1 and 2. The error may be as high as ±3 kcal in some of the curves. Rather than attempt to estimate the reliability of each curve, the source of the data used is reported in the appendix, and the reader may compare these data with newer values as they become available.

Figs. 1 and 2 fail to show values for the fluorides of many important metals. In most cases this is because the entropy of the metallic fluoride is unknown. For preliminary calculations it is often useful to have available the best estimate of an unknown datum, rather than no information at all. With this in mind, Table I lists estimated standard free-energy values for a number of important metallic fluorides not included in Figs. 1 and 2. The values reported in Table I were calculated by Brewer et al.[13] and are based on estimated entropy values. The estimated uncertainty of the values for each fluoride were calculated from the uncertainty values given by Brewer[13] for ΔH°_f and the entropy function.

Table I. Estimated Values of Standard Free Energy of Fluorides*

Kilo-calories per Mol of Fluorine

Compound	Temp. °C				Uncertainty, kcal at	
	25°	227°	727°	1227°	227°C	727°C
2AuF	— 28.2	— 23.0	— 18.0		9	13
2HgF	— 79.4	— 70.0			15	
HgF_2	— 83.1	— 74.5			10	
2CuF	—110.4	—104.0	— 92.0	— 78.0 (l)	8	12
2/3 CoF_2	—116.1	—109.0	— 93.4		7	9
CuF_2	—117.6	—110.5	— 95.0		5	6
2/3 BiF_3	—133.3	—125.7			6	
2/3 SbF_3	—135.3	—128.6			4	
2/3 FeF_3	—146.0	—138.2	—122.0	—106.7 (l)	9	10
NiF_2	—147.3	—140.0	—124.6	—108.5	3	5
CoF_2	—147.9	—141.0	—125.0	—108.5 (l)	3	5
2/3 MnF_2	—148.1	—141.0			4	
SnF_2	—148.5	—141.5			5	
FeF_2	—157.6	—150.5	—133.0	—118.5 (l)	3	5
ZnF_2	—165.6	—158.5	—142.0		4	6
2/3 CrF_3	—166.7	—159.3	—143.3	—131.3 (l)	4	6
CrF_2	—171.9	—165.5	—148.0	—137.0 (l)	4	6
1/2 TiF_4	—175.2	—167.8			10	
1/2 ZrF_4	—211.5	—204.0	—187.5		15	16
BeF_2	—216.9	—210.5	—195.0	—183.5 (l)	5	6

* Based on values estimated by Brewer et al.[13] Values are for the solid compounds, except those marked (l), which are for the liquid fluorides. Uncertainty values take into account the uncertainty in ΔS° as well as ΔH°.

HERBERT H. KELLOGG, Member AIME, is Assistant Professor of Mineral Engineering, Columbia University, New York.

Discussion of this paper, TP 3009 D, may be sent to AIME by April 1, 1951. Manuscript received Sept. 8, 1950. St. Louis Meeting, February 1951.

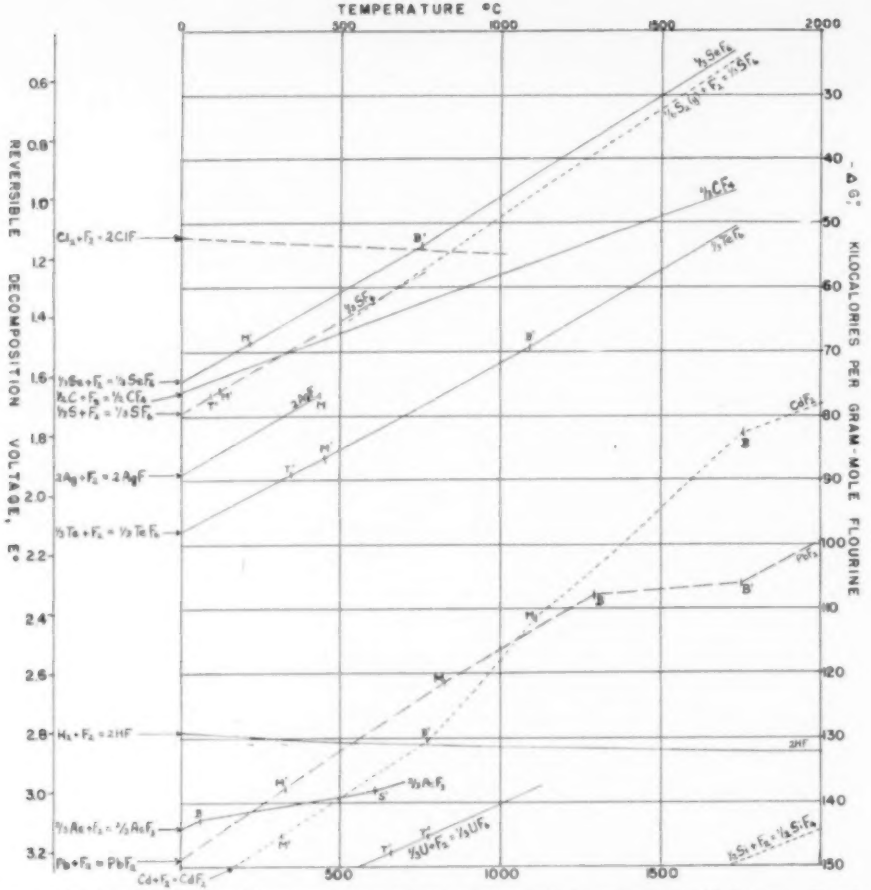

Fig. 1—Standard free energies of formation for metal fluorides as a function of temperature ΔG° between —20 and —150 kcal.

M, B, S, and *T* refer to normal melting, boiling, sublimation, and transition temperatures of the metal fluorides; *M', B', S',* and *T'* refer to the same phase changes for the metal.

Metallurgical Applications

Reduction of Fluorides: It will be recalled that a free-energy vs. temperature diagram such as given in Figs. 1 and 2, is a quantitative affinity series for the compounds listed, which is valid over the temperature range covered. The most stable fluorides are those with the most negative value of the standard free-energy of formation (the alkali and alkaline-earth fluorides at the bottom of Fig. 2). Since the basis for the values reported on Figs. 1 and 2 is 1 mol of fluorine, the subtraction of the value for one fluoride from that of another fluoride, results in the reaction whereby the latter metal replaces the former fluoride to yield the latter fluoride and the former metal. The standard free-energy for this replacement reaction, at any given temperature, is the algebraic sum of the standard free-energies read from Figs. 1 and 2. A negative value for the standard free-energy of any reaction indicates that the reaction is spontaneous when all of the reactants and products are in their standard states.

The positions of the curves on Figs. 1 and 2 (and the data of Table I) show at a glance the possibilities for hydrogen reduction of any given fluoride. The metallic fluorides whose curves lie above the curve for 2HF can be reduced to the metal by hydrogen gas under standard conditions. As the temperature increases the reduction by hydrogen becomes more spontaneous.

A fluoride such as UF_6, whose curve lies slightly below the 2HF curve at 1000°C can be reduced to the metal with hydrogen if the partial pressure of H_2 is kept high and that of HF low, so that the free-energy (ΔG) becomes negative, even though the standard free-energy (ΔG°) is positive (see ref. 5 for details of calculation of ΔG from ΔG°). The fluorides whose curves lie far below the 2HF curve cannot be reduced to the metal by hydrogen under practical conditions.

As with the chlorides, carbon is almost valueless as a reducing agent for metal fluorides. This conclusion is based on the position of the curve for CF_4, which lies far above the curves for most of the

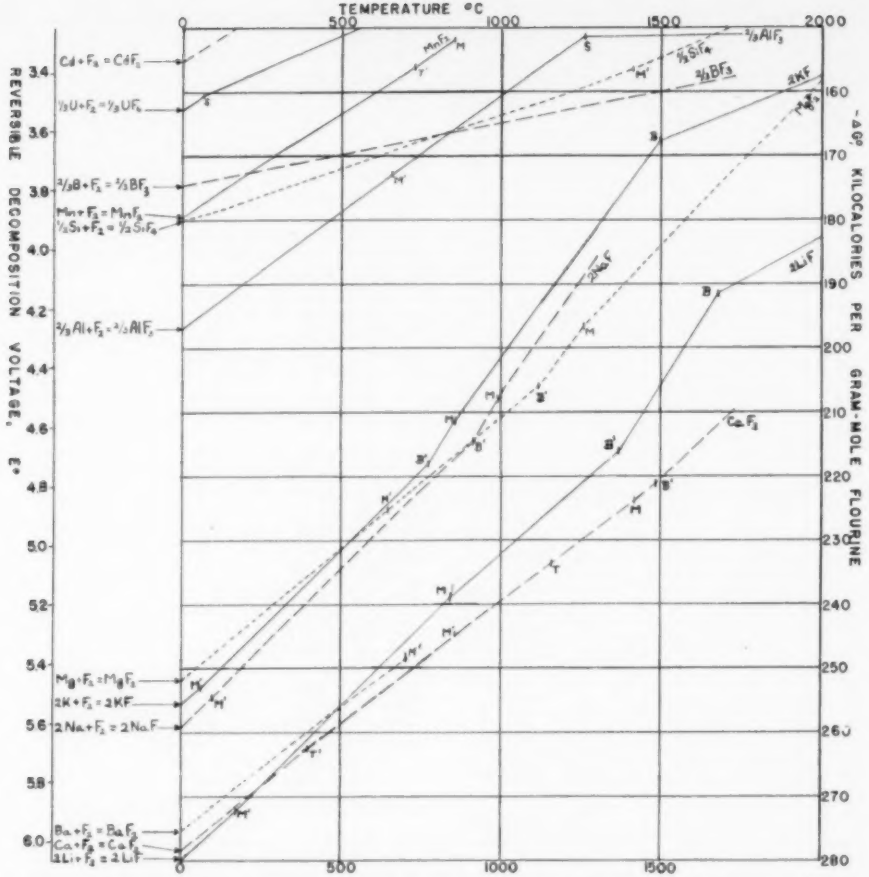

Fig. 2—Standard free energies of formation for metal fluorides as a function of temperature ΔG° between —150 and 280 kcal.

M, B, S, and T refer to normal melting, boiling, sublimation, and transition temperatures of the metal fluorides; M', B', S', and T' refer to the same phase changes for the metal.

other fluorides. Sulphur, selenium, and tellurium are likewise very poor reducing agents for most of the fluorides.

A metal will act as a reducing agent for another metal fluoride, if the curve for the fluoride of the reducing agent lies below the curve for the fluoride to be reduced. Thus, magnesium metal could be used to reduce TiF_4, ZrF_4, SiF_4, etc., in analogy to the Kroll process.[14]

By adjustment of conditions far from the standard states, such as by use of a vacuum process, the direction of many reduction reactions can be reversed. Thus, silicon metal could be used to reduce aluminum fluoride to the metal at 700°C, even though the curve for SiF, lies above the curve for AlF_3 and ΔG° for the reduction reaction is positive.

$$1/2\ Si(s) + 2/3\ AlF_3(s) = 2/3\ Al(l) + 1/2\ SiF_4(g)$$

$$\Delta G^\circ_{700^\circ C} = +171{,}400 - 168{,}400 = +3{,}000\ \text{cal}$$

$$K_{700^\circ C} = 0.212$$

If, for a first approximation, the aluminum and silicon are assumed to remain as pure metals, then:

$$K_{700^\circ C} = 0.212 = \frac{P_{SiF_4}{}^{1/2} \times 1}{1 \times 1}$$

$$P_{SiF_4} = 0.045\ \text{atm} = 34\ \text{mm of Hg}$$

If the reaction were carried out in a vacuum retort, and the pressure kept lower than 34 mm of Hg, the reaction would proceed spontaneously from left to right provided the reaction rate was sufficiently great. For more accurate calculations the alloying of aluminum and silicon would have to be considered.

Electrolysis can be used to reduce any of the fluorides to the metal and fluorine. Figs. 1 and 2 show the reversible decomposition voltage for the electrolysis of the pure fluoride to produce pure metal and fluorine at 1 atm pressure. When the fluoride bath is a mixture of fluorides, appropriate activity corrections must be made to obtain the reversible decomposition voltage under nonstandard conditions (see ref. 5).

In any reaction involving several fluorides, the

possible formation of double fluorides, of which cryolite ($3NaF \cdot AlF_3$) is an example, must be taken into account. Kroll[10] has reported the relative stability of several double fluorides and has shown their importance in fluorine metallurgy. The formation of a double fluoride has the effect of reducing the activity of the individual fluorides in a degree proportional to the stability of the double fluoride.

Fluorination of Oxides, Sulphides, and Chlorides

Tables II, III, and IV list standard free-energies for the type reactions:

$$MO + F_2 = MF_2 + \tfrac{1}{2} O_2 \qquad \text{(Table II)}$$

$$MS + F_2 = MF_2 + \tfrac{1}{2} S_2(g) \qquad \text{(Table III)}$$

$$MCl_2 + F_2 = MF_2 + Cl_2(g) \qquad \text{(Table IV)}$$

The negative values for ΔG° exhibited by all of the reactions in Tables II, III, and IV, indicate that all oxides, sulphides, and chlorides can be fluorinated by fluorine gas under standard conditions. This conclusion emphasizes the unusual stability of the fluorides—they are the most stable general class of compounds.

Despite the fact that the metals and oxides are all thermodynamically unstable with respect to fluorine gas, many metals and certain oxides do not react with dry fluorine gas at room temperature and even higher, because of extremely low reaction rate. Dry fluorine can be handled in glass or silica apparatus at room temperature and somewhat above.[6] Dry fluorine does not appreciably attack steel at 200°C or nickel at 600°C.

When fluorinating a sulphide or chloride with an excess of fluorine gas, the reaction will proceed to the formation of SF_6 and ClF, rather than releasing S_2 and Cl_2 as indicated in Tables III and IV, provided that the reaction rate for the formation of SF_6 or ClF is sufficient at the temperature in question. Thus, the complete reactions will be:

$$\text{(a)}\quad MS + 4F_2 = MF_2 + SF_6$$

$$\text{(b)}\quad MCl_2 + 2F_2 = MF_2 + 2ClF$$

ΔG° for reaction (a) will be more negative (the reaction is more spontaneous) than the values reported in Table III by 198 kcal at 500°C and 147 kcal at 1000°C. The value of ΔG° for reaction (b) will be more negative than the values reported in Table IV by 53.5 kcal at 500°C and 54.8 kcal at 1000°C.

If a limited amount of fluorine gas is used to fluorinate a metal sulphide or chloride, the metal fluoride will be produced rather than the sulphur fluoride or chlorine fluoride, as indicated by the relative stability of the fluorides on Figs. 1 and 2.

Tables II, III, and IV also serve to show standard free-energies of fluorination of the oxides, sulphides, and chlorides by other fluorides. The standard free-energy of fluorination of an oxide by HF is obtained by subtracting eq 3 (Table II) from the equation for

Table II. Fluorination of Oxides by Fluorine Gas*

ΔG° in kilo-calories

Number	Reaction	Temp., °C 25°	500°	1000°
1	$\frac{1}{2} CO_2 + F_2 = \frac{1}{2} CF_4 + \frac{1}{2} O_2$	— 28.7	— 19.8	— 10.8
2†	$\frac{1}{2} TiO_2 + F_2 = \frac{1}{2} TiF_4 + \frac{1}{2} O_2$	— 72.6		
3	$H_2O + F_2 = 2HF + \frac{1}{2} O_2$	— 74.1	— 81.8	— 89.3
4	$1/3\ Al_2O_3 + F_2 = 2/3\ AlF_3 + \frac{1}{2} O_2$	— 74.2	— 67.0	— 59.9
5†	$Cu_2O + F_2 = 2\ CuF + \frac{1}{2} O_2$	— 75.0	— 68.6	— 63.7
6	$\frac{1}{2} SiO_2 + F_2 = \frac{1}{2} SiF_4 + \frac{1}{2} O_2$	— 82.0	— 84.4	— 86.9
7†	$1/3\ Cr_2O_3 + F_2 = 2/3\ CrF_3 + \frac{1}{2} O_2$	— 83.6	— 77.0	— 73.1
8	$Ag_2O + F_2 = 2\ AgF + \frac{1}{2} O_2$	— 86.2		
9†	$\frac{1}{2} ZrO_2 + F_2 = \frac{1}{2} ZrF_4 + \frac{1}{2} O_2$	— 89.0	— 81.6	
10†	$ZnO + F_2 = ZnF_2 + \frac{1}{2} O_2$	— 89.9	— 85.2	
11	$MnO + F_2 = MnF_2 + \frac{1}{2} O_2$	— 92.0	— 84.7	
12†	$NiO + F_2 = NiF_2 + \frac{1}{2} O_2$	—94.7	— 88.7	— 83.5
13†	$CoO + F_2 = CoF_2 + \frac{1}{2} O_2$	— 97.2	— 89.6	— 82.2
14	$CdO + F_2 = CdF_2 + \frac{1}{2} O_2$	— 97.5	— 95.4	— 94.6
15	$1/3\ As_2O_3 + F_2 = 2/3\ AsF_3 + \frac{1}{2} O_2$	— 98.2	—101.1	
16†	$FeO + F_2 = FeF_2 + \frac{1}{2} O_2$	—100.0	— 90.5	— 81.7
17	$PbO + F_2 = PbF_2 + \frac{1}{2} O_2$	—103.0	— 96.8	— 90.8
18	$MgO + F_2 = MgF_2 + \frac{1}{2} O_2$	—112.4	—103.8	— 96.6
19	$CaO + F_2 = CaF_2 + \frac{1}{2} O_2$	—133.3	—125.5	—118.4
20	$BaO + F_2 = BaF_2 + \frac{1}{2} O_2$	—148.9	—141.0	
21	$Na_2O + F_2 = 2\ NaF + \frac{1}{2} O_2$	—169.1	—159.7	—151.3
22	$K_2O + F_2 = 2\ KF + \frac{1}{2} O_2$	—179.1	—170.9	

* Data for fluorides from Figs. 1 and 2 and Table I. Data for Al_2O_3, CaO, CO_2, H_2O, MgO, MnO, SiO_2, Na_2O, TiO_2, Cr_2O_3, CoO, Cu_2O, FeO, from Richardson and Jeffes.[3] Data for Ag_2O, CdO, from Dannatt and Ellingham.[2] Data for NiO, ZnO, PbO, As_2O_3, K_2O, BaO, ZrO_2 from Osborn.[1] Standard states are $F_2(g)$ and $O_2(g)$ at 1 atm, and the forms of the oxide and fluoride which are stable (at 1 atm pressure) at the temperature in question.

† Based on estimated value for standard free-energy of formation of the fluoride.

Table III. Fluorination of Sulphides by Fluorine Gas*

ΔG° in kilo-calories

Number	Reaction	Temp. °C 25°	500°	1000°
1	$1/2\ CS_2 + F_2 = 1/2\ CF_4 + 1/2\ S_2$	— 73.6	— 64.9	— 55.7
2†	$Cu_2S + F_2 = 2CuF + 1/2\ S_2$	— 80.9	— 73.1	— 64.2
3†	$ZnS + F_2 = ZnF_2 + 1/2\ S_2$	—108.5	—103.2	
4	$H_2S + F_2 = 2HF + 1/2\ S_2$	—111.4	—118.3	—124.9
5	$CdS + F_2 = CdF_2 + 1/2\ S_2$	—111.6	—106.3	—102.5
6	$PbS + F_2 = PbF_2 + 1/2\ S_2$	—115.7	—108.7	—103.3
7†	$NiS + F_2 = NiF_2 + 1/2\ S_2$	—116.7	—106.6	— 97.9
8†	$FeS + F_2 = FeF_2 + 1/2\ S_2$	—125.1	—114.3	—105.0
9	$MnS + F_2 = MnF_2 + 1/2\ S_2$	—139.4	—131.2	
10	$CaS + F_2 = CaF_2 + 1/2\ S_2$	—158.0	—149.9	—142.3

* Data for fluorides from Figs. 1 and 2 and Table I. Data for CdS, FeS, Cu_2S, and CS_2 from Dannatt and Ellingham.[2] Data for ZnS, H_2S, PbS, NiS, MnS, and CaS from Osborn.[1] Standard states are $F_2(g)$ and $S_2(g)$ at 1 atm, and the forms of the sulphide and fluoride which are stable (at 1 atm pressure) at the temperature in question.

† Based on estimated value for standard free-energy of formation of the fluoride.

Table IV. Fluorination of Chlorides by Fluorine Gas*

ΔG° in kilo-calories

Number	Reaction	Temp. °C 25°	500°	1000°
1	$2\ AgCl + F_2 = 2\ AgF + Cl_2$	— 36.1		
2†	$HgCl_2 + F_2 = HgF_2 + Cl_2$	— 39.3		
3†	$Cu_2Cl_2 + F_2 = 2\ CuF + Cl_2$	— 54.0	— 53.5	— 51.1
4	$1/2\ C\ Cl_4 + F_2 = 1/2\ CF_4 + Cl_2$	— 67.5	— 67.5	
5	$CdCl_2 + F_2 = CdF_2 + Cl_2$	— 72.7	— 74.2	— 71.9
6	$PbCl_2 + F_2 = PbF_2 + Cl_2$	— 73.0	— 73.4	— 68.2
7	$2/3\ AlCl_3(g) + F_2 = 2/3\ AlF_3(s) + Cl_2$			— 69.3
8	$MnCl_2 + F_2 = MnF_2 + Cl_2$	— 73.2	— 72.7	
9	$2\ NaCl + F_2 = 2\ NaF + Cl_2$	— 74.4	— 71.7	— 66.6
10†	$SnCl_2 + F_2 = SnF_2 + Cl_2$	— 75.6		
11†	$ZnCl_2 + F_2 = ZnF_2 + Cl_2$	— 77.2	— 75.4	
12†	$CoCl_2 + F_2 = CoF_2 + Cl_2$	— 80.3	— 80.3	— 77.4
13†	$NiCl_2 + F_2 = NiF_2 + Cl_2$	— 82.2	— 81.8	— 81.4
14†	$2/3\ BiCl_3 + F_2 = 2/3\ BiF_3 + Cl_2$	— 82.5		
15	$2\ HCl + F_2 = 2HF + Cl_2$	— 83.6	— 83.1	— 82.4
16†	$2/3\ SbCl_3 + F_2 = 2/3\ SbF_3 + Cl_2$	— 83.7		
17†	$FeCl_2 + F_2 = FeF_2 + Cl_2$	— 85.3	— 83.0	— 76.5
18†	$CrCl_2 + F_2 = CrF_2 + Cl_2$	— 86.4	— 84.9	— 81.7
19†	$1/2\ TiCl_4 + F_2 = 1/2\ TiF_4 + Cl_2$	— 93.5		
20	$1/3\ AlCl_3 + F_2 = 2/3\ AlF_3 + Cl_2$	— 94.6	— 85.3	
21	$2/3\ AsCl_3 + F_2 = 2/3\ AsF_3 + Cl_2$	— 96.1	— 96.7	
22	$CaCl_2 + F_2 = CaF_2 + Cl_2$	— 97.7	— 95.0	— 90.9
23†	$1/2\ ZrCl_4 + F_2 = 1/2\ ZrF_4 + Cl_2$	—107.2	—102.9	
24	$MgCl_2 + F_2 = MgF_2 + Cl_2$	—109.4	—107.9	—102.8
25	$1/2\ SiCl_4 + F_2 = 1/2\ SiF_4 + Cl_2$	—111.1	—111.4	—111.0
26	$2/3\ BCl_3 + F_2 = 2/3\ BF_3 + Cl_2$	—113.6	—112.8	—111.7
27†	$BeCl_2 + F_2 = BeF_2 + Cl_2$	—116.1		

* Data for fluorides from Figs. 1 and 2 and Table I. Data for chlorides from Kellogg.[5] Standard states are $F_2(g)$ and $Cl_2(g)$ at 1 atm, and the forms of the chloride and fluoride which are stable (at 1 atm pressure) at the temperature in question.

† Based on estimated value for the standard free-energy of formation of the fluoride.

the oxide. Thus, for the fluorination of MgO by HF at 500°C, we have:

		$\Delta G°$ 500°C
Reaction 18	$MgO + F_2 = MgF_2 + 1/2\ O_2$	—103.8
Reaction 3	$H_2O + F_2 = 2HF + 1/2\ O_2$	— 81.8
Reaction 18 minus Reaction 3	$MgO + 2HF = MgF_2 + H_2O$	— 22.0 kcal

And for fluorination of MgO by FeF_2, we have:

		$\Delta G°$ 500°C
Reaction 18	$MgO + F_2 = MgF_2 + 1/2\ O_2$	—103.8
Reaction 16	$FeO + F_2 = FeF_2 + 1/2\ O_2$	— 90.5
Reaction 18 minus Reaction 16	$MgO + FeF_2 = MgF_2 + FeO$	— 13.3 kcal

In general, fluorination of an oxide by a fluoride will be spontaneous, under standard conditions, if the equation for the oxide on Table II has a more negative value of $\Delta G°$, than does the equation for the fluorinating agent. Thus, the fluorides at the top of Table II are the strongest fluorinating agents.

The free-energy of fluorination of sulphides and chlorides by metal fluorides can be derived from Tables III and IV in a similar manner.

One interesting application of the fluorination of oxides by hydrogen fluoride is afforded by the phosphate processing industry. In the thermal processing of phosphate rock to produce fused tricalcium phosphate, the fluorine content of the rock is driven off as hydrogen fluoride and enters the stack gases. A process for the recovery of the hydrogen fluoride from stack gases has recently been described.[10] The essential feature of the process is the reaction of the HF with a bed of crushed limestone at room temperature. The reaction is:

$$\text{(a)}\quad CaCO_3 + 2HF = CaF_2 + H_2O + CO_2$$

The standard free-energy of this reaction at 25°C can be obtained by combination of the data of Table II with the data on the decomposition of $CaCO_3$ given by Osborn.[4] The result is:

$$\Delta G°_{25°C} \text{ for reaction (a)} = -28{,}100 \text{ cal.}$$

The reaction is therefore spontaneous under standard conditions, and the reaction rate is fast enough to allow efficient absorption of the HF.[10]

When producing superphosphate the evolved fluorine is principally in the form of SiF_4,[17] and it is interesting to see whether limestone could be used to absorb this gas. The reaction would be:

$$\text{(b)}\quad CaCO_3 + \tfrac{1}{2}SiF_4(g) = \tfrac{1}{2}\ SiO_2 + CaF_2 + CO_2(g)$$

Combination of the data of Table II with that of Osborn[4] yields:

$$\Delta G°_{25°C} \text{ for reaction (b)} = -20{,}200$$

This reaction is also spontaneous at room temperature; its rate characteristics have not been reported.

Summary

The uses of fluorine and fluorides in extractive metallurgy today are very few. However, it is reasonable to expect that the increased "know-how" in handling of fluorine and fluorides, the availability of large quantities of fluorine at relatively low prices, and the unusual properties of many of the metallic fluorides will result in new metallurgical processes.

The free-energy values reported in this paper can serve as a valuable tool in any exploratory work in fluorine metallurgy. The importance and use of thermodynamic data in metallurgical calculations have not been discussed in this paper, but will be found in an earlier paper,[5] or in any textbook on thermodynamics.

Acknowledgment

The author is indebted and grateful to Jane Breckwoldt, Research Associate in Mineral Engineering, who performed duplicate calculations for all the material shown on Figs. 1 and 2.

Appendix

Sources of Thermodynamic Data for Figs. 1 and 2

Numbers refer to references at end of paper

	Fluoride				Metal		
	$S°_{298}$	$\Delta H°_{f298}$	Phase Changes	Specific Heat	$S°_{298}$	Phase Changes	Specific Heat
AgF	8	8		[a]	8	10	10
AlF_3	8	8	8	10[b]	8	10	10
AsF_3	8	8	8	8,10	8	8	10[c]
BF_3	8	8		10	8		10
BaF_2	9	8		10	9		10
CF_4	8	8		10	8		10
CaF_2	9	8	10	10	9	10,11,12	10,12
CdF_2	8	8	8	[a]	8	8	10,12
ClF	8	8		[f]	8		[f]
HF	8	8		10	8		10
KF	13	8	10,12	10	9	10,12	10,12
LiF	9	8	8	10[c]	8	8,12	10,12
MgF_2	8	8	8	10	8	8	10,12
MnF_2	8	8		[a]	8	8	10
NaF	9	8	10,12	10	9	10,12	10,12
PbF	8	8	8	10[c]	8	8	10,12
SF_6	8	8		10	8,9	10,8	10
SeF_6	8	8		10	8	8	10
SiF_4	8	8		10	8	8	10
TeF_6	8	8		10	8	8	10[d]
UF_6	8	8	8	19	8	10	10

[a] Estimated.
[b] Neglect ΔCp above 1530°K.
[c] Neglect ΔCp above 883°K.
[d] Estimated Cp for liquid.
[e] Estimated Cp for liquid and gaseous forms.
[f] Neglect ΔCp.

References

[1] H. J. T. Ellingham: *Journal* Soc. Chem. Ind. (London) (May 1944) p. 125.
[2] C. W. Dannatt and H. J. T. Ellingham: Discussion Faraday Soc. (1948) **4**, p. 126.
[3] F. D. Richardson and J. H. E. Jeffes: *Journal* Iron and Steel Inst. (1948) **160**, p. 261.
[4] C. J. Osborn: *Trans.* AIME (1950) **188**, p. 600; JOURNAL OF METALS (March 1950) TP 2720CDE.
[5] H. H. Kellogg: *Trans.* AIME (1950) **188**, p. 862; JOURNAL OF METALS (June 1950) TP 2869D.
[6] A. J. Rudge: *Chem. and Ind.* (1949) pp. 247-253.
[7] Symposium on Fluorine Chemistry: *Industrial Engineering Chemistry* (1947) **39**, pp. 360-434.
[8] Selected Values of Chemical Thermodynamic Properties. National Bureau Standards. Published in installments beginning March 31, 1947.
[9] K. K. Kelley: U. S. Bureau Mines *Bulletin* 477 (1950).
[10] K. K. Kelley: U. S. Bureau Mines *Bulletin* 476 (1949).
[11] K. K. Kelley: U. S. Bureau Mines *Bulletin* 393 (1936).
[12] K. K. Kelley: U. S. Bureau Mines *Bulletin* 383 (1935).
[13] Chemistry and Metallurgy of Miscellaneous Materials. Edited by L. L. Quill. McGraw-Hill Book Co., Inc. (1950).
[14] W. J. Kroll: *Trans.* Electrochem. Soc. (1940) **78**, pp. 35-37.
[15] W. J. Kroll: *Metall u. Erz.* (1940) **37**, pp. 63-67.
[16] T. P. Hignett and M. R. Siegel: *Industrial Engineering Chemistry* (1949) **41**, pp. 2493-2498.
[17] G. C. Finger and F. H. Reed: *Chemical Industry* (1949) **64**, pp. 51-56.
[18] E. F. Westrum, Jr. and K. S. Pitzer: *Journal* Amer. Chem. Soc. (1949) **71**, pp. 1940-1949.
[19] J. Bigeleisen and M. G. Mayer: *Journal Chem. Phys.* (1948) **16**, pp. 442-445.

Cobalt Self-Diffusion: A Study of the Method Of Decrease in Surface Activity

by R. C. Ruder and

C. E. Birchenall

The method of decrease in surface activity was used to determine the rates of diffusion of Co^{60} into cobalt and into nickel. Since the absorption curves for cobalt radiation were quite complex under the conditions of these experiments, the effects of geometry and surface preparation on the diffusion results were investigated. The cobalt self-diffusion coefficients obey the equation

$$D^{Co}_{Co} = e^{-45000/RT} \text{ cm}^2 \text{ per sec.}$$

For dilute cobalt diffusing in nickel,

$$D^{Co}_{Ni} = 1.46\, e^{-45000/RT} \text{ cm}^2 \text{ per sec.}$$

AS part of the general program to measure the self-diffusion and dilute-solution diffusion rates of the iron-group metals, the diffusion coefficients of cobalt into cobalt and nickel have been measured using the radioactive isotope Co^{60}. Self-diffusion studies in iron have been previously reported by Birchenall and Mehl.[1] The technique of measurement used was the decrease in surface activity method described by Steigman, Shockley, and Nix.[2] It has been determined that scattering of the measured beta radiation by the specimen matrix is significantly influenced by the condition of the surface and the counting geometry. Accurate diffusion coefficients can be calculated from the activity data provided that the specimens have plane diffusion surfaces and that the absorption properties of the emitted radiation are determined under geometrical conditions duplicating with external absorbers the absorption and scattering in a thin film at the specimen surface as nearly as possible.

The cobalt used in this research was originally in the form of hydrogen reduced rondels 99.9+ pct pure. The nickel had been prepared by the carbonyl process and was found by spectrographic analysis to contain 0.03 pct Fe, 0.04 pct Co and smaller traces of other metallic elements for a balance purity of 99.9+ pct Ni. Both materials were vacuum melted and cast in rectangular ingots. Specimens $\frac{7}{8} \times \frac{7}{8} \times \frac{1}{4}$ in. were machined from these ingots. The specimens were then ground to 4-0 emery paper and annealed in hydrogen for at least a day at 1200°C. Some of the specimens were used in preliminary experimentation after which their diffusion faces were machined to remove the radioactive material from the previous diffusion experiments. After grinding, the specimens were polished using an electrolytic lapping technique described by Mazia.[3] This lapping was continued until at least 0.005 in. was removed from the diffusion surface. The final surfaces were metallographically smooth except for a few fine scratches caused by the glass cloth. A large percentage of the area was undisturbed as determined by microscopic examination.

The grain diameters of the diffusion specimens varied from 0.1 to 5 mm. There were no effects due to grain boundary diffusion in the experiments

R. C. RUDER, Pigments Dept., E. I. duPont de Nemours and Co., Wilmington, Del., was formerly Graduate Student, Carnegie Institute of Technology; and C. E. BIRCHENALL, Member AIME, is Member of Staff, Metals Research Lab, Carnegie Institute of Technology, Pittsburgh.

Discussion of this paper, TP 3004 E, may be sent (2 copies) to AIME by April 1, 1951. Manuscript, Oct. 16, 1950, revision Dec. 13, 1950. St. Louis Meeting, February 1951.

This paper represents part of a thesis submitted by R. C. Ruder in partial fulfillment of requirements for the degree of Doctor of Science to the Graduate Committee of the Carnegie Institute of Technology.

reported here. Probably none should be expected for the grain sizes and temperatures employed.

Cobalt, containing radioactive Co^{60}, was plated on the diffusion surfaces from a cobalt sulphate solution made slightly basic with ammonium hydroxide. From specific activity calculations the plated film was of the order of 10^{-7} cm thick. The active cobalt was removed from the edges of the specimens and from the diffusion surfaces for a distance of at least $\frac{1}{8}$ in. from the edge. Each diffusion experiment consisted of two specimens placed in an iron boat with their diffusion faces together in order to minimize the loss of the active cobalt through evaporation during the high-temperature anneal. Autoradiographs were made of the diffusion surfaces before and after the diffusion anneals. There was no evidence of any change in the surface distribution of the activity due either to evaporation or surface diffusion. Lateral diffusion was too small to produce a significant change in geometry.

The diffusion anneals were carried out in an atmosphere of hydrogen from which oxygen was removed by hot platinized asbestos, followed by drying over activated alumina. In addition, the presence of powdered iron and the iron of the supporting boat removed the final traces of oxygen in the furnace tube. There was no visible oxidation of the diffusion specimens. The temperature was automatically controlled to ±2°C. In addition, the furnace temperature close to the specimens was checked frequently during the diffusion experiments. The temperature of the specimens was recorded during the heating and cooling of the furnaces, and appropriate correction was made if there was appreciable diffusion occurring during these periods.

The specimens, having nearly equal activities, were counted before and after the diffusion anneals using an argon filled self-quenching tube mounted in a lead counting safe. Counting was continued for times long enough to reduce the statistical counting error well below 1 pct. Relative counting rates were calculated with reference to a standard specimen which was counted frequently during the activity measurements. Appropriate correction was made for background and coincidence errors. At least three counts were made on each specimen to reduce systematic errors in counting rate due to climatic conditions. Agreement within 1 pct was considered satisfactory. Absorption measurements, using nickel, aluminum, and cobalt absorbers, were made on individual specimens before and after diffusion and under various geometric conditions. Details will be considered later.

Calculation of Diffusion Coefficient

Due to the form of the absorption curve, it is impossible to use an analytical method of computing the diffusion coefficient. A graphical integration was required. The diffusion of an infinitely thin layer of one atomic species into a semi-infinite solid of another may be represented by a function of the form:

$$C = \frac{C_o}{\sqrt{\pi\, Dt}}\, e^{-\frac{x^2}{4Dt}}$$

which is the solution of Fick's law appropriate to the boundary conditions, where C is the concentration of the first species of atom at a distance x from the diffusion interface. C_o is the total amount of the first species. D is the diffusion coefficient, and t is the time of the diffusion anneal. The distribution in x is therefore determined by the product Dt. The radiation detected at the surface of the specimen after diffusion from the active material at a distance x from the surface is obtained from the experimentally determined absorption curve. The ratio of the activities after and before diffusion is therefore the integral from the diffusion interface to a point effectively at an infinite distance into the specimen of the product of the concentration-distance function and the absorption-distance function, divided by the integral of the concentration-distance function. Since the activity ratio is a function of the Dt product, this graphical process was carried out for a number of Dt products, and the resulting function of activity ratio vs. Dt was used to calculate the diffusion coefficient by interpolation. Since this function is appropriate to the tracer and geometry used in these experiments only, it is not presented.

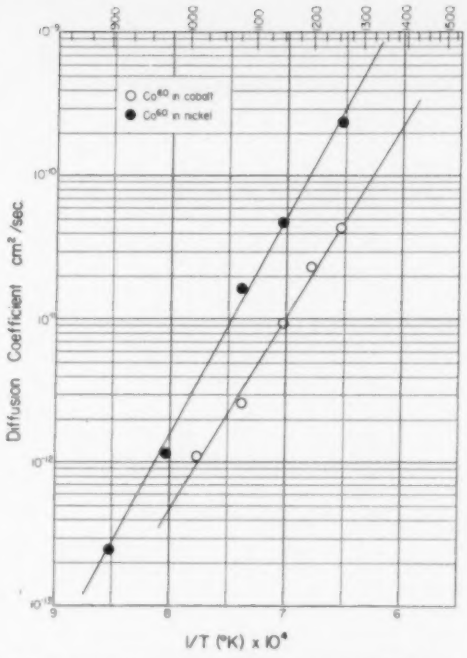

Fig. 1—Temperature dependence of diffusion coefficients for cobalt self-diffusion and for dilute cobalt diffusing in nickel.

The results of these experiments are given in Fig. 1. The standard deviation of the plotted points from the best least square straight line is about 15 pct, which from calculated errors arising from the observed statistical distribution of the counting rates, errors in absorption measurement and variations in temperature measurement, may be considered satisfactory. For cobalt self-diffusion:

$$D = 0.032 \exp\left(\frac{61.9 \pm 3.5}{RT}\right) \text{cm}^2 \text{ per sec}$$

while for very dilute cobalt diffusing into nickel:

$$D = 1.46 \exp\left(\frac{68.3 \pm 2.0}{RT}\right) \text{cm}^2 \text{ per sec.}$$

Here the activation energies are expressed in kcal

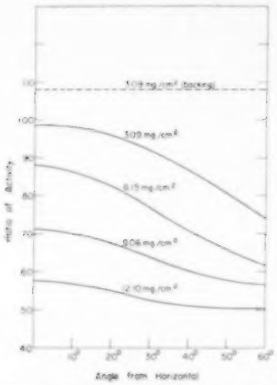

Fig. 2—Ratio of activity of a point source of Co^{60} under an absorber which makes an angle θ with the horizontal plane to the activity of the same source under no absorber.

An exponential correction has been applied for the effectively greater thickness of the absorber due to rotation.

per mol. Cobalt does not show evidence of a change in the diffusion behavior at the Curie point. Nor is there a change at any other temperature in the measured range which might be considered as evidence of a high-temperature phase transformation.

Absorption and Scattering of Beta Particles*

An understanding of absorption and scattering processes is critical for the evaluation of diffusion data by the method of decrease in surface activity. Novey and Elliott[4] and Burtt[5] found maxima in absorption curves when the source was some distance from the detector. The latter also found that the maxima disappeared if the absorbers were placed close to the counting tube rather than close to the source. Willard and Johnston[6] studied the effect of moving an absorber from tube window toward the source using both randomly directed and collimated radiation. The 1.69 mev. maximum energy beta radiation from P^{32} and the 1.1 and 1.3 mev. gamma rays from Co^{60} were used. When the radiation was collimated to allow detection of only those rays going directly from source to counter, the effect of moving the absorber from the tube toward the source was to decrease the counting rate for both gamma and beta radiation, though the effect was much stronger for betas. When the collimator was removed, permitting detection of particles scattered into the solid angle subtended by the tube although their original directions lay outside that angle, the effect of moving the absorber from the tube toward the source was to increase the counting rate about the same amount for both beta and gamma radiations.

These experiments rule out the possibility that the effect could be caused by the creation of secondary radiation and give preliminary indication that the scattering effects are large and significant. The effects could be described in terms of a change in the angular distribution of the radiation as it passes through absorber which also acts as a scattering source. This change in angular distribution would be one in which the component of intensity of the radiation perpendicular to the plane of the absorber is increased at the expense of the component parallel to the absorber plane.

In order to study this angular distribution change as a function of absorber thickness for both front and back scattering, a point source of Co^{60} radiation was placed at the center of a very thin Formvar film mounted in a 1-in. diam hole in a thin aluminum sheet. Absorbers could be attached on either side of the radiation source, and the sheet and absorbers could be rotated with respect to the counter. Measurements were made only to 60° on either side of the original horizontal position to avoid possible effects of scattering by the supporting plate and absorber holders. The point source was on the axis of rotation.

As the angle was increased, the effective absorber thickness increased such that if the angle between the normal to the absorber plane and the direction of the detector was θ, the effective thickness was $x \sec \theta$, where x was the sheet thickness. From the observation that when absorption measurements were made with the source and absorber close to the tube window the absorption was approximately exponential, correction for this increase in thickness was made.

Due to the fact that the active source had to be

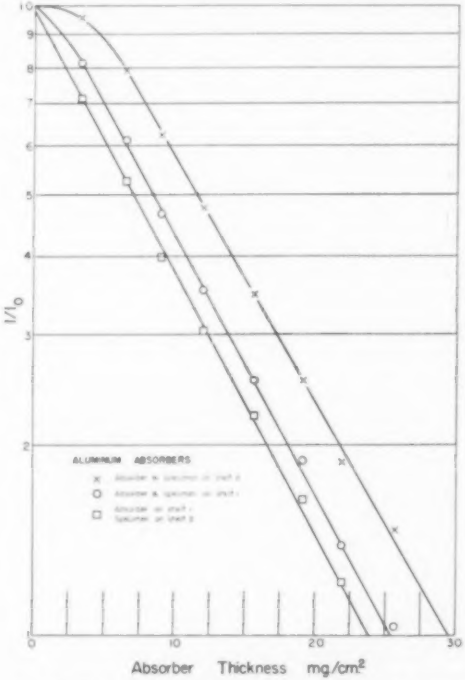

Fig. 3—Effect of counting geometry on the absorption curves obtained on diffusion disks with Co^{60} activity on the surface.

* We were unaware at the time this paper was submitted for publication of the experimental determination of the angular distribution of absorbed P^{32} radiation performed by Yaffe and Justus (L. Yaffe and K. M. Justus: *Journal* Chem. Soc., London, Supplementary Issue No. 2, 1949). It is most interesting to have confirming evidence of his anisotropy with beta radiation from a different source. Our conclusion that back scattering is isotropic is confirmed by these authors only for thin back scatterers. Their results show an increase in anisotropy as the back scatterer becomes thicker. However, as this anisotropy is small compared to the forward scattering anisotropy, the basic argument used in our paper is still valid.

mixed with a small amount of rubber cement to fix the position on the Formvar film, there was a small and irregular variation in the distribution of the radiation. However, the results of the angular distribution measurement shown in Fig. 2 give the ratio of the activities with and without absorber for each position and this irregularity cancels out. The top curve is the result of the back-scattering measurements while the four lower curves give the results of forward scattering for increasing absorber thicknesses. The back-scattering process shows no variation in angular distribution caused by the presence of the backing absorber. The forward-scattering curves show that the effect is greatest for the thinner absorbers and becomes less as the absorber thickness is increased.

On the basis of these measurements, it is possible to understand the dependence of the absorption measurements on the counting geometry. For some solid angle comprising a cone with the axis of rotation normal to the absorber, the number of detected particles will be proportionately greater than were originally in that solid angle before the scattering process. For regions outside of this solid angle, the scattering process will cause a relative depletion in the number of particles. If the counting tube is situated at such a distance that it detects only this critical solid angle, or part of it, the relative counting rate will increase as the absorber thickness increases. However, as Fig. 2 shows that the change in angular distribution becomes less as the absorber thickness increases, the decrease in the counting rates caused by the absorption processes becomes the important factor and the absorption curve becomes more nearly characteristic of the absorption processes alone. If the specimen is located closer to the counting tube, the region detected will include an increasing amount of the loss region and the net effects of scattering are more nearly cancelled out. The optimum geometry is obviously obtained by internal sample counting. If this is impossible, the sample should be brought as close to the tube as conditions permit.

In diffusion measurements the sample itself acts as absorber and scatterer. Therefore it is necessary to measure absorption curves with the absorber as close to the sample as possible to reproduce this condition. The curves in Fig. 3 illustrate these effects. The first counting shelf was located at a distance of 0.729 cm from the tube window while the second shelf was located at a distance of 3.64 cm. The lower curve shows the effect of placing the absorber on the first shelf and the specimen on the second. The lowering of this curve is caused by the collimation of the incident beam by the aluminum shelf which supported the absorber.

Effect of Surface Irregularities

Because of the scattering of electrons, detailed consideration of the diffusion process at the surface of the specimen is necessary. These irregularities may be due to abraiding, chemical etching, or thermal etching of the surface during the diffusion anneals. The detailed consideration for any particular case would of course depend on the exact form of the surface. However, the general situation may be visualized by consideration of a simple case which should provide the worst scattering effects. This will consist of triangular grooves of such steepness that the normals to the microsurfaces form angles with the normal to the macrosurface which exceed the angle of increased activity due to scattering. Analytical solution of the diffusion equation even for this simplified case is difficult, but a qualitative consideration of the diffusion into this type of surface will suffice.

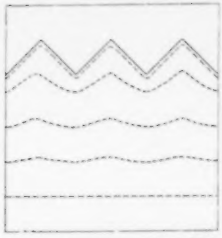

Fig. 4—Iso-concentration lines for different degrees of diffusion penetration into an irregular surface.

As the active atoms first diffuse into the base metal, iso-concentration lines will originally follow the microsurfaces. As diffusion progresses, the iso-concentration lines will begin to approximate the macrosurface and will become essentially parallel to it when the diffusion distances are large with respect to the surface irregularities. This sequence of events is shown schematically in Fig. 4. This, together with consideration of the scattering behavior, will permit discussion of the effects of the surface irregularities on the emitted radiation. The initial active film which is of the order of atomic dimensions will not scatter the radiation to an appreciable extent. Further, backscattering from the irregular surface will not cause a change in the angular distribution of the radiation. Therefore, the deposited layer will emit isotropically. As the active atoms diffuse into the surface, there will be a comparatively large decrease in the measured activity since the radiation will be scattered away from the detector in the direction of the normals to the microsurfaces. As diffusion progresses, the directions of maximum intensity will move from the normals of the microsurfaces in the direction of the normal to the macrosurface and will eventually coincide with it.

The correctness of this picture may be checked experimentally in at least three ways: First, by comparison of diffusion coefficients from specimens with differing surfaces. Three series of experiments were performed which may be compared by consideration of the diffusion coefficients at the same temperature, 1000°C. The first series was abraided with 4-0 emery paper; the second was etched in hot concentrated hydrochloric acid; and the third was electrolytically lapped. This is a sequence of increasing smoothness. The comparison of the apparent cobalt self-diffusion coefficients at 1000°C, calculated on the assumption of plane surfaces, is given in Table I.

It will be observed that the rougher surfaces give the higher rates of diffusion. In order to evaluate the significance of the results, it is necessary to remember that the absorption curves used in the calculation of the diffusion coefficients represent the combined effects of absorption and scattering in a plane parallel film of metal of radiation from an emitting source where the angular distribution of the radiation is isotropic. If there is any scattering of the radiation away from the normal to the macro-

surface, this will be equivalent to higher absorption in the specimen, indicating a greater depth of penetration and a higher rate of diffusion. As diffusion into polished surfaces most nearly duplicates the assumed conditions only the work done on these surfaces is presented as representing the true diffusion rates.†

The second check on the validity of the above picture is the dependence of the calculated diffusion coefficients on the amount of diffusion as measured by the ratio of activity of the specimens after and before diffusion for specimens with irregular surfaces. As there is an initial scattering of the radiation away from the normal to the macrosurface which becomes less as diffusion proceeds, the calculated diffusion coefficients should be high after short times and decrease as the activity ratio decreases. This conclusion was experimentally verified by interrupting the diffusion process at various times for activity measurements. Table II shows the results on a cobalt specimen pair with etched surfaces diffused for increasing times at 1000°C.

The third check is provided by comparison of diffusion coefficients calculated from activity ratios measured at different distances from the tube using absorption measurements made at those distances. Two cobalt specimens were diffused at 970°C for 4.93×10^5 sec. The activity ratios and calculated diffusion coefficients are shown in Table III.

Although the measured activity ratios are quite different using the two geometries, the diffusion coefficients calculated using the absorption curve appropriate to each geometry show good agreement.

Much work remains to be done in order to fully understand and interpret this scattering effect. As only one radiation source was used in these experiments, the effect of such variables as particle energy is not known. However, as this method of measuring diffusion coefficients provides a more rapid and potentially more accurate technique for low diffusion rates than the conventional sectioning methods, further investigation of these scattering phenomena should be of great interest.

Table I. Cobalt Self-diffusion Coefficients at 1000°C

Abraided	5×10^{-12} cm² per sec
Etched	2.4×10^{-12} cm² per sec
Electropolished	0.7×10^{-12} cm² per sec

Table II. Activity Measurements of a Cobalt Specimen Pair

Time, sec x 10^{-5}	Activity Ratio	Apparent Diffusion Coefficient cm² per sec x 10^{12}
0.2688	0.850	4.78
0.9162	0.757	3.93
2.033	0.674	2.94
3.823	0.595	2.58

Table III. Activity Ratios and Calculated Diffusion Coefficients of Two Cobalt Specimens

	Shelf One		Shelf Two	
Specimen	Activity Ratio	Diffusion Coefficient, cm² per sec x 10^{12}	Activity Ratio	Diffusion Coefficient, cm² per sec x 10^{12}
13	0.544	1.29	0.672	1.23
14	0.510	1.64	0.616	1.76
avg.	0.527	1.45	0.644	1.48

Much work remains to be done in order to fully understand and interpret this scattering effect. As only one radiation source was used in these experiments, the effect of such variables as particle energy is not known. However, as this method of measuring diffusion coefficients provides a more rapid and potentially more accurate technique for low diffusion rates than the conventional sectioning methods, further investigation of these scattering phenomena should be of great interest.

Summary

The cobalt self-diffusion coefficients have been measured using the decrease in surface activity method and found to satisfy the equation:

$$D = 0.032 \exp\left(\frac{61.9 \pm 3.5}{RT}\right) \text{cm}^2 \text{ per sec}$$

The diffusion coefficients for very dilute cobalt in nickel measured in the same way have been found to satisfy the equation:

$$D = 1.46 \exp\left(\frac{68.3 \pm 2.0}{RT}\right) \text{cm}^2 \text{ per sec}$$

(The activation energies are in kcal per mol.)

Scattering of the beta radiation was measured and found to influence the calculated diffusion coefficients to a very significant extent.

Acknowledgments

The authors wish to express their gratitude to the Office of Naval Research for the support of this work, to R. F. Mehl for numerous discussions during the course of these studies, and to L. F. Gronholz and J. Ferrin for much of the radioactive counting. The Co^{60} used in these experiments was obtained from the Isotopes Division, U. S. Atomic Energy Commission.

References

[1] C. E. Birchenall and R. F. Mehl: *Trans.* AIME (1950) **188**, pp. 144-149; JOURNAL OF METALS (Jan. 1950) TP 2752E.

[2] J. Steigman, W. Shockley, and F. C. Nix: *Physical Review* (1939) **56**, p. 13.

[3] J. Mazia: *Steel* (1947) **120**, p. 84.

[4] R. M. Barrer: Diffusion In and Through Solids. Cambridge. (1941).

[5] T. B. Novey and N. Elliott: Plutonium Project Record *9B*, 2.2.2.

[6] B. P. Burtt: *Nucleonics* (1949) **5**, No. 2, pp. 28-43.

[7] E. J. Willard and F. Johnston: *Science* (1949) **109**, p. 11.

† After this manuscript was prepared a note on cobalt self-diffusion appeared: F. C. Nix and F. E. Jaumot, Jr., *Physical Review* (1950) **80**, 1191. Their equation, $D = 0.367\ e^{-67900/RT}$ cm² per sec for points at 1050°, 1150°, 1250°C., corresponds to higher diffusion coefficients than those reported here, but lower than unreported values obtained on ground (4-0 emery paper) and etched surfaces. In the absence of a description of their surface preparation, no conclusions may be drawn.

Correction

In the January 1951 issue: TP 2989 D. *Industrial Hygiene in American Smelting and Refining Company* by John N. Abersold and K. W. Nelson. P. 36, Ref. 2 should read: B. R. Small, with appendix by C. A. Stevenson: Air Conditioned Crane Cabs. Engineering Series Bulletin 4. Industrial Hygiene Foundation of America. Mellon Institute, Pittsburgh, Pa. (1947).

Formation and Behavior of Subboundaries in Silicon Iron Crystals

by C. G. Dunn and F. W. Daniels

IN recent publications[1-5] the existence and behavior of subgrain boundaries in high-purity metals has been clearly brought to light. Lacombe and Beaujard[1] by means of special etching methods disclosed in polycrystalline sheets of aluminum the existence of substructures differing in orientation by small amounts (about ¼°). Boundaries of these structures at relatively high temperatures had the remarkable property of moving about while the ordinary boundaries remained stationary. Cahn[2] also observed substructures in bent and annealed single crystals of aluminum, zinc, magnesium, and rock salt. The position of subboundaries could be explained in terms of a *dislocation mechanism of polygonization* in which dislocations move into lines at right angles to the bent glide planes thereby relieving elastic stresses in these planes. Guinier and Tennevin[4, 5] disclosed the further interesting feature that polygonized structures coarsened significantly upon prolonged annealing.

Somewhat similar subgrain phenomena have been observed in silicon iron of commercial purity. Although some evidence for the development of macromosaic structures in silicon iron already has been reported by one of the authors[6, 7] under the phenomenological term "crystal recovery," much better evidence recently has been obtained due to improved etching techniques. In addition, phenomena regarding structural changes have been uncovered.

The present investigation is divided into three parts: (1) The phenomenon of Laue spot sharpening on annealing cold-rolled crystals, (2) the phenomena of polygonization and subgrain coarsening

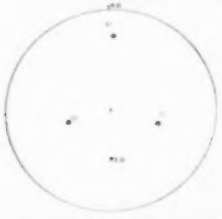

Fig. 1—Stereographic projection of {100} cube poles and the probable most active <111> slip direction. Open circles give original orientation and solid circles the orientation after cold rolling.

in (a) bent single crystals and (b) cold-rolled crystals, and (3) boundary and subboundary interactions.

Procedure

The material used in the present investigation was high-grade commercial silicon iron sheet of nominal composition, 3.3 pct Si, 0.004 C, 0.011 P, 0.010 S, 0.04 Mn, 0.01 Al, 0.04 Cu, 0.01 Sn. Large single crystals of this material were prepared for cold-rolling or bending as scheduled. Cold-rolling of 12 pct was carried out on a laboratory 8-in. diam rolling mill. The bending deformations were performed by pressing the crystals between a solid round bar and a mating half cylinder, both heavily greased. Individual specimens were cut from the deformed crystals, and the cut edges were deeply etched prior to annealing. Laue photographs were made using 40-kv tungsten radiation. The technique used to disclose the various subboundaries was an electropolish and electroetch in a bath of chrome-acetic acid.[8] The anodic polishing done at 22 v was immediately followed by etching at a reduced voltage, which was dependent upon the nature of the subboundaries.

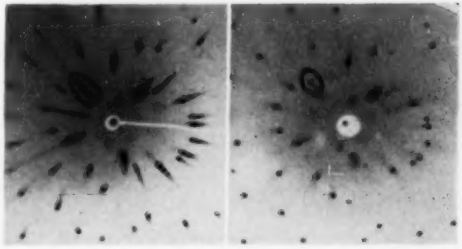

Fig. 2—Illustrative Laue patterns to show Laue spot sharpening. *a* (left)—Specimen as cold rolled. *b* (right)—After 18 hr at 1400°C.

Phenomenon of Laue Spot Sharpening on Annealing Cold-Rolled Crystals

Fig. 1 gives the initial and final orientations of the specimens cold-rolled 12 pct. Each specimen was annealed at a temperature and for a time which caused significant structural changes as evidenced by alterations in Laue patterns.

Representative Laue patterns and micrographs showing the essential changes are given in Figs. 2, 3, and 4. The essential points to be derived from these illustrations follow:

1. Annealing at 950°C clearly develops a substructure with the orientation of the cold-rolled specimen.
2. The subboundaries formed obviously separate regions of nearly the same orientation. Some of the subboundaries appear as a sequence of dots similar to those observed in aluminum by Lacombe and Beaujard,[1] but whether this is due to extremely small differences in orientation is not known at present.
3. The substructure coarsens upon prolonged annealing.
4. Prolonged annealing also causes a decrease in orientation spread according to Laue spot sharpening.

C. G. DUNN, Member AIME, is Research Physicist, and F. W. DANIELS, is Metallurgist, General Electric Co., Pittsfield, Mass.

Discussion of this paper, TP 3005 E, may be sent (2 copies) to AIME by April 1, 1951. Manuscript, Oct. 9, 1950. St. Louis Meeting, February 1951.

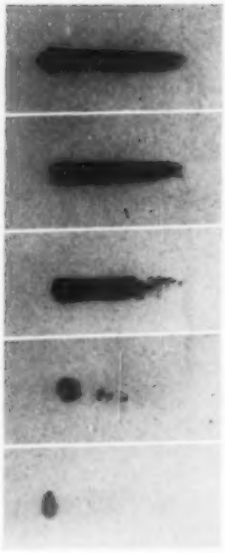

Fig. 3 (left)—Enlarged Laue spot for encircled position of Fig. 2.

a—Cold rolled. b—10 min at 950°C. c—5 hr at 1000°C. d—1 hr at 1200°C. e—48 hr at 1400°C.

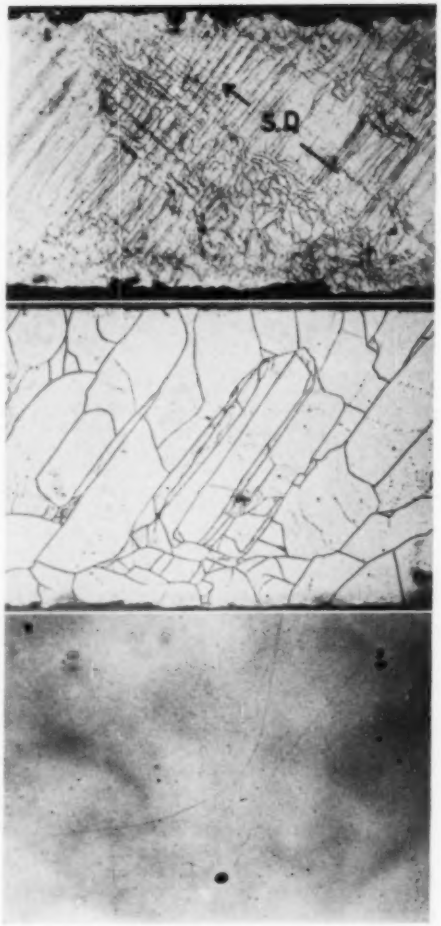

Fig. 4 (right)—Micrographs of cold-rolled specimens after various anneals.

Electro etch. X200. Reduced approximately 33 pct for reproduction. a (top)—10 min at 950°C, longitudinal section. b (center)—1 hr at 1200°C, longitudinal section. c (bottom)—48 hr at 1400°C, transverse section.

5. These alterations in the Laue photographs and the accompanying coarsening of the structure may be interpreted to mean that a *selective* growth of subgrains has occurred. Stated another way subgrains with orientations further removed from the average orientation of the composite are consumed by those closer in orientation to the average.

Phenomena of Polygonization and Subgrain Coarsening

Bent Single Crystals: A number of bent specimens were prepared from a large single crystal 0.025 in. thick. Fig. 5 gives the pertinent crystallographic directions and the axis of bending which coincides with a $[12\bar{1}]$ direction. Preliminary X-ray and micrographic data for annealed specimens disclosed that high-temperature annealing produced many lamellar shaped subgrains within each original crystal. X-ray data, for example, disclosed that each Laue spot changed to a discrete set of smaller spots (a fine structure) covering the original orientation range. Fig. 6 shows such a set obtained by using an X-ray camera in a focusing position to obtain maximum sharpness of the spots. The average difference in orientation from these patterns is (a) 0.22° or (b) 0.23°. Fig. 7 shows the accompanying microstructure in a plane perpendicular to the axis of bending, see Fig. 5. The structure was disclosed by a thermal etch—a method often superior to ordinary chemical etches but far inferior to the chrome-acetic acid electroetch. One may speak of the foregoing structure as polygonized.*

Regarding the boundary orientations, the present boundaries lie approximately 90° to the [111] direction as shown in Fig. 7, and this raises a question regarding possible crystallographic relationships between boundary directions and active slip planes as predicted by the dislocation mechanism of polygonization.

To check the crystallographic relationships for formation of the new boundaries, visible traces of active slip planes were obtained before annealing and compared with the boundaries formed in a subsequent anneal. Fig. 8*a* shows that there are two sets of slip lines corresponding to slip on the $(10\bar{1})$ and (011) planes. Fig. 8*b* shows the final subboundary for the identical area after a high-temperature anneal (subboundaries are very faint) and Fig. 8*c* also shows a representative structure at this point. Comparison of the photographs discloses that the boundary lines are perpendicular to the $(10\bar{1})$ slip lines which, in this case, coincide with the [111] direction. Disregarding slip on (011) planes, the results agree well with those predicted on the basis of movement of dislocations ($[\bar{1}2\bar{1}]$-edge dislocations which are perpendicular to the plane of the microsection) until they form subgrain boundaries at 90° to the (101) slip plane (this plane is in the maximum shear position and, therefore, probably the most active one during plastic bending). More will be said about this later.

* The descriptive term *polygonized* was supplied by E. Orowan and R. W. Cahn to indicate that the line of atoms in a specific crystallographic direction taken in each subgrain along the arc of the bend forms part of a polygon. Also if the lattice is elastically bent prior to annealing, there is no polygonized state until a subdivision into unbent units occurs. This breakup into unbent units is called *polygonization*.

Fig. 5 (left)—Stereographic projection showing {100} poles of crystal in approximately (210) orientation, important {110} slip planes, axis of bending, and plane of the microsections.

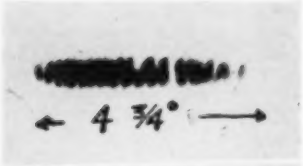

Fig. 6 (left)—Enlarged Laue spots of bent specimen P5, 3/8 in. radius, after 22 hr at 1300°C.
a (top)—0.030 in. pinhole system. *b* (bottom)—0.010 in pinhole system.

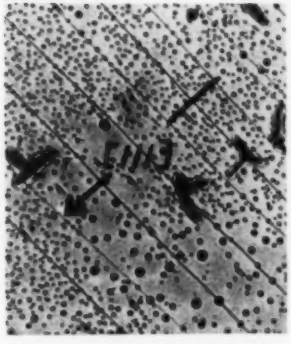

Fig. 7 (left)—Microstructure of specimen P5 after 22 hr 1300°C anneal in argon. Thermal etch. X200.

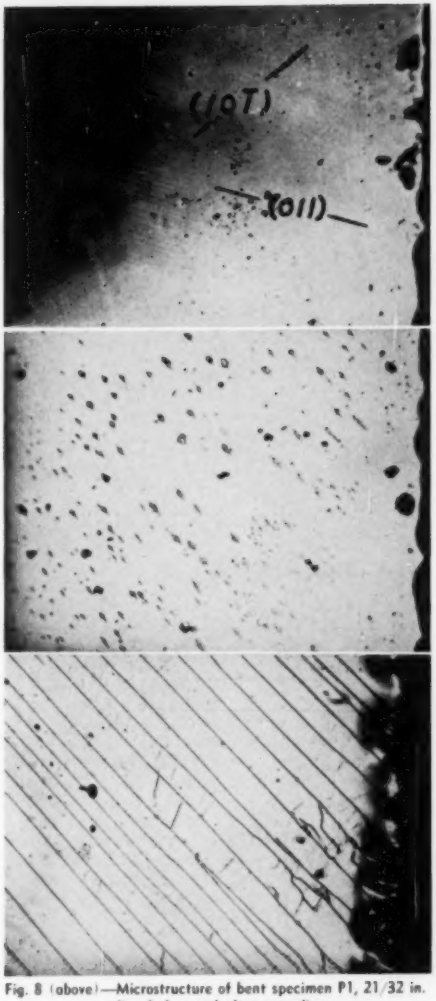

Fig. 8 (above)—Microstructure of bent specimen P1, 21/32 in. radius, before and after annealing.
X150. Reduced approximately 33 pct for reproduction. *a* (top)—Polished then bent. *b* (center)—After 1 hr at 1300°C in argon. Same area as *a*. Thermal etch. *c* (bottom)—Representative structure. Electro etch.

Other specimens were used to investigate the early stages of formation of the polygonized structure and also the effect of amount of bending. Three parts (*P*2, *P*3, and *P*4) of the original crystal were bent to radii of 21/32, 3/8, and 3/32 in., respectively. Each part was further divided into a number of specimens for various treatments. Fig. 9 shows the microstructure of some *P*3 specimens before and after heat treatment, the latter three being a sequence on a single specimen. Another *P*3 specimen of importance but not photographed was annealed 15 min at 775°C.

The micrographs disclose a coarsening of the substructure as well as the formation of subboundaries 90° to the direction of $(10\bar{1})$ slip lines. The slip lines here are revealed after sectioning and therefore are representative of interior regions of the bent crystal. These lines are not called subboundaries. The subboundaries initially formed are very wavy and often appear to terminate in the matrix; only later in the annealing do they become relatively straight. Some areas in the 775°C annealed specimen disclosed no subboundaries, other areas did. Among these subboundaries there were some that extended only from one slip line to another.

Figs. 10 and 11 show micrographs for the *P*2 and and *P*4 series, respectively. *P*2 appears incompletely transformed after 10 min at 950°C. Lines that coincide with the original slip lines are still present and the structure in general is quite heterogeneous. The increase in subgrain size on prolonged annealing at 950°C is very striking. Specimen *P*4 reacted to the 950°C anneals in somewhat similar fashion, the coarsening, however, being less pronounced. The 1300°C treatment converted *P*4 to a single crystal of new orientation. Unlike the subgrains, which had a common $[1\bar{2}1]$ direction, this new crystal had a different orientation and therefore could not have been one of the observed subgrains which had grown at the expense of others. The origin of this grain is beyond the scope of the present paper; it

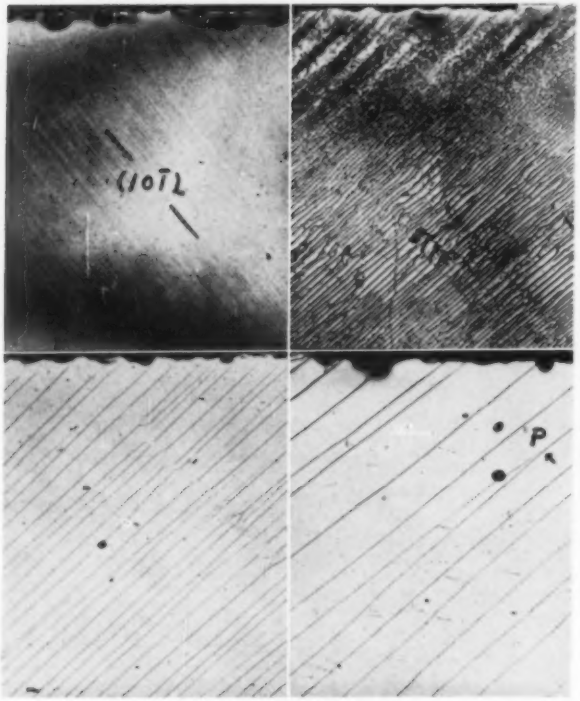

Fig. 9—Microstructure of bent specimen P3, 3/8 in. radius, before and after various anneals.

Electro etch. X200. Reduced approximately 33 pct for reproduction. *a* (upper left)—Bent and sectioned to show slip lines. *b* (upper right)—After 10 min at 950°C. *c* (lower left)—After 24 hr at 950°C. *d* (lower right)—After 4 hr at 1300°C.

is more properly dealt with under the phenomenon of primary recrystallization.

X-ray data representing early and late stages of the treatments are shown in Figs. 12 to 14. Annealing for 10 min at 950°C appears to have produced a change in the uniformity of the Laue spot for specimen *P*3. No such change, however, is apparent for *P*2, and a nonuniform Laue spot for specimen *P*4 is present both before and after annealing. It might be concluded from these X-ray data that specimen *P*4 was partly polygonized before annealing, that specimen *P*3 polygonized some in the 10-min 950°C anneal, and that *P*2 did not polygonize at all in the same anneal. However, the micrographic data indicate degrees of polygonization not resolvable by the present X-ray technique. No refined technique such as that employed by Guinier[4] was attempted, however, since the micrographs were entirely satisfactory for revealing early structures. After appreciable subgrain coarsening, ordinary X-ray techniques sufficed to determine the nature of the substructure.

Table I. Average Width of Subgrains in Microns

Anneal	*P*2	*P*3	*P*4	*P*5
10 min at 950°	3.5	5.1	2.2	
24 hr at 950°	18.3	13.7	3.7	
4 hr at 1300°	42.5	33.3		
22 hr at 1300°				39.5

Table II. Angle of Separation θ in Degrees

Anneal	*P*2	*P*3	*P*4	*P*5
10 min at 950°	0.017	0.043	0.075	
24 hr at 950°	0.088	0.12	0.13	
4 hr at 1300°	0.21	0.30		0.19

The widths of lamellar subgrains were measured to obtain the values given in Table I.

Using an angle of 45° for the directions of the boundaries and assuming a progressive rotation of the subgrains, geometry considerations indicate that the average angle between adjacent lamellae should be, to a good approximation:

$$\theta = \frac{W \times 57.3}{R\ (0.707)} \qquad [1]$$

where *W* is the average width of the subgrains and *R* is the radius of bend. With this equation and the foregoing data the values given in Table II were obtained.

The largest subgrains were approximately double the average size. The values of 0.19° for specimen *P*5 and 0.21° for *P*2 obtained from eq 1 agree well with the X-ray diffraction value of 0.22° or 0.23° given previously for specimen *P*5. This agreement justifies the assumption of a progressive rotation of the subgrains *after coarsening*. On the other hand it does not prove that the *initial subgrains* actually differed in orientation by 1′ to 4′ (0.02° to 0.07°) as calculated in Table II.

Cold-rolled Crystals: In Fig. 4*a*, there are narrow lamellae in certain regions of the microstructure, which look very similar to the lamellae developed in bent specimens. The crystallographic relationship obtained from Figs. 1 and 4*a* show that the parallel boundary lines are approximately 90° to a <111> direction, S.D., which should have been active according to the orientation change produced during deformation. This part of the transformation, therefore, appears to be identical with that occurring in bent specimens and suggests that local regions of the lattice were bent during cold-rolling.

The structure in such local regions after annealing, therefore, may be described as polygonized. As the structure coarsens, however, it has less and less the characteristics of a polygonized one, not because the lamellar structures vanish but because larger units no longer have simple relationships in an orientation sequence. The coarsened structure is probably better described as macromosaic. At the stage of coarsening represented by Figs. 3*d* and 4*b*, however, there still are present a number of parallel boundaries in the direction of the original polygonized lines and this indicates some persistence of the structure. A similar situation appears to have been the case in an example of crystal recovery cited by Dunn[7] (see his Figs. 8, 9, and 10), because if <111> directions are added to Fig. 10, they fall roughly 90° to the subboundaries of the micrograph.

Boundary and Subboundary Interactions

The results of boundary and subboundary interactions reported in this section are largely of a preliminary and qualitative nature.

The simplest example of interaction involves two grains, one in a strain free state, the other containing considerable substructure as shown in Fig. 15, for example. As in the case of specimen *P4* described previously, grain *A* is the result of primary recrystallization but, in this example, has not completely consumed the polygonized grain. Although primary recrystallization may provide suitable examples of interaction as illustrated above, greater control of the variables is possible if two-grain specimens are made in another way.

In the controlled method one grain is grown until about half of a fine-grained specimen is transformed. The entire specimen is then bent and the untransformed area is converted to a second grain. In this second step the first grain undergoes polygonization. A Laue photograph, such as Fig. 16*a* taken at the grain boundary of a completed specimen, would show one grain in the strained condition and the other strain free as evidenced by Laue asterism and sharp Laue spots, respectively. Micrographs of such specimens, however, show that the strained grains actually are polygonized.

When a specimen is annealed at temperatures of 1200° to 1300°C, the strain free grain grows at the expense of the polygonized grain, with parts of the boundary often moving away from their centers of curvature. In other words the situation appears to be similar to that of growth into a strained matrix. Since the surface tensions of the subboundaries no doubt are small, one should expect near 180° grain boundary angles at boundary and subboundary junctions and consequently little evidence for subboundary driving energy from the geometry of the boundary, see Fig. 15. Nevertheless, the major driving energy in the present illustrations reasonably resides at the subboundaries. The ideas of Bragg,[9] Burgers,[10] and Smith[11] on subboundaries and subboundary energies are particularly pertinent to this view although some of the ideas apply more specifically to the cold-worked state.

A more complicated type of interaction involves two grains each with subboundaries. For example, a two-grain specimen may be cold rolled and annealed with each part behaving as in the early illustration—that is, developing substructures, which coarsen while the subboundaries apparently balance out at the boundary. Such coarsening of a substructure was of course not observed in previously published work on silicon iron[6, 7] where the ordinary boundaries remained essentially unchanged during Laue spot sharpening. However, since the conditions of deformation and annealing were similar to those of the present work, it is believed that subgrain coarsening did occur and was responsible for the observed sharpening of Laue spots.

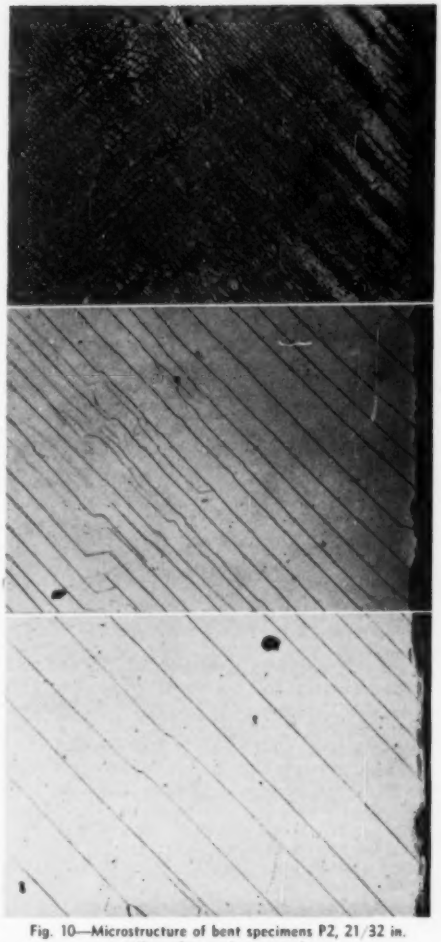

Fig. 10—Microstructure of bent specimens P2, 21/32 in. radius, after various anneals.

Electro etch. X200. Reduced approximately 33 pct for reproduction. *a* (top)—After 10 min at 950°C. *b* (center)—After 24 hr at 950°C. *c* (bottom)—After 4 hr at 1300°C.

Some cases have been observed in cold-rolled specimens where one grain grows at the expense of the other (a case of unbalanced subboundaries). Examination of the area swept by the grain boundary usually discloses the presence of subboundaries, which continue back to the original position of the boundary. This means that subboundaries are "pulled along" with the boundary as it moves. Some of the subboundaries produced in this way separate regions differing in orientation by a degree or two. The appearance of grain boundaries in the strain-induced grain boundary migration experiments in high-purity aluminum of Beck and Sperry[12] indicate that subboundaries no doubt would be formed

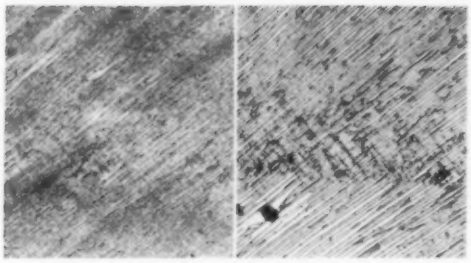

Fig. 11—Microstructure of bent specimens P4, 3.32 in. radius, after various anneals.
Electro etch. X200. *a* (left)—After 10 min at 950°C. *b* (right)—After 24 hr at 950°C.

similarly in the traversed areas. It is, therefore, not very surprising that the strain-anneal method for producing large crystals in high-purity aluminum often produces rather imperfect crystals as reported by Lacombe.[10]

That an unbalance of subboundaries adjacent to an ordinary boundary will promote migration of the latter can readily be shown. To illustrate, if the specimen of Fig. 16*a* is again bent and polygonized (see Fig. 16*b*), the resulting two grains differ in their subboundary energy per unit volume and the one that is least bent (lowest energy in this case) will grow at the expense of the other. In a 1300°C, 3-hr anneal the boundary for this case actually moved a small amount. X-ray and micrographic data disclosed that the subboundaries moved along with the grain boundary, altering but not removing polygonization in the traversed area. The polygonized state in the area traversed by the boundary clearly did not originate through a *dislocation-mechanism of polygonization* as described by Cahn; rather it arose from growth of a polygonized region adjacent to it. Since this phenomenon may occur under less controlled conditions, it follows that simple growth processes may play a role in the development of polygonized areas. Alterations in the substructure and thus alterations in the detailed picture of a polygonized state through growth of the subgrains have, of course, already been discussed.

Energetics of Boundary and Subboundary Migration

Boundary Migration: The grain boundary energy equation of Shockley and Read[14] should apply especially well to subboundaries, because the orientation differences involved are very small. The equation is:

$$E = E_o\theta\,(A - \ln\theta) \qquad [2]$$

where E is the energy per unit area of grain boundary, θ is the difference in crystal orientation, and E_o and A are approximately constants.

Assuming eq 2 applies and that the energy reaches a maximum at θ equal to 30°, it follows that the energy in a subboundary of coarsend substructure (θ equal to 0.2°) is about 1/25 the maximum value (i.e., approximately 1/25 that of an ordinary boundary). With smaller θ's the energy would be less than this.

The energy per unit volume, or the driving force, is more important for boundary migration. Assuming a uniform lamellar substructure of width w equal to 40μ and a θ value of 0.2°, it follows that the energy per unit volume would be:

$$\frac{E\,(0.2^\circ)}{w} = \frac{E_m}{25w} = 10E_m \qquad [3]$$

This value of available driving force is approximately the same as that obtained in grain-growth experiments on two-grain specimens of silicon iron carried out at temperatures of 1300° to 1400°C and appears to be near a lower limit for ordinary grain-boundary migration at these temperatures.[15] An estimate of the absolute value of this energy per unit volume indicates that it would be about 10^{-5} that measured for heavily cold worked iron.†

Growth of a grain at the expense of another because of subboundary energy in one of them, as was illustrated in Fig. 15, would be expected to be slow, therefore, according to these estimates of available driving force.

A more general energy relationship for lamellar subgrains can be written in terms of the orientation difference θ and the radius of bend R, since these quantities together with the boundary direction ϕ determine the width of the subgrains. From eqs 1 and 2 it follows that:

$$\text{Energy per unit volume} = \frac{E_o\,(A - \ln\theta)}{R\,\text{Cos}\,\phi} \qquad [4]$$

where ϕ generally is near 45°.

According to this equation the average driving force for boundary migration decreases with increasing values of θ and R indicating: (1) That subgrain coarsening lowers the total energy as it should and (2) with constant θ, less bending of the lattice leads to less energy, which also is reasonable.

When boundary migration involves subboundaries on both sides of the boundary, the driving force is

† Perhaps significant in this connection is some unpublished work on microhardness vs. crystal recovery in silicon iron crystals which has shown almost 100 pct removal of work hardening for equivalent anneals to those producing polygonization in the present investigation.

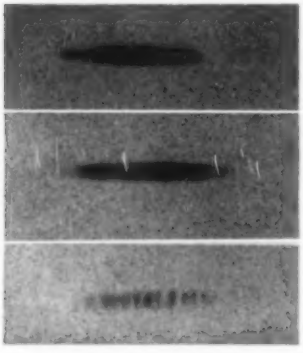

Fig. 12 (left)—Enlarged Laue spot of specimen P2.
a (top)—As-bent. *b* (center)—After 10 min at 950°C. *c* (bottom)—After 4 hr at 1300°C.

Fig. 13 (right)—Enlarged Laue spot of specimen P3.
a (top)—As-bent. *b* (center)—After 10 min at 950°C. *c* (bottom)—After 4 hr at 1300°C.

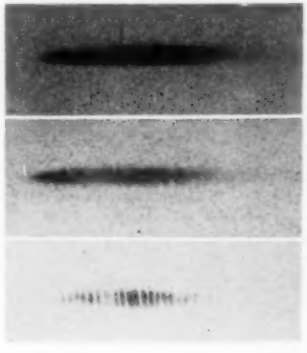

obtained as a difference in subboundary energy per unit volume. If this difference is zero, there is no net driving force to move the grain boundary. Instances may occur where the difference is so small that little movement of ordinary boundaries could be expected. This may account, therefore, for stationary grain boundaries[1] as well as the phenomenon of growth retardation through straining.[10] On the other hand, it is well known that grains in a deformed polycrystalline specimen have different degrees of straining, and this leads to the belief that many situations of unbalanced subboundaries could arise. It is suggested that strain-induced grain-boundary migration, reported by Beck and Sperry,[12] probably is this phenomenon.

Subboundary Migration and Subgrain Coarsening: Coarsening may be considered apart from any mechanism for release of subboundary energy. According to eq 4 the average energy per unit volume for a uniform substructure decreases logarithmically with θ. This means that the available driving force for doubling the subgrain size is constant regardless of the initial size. If half the volume transforms to produce doubling, we have

$$\text{Driving force} = \frac{2E_o \ln 2}{R \cos \phi} \qquad [5]$$

and this is somewhat less (a factor of 0.23) than the residual energy per unit volume for θ equal to 0.2°.

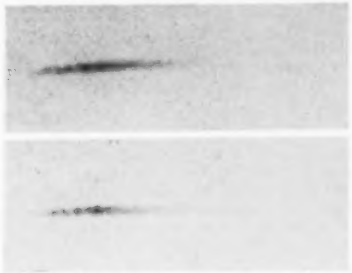

Fig. 14—Enlarged Laue spot of specimen P4. *a* (upper)—As-bent. *b* (lower)—After 10 min at 950°C.

Theoretically two thirds of the volume could transform with θ increasing to 3θ due to the coalescence of three boundaries with a

$$\text{Driving force} = \frac{3E_o \ln 3}{2R \cos \phi} \qquad [6]$$

and this is about 0.27 times the 0.2°—residual. The coalescence of three subboundaries to form one, therefore, provides slightly more driving force than the coalescence of two, but the driving force is of course not large for either case.

The probability of one lamella growing at the expense of others as in exaggerated grain growth, for example, should be low in spite of an even more favorable driving force. At the start any one lamella is not favored to grow because the driving force is $\frac{2E_o \ln 2}{R \cos \phi}$ for each. After one lamella has doubled, however, the driving energy for its further growth is greater, because coalescence of a 2θ-boundary and a θ-boundary releases more energy for the same volume change than the coalescence of two θ-boundaries. The situation then improves with growth but not in a rapid manner; consequently other lamellae probably would grow also before one could become particularly large.

It must be remarked here that growth of a new grain at the expense of a polygonized grain (treated previously) does not have a constant driving force if growth alters the type of boundary enough to increase or decrease its specific energy.

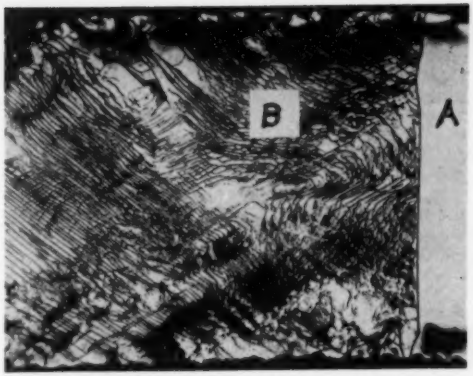

Fig. 15—Micrograph showing boundary and subboundaries of two grains A and B, with grain B in a complex polygonized state, after 4 hr at 1300°C.
Electro etch. X150. Reduced approximately 33 pct for reproduction.

If the driving energy is roughly constant for each stage of doubling as the above analysis would indicate, it is not at all clear why the coarsening should slow down at high temperatures. However, there must be a mechanism for the release of energy. We believe it is one of subboundary interaction quite analogous to that for ordinary grain growth. With increased annealing the reduction in number of interaction points such as that at P in Fig. 9*d* seems significant; interactions could move such points to the surface and thus coarsen the structure. When all have been used, coarsening should stop. On the other hand if sidewise movement of the subboundaries should occur because of unusual mobility (this is not a mechanism), some subboundaries occasionally would disappear during coarsening. Others should define very narrow lamellae just prior to disappearance, but the microstructures gave no strong evidence of this kind.

When parallel subboundaries are very close together, as they may be during polygonization, a force of attraction may exist between them, which would tend to make them coalesce. According to eq 2 if two like boundaries coalesce with one lamella going to zero width, the energy for the final subboundary will be less than that of the sum of the two initial subboundaries; so coalescence will reduce

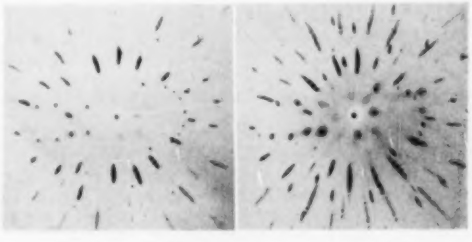

Fig. 16—Laue photograph of boundary position in a two-grain specimen.
a (left)—As-prepared. Lattice of one grain strain free, lattice of other strained to 21/32 in. radius bend. *b* (right)—After additional bending and a 3-hr anneal at 1300°C.

the energy. Now if it is assumed that the change in energy occurs continuously, it follows that the force of attraction is the rate of energy variation with distance of separation. Somewhat larger forces of attraction reasonably could occur for polygonized cold-rolled crystals because adjacent boundaries could consist of dislocations of opposite signs whereas boundary dislocations in a bent sample are only of one kind.

The observed coarsening of subgrains in cold-rolled crystals may be likened to normal grain growth, except for the addition of a selective growth feature. Selective growth with removal of the orientation spread, of course, leads to a lower final energy state (because energy increases with difference in orientation) and should be favored therefore on a probability basis. On the other hand the selective growth may also involve subgrain sizes, smaller subgrains having orientations farthest from the average.

Although the removal of subboundary interaction points seems to account for the slowing down of coarsening in polygonized samples at high temperatures, the amount of movement of subboundaries at low temperatures, note Figs. 10*a* and 10*b*, suggest that some feature of the kinetics besides simple interaction and energy per unit volume may be involved. In a simple polygonization process the first lamellae formed have much smaller differences in orientation than those formed later as a result of coarsening. It would appear that a small difference in orientation favors subboundary movements. Generally, however, grain-boundary migration is favored by an appreciable difference in orientation. These somewhat contradictory facts can be reconciled if it is assumed that ease of boundary migration decreases at first with difference in orientation θ, reaches a minimum value for a relatively small value of θ (possibly about one degree) and then increases again.‡ According to dislocation theory, mobility should be high for very small values of orientation difference, but theory apparently has not advanced far enough to completely explain the role of orientation relationships. For that matter much remains to be done experimentally on the same problem.

Summary

Single crystals of silicon iron were plastically deformed either by cold-rolling or by bending and were subsequently annealed. Results of a micrographic and X-ray investigation disclosed the following:

1. The phenomenon of removal of asterisms in Laue spots of cold-rolled single crystals without recrystallization results from two processes: (a) Polygonization, which produces a relatively fine subgrain structure and (b) subgrain growth of a fairly uniform kind like normal grain growth but selective in nature, removing the major spread in orientation and thereby producing a more nearly perfect single crystal of low subboundary energy.

2. Polygonization occurs in bent single crystals with subboundaries 90° to the active slip plane. As first formed the subboundaries are far from continuous and straight. With continued annealing irregularities disappear concurrently with coarsening of the lamellar substructure, which in one instance went as far as a ten-fold increase in lamellar width. Theoretical considerations of the kinetics involved indicate a relatively small driving energy for coarsening.

Two-grain specimens were prepared in which either one or both of the grains contained subgrains. Annealing at high temperatures disclosed the following:

1. When one grain alone contains subboundaries, the other grain grows quite readily, apparently through interaction of the subboundaries with the ordinary boundary.

2. When both grains contain subboundaries, the ordinary boundary sometimes fails to move, apparently from lack of driving energy. At the same time, however, the subgrains grow larger. At other times the boundary does move, but in general the area swept is not free of subboundaries. Subboundaries are "pulled along," so to speak, since the ordinary boundary actually separates two sets of subgrains instead of two perfect crystal lattices. The available driving energy for the movement is the difference in subboundary energy per unit volume.

‡ This view of the effect of orientation difference on rate of growth was developed in a discussion of growth phenomena with David Turnbull.

References

[1] P. Lacombe and L. Beaujard: The Application of Etch-Figures on Pure Aluminum (99.99%)—to the Study of some Micrographic Problems. *Journal* Institute of Metals (1948) **74**, p. 1.

[2] R. W. Cahn: Recrystallization of Single Crystals after Plastic Bending. *Journal* Institute of Metals (1949) **72**, p. 121.

[3] A. Guinier and J. Tennevin: Etude aux Rayons X de la Texture Fine des Cristaux d'Aluminium. *Comptes Rendus* (1948) **226**, p. 1530.

[4] A. Guinier and P. Lacombe: L' état "polygonizé" du Cristall Métallique. *Metaux et Corrosion* (1948) **23**, p. 212.

[5] A. Guinier: Substructures in Crystals. N.R.C. Conference on Crystal Imperfections (1950). An excellent review as well as results of recent investigations.

[6] C. G. Dunn: Recrystallization and Twin Relationships in Silicon Ferrite. *Trans.* AIME (1944) **158**, p. 372; METALS TECHNOLOGY (Feb. 1944) TP 1691 E.

[7] C. G. Dunn: Some Aspects of Crystal Recovery in Silicon Ferrite. *Trans.* AIME (1946) **167**, p. 373; METALS TECHNOLOGY (Aug. 1946) TP 1991 E.

[8] C. E. Morris: Electropolishing of Steel in Chrome Acetic Acid Electrolyte. *Metal Progress* (1946) **56**, p. 5.

[9] W. L. Bragg: The Structure of a Cold Worked Metal. *Proc.* Physical Soc. (1940) **52**, p. 105.

[10] W. G. Burgers: Recovery and Recrystallization Viewed as Processes of Solution and Movement of Dislocations. Koninkl. Nederland, Akad. Wentenschap., *Proc.* (1947) **50**, p. 452.

[11] C. S. Smith: Discussion on Effect of a Dispersed Phase on Grain Growth in Al-Mn Alloys. *Trans.* AIME (1949) **185**, p. 310; JOURNAL OF METALS (May 1949). Also private communication.

[12] P. A. Beck and P. R. Sperry: Strain Induced Grain Boundary Migration in High Purity Aluminum. *Journal of Applied Physics* (1950) **21**, p. 150.

[13] P. Lacombe: Subboundary and Boundary Structures in High Purity Aluminum. Physics Soc. Report of Conference on Strength of Solids (1948), p. 91.

[14] W. Shockley and W. T. Read: Quantitative Predictions from Dislocation Models of Crystal Grain Boundaries. *Physical Review* (1949) **75**, p. 692. Also Dislocation Models of Crystal Grain Boundaries. *Physical Review* (1950) **78**, p. 275.

[15] C. G. Dunn, F. W. Daniels, and M. J. Bolton: On the Problem of Grain Boundary Movement. *Trans.* AIME (1949) **185**, p. 708; JOURNAL OF METALS (Oct. 1949) TN 25 E.

[16] W. G. Burgers: Rekristallisation, Verformter Zustand und Erholung. Akad. Verlagsges. Berlin (1941). Also Edwards Brothers, Inc. Ann Arbor, Mich. (1944) p. 176.

Interface and Marker Movements in Diffusion In Solid Solutions of Metals

by Luiz C. Correa da Silva and Robert F. Mehl

An experimental study of the movement of markers in the systems Cu/α-brass, Cu/Snα-solid solution, Cu/Alα-solid solution, Cu/Ni, Cu/Au, Ag/Au, employing many types of markers and a variety of temperatures. Marker movement is confirmed and undoubtedly associated with the manner in which atoms move during diffusion.

SEVERAL years ago Smigelskas and Kirkendall[1] reported measurements on the interdiffusion of copper and α-brass and on the movement of inert markers placed at the original join. These markers were observed to move toward the α-brass side of the join, and from this it was inferred that zinc diffuses in α-brass more rapidly than copper. Similar results were reported a little earlier for the diffusion of solvents into high polymer solids.[2] This has attracted much attention, particularly from those interested in the mechanism and the theory of diffusion: Seitz[3] has employed it in supporting the vacancy theory of diffusion; from the data Darken[4] has calculated separate diffusion coefficients for copper and zinc, developing a "phenomenological" theory of diffusion; and Bardeen[5] has employed it in constructing a general theory, including therein the work of Seitz and Darken, as has Le Claire.[6] These matters have recently been reconsidered in a symposium.[7]

Some reason has existed for questioning the work of Smigelskas and Kirkendall.[1] Their technique consisted in electroplating copper on α-brass, upon the surface of which Mo-wires had been secured, and then diffusing, measuring the extent of diffusion along the normal to the join, and measuring the marker displacement in the same direction by a comparator determination of the distance between Mo-wires on opposite sides of the electroplated brass sample. It has been suspected that the copper plate might have been porous, and that the original interface might have been an imperfect join, both contributing to the transfer of the volatile zinc by vapor transfer;[8] it has also been questioned whether the marker movement might not in a measure be a property of the marker itself; etc. These legitimate questions require experimental answers; the present paper offers such answers.

Moreover, Smigelskas and Kirkendall studied the effect only in the Cu-Zn system and at one temperature; the attention which the work of Smigelskas and Kirkendall has commanded recommends similar

Table I. Diffusion Couples

Designation	Nominal Composition in Specimen (W/o)	Total Time of Diffusion, hr	Temp of Diffusion, °C	Atmosphere Used
Cu-Zn System				
B 20	Cu/70Cu,30Zn/Cu	119	880	H_2N_2
B 35	70Cu,30Zn/Cu/70Cu,30Zn	691	784	N_2
B 36	70Cu,30Zn/Cu/70Cu,30Zn	507	834	H_2N_2
B 37	70Cu,30Zn/Cu/70Cu,30Zn	197	885	N_2
B 42*	70Cu,30Zn/Cu/70Cu,30Zn	533	784	N_2
B 45*	70Cu,30Zn/Cu/70Cu,30Zn	185	883	N_2
C 1*	Cu/70Cu,30Zn/Cu	257	882	N_2
C 3*	Cu/70Cu,30Zn/Cu	267	883	N_2
C 11*	70Cu,30Zn/Cu/70Cu,30Zn	85	882	N_2
C 14*	Cu/70Cu,30Zn/Cu	112	884	N_2
C 17	Cu/80Cu,20Zn/Cu	66	923	N_2
C 19*	Cu/70Cu,30Zn	73	884	N_2
C 20*	Cu/70Cu,30Zn/Cu	27	884	N_2
E 1	Cu/70Cu,30Zn/Cu	46	884	N_2
C 22	52Cu,48Zn/81Cu,19Zn/52Cu,48Zn	18 hr 50 min	733	N_2
Cu-Al System				
B 22	Cu/93Cu,7Al/Cu	165	977	He
B 34	Cu/93Cu,7Al/Cu	606	948	Vacuum
B 39	Cu/93Cu,7Al/Cu	305	889	N_2
C 6*	Cu/93Cu,7Al/Cu	186	994	N_2
Cu-Sn System				
B 23	Cu/90Cu,10Sn/Cu	224	804	N_2
B 28*	Cu/90Cu,10Sn/Cu	164	812	Ar
B 33	Cu/90Cu,10Sn/Cu	524	808	N_2
B 41*	Cu/90Cu,10Sn/Cu	695	733	N_2
B 46	Cu/90Cu,10Sn/Cu	504	733	N_2
Cu-Ni, Ag-Au, and Cu-Au Systems				
B 38	Cu/Ni	362	947	Vacuum
C 4	Cu/Ni/Cu	312	1054	N_2
C 21*	Cu/Au/Cu	92	839	N_2
D 2*	Ag/Au/Ag	96	910	Ar
D 3*	Ag/Au/Ag	50	925	Vacuum

* Not analyzed.

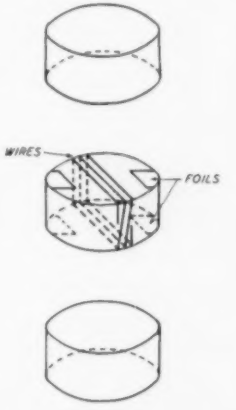

Fig. 1 — Arrangement of markers of wire and foil in a (double) diffusion couple to be welded.

LUIZ C. CORREA DA SILVA, formerly Graduate Student, Department of Metallurgical Engineering, Carnegie Institute of Technology, is now Research Engineer, Instituto de Pesquisas Tecnologicas, Sao Paulo, Brazil. ROBERT F. MEHL, Member AIME, is Professor of Metallurgical Engineering, Carnegie Institute of Technology, Pittsburgh.

Discussion of this paper, TP 3003 E, may be sent (2 copies) to AIME by April 1, 1951. Manuscript, Oct. 20, 1950; revision, Dec. 13, 1950. St. Louis Meeting, February 1951.

This paper represents part of a thesis by Luiz C. Correa da Silva submitted in partial fulfillment of requirements for the degree of Doctor of Science in Metallurgical Engineering to the Graduate Faculty of the Carnegie Institute of Technology.

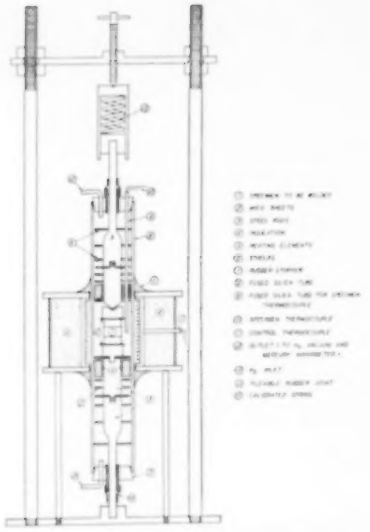

Fig. 2—Welding apparatus.

studies on other systems over a range of temperatures; the present paper offers similar studies upon six alloy systems. Diffusion couples in the following systems have been studied: (1) Cu/α-brass, 30 pct Zn and 20 pct Zn; (2) Cu/Cu-Al, α-solid solution, 7 pct Al; (3) Cu/Cu-Sn, α-solid solution, 10 pct Sn; (4) Cu/Ni; (5) Cu/Au; (6) Ag/Au. The diffusion couples were welded disks, and of the 29 couples all were double couples ("sandwiches"), e.g., Cu/Ni/Cu, except two. Table I lists the couples employed; it also gives times and temperatures of diffusion and the protective atmosphere employed.

Materials

Most of the alloys were prepared through the courtesy of D. K. Crampton, of the Chase Brass and Copper Co. The analyses are listed in Table II. The 30 pct Zn alloy was received in the form of rolled slab, 1 in. thick; the Cu-Sn alloy was a forged flat bar ½ in. thick; and the Cu-Al alloy was a forged round bar 1½ in. in diam. In addition to the 30 pct Zn α-brass supplied, one other brass was made of nominal composition 20 pct Zn; this was made from

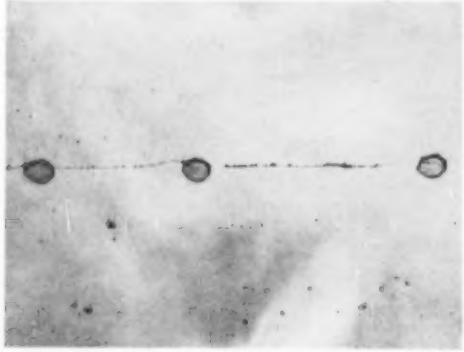

Fig. 3—Imperfect weld showing wire markers and imperfectly welded join. X100. Reduced approximately 33 pct for reproduction.

Table II. Compositions of the Copper Alloys

Nominal	Cu	Pb	Fe	Ni	Sn	Al	Si	Mn	Zn
70/30Zn	68.92	<0.01	0.025	0.014	0.039				Rem.
90/10Sn	89.82	0.009	0.004	<0.001	Rem.	<0.001	<0.002	0.005	<0.01
93.7Al	92.65	0.002	0.030	<0.005		Rem.	<0.002	0.002	<0.01

OFHC copper and zinc of 99.99 pct Zn; it was melted in a graphite crucible under borax in an induction furnace. The 20 pct Zn alloy was cold-rolled 50 pct and annealed; this alloy appears in the couple C-17 (Table I). The copper was in the form of cylinders 3 in. in diam; the nickel was high-purity Mond nickel, received as disks 1 in. in diam and ¼ in. thick.

Disks were cut to a diameter of 1¼ in. (except in the case of Ni, left at 1 in.) and to thicknesses of ¼ in. (for the Cu/Ni couples) or ½ in. (for all others). For the purposes of the experiments, the opposite faces had to be as nearly parallel as possible; with care this was done to ± 0.0005 cm; after machining the disks were polished carefully, usually with a finish from 4/0 emery paper. The surfaces were cleaned, degreased, and lightly etched with HNO_3.

The interface join markers employed were, variously:

Type *a*. Molybdenum wire, 0.0075 cm diam.
Type *b*. Tungsten wire, 0.0050 cm diam.
Type *c*. Tungsten wire, 0.0010 cm diam.
Type *d*. Platinum wire, 0.0075 cm diam.
Type *e*. Platinum wire, 0.0025 cm diam.
Type *f*. Platinum wire, silver coated, 0.0005 cm diam.
Type *g*. Nickel wire, 0.0075 cm diam.
Type *h*. Iron foil, 0.0025 cm thickness.
Type *i*. Tantalum foil, 0.0025 cm thickness.
Type *j*. Platinum foil, 0.0050 cm thickness.
Type *k*. Nickel foil, 0.0075 cm thickness.
Type *l*. Carbonaceous "wire"—made by carbonizing silk thread in vacuum.
Type *m*. Al_2O_3 powder (of polishing grade).
Type *n*. Iron oxide "wire"—made by oxidizing a fine iron wire.

Welding

The pressure applied for welding was the minimum possible for successful welding, usually in the neighborhood of 100 lb. The welding time was usually about 1 hr.

The specimens used usually consisted of three disks, the two outer disks identical, assembled as shown in Fig. 1. The markers in wire form were wound around the middle disk, as shown; this figure also shows the placing of foils. The composite of three disks were initially compressed hydraulically to 5000 to 15,000 lb to set the markers; this prepressing made subsequent welding much easier. After placing the disk composite in the furnace, the furnace was evacuated, then filled with hydrogen, the operation repeated several times at room temperature, and finally repeated several times while heating the furnace to 600°C; the latter operation was omitted in the case of the brasses, owing to the risk of dezincing. In the case of the Cu-Al samples, special care was taken to remove all traces of oxygen (since hydrogen will not reduce Al_2O_3)—some Mg dust was employed as a getter. The time of welding was 1 hr or longer.

The metal disks were welded in the furnace sketched in Fig. 2. Heating was provided by resist-

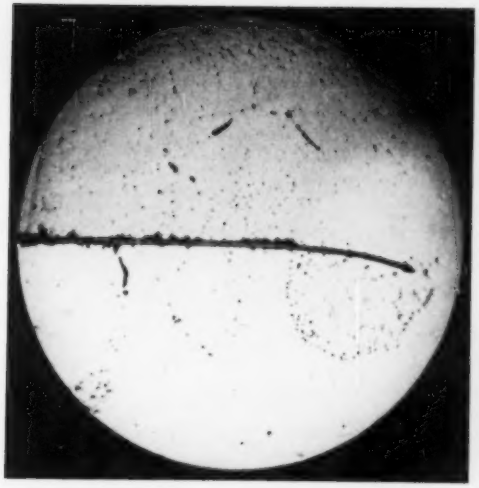

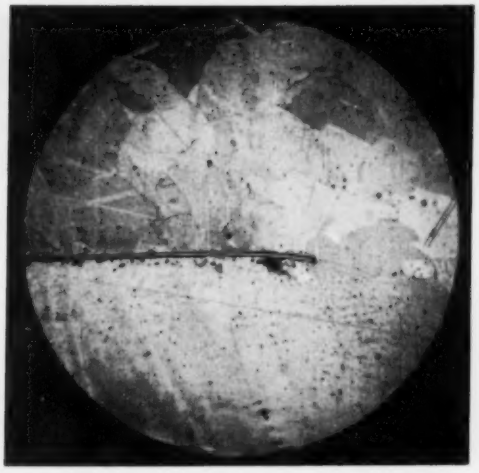

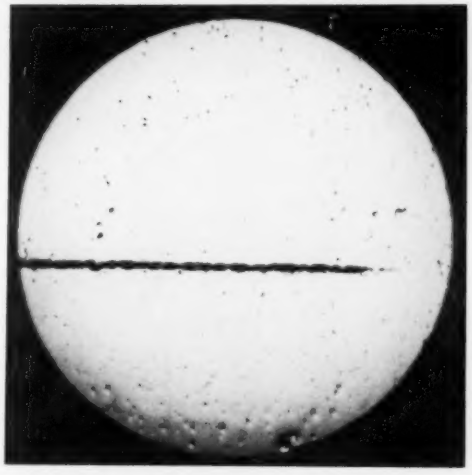

Fig. 4 (upper left)—Sample C1 with foil marker after diffusion, unetched. X25.

Fig. 5 (upper right)—Sample E1 with foil marker after diffusion, etched. X25.

Fig. 6 (lower right)—Sample C3 with foil marker after diffusion showing final straightening of foil after prolonged diffusion.

ance elements; mechanical pressure was applied to the disks, through steel rods as shown; vacuum or controlled pressures of any desired gas was maintained through pump and manometer control. The heating element was Kanthal; rapid heating was possible—the disks could be brought to a welding temperature in 20 min; the temperature was kept constant during welding by a Celectray control. Other details in the welding operation are obvious from Fig. 2. The thermocouple registered nominal temperatures only; these were high, approximating the melting point of the low-melting alloy; but the disks, held between steel plates, were actually at a substantially lower temperature; the thermocouple served only as a guide to reproduce the welding operation; the actual temperatures of the disks were not measured.

After welding, the specimens were machined with very great care, using a very sharp tool, the last layers removed were never thicker than 0.008 in., in order to minimize distortion, to produce two opposite planes accurately perpendicular to the welding zone and the marker; in the case of foil markers, four such surfaces were produced, related by right angles. This machining served two purposes: to reveal faulty welds on microscopic examination (whence many faulty specimens were discarded) and to provide an opportunity to establish the initial marker position. In the case of Cu-Zn alloys, this machining was deep enough to remove completely any dezinced outer layer. Fig. 3 shows the position of the wire marker with respect to the weld join (in an imperfect weld); other figures herein illustrate the weld zone in properly welded specimens. The inter-marker distance was determined with a comparator capable of yielding measurements reproducible within 0.0004 cm. Microscopic inspection showed the markers to be effectively equally imbedded in the opposing disks; the line of weld could be readily recognized.

Diffusion Treatments

The welded disk composites, when including brass, were annealed for diffusion in a steel container packed with brass chips (of the same composition as that in the disk composite) and lampblack (to prevent sticking of the charge), in order to avoid dezincing. As a result the Cu disks in all such composites were uniformly coated with a layer of brass, and the whole sample thus presented to the ambient a surface of the same composition, that of the high-Zn disk. For other disk composites hydrogen was used in general; Cu-Al alloys heated in hydrogen were observed to swell, perhaps because of hydrogen reduction of included oxides, and for this system nitrogen was used as a protective atmosphere. Cu-Al and Cu-Ni alloys were annealed in vacuum. Diffusion temperatures were maintained to ± 2°C.

Measurements on Diffused Couples

After diffusion, the flat longitudinal planes were re-machined, with similar care, in the case of Cu-Zn alloys this machining sufficed to remove completely

Table III. Displacement of Interfc.e Markers

Speci-men	Type of Markers at Each Interface	Temp. °C	Time of Diffusion, hr	Shift at Each Interface, cm	Method of Measure-ment	Observations
Cu-Zn System						
B 20	3 W wires 0.0050 cm	800	119	0.0109	Diff. curve	From B 20-I
B 35	5 Mo wires 0.0075 cm	784	157	0.0038	Direct	
			691	0.0110	Direct	
			691	0.0086	Diff. curve	From B 35-II
			691	0.0062	Diff. curve	From B 35-I
B 36	5 Mo wires 0.0075 cm	834	119	0.0076	Direct	
			289	0.0115	Direct	
			507	0.0180	Direct	
			507	0.0190	Diff. curve	From B 36-II
B 37	5 Mo wires 0.0075 cm	885	97	0.0105	Direct	
			197	0.0146	Direct	
			197	0.0148	Diff. curve	Average from B 37-I and B 37-II
B 42	3 Mo wires 0.0075 cm and 2 Fe foils 0.0025 cm	794	123	0.0067	Direct	Total shift
			123	0.0046	Direct	Rel. to foils
			245	0.0105	Direct	Total shift (Foils irregular)
			533	0.0155	Direct	Total shift
			533	0.0094	Foil bend	
B 45	3 Mo wires 0.0075 cm and 2 Ta foils 0.0025 cm	883	19	0.0059	Direct	Total shift
			19	0.0047	Direct	Rel. to foils
			85	0.0127	Direct	Total shift
			85	0.0105	Direct	Rel. to foils
			85	0.0089	Foil bend	
			185	0.0180	Direct	Total shift (Foil reference lost)
C 1	3 Mo wires 0.0075 cm and 1 Fe foil 0.0025 cm and 1 Ta foil 0.0025	882	19	0.0052	Direct	Total shift
			19	0.0035	Direct	Rel. to Ta foil (Zn crossed Fe foil)
			85	0.0075	Direct	Total shift
			157	0.0084	Direct	Total shift (Foil ref. lost)
			257	0.0089	Direct	Total shift
C 3	3 Mo wires 0.0075 cm and 1 Fe foil 0.0025 cm and 1 Ta foil 0.0025 cm	883	72	0.0052	Direct	Total shift (Foil ref. lost)
			167	0.0066	Direct	Total shift
			267	0.0085	Direct	Total shift
C 11	3 Mo wires 0.0075 cm and 2 Pt foils 0.0050 cm	883	19	0.0050	Direct	Total shift (Pt foils dissolved)
			85	0.0089	Direct	Total shift
C 14	3 W wires 0.0012 cm and 2 Mo wires 0.0075 cm 3 Pt wires 0.0050 cm	884	66	0.0027	Direct	Total for Mo, W (Pt wires dissolved)
			112	0.0040	Direct	Total for Mo, W
C 17	2 Mo wires 0.0075 cm 2 Ni wires 0.0075 cm 1 Pt wire 0.0012 cm	923	66			Cu-20Zn brass/Cu (Sample visibly expanded due to gas reaction)
C 19	2 sets of Fe foils in brass disks, perpendicularly to interface	884	73	0.0007	Direct	Lateral change in dimensions of the brass, at the interface
C 20	Wires: 2 Mo-0.0075 cm 2 W-0.0050 cm 2 Ni-0.0075 cm 2 Pt-0.0012 cm Foils: 1 Fe-0.0025 cm 1 Pt-0.0050 cm 1 Ni-0.0050 cm 1 Ta-0.0025 cm *Others:* Fe_2O_3 Al_2O_3 Carbon	884	27	0.0024	Direct	Total, for all markers (All foils except one Ta were crossed by Zn or dissolved)

Table III, Cont. Displacement of Interface Markers

Specimen	Type of Markers at Each Interface	Temp, °C	Time of Diffusion, hr	Shift at Each Interface, cm	Method of Measurement	Observations
E 1	3 Mo wires 0.0075 cm 2 Ta foils 0.0025 cm	884	46 46 46 46 46	—0.0027 +0.0025 —0.0052 —0.0079	Direct Direct Direct Foil bend	Total for wires Total for foils Rel. to foils
C 22	2 Mo wires 0.0075 2 Pt wires	733	2 2	+0.0065 —0.0196	Direct Direct	Total for Mo wires Total for interface
			18.8 18.8	+0.0210 —0.0685	Direct Direct	Total for Mo wires Total for interface
Cu-Al System						
B 34	5 Mo wires 0.0075 cm	948	147	0.0014 0.0015	Direct Direct	Total shift Total shift
			341	0.0022 0.0021	Direct Direct	Total shift Total shift
			608	0.0024 0.0022	Direct Direct	Total shift Total shift
B 39	5 Mo wires 0.0075 cm	889	305	0.0011	Direct	Total shift
C 6	5 W wires 0.0012 cm	994	186	0.0029 0.0023	Direct Direct	Total shift Total shift
Cu-Zn System						
B 23	4 W wires 0.0050 cm	804	224	0.0029 0.0031	Direct Direct	Total shift Total shift
B 28	4 Mo wires 0.0075 cm	812	164	0.0026 0.0030	Direct Direct	Total shift Total shift
B 41	5 Mo wires 0.0075 cm and 2 Fe foils 0.0025 cm	733	191 695	0.0002 0.0012 0.0020 0.0024	Direct Direct Direct Direct	Total, uncorrected Rel. to foils Total, uncorrected Rel. to foils
B 46	3 Mo wires 0.0075 cm	733	504	0.0023	Direct	Total shift
Cu-Ni, Ag-Au, and Cu-Au Systems						
B 38	3 Mo wires 0.0075 cm	947	362	0.0039	Diff. curve	
C 4	3 Mo wires 0.0075 cm	1054	312	0.0094 0.0140	Direct Diff. curve	Total shift From C 4-I
C 21	2 Mo wires 0.0075 cm	839	24½ 92	0.0007 0.0020	Direct Direct	Total shift Total shift
D 2	4 W wires 0.0012 cm	910	96	0.0113	Direct	Total shift
D 3	3 Mo wires 0.0075 cm	925	50	0.0113	Direct	Total shift

the outer layer which had absorbed Zn. The surfaces then were polished and etched; samples revealing faulty welds were discarded. The markers (and sometimes the original join) were visible on the final surface.

The diffusion-penetration curves (herein designated as c-x curves whatever units were used to express concentration and distance) were obtained from samples procured by machining. Machining was a critical operation; accurate specimen alinement with the lathe axis was obtained by the use of a mounted telescope with reticule, sighting upon the readily visible markers, rotating the specimen and adjusting; in some cases the weld line on an etched sample served equally well. Successive layers were machined normal to the lathe axis (parallel to the markers and join); the thickness of layers varied with the extent of diffusion; with small amounts of diffusion, and with nearly symmetrical diffusion-penetration curves, it was 0.0050 cm, or 0.0075 cm; in others, these same thicknesses were taken when the c-x curve varied sharply with distance, but when it varied but slowly thicker layers, 0.0150 and 0.0200 cm, were taken. The machined layers were analyzed chemically; in the Cu-Zn system usually Cu only was determined by chemical analysis, though both Cu and Zn were determined in sample B20-II. Some 20 machined samples were analyzed for each c-x curve.*

Measurement of Marker Position and Marker Shift

Direct Method: The initial distances between markers in double couples (sandwiches) were established after welding as noted above; after diffusion these distances were determined again in the same way; this is effectively the method employed by Smigelskas and Kirkendall[1]; it is denoted herein as the "direct method"; as in Figs. 47 to 55 and Table III these were reproducible to ±0.0004 cm; since the markers were pressed between the metal disks before welding, the wires were imbedded in both disks (in Smigelskas and Kirkendall's electroplating technique the wires were not centered exactly at the join, but lay just off the join, imbedded in the electroplate); it was easy to locate the wires with respect to the welded join, and to observe the penetration of the disks by the markers, Fig. 3; in the Cu/α-brass couples, the wires penetrated the Cu a little more than the α-brass. Microscopic inspection showed that inclusions at the join move as do the markers; they thus also serve as markers. The

* For the data from which c-x curves were plotted order Document 3115 from American Documentation Institute, 1719 N St., N.W., Washington 6, D. C., remitting $1.00 for microfilm (images 1 in. high on standard 35 mm motion picture film) or $1.05 for photocopies (6x8 in.) readable without optical aid.

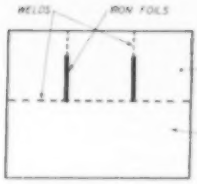

Fig. 7 (left)—Showing placement of foil markers for measurement of changes in lateral dimensions.

Fig. 9 (right)—c-x curve for sample B20-I, Cu/α-brass.

direct method is not the best (as the data will show), for it probably suffers from secondary effects of creep, internal gas reactions, and possibly, though not certainly, dimensional changes resulting from internal stresses and recrystallization.

Diffusion Curve Method: The procedure of machining layers to determine the c-x curve served to place the markers upon the c-x curve, for when the markers were encountered during machining they could be recognized readily and thus associated with the composition of the layer machined at that point. The accuracy of the placement of the markers by this method was thus that of the thickness of the machined layer. As shown elsewhere, the position of the Matano interface was found to agree with the position of the original join, when lattice space is

Table IV. Matano Areas Observed in the Specimens Studied

Specimen	Time, hr	Temp, °C	Matano Area (cm) (A/o)
B 20-I	119	880	0.95
B 35-I,II	691	784	0.98
B 36-II	507	834	1.33
B 37-I,II	197	885	1.36
B 22-I	165	977	0.99
B 34-I	608	948	1.09
B 39-I	305	889	0.59
B 23-I	224	804	0.10
B 33-I	524	808	0.16
B 46-I	504	733	0.07
B 38	362	947	0.51
C 4-I	312	1054	0.96

employed; thus the difference in position of the marker and the Matano interface is the shift; this method is denoted herein as the "diffusion curve method," see Figs. 47 to 55 and Table III. A single couple will suffice for this method.

Foil Reference Method: Impermeable foils inserted in the original join served as reference points for other, mobile markers; as noted elsewhere, this is a good method, for if the movement of the mobile markers is corrected for the (slight) movement of the centers of the "static" foils, then secondary effects of creep, etc., are excluded. In Figs. 47 to 55 and Table III, this is denoted as the "relative to foil" method.

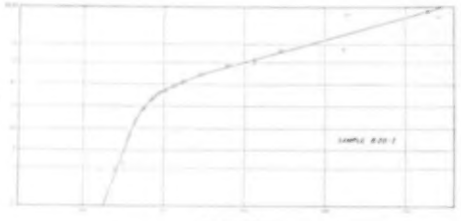

Fig. 8—Probability plot of c-x curve for sample B20-I.

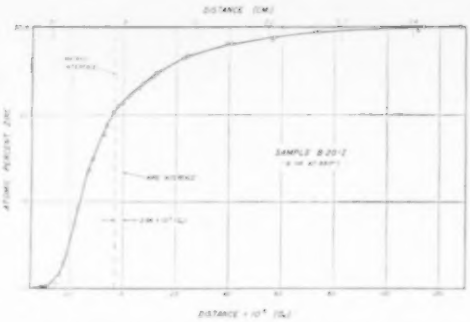

Foil Bend Method: This method is based upon the new observation that the edge of a foil placed at the join will bend progressively as diffusion occurs around it, Figs. 4 and 5. The middle portion of the "impermeable" foil will stay fixed as long as it is not affected by the diffusion occurring around the edges.

This also appears to give a reliable experimental method for obtaining the shift of markers caused by diffusion, since the movement of the foil tip can be measured (with respect to the unaffected middle portion) and such a measurement will not be affected by secondary volume changes occurring in the disks themselves. This method is denoted as the "foil bend method" in Figs. 47 to 55 and Table III. Interestingly enough, on very extensive diffusion, when diffusion had extended thoroughly around the foil, the foil "unbent," becoming flat again, Fig. 6.

Measurement of Shift in Lateral Dimensions

All treatments of the work of Smigelskas and Kirkendall (and of other work) assume that there is no change in lateral dimensions, i.e., perpendicular to the direction of the diffusion current, though there have been no measurements of this. This measurement was made on a multiple sandwich, sample C19, with foils placed parallel to the diffusion direction, as sketched in Fig. 7. Three blocks of 30 pct Zn brass were welded with two iron foils placed as shown; this specimen then was machined to produce a plane surface perpendicular to the foil markers and then welded to a copper disk. Movement of these markers, spaced at a distance of 1.05 cm with respect to one another, served to evaluate

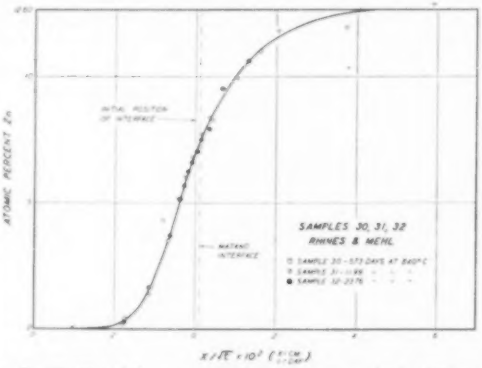

Fig. 10—Plot of three c-x curve for Cu/α-brass couples for different values of time, abscissas $x/t^{1/2}$.

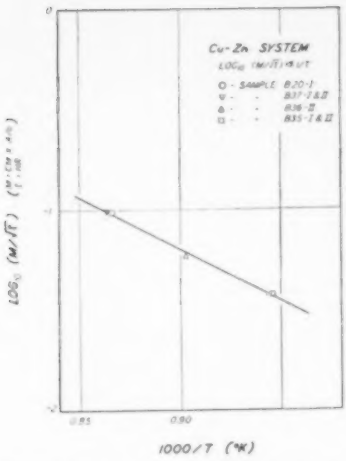

Fig. 11 (left)—Log $M^{1/2}$ vs. 1/T, Cu/α-brass couples.

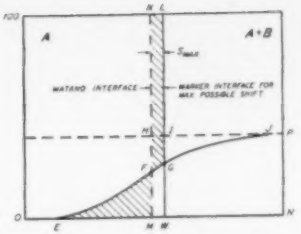

Fig. 12 (right)—Graphical determination of maximum possible marker shift.

Table V. Values of K_M and Q_M

System	Nominal Conc. Range A/o	K_M (cm) (A/o) / (hr) $^{1/2}$	Q_M cal/mol
Cu-Zn	0-30	$1.38(10)^8$	44,300
Cu-Al	0-16	$3.53(10)^8$	53,400
Cu-Sn	0-5.5	$0.246(10)^8$	45,100
Cu-Ni	0-100	$0.147(10)^8$	41,800

lateral dimensional change. Measurements were made between the foils very near the interface and at a point well beyond the diffusion zone; some movement might be expected in the latter because of creep, etc.; the lateral shift is taken as the difference between the movements of the foils at the interface and those beyond the diffusion zone. The diffusion temperature was 884°C and the time 73 hr. Diffusion-penetration curves were not made, but can be calculated from the other data for this system.

Methods of Plotting Results

The c-x curves are plotted conventionally as concentration, either in weight or atomic percentage, vs. distance in usual units. As is well known (see, for example, ref. 9), if the diffusion coefficient D does not vary with the concentration, this plots as a straight line on probability paper; if D varies with concentration ($D = f(c)$) the curve is bent, as in all cases herein. Such a plot, however (Fig. 8), serves to "normalize" the curve—it is much easier to draw a "best fit," to eliminate clearly spurious points. The curve drawn can then be used to redraw the conventional curve (Fig. 9), and to calculate $D = f(c)$; this is the method adopted in all cases.

Diffusion in solids occurs in a lattice; atomically, it appears that the process must consist of atom jumps from one lattice point to another, the distance of closest approach of atoms; it is unlikely that this elementary process should involve a multiple of this distance. Whatever the distance, movement must occur in steps in lattice space, which may be taken as the side of the unit cell, a_o (or the distance of closest approach). Cartesian space is thus indirect in the process; advantages should accrue to plotting lattice space (or distance) instead of Cartesian space (or distance) and this method has been adopted. Such a plot obviously avoids the necessity for any correction of distance measured at room temperature to distance at the temperature of diffusion; on this basis a comparison of D at one concentration with D at another should be more fundamental. In studying marker displacement, this method has a special advantage: marker displacements originating in density changes are eliminated. The transformation from distance in terms of centimeters to distance in terms of the number of lattice (a_o) spacings, can readily be accomplished graphically; Fig. 9 is drawn on this basis. Diffusion coefficients calculated from such curves will have the dimensions $(a_o)^2$ per sec. The ordinate should be the number of atoms in the unit cell, although, since atomic percentage is linearly related to this in substitutional solid solutions, atomic percentage may be used. This method of plotting has been used wherever the precision of the data seemed to warrant the labor.

Since the present work is primarily a general experimental exploration of marker shift, only a few measurements were made on the rate of marker movement at one temperature (known from Smigelskas and Kirkendall[1] and Darken[4] to be parabolic);

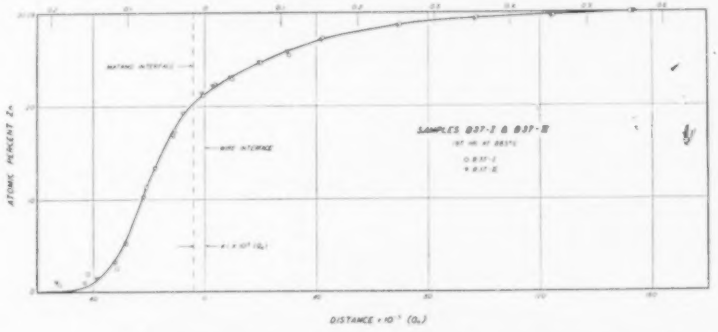

Fig. 13—c-x curve and marker position for samples B37-I and II, Cu/α-brass.

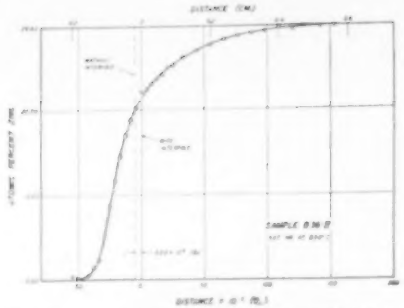

Fig. 14— curve and marker position for sample B36-II, Cu/α-brass.

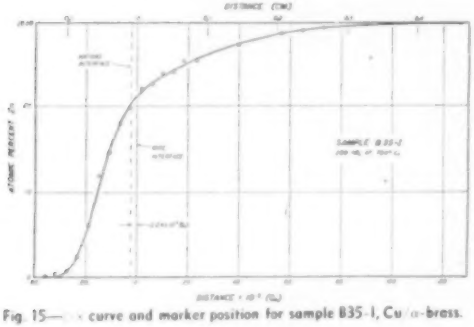

Fig. 15— curve and marker position for sample B35-I, Cu/α-brass.

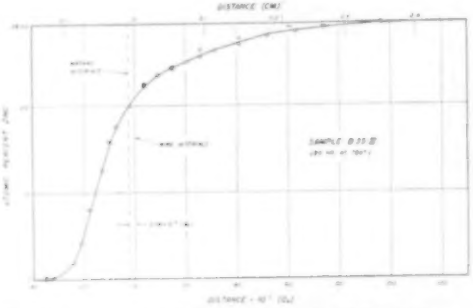

Fig. 16— curve and marker position for sample B35-II, Cu/α-brass.

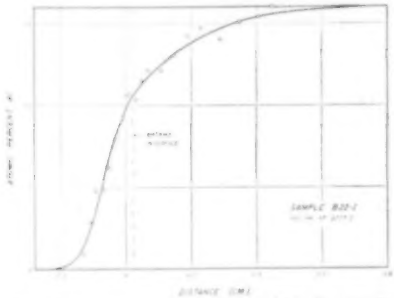

Fig. 17— curve and marker position for sample B22-I, Cu/αCu-Al.

Table VI. Marker Shifts and Matano Areas

Specimen	Matano Area (cm) (A/σ)	Shift of markers (cm)	Observations
Cu-Zn System			
B 20	0.96	0.0109	From diff. curve
B 35	0.96	0.0084	From diff. curve
B 36	1.34	0.0190	From diff. curve
B 37	1.29	0.0148	From diff. curve
B 42	0.42	0.0048	Rel. to foils
	0.85	0.0094	Foil bending
B 45	0.40	0.0047	Rel. to foils
	0.94	0.0105	Rel. to foils
	0.84	0.0089	Foil bending
C 1	0.40	0.0035	Rel. Ta foil
E 1	0.62	0.0052	Rel. to foils
	0.62	0.0079	Foil bending
Cu-Al System			
B 34	0.72	0.0014	Total shift
	1.11	0.0021	Total shift
	1.48	0.0023	Total shift
B 39	0.60	0.0011	Total shift
C 6	1.21	0.0026	Total shift
Cu-Sn System			
B 23	0.102	0.0030	Total shift
B 28	0.094	0.0028	Total shift
B 41	0.046	0.0012	Rel. to foils
	0.087	0.0024	Rel. to foils
B 46	0.072	0.0023	Total shift
Cu-Ni System			
B 38	0.51	0.0039	From diff. curve
C 4	0.96	0.0140	From diff. curve
		0.0094	Direct measure
Ag-Au System			
D 2	3.4K	0.0113	Direct measure
D 3	2.7K	0.0113	Direct measure

a variety of temperatures and times was used. It would be useful to have a method to compare the results obtained. An approximate method has been derived and will be employed in treating some of the data.

The penetration x, for a given concentration, (c), depends upon time, as is well known, by the relation:

$$x(c) = k(c) \cdot t^{1/2}$$

Since all points in a diffusion curve obey this relation, it is obvious that, from a single diffusion curve for a given time, the diffusion curve corresponding to any other time (at the same temperature) may be derived. The inverse, of course, is also true: we can reduce all diffusion curves (for different times, at a given temperature) to a single master curve, if instead of distance x we plot $(x \cdot t^{-1/2})$, Fig. 10 (plotted from the data of Rhines and Mehl[10]).

If we wish to compare diffusion curves (or shifts) obtained at different temperatures, the following approximate treatment may be used:

The usual expression for D:

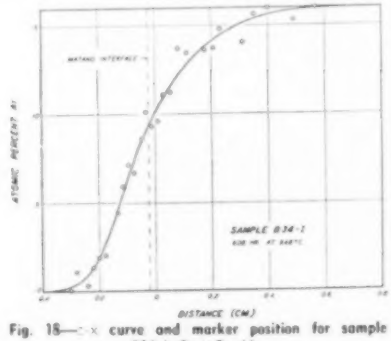

Fig. 18— curve and marker position for sample B34-I, Cu/αCu-Al.

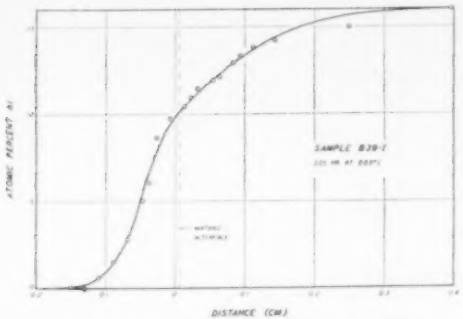

Fig. 19—C-x curve and marker position for sample B39-1, Cu/αCu-Al.

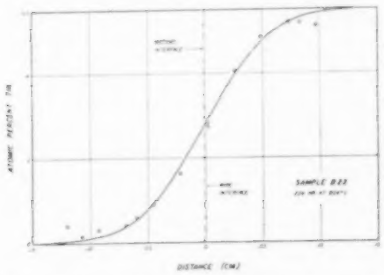

Fig. 20—C-x curve and marker position for sample B23, Cu/αCu-Sn.

$$D = A \cdot e^{-Q/RT}$$

can be written:

$$D(c,T) = A(c) \cdot e^{-\frac{Q(c)}{RT}} \qquad [1]$$

indicating that, for a given solid solution, D, A, and Q depend on the concentration. If we are dealing with relatively small temperature intervals, or if we are satisfied with only an approximate treatment, we may substitute an average, constant value Q_{av} for the function $Q(c)$:

$$D(c,T) = A(c) \cdot e^{-\frac{Q_{av}}{RT}} \qquad [2]$$

Consequently, if we know the function $D(c,T)$ for a temperature T_1, its value at T_2 is given by:

$$D_2(c) = e^{\frac{Q_{av}}{R} \cdot \frac{T_2 - T_1}{T_2 T_1}} \cdot D_1(c) \qquad [3]$$

which is equivalent to the displacement of $D = f(c)$ by a constant amount:

$$D_2(c) = K \cdot D_1(c) \qquad [4]$$

In this treatment, then, passage from temperature T_1 to T_2 is equivalent to multiplying the coordinates x of the diffusion curve by a constant $\sqrt{K}$.

Thus, we may write, as an approximation (eq 3 above):

$$D_2(c) = e^{\frac{Q_{av}}{R} \cdot \frac{T_2 - T_1}{T_2 T_1}} \cdot D_1(c) \qquad [3a]$$

and

$$x_2(c) = e^{\frac{Q_{av}}{2R} \cdot \frac{T_2 - T_1}{T_2 T_1}} \cdot x_1(c) \qquad [5]$$

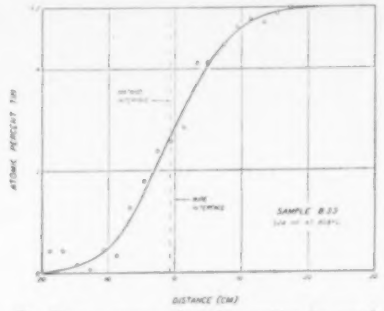

Fig. 21—C-x curve and marker position for sample B33, Cu/αCu-Sn.

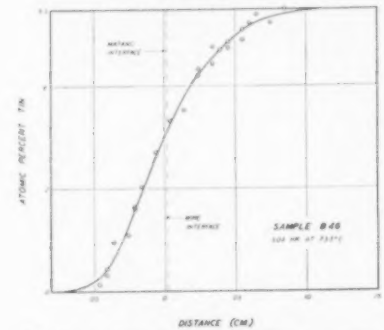

Fig. 22—C-x curve and marker position for sample B46, Cu/αCu-Sn.

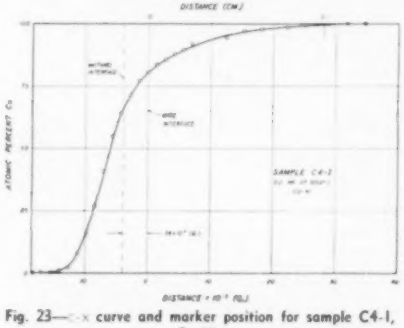

Fig. 23—C-x curve and marker position for sample C4-1, Cu-Ni.

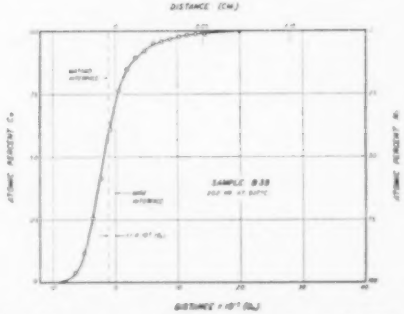

Fig. 24—C-x curve and marker position for sample B38, Cu-Ni.

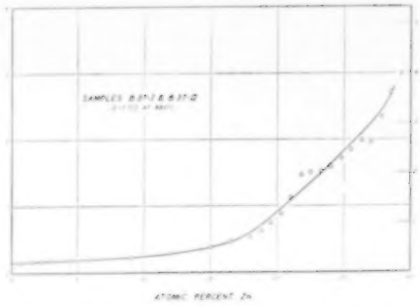

Fig. 25—D = f(c) for samples B37-I, II, Cu/α-brass.

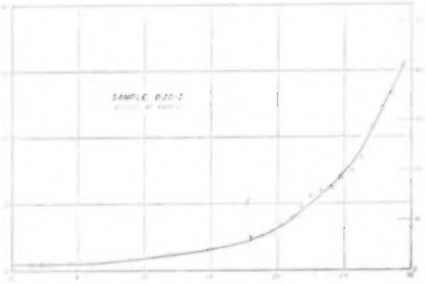

Fig. 26—D = f(c) for sample B20-I, Cu/α-brass.

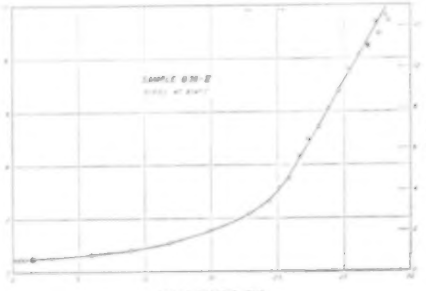

Fig. 27—D = f(c) for sample B36-II, Cu/α-brass.

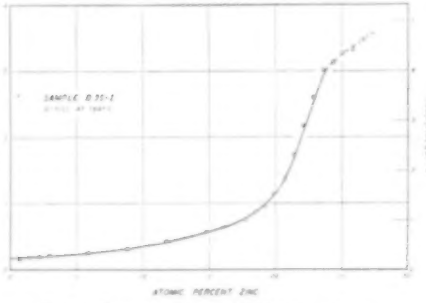

Fig. 28—D = f(c) for sample B35-I, Cu/α-brass.

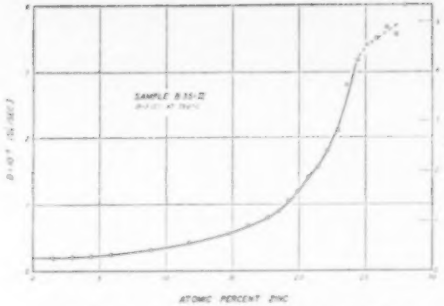

Fig. 29—D = f(c) for sample B35-II, Cu/α-brass.

If the time also varies, then:

$$x_2(c) = \sqrt{\frac{t_2}{t_1}} \cdot e^{\frac{Q_{av}}{2R}\left(\frac{T_2 - T_1}{T_2 T_1}\right)} \cdot x_1(c) \qquad [6]$$

or, in general:

$$x(c) = K(c) \cdot t^{1/2} \cdot e^{-\frac{Q_{av}}{RT}} \qquad [7]$$

This is approximate, but it predicts the actual shape of the diffusion curve quite well, knowing the diffusion curve for a given t and a given T.

The Boltzmann-Matano area (hereinafter the "Matano area") is that on either side of the Boltzman-Matano interface (the "Matano interface"). These areas, as measured from the diffusion curves, are given in Table IV. This area measures the amount of diffusion; if atoms are conserved on lattice points, it represents the number of atoms diffused. It varies linearly with x and $t^{1/2}$ and can be written:

$$M = K_M \cdot t^{1/2} \cdot e^{-\frac{Q_M}{RT}} \qquad [8]$$

Again Q is averaged over a concentration range. This area is less subject to error since slopes and small areas are not measured, as they are in calculating D.

The values of K_M and Q_M in eq 8 may be obtained from a plot of $\log_e(M/t^{1/2})$ vs. $1/T$, employing the data from Table IV; Fig. 10 gives the plot for the system Cu-Zn (similar plots were made for the other systems); the plots serve to show that eq 8 is satisfactory; the derived values for K_M and Q_M are given in Table V. Using eq 8 and the data in Table V, the Matano areas have been calculated for those specimens in which marker displacements have been measured; these marker displacements and corresponding Matano areas are given in Table VI. These are the data used in Figs. 11 to 15; since the marker shift varies with $t^{1/2}$, it should also vary linearly with the Matano area.

In the Ag-Au system values of K_M and Q_M were not available, the comparison of the two measured shifts was approximated by assuming a Q-value of 26,600 cal per mol.[11] This value may be too low.

Maximum Possible Shift

If it is assumed, as others have, that the marker shift results from unequal countercurrent diffusion flow, it is possible to calculate, in some of the present cases, the marker displacement that would result if the diffusion coefficient of one of the atomic species were zero—if one of the atomic species did not cross the marker at all. This shift will be desig-

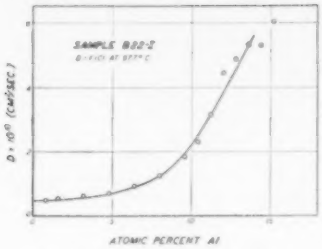

Fig. 30—D = f(c) for sample B22-I, Cu/αCu-Al.

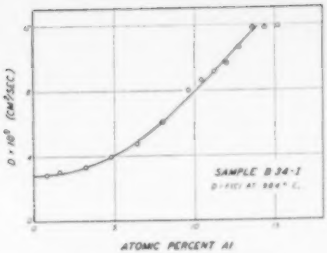

Fig. 31—D = f(c) for sample B34-I, Cu/αCu-Al.

nated as the "maximum possible shift," S_{max}. Such a calculation assumes that no measurable voids are created, and that all dimensional changes are in the direction of diffusion flow.

Fig. 12 represents a diffusion curve in lattice units, for diffusion between a metal and its terminal solid solution. Areas in this diagram are proportional to numbers of atoms. At the outset, the number of *B* atoms is proportional to the area *MHPN*. If *B* atoms cross the markers toward the left without any *A* atoms crossing toward the right, the markers will move to a new position *WL* in such a way that the area *EFM* and *FKLG* will be equal. The maximum possible shift would then be the shift from *MK* to *WL*. The values of S_{max} in terms of lattice units are then reconverted to cm, and plotted against cm, as in Figs. 48 to 53.

c-x Curves

The data are plotted in Figs. 9 and 13 to 24; the abscissas are lattice spacings where possible. As noted, Fig. 13 plots data for both couples in a sandwich; the correspondence speaks well for the reproducibility of such data.

D = f(c)

From the above curves, the variation of *D* with concentration can be plotted ($D = f(c)$); the results are plotted in Figs. 25 to 36. Fig. 37 is a comparison of the $D = f(c)$ curve for the Cu/20 pct Zn couple, as determined at 923°C as compared with a similar curve for the couple Cu/30 pct Zn, extrapolated from the curves for this couple obtained at lower temperatures. In the Cu/20 pct Zn couple, the *D*-values above about 10 pct Zn are for compositions losing Zn during diffusion, below 10 pct Zn for compositions gaining Zn. In the Cu/30 pct Zn couple the dividing composition is about 15 pct. The curves suggest that for a given composition, the *D*-value is the higher when that composition is losing Zn than when gaining, as though the act of losing Zn creates a structural degeneracy which favors a higher mobility. Fig. 38 is a recalculation of the earlier data of Rhines and Mehl,[9] for somewhat similar couples. The results are essentially the same. This result is highly tentative, for the comparison for the Cu/20 pct Zn couple is necessarily made for the high-Zn side, i.e., near one end of the diffusion-penetration curve where the accuracy is not good. The curves for the Cu/30 pct Zn couple, comparing the present results with the earlier ones

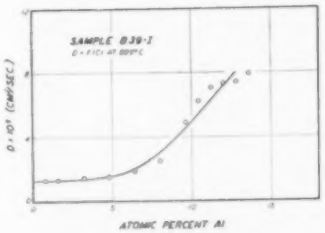

Fig. 32—D = f(c) for sample B39-I.

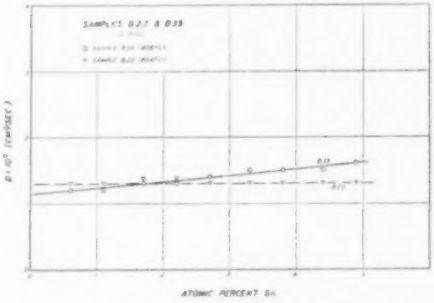

Fig. 33—D = f(c) for samples B23 and B33, Cu/αCu-Sn.

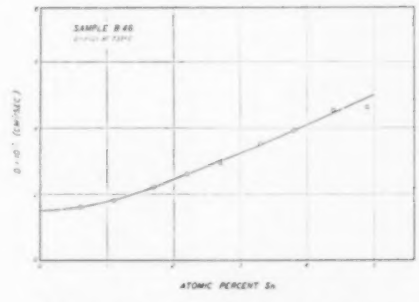

Fig. 34—D = f(c) for sample B46, Cu/αCu-Sn.

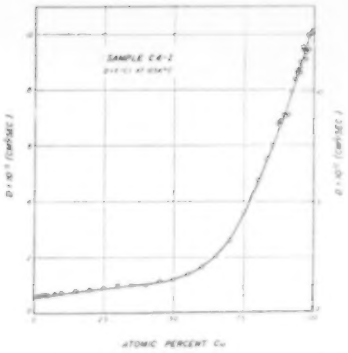

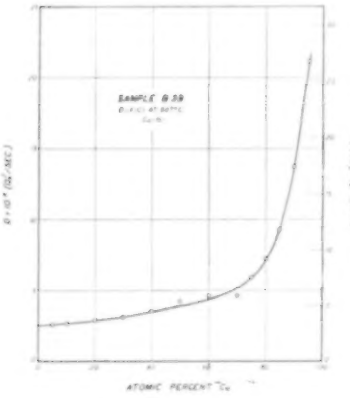

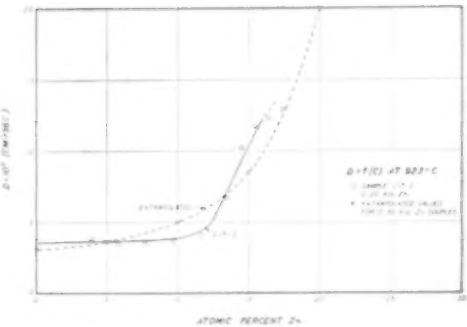

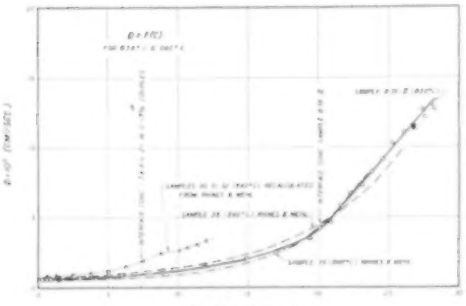

of Rhines and Mehl show remarkably good agreement.

Activation Plots

From the preceding data, eq 1 may be plotted for the systems Cu-Zn, Cu-Al, Cu-Sn, and Cu-Ni, Figs. 39 to 42. The activation plot for Cu-Ni, Fig. 42, and the plot of $Q = f(c)$, Fig. 45, are surprising; probably further study is needed. The activation plot for Cu-Zn, Fig. 39, shows wide scatter, possibly reflecting appreciable variation in measured D-values as a result of grain-size differences at low temperatures.[17]

Q = f(c)

The values of the activation energy Q as a function of concentration ($Q = f(c)$) may now be plotted, Figs. 43, 44, 45, and 47. These values for the systems Cu-Zn, Cu-Al, and Cu-Sn are in fair agreement with those of Rhines and Mehl;[16] in all cases the direction of change of Q with increasing concentration is the same. The values of Q calculated by Rhines and Mehl were known to be highly approximate; these new values are probably better. Fig. 46 plots the frequency factor A as a function of concentration for the system Cu-Zn.

Marker Displacement

The methods are given above. The measurements are listed in Table III. The results are plotted in Figs. 48 to 56; in several of these the ordinate is $t^{1/2}$, in others the Matano area.

Table III gives the types of markers, the temperature and the time of diffusion, the shift measured, and the method used. Note that several methods are occasionally included in one sample, such as B-45, E-1, etc. Moreover, in some cases markers of different materials were included in one sample, of which sample C-20 is an important example. In this case and in other cases, all markers, whatever their nature, moved by exactly the same amount; the amount of bending of foil markers, whatever their composition, was the same. These materials vary markedly in chemical nature and in physical form and dimension.

Inasmuch as some possibility obtained that marker movement might be related to transport of matter at the interface around an insoluble wire (and therefore be related to diffusion only most indirectly), wire markers were used which dissolved in the matrix; these were of Ni and Pt; Ni dissolved too rapidly; Pt, however, in wire form, 0.001 in. diam, was useful: though it dissolved, the point where it had been (and where the Pt concentration was still high) could be recognized clearly upon etching; this marker moved the same distance as all the others. As noted, the Matano areas, and corresponding marker shifts, are given in Table VI.

Fig. 48 gives the data for the Cu-Zn system at 882°C plotted against $t^{1/2}$. As remarked above, data from the direct method are probably most unreliable; these points are represented by open circles, triangles, etc.; the data from the presumably more trustworthy experiments, resulting from application of the other methods ("reference to foils," etc.),

Fig. 35 (top)—D = f(c) for sample C4-1, Cu-Ni.

Fig. 36 (second from top)—D = f(c) for sample B38, Cu-Ni.

Fig. 37 (third from top)—D = f(c) for sample C17-1, Cu/α-brass.

Fig. 38 (bottom)—Comparison of diffusion data for 834° and 840°C, Cu/α-brass.

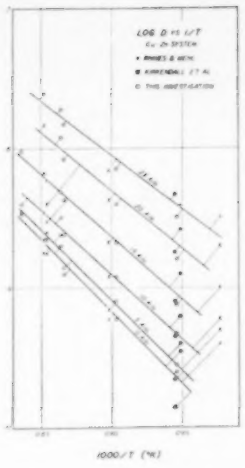

Fig. 39—Log D vs. 1/T, Cu/α-brass.

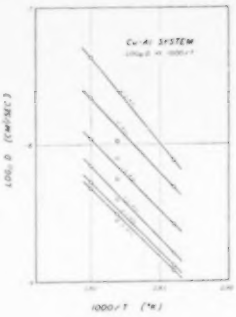

Fig. 40—Log D vs. 1/T, Cu/αCu-Al.

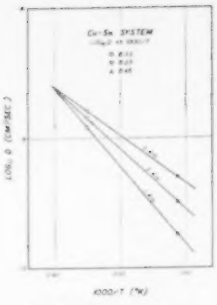

Fig. 41—Log D vs. 1/T, Cu/αCu-Sn.

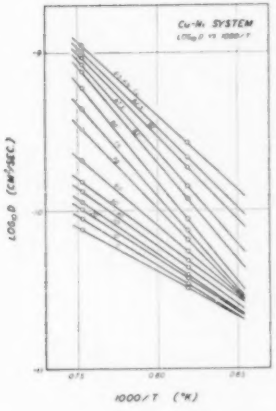

Fig. 42 (right)—Log D vs. 1/T, Cu-Ni.

are represented by filled-in points; the curves "observed shift" are drawn from these, ignoring the others. The great scatter shown in the points from the "direct method" is evidence that this method does not yield consistent data and is presumably somewhat unreliable. Using only the filled-in points, the parabolic law is reasonably obeyed. The shift is toward the high-Zn side of the couple (see Figs. 48 to 51) and is nearly the maximum possible shift. Fig. 49, representing data for 834°C, seems to show that the maximum possible shift is nearly attained, though the data are few.

Fig. 50 is a similar plot for a temperature of 784°C; again the shift is near to the maximum possible. The data of Smigelskas and Kirkendall are placed on this diagram; the agreement with the current data is fairly good. The points represented by upright triangles probably should be disregarded, for reasons noted above, and have been disregarded in drawing the curve of observed shift; all points from the direct method have been disregarded. These data include reversed couples, i.e., both Cu/30 pct Zn/Cu couples (as employed by Smigelskas and Kirkendall) and 30 pct Zn/Cu/30 pct Zn couples. No significant difference in the marker shift upon couple reversal is evident.

Fig. 51 combines the data, plotting the Matano area as abscissa. The parabolic law is evident; the current data (here as elsewhere) suggest that the shift is somewhat greater than that measured by Smigelskas and Kirkendall; it shows also that the shift is not far from the maximum possible.

Fig. 52 gives a similar plot for the Cu-Al system. The marker displacement is toward the high-Al side of the couple. It is but a fraction of the maximum possible shift.

The marker displacement in the Cu-Sn system, Fig. 53, is toward the high-Sn side of the couple. Most surprisingly, the shift is greater than the "maximum possible"; the data are few, however, and difficulties in chemical analysis (especially in

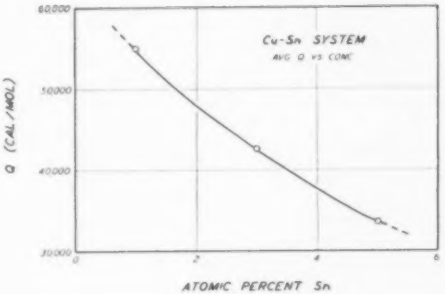

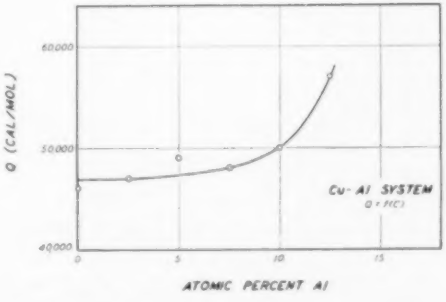

Fig. 43 (second from bottom)—Q = f(c), Cu/αCu-Sn.

Fig. 44 (bottom)—Q = f(c), Cu/αCu-Al.

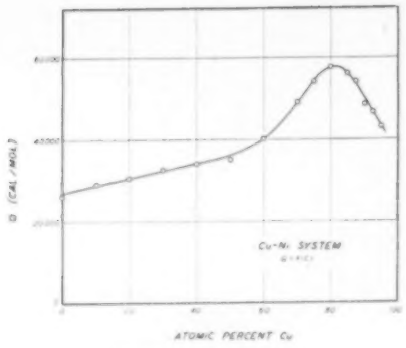

Fig. 45—Q = f(c), Cu-Ni.

view of the small concentration range involved, viz., 5.5 atomic pct) may render them untrustworthy. The unexpected and even startling nature of these results recommend further study. The results on the systems Cu-Al and Cu-Sn probably suffer from inferior accuracy.

In the Cu-Ni system, the shift is toward the high-Cu side of the couple, Fig. 54. The data are too few to permit a detailed study.

Fig. 55 is an approximation (as noted elsewhere) for the shift in the Ag-Au system, as plotted against (an approximation of) the Matano area. The shift is toward the high-Ag side of the couple.

Fig. 56 is a plot of the shift for the system Cu-Au, plotted against $t^{1/2}$. The shift is toward the high-Au side of the couple.

Lateral Shift

The method used has been described above; the results are given in Table III, sample C-19. The lateral shift is 0.0007 cm; this is a value for the shift observed in the foils at the interface, corrected for a small shift observed at the other ends of the foils (caused, presumably, by creep, etc.). At the beginning of the diffusion treatment, the composition at the Cu/α-brass interface was 30 atomic pct Zn; after diffusion this became 21 atomic pct; the lateral shift due to lattice parameter change at this point should be 0.0075 cm, and this should be a decrease in the inter-foil distance at the Cu/α-brass interface. The observed shift is but one tenth of this. Moreover, if all dimensions of the brass were to decrease by the amount which the ordinary markers shift, i.e., if the shift of the ordinary markers reflects a simple decrease in volume of the brass, then a further contraction of 0.0080 cm should occur. These special foil markers thus seem quite inert.

This single observation seems to indicate that dimensional changes are entirely unidirectional—in the direction of the diffusion stream. This validates the common theoretical assumption, though the oddity of the phenomenon would appear to demand further study.

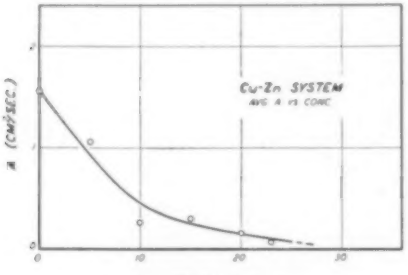

Fig. 46—A = f(c), Cu/α-brass.

Micrographic Studies

Figs. 56 to 58 illustrate the grain structure obtaining at the interface. Apart from deliberately inserted markers, which can readily be seen, some inclusions are visible (on unetched as well as on etched samples, though not easy to show in reproduction); as noted, these inclusions also constitute markers, and move as others do; the micrographs serve also to show the markers in relation to the join.

On the original welded samples, the weld join is, of course, a straight line forming a linear multigrain boundary. This multigrain boundary tends to persist with diffusion, frequently remaining quite straight though sometimes curved; thus grain growth occurs at this point, since the markers move and the grain boundary moves with the markers, during diffusion. It is possible that this is evidence for strain accompanying diffusion, with the generation of imperfections including those of the dislocation type. The long times and the high temperatures of diffusion cause general grain growth; observations of the couples after diffusion are given in Table VII. Much study remains to be done with respect to grain structure changes during diffusion, and it is more than possible that this will contribute much to the subject and even to the theory of diffusion.†

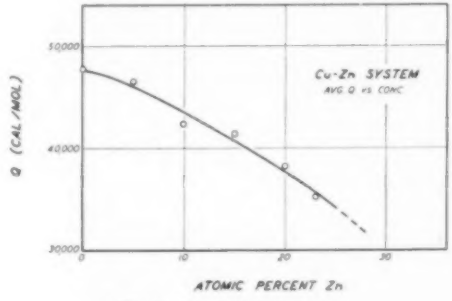

Fig. 47—Q = f(c), Cu/α-brass.

In couples in the Cu-Zn system, some porosity is evident. This porosity (to be distinguished from the very slight traces of "porosity" normally seen in polished sections of alloys, to be ascribed to the embedding of abrasive particles) occurs on the high-Zn side of the couple, Fig. 59. This is the "porosity" observed by Smigelskas and Kirkendall. It is evident, though barely so, in unetched specimens; etching presumably exaggerates it. It does not occur in the high-Cu side of the markers, nor in the immediate neighborhood of the markers, but a very little distance from it. The porosity appears abruptly and is greatest near the marker and decreases in amount with distance from the marker. It occurs only in the diffusion zone—it does not extend beyond it.

† These studies are under way, with special emphasis on the use of single crystals and the structural changes that occur in these.

Table VII. Grain Sizes Observed on Couples After Diffusion

Specimen	Couple	Treatment	Grain Size, mm
C-3	Cu/70Cu-30Zn/Cu	267 hr at 883°C	α-brass:1-4;Cu:0.5
C-11	70Cu-30 Zn/Cu/70Cu -30Zn	85 hr at 882°C	α-brass:2-4;Cu:1-4
C-14	Cu/70Cu-30Zn/Cu	112 hr at 884°C	α-brass:3-8;Cu:1-3
B-22	Cu/93Cu-7Al/Cu	165 hr at 977°C	bronzes:2-4;Cu:3-5

Very interestingly, the porosity is evident around the edge of a reference foil, Fig. 4. Despite some effort, this type of porosity was not found in general in the other systems studied, though some slight evidence for it was exhibited in the Cu-Al samples. It suggests, very tentatively, a degeneracy of the structure caused by diffusion.

Hardness Studies

The suggestion that the observed porosity may be evidence of structural degeneracy led to a study of the Knoop microhardness, with 100 g loads (heavier loads did not show the effect) across the diffusion interface. Nine sets were made on the polished sample, normal to the join. Each set consisted in ten measurements, at intervals of 0.0125 cm. These nine sets were arranged so that the different results on different grain orientations would be averaged and this variable eliminated. The total range studied was 0.050 cm, corresponding to a concentration range of 18 to 24 atomic pct Zn. The results are given in Fig. 60. The microhardness of pure Cu was

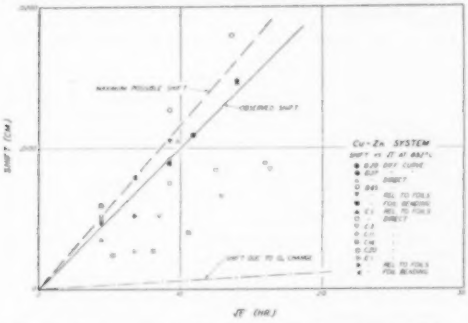

Fig. 48—Data on marker shift, $S = K\sqrt{t}$, Cu/α-brass, 822°C.

found to be 95, and that of the 70-30 composition 120; under the conditions of measurement, these values are wholly relative, though proportional to the usual Knoop hardness values. It would be expected that the hardness would change continuously, but the results show a sudden drop on the high-Zn side; this sudden drop appears at about the point where "porosity" becomes evident, and the hardness remains anomalous in the zones of porosity. This is what might be expected in a porous or otherwise degenerate structure. The results previously noted on diffusion-penetration curves, Figs. 37 and 38, might lead to a similar conclusion: that degeneracy obtains in these parts of a couple that lose Zn. This is wholly tentative; further study is certainly required.

Discussion

Phenomenological: The movement of inert markers in diffusion couples involving a single solid solution is real in the sense that it is a direct concomitant of the diffusion process only and is not an effect originating in nondiffusional processes. The

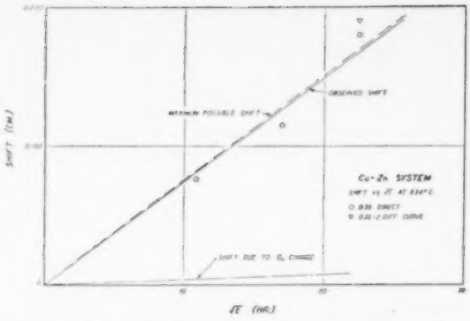

Fig. 49—Data on marker shift, $S = K\sqrt{t}$, Cu/α-brass, 834°C.

effect occurs whatever the nature of the marker, and the magnitude of the effect is identical with all markers, even in the case when the marker is not inert but dissolves. Neither the occurrence of the effect nor its magnitude is dependent upon the method of joining the couple (when metallic contact is intimate)—welding and electroplating give nearly the same result. Neither the effect nor its magnitude is dependent upon: (1) The outer geometry of the sample, for the result is the same for couples in which one side is a thin electroplate[1] as for couples in which both parts are heavy blocks, as in the present work; (2) couple reversal, for the marker displacement of a couple of the type *A/B/A* is identical with that for a reversed couple, *B/A/B*; (3) differences in the specific reactivities of the surfaces of the component metals with respect to the formation of vacancies, for the surfaces of both parts of the Cu/α-brass couples were coated with a layer of α-brass of uniform composition (see discussion below).

The effect occurs in lattice space, and methods are given by which the magnitude of the effect in lattice space may be shown. The effect seems to be unidirectional, occurring only in the direction of diffusion flow, judging from only one—though albeit quite careful—experiment which demonstrated no dimensional change perpendicular to the direction of diffusion flow.

The effect and its magnitude can be affected by secondary factors, such as creep, internal gas generation, and possible recrystallization, but these (except recrystallization) can be experimentally avoided and the basic effect confirmed and accurately measured by newly developed techniques;

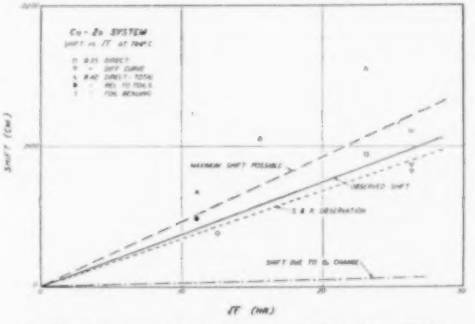

Fig. 50—Data on marker shift, $S = K\sqrt{t}$, Cu/α-brass, 784°C.

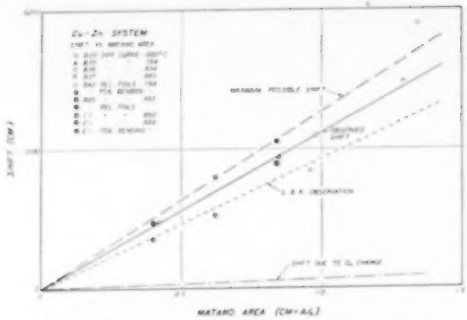

Fig. 51—Data on marker shift, plotted against Matano area, Cu/α-brass.

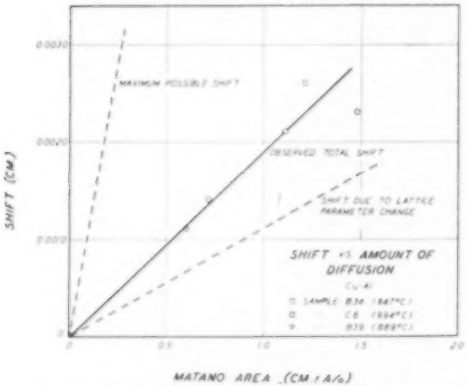

Fig. 52—Data on marker shift, plotted against Matano area, Cu/αCu-Al.

spurious effects are especially pronounced at high temperatures—thus, in Cu/α-brass couples they are negligible at 785° and 834°C, but appreciable at 882°C; the direct method (used by Smigelskas and Kirkendall) gives results which agree with those obtained by better methods of measurement at the two lower temperatures, but not at the high temperature.

The original interface is unambiguously given by the original positions of the unbent portions of the foil markers; the number of atoms on either side is unchanged since there is no diffusion normal to the unbent portions. The bending of the foil edge, as measured from the unbent portion, is thus the shift with respect to the original interface. Inasmuch as all other markers move quantitatively identically with the bending of the foil edge, then all marker shift is referred to the original interface as defined by the unbent foil. Measurements show that the amount of movement is identical with the marker movement referred to the Matano interface. The Matano interface thus defines the original interface. Inasmuch as the whole diffusion area is computed in determining the Matano interface, atoms are conserved on lattice points (else volume increases caused by lattice degeneracy—voids, etc.—would have given a discrepancy between the Matano interface and the original interface). Accordingly, volume anomalies, such as voids (porosity) are too small to be detectible; no change in normal lattice site vacancies would be expected to give a measurable volume anomaly, for appraisals of the probable fraction of vacant lattice sites show this effect to be beyond these measurements.

Mechanism: Smigelskas and Kirkendall proposed that the movement of markers may be taken as evidence that one component of the solid solution diffuses more rapidly than Cu and that the markers move with a bulk movement. All subsequent writers have adopted this point of view. Darken,[4] taking the marker as the origin of a frame of reference for diffusion flow and counterflow, provided a method of calculating the respective dual diffusion coefficients, finding $D_{Zn} > D_{Cu}$. Similar calculations can be made for the measurements on the several systems reported herein. (In passing, it should be noted that this in no way invalidates the Matano analysis; this remains a complete quantitative description of c-x diffusion curves.[5])

Darken's presumption depends upon the somewhat difficult concept of the movement of the "body" of the lattice, which the markers accompany. The validity of this concept, however, appears undoubted in view of the present observation that dissolved Pt markers move as do inert, insoluble markers, for the high-Pt regions are patently integral with the lattice; the much lower magnitude of the diffusion coefficient of Pt renders these regions relatively immobile. (At 800°C the diffusion coefficient of Pt in Cu[12] is one to two hundredth of that of Zn in α-brass.[13]) Radioactive tracers, used recently in this laboratory as markers in the study of multiphase oxidation layers, would doubtless provide similar evidence.

Darken's treatment is purely "phenomenological," i.e., it provided a quantitative treatment of the phenomena but did not contrive a mechanism. Seitz[3] pointed out that diffusion by means of direct atom interchange cannot offer a basis for marker movement, though diffusion through the action of vacancies can, recalling[14] that calculations of diffusional activation energies from first principles for face-centered cubic substitutional solid solutions of a Cu prototype show a preference for diffusion by vacancies over diffusion through interstices, and show that simple two-atom interchange would require prohibitively high energies. Recent calculations by Zener,[15] while altering some numerical values, retain this order of preference; Zener showed on a basis of energetics that a four-atom ring interchange, though requiring more energy than vacancy interchange (though not much) in

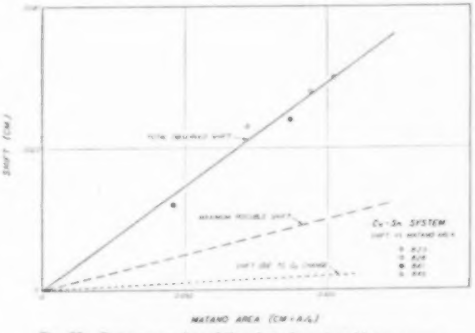

Fig. 53—Data on marker shift, plotted against Matano area, Cu/αCu-Sn.

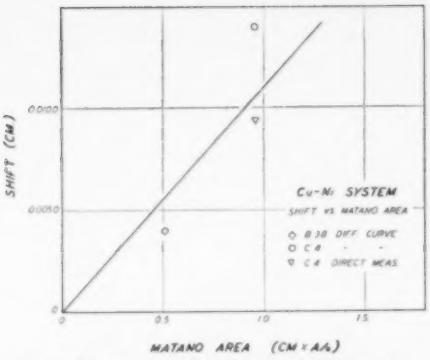

Fig. 54—Data on marker shift, plotted against Matano area, Cu-Ni.

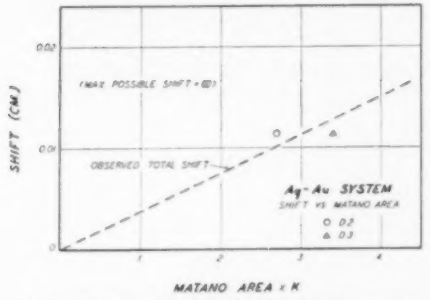

Fig. 55—Data on marker shift, plotted against Matano area, Ag-Au.

face-centered cubic lattices, may be the preferred mechanism in body-centered cubic lattices. Presumably, then, marker movement would not occur in the latter type of lattice (a matter now under study in this laboratory). These calculations are based, to be sure, upon geometrically ideal lattices; whether in real lattices, characterized by subgrain structural units of various types, vacancy diffusion alone obtains, cannot be said. If there be a fine structure to diffusion processes (a possibility deserving attention), with rapid diffusion along the surfaces of imperfection, then a real diffusion process must be represented by a series of fundamental diffusion equations of type 1, each applying to a single structural type of diffusion, as Smekal early proposed,[15] and the atom movement process would be a combination of several types, and, indeed, atom movement mechanisms prohibited in perfect lattices might well occur in the disorder of imperfections.

Seitz,[8] accepting Smigelskas and Kirkendall's idea of mass flow and Darken's analysis, then proposed that the result $D_{Zn}>D_{Cu}$ means fundamentally that the interchange Zn-vacancy is easier than the interchange Cu-vacancy, so that in the couple Cu/α-brass vacancies stream predominantly from left to right and Zn atoms from right to left. The accumulation of vacancies to the right was thought to produce voids (manifesting porosity) which in time disappeared by a sintering process, thus providing mass flow; this requires a source of vacancies; he thought the electroplated Cu might be characteristically high in voids and hence vacancies, but conceived the abiding source to be the outer surface of the sample. On this basis, mass flow was held to occur over a much greater volume than that of the diffusion zone; Darken held it to be restricted to the diffusion zone; Seitz stated that the issue would be resolved by couple reversal, saying that if α-brass were on the outside of the couple and Cu inside the marker movement would be reversed also. The present work favors Darken on the latter point and greatly limits the possibilities as to the source of vacancies.

The proposal that the stimulating vacancy flow originates at the specimen surface appears quite unlikely: the present experiments show that the marker movement does not vary in any way with the geometry of the sample; couple reversal is without result; the thickness of the Cu portion of the couple is without effect, since nearly the same result was obtained in the present work, where thick Cu disks were used as in Smigelskas and Kirkendall's work, where a thin electroplate was employed. Vacancies in any event could hardly, in the present experiments, have originated in the surface, for the Cu/α-brass couples were in fact completely covered with α-brass of the same composition, presumably providing vacancies equally to both elements in the couple, yet the results were nearly the same as those of Smigelskas and Kirkendall where the couple exhibited the surface of only Cu to the ambient. If the porosity observed in the α-brass portion of the Cu/α-brass couples is intimately related to mass flow process, then, so far as this portion of the couple is concerned, the effect does not extend throughout the volume of the sample, but is restricted to the diffusion zone.

The vacancy mechanism requires that (1) vacancies be created in the Cu side of the Cu/α-brass couple, and (2) that (after diffusing) they be destroyed on the α-brass side. In the light of the present findings, these processes must be limited to the diffusion zone; and in view of the finding that the lateral dimension does not appreciably change, the creation of vacancies in Cu and their diffusion toward and destruction in the α-brass must remove lattice planes perpendicular to the direction of diffusion in the α-brass and add perpendicular planes in the Cu.‡

The migration of vacancies from the Cu to the α-brass is not enough to explain mass flow, for it does not in itself explain how lattice planes are added on the Cu side and destroyed on the α-brass side while maintaining lateral dimensions unchanged. Dislocations might here be advanced as a helpful aid: Fig. 61 illustrates the shrinkage of the α-brass side of the couple in terms of a simple edge type of dislocation. On this side of the couple,

‡ For simplicity in discussion the Cu/α-brass couple will be used as a prototype, with what is said applying also to the other systems studied.

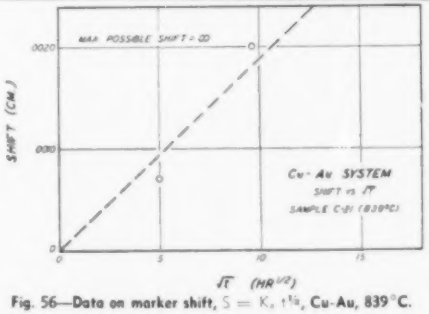

Fig. 56—Data on marker shift, $S = K_o t^{1/2}$, Cu-Au, 839°C.

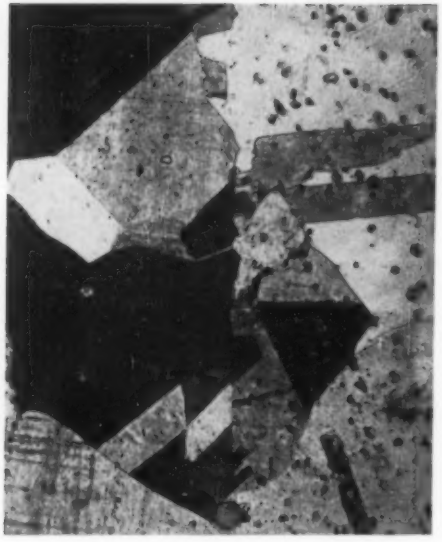

Fig. 57—Micrograph of sample B22, Cu/α-brass, $K_2Cr_2O_7$ etchant, Cu to left, showing one wire. X100.

Fig. 58—Micrograph of sample B22, Cu/αCu-Al, $K_2Cr_2O_7$ etchant, showing one wire. X100.

vacancies presumably could combine, forming a line of vacancies perpendicular to the direction of diffusion flow; this combination could then shrink to a dislocation of the type shown in Fig. 61 IV. This effectively destroys a lattice plane, giving marker movement as pictured, and maintains the constancy of lateral dimensions. Any three-dimensional void would provide three-dimensional contraction, and dislocations oriented otherwise than pictured would do likewise. Presumably it is the elastic restraint of the couple as a whole that restricts contraction to

Fig. 59—Micrograph of sample B35, Cu/α-brass, $K_2Cr_2O_7$ etchant, showing one wire. X100

the plane perpendicular to direction of diffusion flow.

Inasmuch as there is reason to believe that even annealed metals exhibit a characteristic concentration of dislocations, Zn atoms wandering toward the Cu, there find dislocations awaiting, and by a simple reversal of the process shown in Fig. 61, destroy a dislocation by occupying positions between dislocation edges, thus ultimately creating a new lattice plane.‡ This is a simple scheme offering possibilities of elaboration.**

This mechanism meets the requirements: lattice planes are destroyed on the α-brass side and created on the Cu side. The interaction of vacancies and dislocations is fundamental. It is probably oversimple to think of the two processes of destruction and creation as restricted respectively to the extremes of the diffusion zone; they would probably overlap within that zone. The creation of voids or porosity is not necessary, and indeed voids are not found in some systems studied herein, as noted above; whether or not voids form probably relates to the ease with which dislocations may form.

The marker shift varies greatly from system to system. In the Cu-Zn, Cu-Al, Cu-Sn systems the markers moved away from the Cu side of the couple; in the Cu-Ni system, toward the Cu side; in the Ag-Au system, toward the Ag side; in the Cu-Au system, toward the Au side. The magnitude of the marker shift varies greatly: it is relatively great in the Cu-Zn, Cu-Ni, and Ag-Au systems, and relatively small in the Cu-Al and Cu-Sn systems. As Darken's analysis[4] shows, these movements can be referred to the respective values of two diffusion coefficients for each system. And in turn this implies a greater rate of interchange with vacancies

‡ In those systems in which there is a marked change in lattice dimensions with concentration, stresses may well arise causing plastic flow and resultant recrystallization and grain growth, multiplying the dislocation concentration and facilitating the process pictured; there is ample evidence that recrystallization, or at least grain boundary movement, does occur in diffusion in α-brass.[32]

** Having seen this proposal, Seitz[19] has further developed it, employing dislocations of the ring type.

of the atom with the greater separate diffusion coefficient. No *a priori* way of predicting this is available.

If one assumes that diffusion is by the vacancy mechanism, with maintenance of equilibrium or near equilibrium of vacancy concentration, and with no sensible voids created, then self-diffusion measurements in alloys might possibly be taken to predict the direction of movement of markers; from Johnson's results on self-diffusion coefficients in a 50:50 atomic pct Ag-Au alloy,[10] it would then be predicted that the marker would move toward the silver side of the couples, which indeed it is observed to do in the experimental work given above. Whether self-diffusion coefficients in the pure components could be used somewhat similarly cannot be said, for such coefficients are either not available, or too uncertain in accuracy, or not applicable (as in the case of Zn, where the data apply to hexagonal Zn, not to the cubic lattice concerned).

Summary

This is an experimental study of the movement of markers during diffusion in solid solutions, the phenomenon discovered by Kirkendall. Six systems have been investigated, at a series of temperatures: Cu/α-brass; Cu/Snα-solid solution; Cu/Al α-solid solution; Cu/Ni; Ag/Au; Cu/Au; diffusion couples have been made by welding. Markers of many types have been used, including W, Mo, Ni, Pt wires; Pt, Ta, Fe, Ni foils; C, Al_2O_3, Fe_2O_3 powders. All markers move, and by the same amount in a given system, the phenomenon is thus not a property of the marker; the movement, with respect to the Matano interface, has been measured for the separate systems. In the Cu/α-brass couples, the markers move toward the high-Zn side; in the Cu-Al system, toward the high-Al side; in the Cu-Sn system, toward the high-Sn side; in the Cu-Ni system, toward the Cu; in the Ag-Au system, toward the Ag; in the Cu-Au system, toward the Au. Measurements agree reasonably well with Kirkendall's, showing that the technique of joining is unimportant. The Matano interface agrees with the original interface, showing conservation of atoms on lattice sites, and showing porosity to be negligible.

The amount of marker shift differs from system to system, for unexplained reasons; the amount of shift is sometimes near the maximum possible; it is large in Cu-Zn and Cu-Ni systems, smaller in others. Dimensional changes seem to be restricted to the direction parallel to diffusion flow. Cu/α-brass couples exhibit apparent traces of porosity in the diffusion zone (and anomalously low hardness there), while no such porosity could be found in other systems. Only the vacancy mechanism of diffusion appears to be useful in explaining these phenomena, though several theoretical points remain to be explored. Inasmuch as the amount of shift is independent of the nature of the external surface of the diffusion couple, and of the dimensions of the couple, it appears that operating vacancies cannot come from external surfaces but must be generated within the diffusion zone itself. A dislocation mechanism is proposed to explain marker shift.

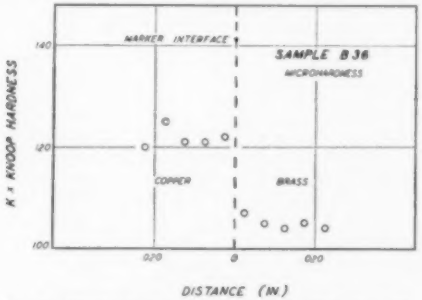

Fig. 60—Microhardness traverse on sample B36, after diffusion, Cu/α-brass.

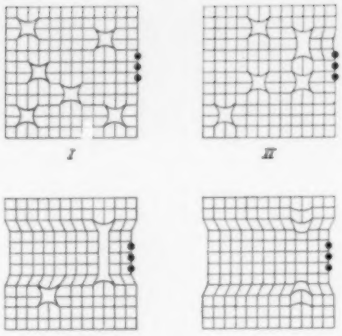

Fig. 61—Vacancies (I), coagulating to voids (II and III), resulting in dislocations (IV), and resultant mass flow and marker (small dot) displacement.

Acknowledgment

We wish to express our gratitude to the Office of Naval Research for support of the experimental work; to the Instituto de Pesquisas Tecnologicas of São Paulo, Brazil, for having generously supplied a fellowship to one of us; and to C. E. Birchenall and other members of the staff of the Metals Research Laboratory for advice and help.

References

[1] A. D. Smigelskas and E. O. Kirkendall: *Trans.* AIME (1947) **171**, p. 130; METALS TECHNOLOGY (Oct. 1946) TP 2071; see also earlier paper: E. O. Kirkendall: *Trans.* AIME (1942) **147**, p. 104.
[2] G. S. Hartley: *Trans.* Faraday Soc. (1946) **42B**, p. 6; C. Robinson: ibid. p. 12; G. S. Hartley: *Trans.* Faraday Soc. (1949) **50**, p. 820.
[3] F. Seitz: *Physical Review* (1948) **74**, p. 1513.
[4] L. S. Darken: *Trans.* AIME (1948) **175**, p. 184; METALS TECHNOLOGY (Jan. 1948) TP 2311; see also discussion to ref. 1.
[5] J. Bardeen: *Physical Review* (1949) **76**, p. 1403.
[6] A. D. LeClaire: Progress in Metal Physics, I. p. 306 (1949) New York. Interscience Publishers Inc.
[7] Atomic Movements Seminar. A.S.M. Chicago. Oct. 21-22, 1950.
[8] See extended discussion to ref. 1.
[9] W. A. Johnson: *Trans.* AIME (1941) **143**, p. 107.
[10] R. N. Rhines and R. F. Mehl: *Trans.* AIME (1938) **128**, p. 185.
[11] R. M. Barrer: Diffusion in and through Solids. (1941) Cambridge. The University Press.
[12] C. Matano: Japan *Journal Physics* (1934) **9**, p. 41.
[13] H. B. Huntingdon and F. Seitz: *Physical Review* (1942) **61**, p. 315.
[14] C. Zener: *Acta Cryst.* (in press).
[15] A. Smekal: Handbuch der Physik (1933) **24**, II.
[16] F. Seitz: *Acta Cryst.* (in press).
[17] F. N. Rhines and C. Wells: *Trans.* A.S.M. (1939) **27**, p. 625.
[18] W. A. Johnson: *Trans.* AIME (1942) **147**, p. 331.
[19] F. Seitz: Conference on Imperfections in Crystals (1950), *Physical Review* (in press).

Effect of Ternary Additions on the Age-Hardening Of a Copper-Silver Alloy

by Harold Margolin and Walter R. Hibbard, Jr

The effect of ten ternary additions on the aging of a Cu-Ag alloy was measured by X ray, microstructure and hardness. A supersaturated copper-rich transition structure was found. The effect of the ternary element was related to differences between transition and precipitate lattice parameters and analogies with solution and strain hardening.

IN addition to the prerequisite of diminishing solid solubility with falling temperature, the theory of coherency hardening[1] proposes that the principal source of hardening during precipitation is strain caused by coherency between the matrix and precipitate. For a given system greater coherency hardening would result from lengthening the period of coherent growth and/or increasing the number of nuclei, other things remaining equal. However, the hardness change during aging is a function of a number of phenomena in addition to coherency hardening, such as dispersion hardening, loss of coherency, solute depletion, matrix recovery or recrystallization, coalescence, and their relative time sequences.

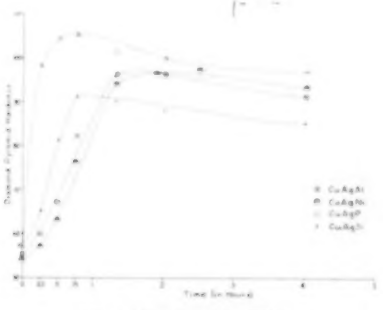

Fig. 1—Aging curves for 500°C.

The present investigation was undertaken to study the effect of ternary additions on the age-hardening of Cu-Ag alloy. For this purpose a series of alloys were made containing as ternary constituents Mg, Al, Si, P, Mn, Ni, Zn, As, In, and Sb. These elements were added to a master 5 wt pct Ag in Cu alloy in such amounts as to obtain alloys listed in Table II containing the following approximate atomic percentages: 96 pct Cu, 3 pct Ag, 1 pct ternary addition. A 97 atomic pct Cu, 3 atomic pct Ag alloy was used as a comparison standard.

HAROLD MARGOLIN is Research Associate, Research Div., New York University, New York, and WALTER R. HIBBARD, JR., Member AIME, is Associate Professor of Metallurgy, Yale University, New Haven, Conn.

Discussion of this paper, TP 3002 E, may be sent (2 copies) to AIME by April 1, 1951. Manuscript, Oct. 16, 1950; revision, Dec. 6, 1950. St. Louis Meeting, February 1951.

This paper is part of a dissertation by Harold Margolin presented in partial fulfillment of requirements for the degree of Doctor of Engineering to Faculty, School of Engineering, Yale University.

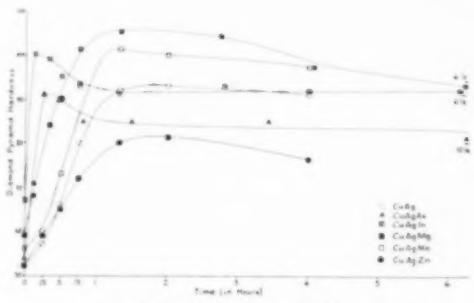

Fig. 2—Aging curves for 500°C.

There have been numerous investigations of age-hardening in Cu-Ag alloys[2-10] but few of ternary Cu-Ag alloys. Pfister and Weist[11] found that 1 wt pct Ni reduced the solubility of Ag in Cu above 600°C and that the rate of precipitation was slower than in polycrystalline Cu-Ag alloys of similar silver content. More recently Hodge, Jaffee, Dunleavy, and Ogden[12] investigated the effect of ternary additions of Mg, Li, P, Cd, Zn, Zr and Be on strength properties of Cu-Ag alloys. Mg, Cd, and P were found to increase strength in the aged and cold-worked condition.

Experimental Procedure

Charges weighing 7.5 lb were melted in a closed carbon crucible under a reducing atmosphere* of nitrogen and hydrogen. A Durville-type casting procedure with a hot-top arrangement was used to obtain a sound casting, 2x2x4¾ in. Prior to rolling and annealing of the ingots, a trial solution anneal of rolled sections of the hot-top portions indicated that at 780°C melting was avoided except for the Cu-Ag-Sb alloy. This alloy could not be produced as a single phase within the limits of temperature control, ± 3° to 5°C, since melting occurred at 640°C, and below this temperature precipitation was

* This gas, a nonexplosive reducing mixture containing 93 pct N_2 and 7 pct H_2, dried by passing through H_2SO_4, was also used in all annealing and aging treatments.

Table I. Lattice Parameters for Various Alloys

Alloy	Cu, A	Ag, A	Cu Transition, A	Aging Time at 550°C, Hr
Cu-Ag	3.6137	4.069	3.658	90
Cu-Ag-Al	3.6130	4.068	3.657	24
Cu-Ag-As	3.6194	4.065	3.668	24
Cu-Ag-In	3.6151	4.103	3.710	24
Cu-Ag-Mg	3.6132	4.068	3.670	29.5
Cu-Ag-Mn*	3.6130	4.074	3.656	29.5
Cu-Ag-Ni	3.6114	4.073	3.653	29.5
Cu-Ag-P	3.6139	4.066	3.655	24
Cu-Ag-Sb	3.6236	4.062	3.662	44
Cu-Ag-Si	3.6131	4.068	3.654	44
Cu-Ag-Zn	3.6142	4.072	3.648	24

* In addition to the silver and transition copper lines, other unidentified lines were seen.

found. Prior to the final solution treatment the alloy was not heated above 630°C.

Specimens for hardness tests were produced by step-wise cold rolling and annealing longitudinally split sections of the casting, approximately 1 in. thick, to a common thickness of 0.165 in. and thence in two reductions of 30 pct each to a final thickness of 0.080 in. Wire specimens for lattice parameter measurements, prepared by a schedule similar to that for hardness specimens, were 0.077 to 0.080 in. in diam. These wires were not etched. Both hardness and lattice parameter specimens were in the cold-worked state prior to the final solution treatment.

With the exception of Cu-Ag-Mg, which was annealed at 800°C, and Cu-Ag-Sb, which was annealed at 650° to 675°C, the alloy specimens 1x$\frac{3}{8}$x 0.080 in. were solution-annealed from 24 to 48 hr at 775°C and quenched in water.

A Rockwell hardness tester, fitted with a 136° diamond pyramid penetrator and a total load of 27.6 kg was employed to obtain the diamond pyramid hardness values.

Debye-Sherrer X-ray patterns were obtained with copper radiation, monochromated by reflection from a cleavage section of penta-erythritol. Exposures of one to three days were required, and, because of the large grain sizes, rotation of the specimens did not always eliminate spottiness. Lattice parameters based on the 420 $K\alpha_1$ and $K\alpha_2$ and the 331 $K\alpha_1$ and $K\alpha_2$ for the stable copper solid solution were determined by Cohen's method[10] of extrapolation and checked against a $\cos^2\theta$ extrapolation. Parameters determined by these methods checked within 0.0003A. The errors

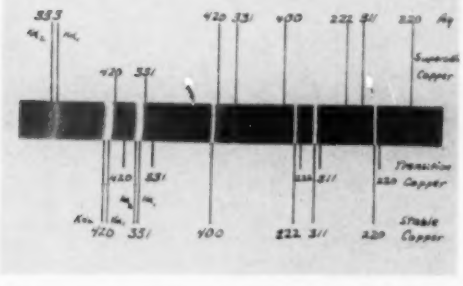

Fig. 3—Debye-Sherrer pattern of Cu-Ag-Al aged 24 hr at 550°C.

Fig. 4 (top)—Cu-Ag solution treated 120 hr at 775°C and quenched.

Fig. 5 (bottom)—Same as Fig. 4 but aged 20 hr at 550°C.

in the transition copper parameters based on the 420 $K\alpha_1$ and 331 $K\alpha_1$ lines and the silver parameters determined from the 333 reflections are estimated to be ±0.0025 and ±0.002A, respectively.

Evaluation of Quenching Conditions

The as-quenched hardness of the alloys varied considerably from 52 for Cu-Ag to 69 for Cu-Ag-In. Hardness tests and microscopic examination of three specimens selected at random from a group of 24, which had simultaneously been solution annealed and quenched, and three specimens individually suspended but otherwise given the same treatment, indicated that the quenching conditions were constant within the errors of hardness measurement and random selection of specimens.

Hardness Deviations

In general each hardness value was obtained by averaging the hardness of three specimens upon which four impressions each had been made, a total of 12 values. The as-quenched hardness values varied very little. However, in some aged specimens deviations occurred up to 33 DPH points, which exceeded the maximum measurement error of ±2 DPH points.

An analysis of the hardness data revealed no correlation with grain size or temperature of treatment. However, the deviations in intermediate (Cu-Ag-Ni) and high (Cu-Ag-P and Cu-Ag-Mg) hardness alloys were greater than those in the low hardness alloys (Cu-Ag-Si and Cu-Ag-Zn). This suggests that hardening did not take place uniformly in all ternary Cu-Ag alloys exhibiting high hardness and having intermediate to large grain size.

Experimental Data

Aging treatments were carried out at 350°, 400°, 450°, and 500°C. Typical hardness vs. time curves obtained for aging at 500°C are shown in Figs. 1 and 2. Debye-Sherrer patterns were obtained from specimens overaged at 550°C for periods of 24 to 90 hr. Films, shown in Fig. 3, of all overaged alloys revealed three sets of lines, two of which were clearly identifiable as (*a*) intense Cu solid solution lines and (*b*) broad less intense Ag solid solution lines. The third fainter set of lines was displaced from the intense Cu rings, so as to correspond to reflections from a greatly expanded and probably transitional copper-type lattice. Calculations of lattice parameters on this basis are given in Table I. Lines due to the unstable, supersaturated Cu solid solution appeared for all alloys after aging at 550°C, even after 90 hr at temperature for binary Cu-Ag.

To determine the source of the expanded copper lattice, X-ray exposures were made of Cu-Ag in the solution annealed and in the aged conditions. The pattern obtained after a 120 hr solution anneal and quench, shown in Fig. 4, disclosed only sharp copper lines. After this specimen was given a 20 hr overaging treatment at 550°C, transition copper and

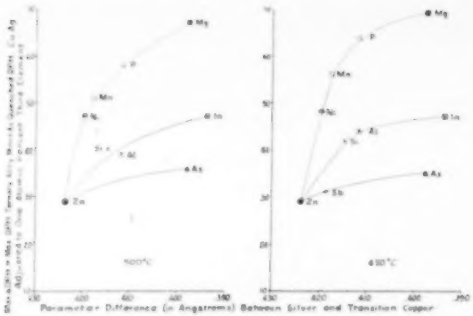

Fig. 6 (left)—Effect of lattice parameter difference on the adjusted age-hardening increment for 500°C.

Fig. 7 (right)—Same as Fig. 6 for 450°C.

silver lines appeared in addition to the stable copper solid solution lines, see Fig. 5. Thus the expanded lattice producing the transition copper lines is formed during aging, probably the result of segregation of silver beyond the equilibrium solubility limits, which would be a logical step in the formation of silver precipitate and the transition phase.

Distribution of the Third Element

With the exception of the lattice expansion found in Cu-Ag-In and Cu-Ag-Sb, the silver precipitate parameters show changes which lie within the limits of error of measurement. However, this is in contrast to the transition copper lattice parameters, which experience the greatest changes, and the stable copper solid solution matrix lattice parameters. There appears to be no general correlation between expansion or contraction of the transition lattice parameters and those of the copper matrix or between the variations of copper matrix and silver lattice parameters. The changes in parameter of the silver and transition copper in the ternary alloys are unpredictably greater or less than the change in the Cu-Ag alloy, indicating that the third element does not always act to cause closer matching between the silver and transition copper phases which are assumed to be coherent during the early stages of growth of the silver precipitate.

Where the third element does not affect silver lattice parameters, but is probably present in the transition and/or the stable copper solid solution, changes in their lattice parameters may be the result of a redistribution of the third element after silver has precipitated. Variations in the transition copper lattice may be caused, in the case of expansion, by local concentration of the third element. A contraction of this lattice, however, may result from diminished solubility of silver in the transition structure.

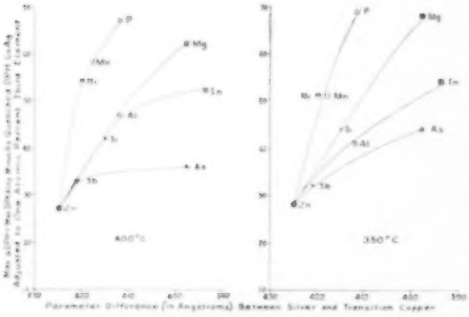

Fig. 8 (left—Same as Fig. 6 for 400°C.

Fig. 9 (right)—Same as Fig. 6 for 350°C.

Maximum Hardness

Since the precipitation mechanism of this series of alloys is similar, it would appear that the maximum hardness values should be related to the degree of matching or difference between the lattice parameter of the silver and the transition copper phases. Since the recrystallization phenomenon is less significant at higher aging temperatures,[10, 11] this relationship would be more distinguishable for the data at these temperatures. Plots of maximum hardness at 450° and 500°C vs. parameter difference indicate that as the sizes of the two lattices converge the hardening increases.

These plots, however, do not take into account small differences in solution hardening nor the variations in the exact atomic composition, see Table II. Therefore, if the difference between the maximum hardness attained by a ternary alloy at any particular aging temperature and the as-quenched Cu-Ag hardness is considered as a measure of the hardness increment added to the basic alloy by the third element, this increment (ΔH) can be extrapolated or interpolated to exactly 1 pct, as necessary.

Table II. Atomic and Weight Percentages of Alloys

Alloy	Ag, Wt Pct	3rd Element, Wt Pct	Ag, Atomic Pct	3rd Element, Atomic Pct
Cu-Ag	4.95		2.98	
Cu-Ag-Al	4.88	0.48	2.92	1.14
Cu-Ag-As	4.88	1.025	2.94	0.89
Cu-Ag-In	4.75	1.64	2.88	1.05
Cu-Ag-Mg	4.79	0.31	2.87	0.82
Cu-Ag-Mn	4.83	0.84	2.90	0.99
Cu-Ag-Ni*	4.52	0.94	2.71	1.04
Cu-Ag-P	4.76	0.45	2.85	0.94
Cu-Ag-Sb	4.78	1.47	2.89	0.79
Cu-Ag-Si	4.88	0.43	2.92	0.99
Cu-Ag-Zn	4.87	0.075	2.93	0.97

* The analysis of all alloys except Cu-Ag-Ni was performed by Lucius Pitkin, Inc., New York.

Figs. 6, 7, 8, and 9 show the adjusted values of ΔH for the temperatures of aging employed. It can be seen, first, that as the differences between the silver and the transition copper lattices decrease, the hardness increases; second, that several rates of hardness changes are evident; and, third, that these relationships exist for all aging temperatures investigated. Thus, there is good general agreement with predicted behavior, although certain detailed differences in hardness change cannot be correlated with individual parameter difference (e.g., Cu-Ag-Al, Cu-Ag-Si, and Cu-Ag-P) or with periodic sequence of the ternary elements. The hardness values for Cu-Ag-In and Cu-Ag-Sb essentially represent measurements of recrystallized material, since in both cases almost complete recrystallization takes place before the hardness maximum is attained. A comparison of hardness values for certain alloys at 450°C indicated that, depending on the alloy and, possibly, the time of aging, the nonrecrystallized areas were as hard and sometimes harder by from 10 to 20 DPH points as the corresponding recrystallized areas. Guy, Barrett and Mehl[10] have shown that a separate, more rapid rate of hardness change exists for the recrystallized areas in Cu-Be alloys.

The ternary solute elements, arranged in decreasing order of the maximum hardness increment, are P and Mg, Mn, Ni, In, Al, Si, As, Sb, and Zn. Hodge et al.[12] have also found that phosphorus and magnesium strengthen Cu-Ag but find "very little effect on the tensile strength" when 1 to 3 wt pct Zn is added to a 6 pct Cu-Ag alloy.

Rate of Hardening

Examination of the hardness-time curves indicated that certain alloys consistently hardened more rapidly than others. A correlation similar to that for ΔH was found for the time to attain one half maximum hardness and the difference between the lattice parameters of silver and transition copper phases. If, at any particular temperature, the difference between the time for each ternary alloy and the basic Cu-Ag alloy to attain one half maximum hardness is adjusted for exactly 1 atomic pct third element, and these adjusted values are plotted against the difference between the silver and transition copper lattice parameters similar figures also are obtained as shown in Figs. 10, 11, 12, and 13.

It will be seen that in general the data for each temperature are scattered along two straight lines which are included to indicate qualitative trends. With the exception of Cu-Ag-P and Cu-Ag-Mg those alloys hardening most rapidly have the lower adjusted maximum hardness increment values. It may be noted that, as the parameter difference increases, the rate of hardening decreases. Moreover, those elements which, when dissolved in copper distort its lattice the least, are generally at the low hardening rate end of their respective lines. This suggests that the rate of age hardening may follow a pattern similar to the rate of strain hardening experienced by binary copper, solid solution alloys. Some data on binary copper alloys are available from Martin,[10] in which the hardness of alloys after constant reduction is plotted against the atomic percent of solute. For the Cu-Ag base alloys, the hardness difference between the unworked alloys and those given 20 and 60 pct reduction have been adjusted to exactly 1 atomic pct solute, and plotted against the parameter difference between silver and transition copper phases. The resulting graphs are shown in Figs. 14 and 15. With the exception of magnesium there is good agreement between Martin's data and the authors', suggesting that the third element dissolved in the transition phase and/or the matrix during coherent growth of the precipitate has a similar effect on coherency hardening as it does on work hardening, i.e., more rapid coherency and work hardening occur with increased lattice distortion. Since the rate of recrystallization is slow in Cu-Ag-P, the high rate of hardening may possibly be the result of a high rate of nucleation and possibly by more extended coherent growth.

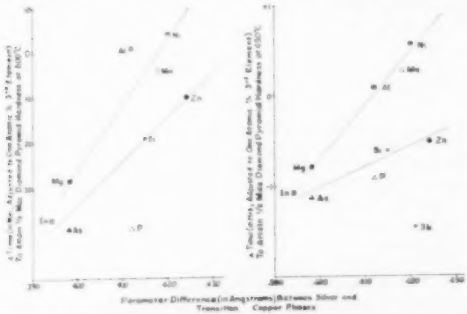

Fig. 10 (left)—Effect of lattice parameter difference on the adjusted time increment for half hardening at 500°C.

Fig. 11 (right)—Same as Fig. 10 for 450°C.

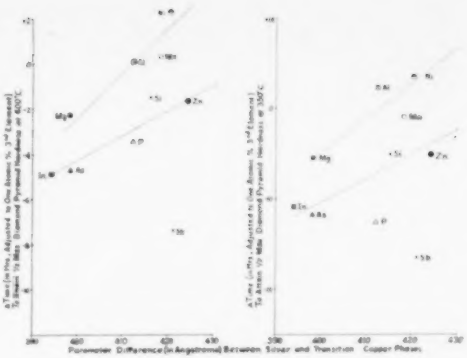

Fig. 12 (left)—Same as Fig. 10 for 400°C.

Fig. 13 (right)—Same as Fig. 10 for 350°C.

The elements, arranged in decreasing order of their influence on the rate of hardening are Sb, As, In, Mg, Si, Zn, Al or Mn, and Ni.

Microstructure

Examination of specimens mechanically polished and etched with copper-ammonium-chloride was principally confined to hardness specimens aged at 450° and 500°C and lattice parameter specimens aged at 550°C. The observed phenomena may be classified in the sequence in which they occur, (a) precipitation within the grain, (b) grain boundary reaction, and (c) coarsening of precipitate.

Precipitation Within the Grain: The procedure employed in obtaining hardness-time curves was to use individual specimens for several different accumulative isothermal aging times at a given temperature. Accelerated precipitation occurred in slipped regions around hardness impressions. Fig. 16 shows one of these areas in a specimen of Cu-Ag-P aged

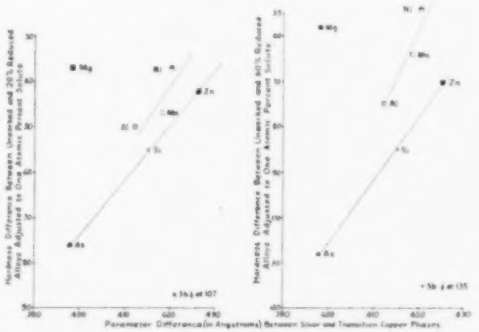

Fig. 14 (left)—Effect of lattice parameter difference on the adjusted work-hardening increment for 20 pct reduction.

Fig. 15 (right)—Effect of lattice parameter difference on the adjusted work-hardening increment for 60 pct reduction.

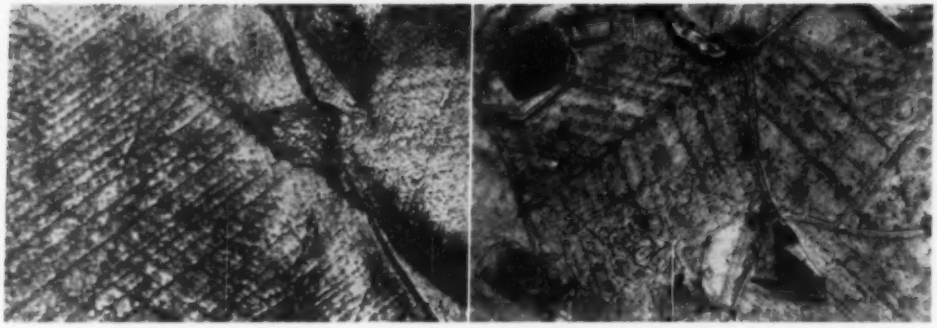

Fig. 16 (left)—Cu-Ag-P aged 1¾ hr at 450°C. Area of photograph near hardness impression. Copper-ammonium-chloride etch. X800.
Fig. 17 (right)—Cu-Ag-Mn aged 1½ hr at 448°C. Copper-ammonium-chloride etch. X200.
Former slip planes along which precipitation has taken place. These planes traverse intragrain boundaries without deviation.

approximately to maximum hardness after 1¾ hr at 450°C.

Fig. 17 shows a type of structure which at 450°C is common to all alloys except Cu-Ag-P, Cu-Ag-As, Cu-Ag-In, and Cu-Ag-Sb. The interior of grains are subdivided by irregular boundaries. It was suspected at first that these boundaries might be a freak etching effect. A specimen of Cu-Ag-Al was polished and etched with copper-ammonium-chloride, and these lines were developed. The specimen, repolished and etched with ammonium persulphate, did not reveal these boundaries. However, when the as-ammonium-persulphate-etched specimen was re-etched with the first etchant the sub-boundaries, together with the precipitation associated with hardness impressions, reappeared.

These lines are similar in appearance to grain boundaries. Both regions are bordered by a light etching area which suggests that silver, at least, must diffuse from these light etching regions to the boundaries in order to precipitate. The internal boundaries differ from grain boundaries in that the recrystallization phenomenon rarely begins in these areas, although it is often seen at grain boundaries. The two also differ in that the subboundaries enclose regions differing slightly in orientation, as shown by Fig. 17.

It is possible that the internal boundaries were formed prior to aging and that precipitation in these boundaries reveals them. Wood and Rachinger[11] working with aluminum found similar structures which were best revealed by slow deformation at high temperatures, conditions which did not apply in the present study. Intra-grain boundaries readily seen as comparatively short aging times were less distinguished in some specimens of the same alloy aged longer times at 450°C. The internal subdivisions are not at all evident in lattice parameter specimens aged at 550°C. Possibly an explanation of this phenomenon may require consideration of a time-temperature-supersaturation relationship.

A Widmanstätten structure was found in all alloys, but for Cu-Ag-In, Cu-Ag-Sb, Cu-Ag-As, and Cu-Ag-P only in the lattice parameter specimens aged at 550°C. The structure of Cu-Ag-P was most difficult to resolve, a fact which suggests that the high hardness of this alloy may be due to a high rate of nucleation. A Widmanstätten structure was seen before maximum hardness in several instances (Cu-Ag, Cu-Ag-Mg, Cu-Ag-Si, and Cu-Ag-Zn) and most likely represents localized overaging. No attempt was made to identify the planes of precipitation, but where the precipitate was clearly resolvable no more than three directions of plates were seen.

Grain Boundary Reaction: The grain boundary or recrystallization reaction occurred early in the precipitation process and was found to diminish in amount as the aging temperature increased. At high magnifications or where the precipitate was coarse, the recrystallized regions showed a pearlitic-like arrangement of phases.

The procedure of aging and hardness testing adopted afforded some opportunity to observe the effect of cold work on the recrystallization reaction. Generally more recrystallization was revealed near and within the hardness impressions, although the extent varied from alloy to alloy. Fig. 18 shows a region near a hardness impression in which recrystallization has begun, but the direction of most rapid growth is not along the most severely deformed directions. On the other hand, Fig. 16 reveals an instance where growth proceeds along deformation lines in regions of high energy. Therefore, it appears likely that there is an orientation as well as energy dependency for this type of recrystallization.

It was observed frequently during use of the Tukon microhardness tester that slip lines (emanating from hardness impressions) within a given grain changed direction upon entering the recrystallized areas associated with this grain. In some regions traversing slip lines disclosed twins, as shown in Fig. 19.

Coarsening of Precipitate: During growth of the recrystallized grains at 450°C the silver particles within them grew resolvable and the spacing between the particles increased. The transition was quite gradual and no boundaries between the two regions could be seen. However, in Cu-Ag alloys aged 9½ hr at 450°C the coarsening of silver commenced at the recrystallized grain boundaries, as shown in Fig. 20; and in Cu-Ag-In, also aged 9½ hr at 450°C, at the original grain boundaries as well, although the specimen is almost entirely recrystallized. At 1500X, as shown in Fig. 21, it can be seen that the new precipitate tends to form perpendicular to the advancing interface as in growing pearlite nodules.[12] Some lattice parameter specimens, aged at 550°C, particularly Cu-Ag, also revealed the

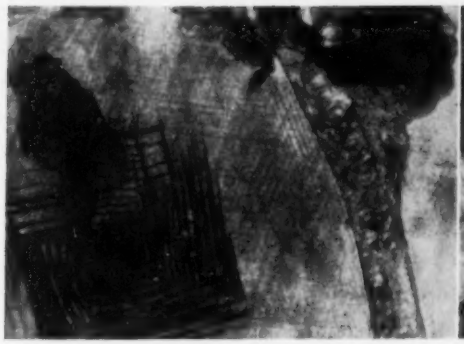

Fig. 18 (left)—Cu-Ag-P previously hardness tested and aged 1¾ hr at 450°C. Copper-ammonium-chloride etch. X100.
Recrystallization at hardness impression.

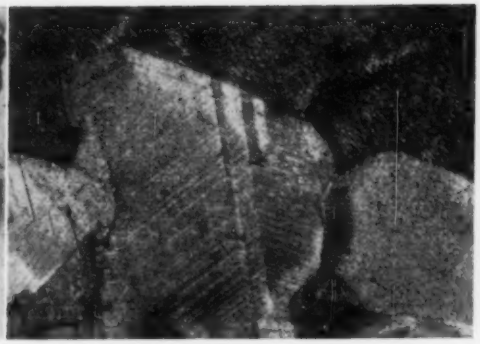

Fig. 19 (right)—Cu-Ag aged 3½ hr at 450°C. Copper-ammonium-chloride etch. X500.
Twins outlined by slip lines in recrystallized grains.

coarsening phenomenon. At 450°C the coarsening reaction occurred primarily at the original grain-recrystallized grain interface, whereas the reaction in the parameter specimens took place primarily at recrystallized boundaries. The general characteristics of the coarsening phenomenon at the recrystallized grain boundaries suggest that a second reorientation of the precipitate may be taking place.

The Precipitation Reaction

Precipitation in Cu-Ag and ternary Cu-Ag alloys appears to include the following phenomena:

1. Segregation of silver (and third element where involved) beyond equilibrium solubility limits† in the case of Cu-Ag, and probably in the ternary alloys as well, to form a transition copper-base structure rich in silver
2. Limited coherent growth of the precipitate, involving coherency possibly between precipitate and transition copper lattice and coherency between transition copper and the matrix copper lattice poorer in silver
3. Breaking away of the precipitate, recrystallization, and coarsening

It is entirely possible that the silver precipitate during its coherent growth may exist in a transition form, the entire mechanism thus being similar to that described by Geisler and Newkirk[20] for permanent magnet alloys. However, no evidence was found relating to a transition silver-base lattice.

The existence of the transition lattice for extended periods of time at relatively high temperatures may be rationalized on the basis of the experimental fact that large Widmanstätten plates form before maximum hardness is attained. This suggests that coherency does not extend for long times, since loss of coherency and growth of the precipitate in some areas must occur quite rapidly, even before the coherent precipitate is formed in other areas. In view of the sluggishness of the diffusion of silver in copper and the reduction of supersaturation during precipitation, a marked reduction in rate of precipitation during its latter stages might be expected. Evidence of an expanded copper phase on films of all specimens aged at 550°C lends support to this suggestion. Another possible reason for the existence of transition copper lines is connected with the occurrence in certain alloys of the second recrystallization or coarsening phenomenon which must involve resolution and reprecipitation of the silver phase.

† Minimum size of transition copper lattice was measured at 3.648A (Cu-Ag-Zn), and for the transition phase of Cu-Ag the parameters were measured as 3.658A. The lattice parameter of copper containing the maximum equilibrium content of 4.87 atomic pct Ag[19] is 3.633A. Based on the assumption that Vegard's law holds in this enforced solid solution, the silver contents of the transition phases of Cu-Ag-Zn and Cu-Ag are approximately 8 and 10 atomic pct, respectively.

Fig. 20 (left)—Cu-Ag aged 9½ hr at 450°C. Copper-ammonium-chloride etch. X500.
Coarsening phenomenon beginning at recrystallized grain boundaries.

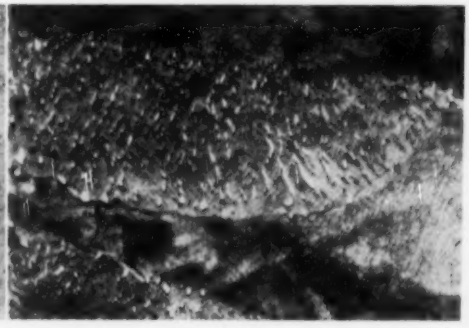

Fig. 21 (right)—Cu-Ag-In lattice parameter specimen aged 24 hr at 550°C. Copper-ammonium-chloride etch. X1500.
Coarsening reaction. (Oblique illumination)

The recrystallization phenomenon appears to be associated with internal stress, for this process occurs most readily in areas immediately surrounding hardness impressions and at low temperatures where hardness and relatedly internal stresses are greatest. When aging temperatures are raised, the extent of recrystallization diminishes and in Cu-Ni-Co[20] and Cu-Ag[21] alloys the phenomenon can be completely suppressed by slow cooling. In experiments on Cu-Be tri-crystals, Guy, Barrett, and Mehl[22] have shown that during aging at 200° and 300°C cracking occurs along grain boundaries where the recrystallization reaction has occurred. No further grain boundary precipitation took place after the formation of cracks, and if aging was carried out at 400°C, no cracking occurred.

Jones, Leech and Sykes[10] have suggested that recrystallization, i.e., discontinuous precipitation, takes place when the temperature is low and the supersaturation high, and that continuous precipitation is prevalent at high temperatures when supersaturation is low. The necessary definitive experiment, i.e., aging alloys of the same constituents but of different compositions at temperatures where the respective degree of supersaturation is the same, has not been performed. Indeed, considerable information is lacking as regards the observed coarsening reaction, subsequent to recrystallization. A program of study involving microstructure examination of large grained specimens during aging and possibly orientation relationships between recrystallized and unaltered areas[23] would probably disclose useful information concerning both phenomena.

Summary

1. A transition copper-base structure, quite rich in silver, has been found during aging in all the investigated alloys, which are Cu-Ag, Cu-Ag-Al, Cu-Ag-As, Cu-Ag-In, Cu-Ag-Mg, Cu-Ag-Mn, Cu-Ag-Ni, Cu-Ag-P, Cu-Ag-Sb, Cu-Ag-Si, and Cu-Ag-Zn.

2. The ternary elements do not generally appear to be distributed in such a manner as to bring about a closer matching between the silver precipitate and the transition copper lattices. The lattice parameters of the transition phases are most affected by the presence of the third element, whereas with exceptions of Cu-Ag-As, Cu-Ag-In, Cu-Ag-N, and Cu-Ag-Sb the parameters of the copper solid solution and the silver precipitate are relatively unchanged.

3. In general, the maximum increment of hardness, adjusted to exactly 1 atomic pct third element, increases with diminishing difference of the silver and transition copper lattice parameters.

4. Rates of hardening, adjusted for exactly 1 atomic pct third element, generally show an increase with decreasing difference between the silver and transition copper parameters. Those ternary elements, which cause the greatest solution hardening in binary copper alloys, effect the most rapid response to coherency and strain hardening.

5. Microstructure examination has revealed precipitate in Widmanstätten form, along intra-granular boundaries, and in recrystallized nodules prior to attainment of maximum hardness. The intra-granular boundaries differ from grain boundaries in that the former do not appear to enclose regions differing widely in orientation and do not serve as sites at which recrystallization begins. It is also seen that the recrystallization phenomenon, commencing almost completely at grain boundaries, is followed by a coarsening reaction, which is seen at the interfaces between recrystallized and nonrecrystallized grains and at recrystallized grain boundaries.

Acknowledgment

The authors wish to thank Marritt L. Kronberg, who designed and put into operation the monochromating system without which much of the X-ray data could not have been obtained. One of the authors also wishes to express his appreciation to the International Nickel Co., Inc. under whose fellowship this work was carried out.

References

[1] A. H. Geisler: Property Changes During Aging. *Trans.* AIME (1949), **180**, p. 230; METALS TECHNOLOGY (Aug. 1948) TP 2436 E.

[2] N. Ageew, M. Hansen, and G. Sachs: Decomposition and Change in Property of Supersaturated Silver-Copper Alloys. *Ztsch. fur Physik* (1930) **66**, p. 350.

[3] P. Wiest: X-ray Study of the Solubility of Silver in Copper. *Ztsch. fur Physik* (1932) **74**, p. 225.

[4] C. S. Smith and E. W. Lindlief: The Equilibrium Diagram of the Copper-Rich Silver Alloys. *Trans.* AIME (1932) **99**, p. 101.

[5] P. Wiest: On the Relation of the Precipitation Process in Single Crystals and Polycrystalline Material. *Metallwirtschaft* (1933) **12**, p. 47.

[6] P. Wiest: Age Hardening Processes in Silver-Copper Single Crystals. *Ztsch. fur Metallkunde* (1933) **25**, p. 238.

[7] P. Wiest and U. Dehlinger: Comparison of the Hardness of a Worked and of a Cast Alloy. *Ztsch. fur Metallkunde* (1934) **26**, p. 150.

[8] H. Bumm and U. Dehlinger: Kinetic Differences Between Cast and Worked Metal. *Metallwirtschaft* (1936) **15**, p. 89.

[9] W. F. Cox and C. Sykes: Precipitation in the Alloys of Copper and Silver During Age Hardening. *Journal* Inst. of Metals (1940) **66**, p. 381.

[10] F. W. Jones, P. Leech, and C. Sykes: Precipitation in Single Crystals of Silver-Rich and Copper-Rich Alloys of the Silver-Copper System. *Proc.* Royal Soc., London (1942-1943) **181A**, p. 154.

[11] H. Pfister and P. Wiest: On the Influence of a Nickel Addition on the Solubility and the Course of Precipitation in the Silver-Copper System. *Metallwirtschaft* (1934) **13**, p. 317.

[12] W. Hodge, R. I. Jaffee, J. G. Dunleavy and H. R. Ogden: A High Strength-High Conductivity Copper-Silver Alloy Wire. *Trans.* AIME (1948) **180**, p. 15; METALS TECHNOLOGY (June 1948) TP 2366 E.

[13] M. U. Cohen: Precision Lattice Constants from X-ray Powder Photographs. *Review of Scientific Instruments* (1935) **7**, p. 155.

[14] M. L. V. Gayler and W. E. Carrington: Metallographic Study of the Precipitation of Copper from a Silver Rich Silver-Copper Alloy. *Journal* Inst. of Metals (1947) **73**, p. 625.

[15] A. G. Guy, C. S. Barrett, R. F. Mehl: Mechanism of Precipitation in Alloys of Beryllium in Copper. *Trans.* AIME (1948) **175**, p. 216; METALS TECHNOLOGY (Feb. 1948) TP 2341 E.

[16] D. L. Martin: A Study of the Rolling and Annealing Characteristics of Some Copper Alpha Solid Solutions. Yale Thesis (1942).

[17] W. A. Wood and W. A. Rachinger: The Mechanism of Deformation in Metals with Special Reference to Creep. *Journal* Inst. of Metals (1949) **76**, p. 237.

[18] C. S. Smith: Grains, Phases, and Interfaces; An Interpretation of Microstructure. *Trans.* AIME (1948) **175**, p. 15; METALS TECHNOLOGY (June 1948) TP 2387 E.

[19] ASM Metals Handbook 1939 and 1948.

[20] A. H. Geisler and J. B. Newkirk: Mechanism of Precipitation in a Permanent Magnet Alloy. *Trans.* AIME (1949) **180**, p. 101; METALS TECHNOLOGY (Aug. 1948) TP 2444 E.

[21] C. S. Barrett, H. F. Kaiser, R. F. Mehl: Studies Upon the Widmanstätten Structure, VII—The Copper-Silver System. *Trans.* AIME (1935) **117**, p. 39.

[22] M. L. Kronberg: Private Communication.

AIME Salutes

- Officers
  - Directors
    - Division Chairmen
      - Legion of Honor
        - Annual Meeting Chairmen

W. M. PEIRCE
President, AIME, 1951

Willis McGerald Peirce, an AIME member since 1927, will assume the Presidency at the Annual Meeting in St. Louis this month. The new President has been active in Institute affairs for many years, serving as Chairman of the Institute of Metals Div. in 1935, IMD lecturer in 1944, as a Director for seven years, and as Vice-President from 1940 to 1943. Born in Buffalo, N. Y., Mr. Peirce went to Pennsylvania State College, took his B.S. in 1918 from the University of Illinois, and an M.S. from Yale two years later. He had begun his professional career in 1919 and attended Yale on a New Jersey Zinc Co. fellowship. He has been with the company, in Palmerton, Pa., ever since, as a research investigator, as head of the metal research div., and, since 1946, as assistant to the general manager of the technical dept. Noted for his work on zinc and for the research organization he has built up, Mr. Peirce has given freely of his time and knowledge as a contributor to AIME literature. Our new President boasts a son, a daughter, and five grandchildren. Hunting, farming and horseback riding occupy his spare hours.

Joseph Lincoln Gillson became an AIME member in 1923, when he was an instructor in Mineralogy and Petrography at MIT. He had received his B.S. and M.A. degrees from Northwestern and his Ph.D. from MIT, where, by 1928, he was an associate professor. The following year he returned to Northwestern, as associate professor of Economic Geology. In 1930 he joined E. I. du Pont de Nemours & Co., Wilmington. Dr. Gillson was Chairman of the Industrial Minerals Div., AIME, in 1947, and was recently Chairman of the AIME Committee on Democratization.

J. L. GILLSON

M. L. HAIDER

Michael L. Haider was Chairman of the publications committee of the AIME Petroleum Div., for several years, Chairman of the Petroleum Div., in 1945, and active on numerous other committees. He is vice-president and general manager of the production dept. of the Imperial Oil Co. Ltd., Toronto, going there about five years ago from the Standard Oil Co. (N.J.). After graduation from Stanford in 1927, he worked for the Portland Cement Co., the Richfield Oil Co., and the Carter Oil Co.

Leo F. Reinartz, assistant vice-president and manager of the Armco Steel Corp., Middletown, Ohio, has served AIME with great distinction since he joined in 1925. He was Howe Memorial Lecturer in 1943, a Vice-President in 1946 and 1947, and served on the Board of Directors from 1944 to 1948. Perhaps his greatest service has been his 19 successful years of service as Chairman of the National Open Hearth Committee. Born in East Liverpool, Ohio, Mr. Reinartz graduated from Carnegie Institute of Technology in 1909. He went to work for the American Rolling Mill Co. that year, and eight years later became superintendent of open hearth furnaces. By 1938 he was manager of the company.

Thomas Gaunt Moore began his present association with the American Metal Co., New York, in 1935 as field engineer in the mining dept. Following graduation from Harvard in 1931, he became geologist in charge of the Morococha mine of Cerro de Pasco. After three years in Peru, he returned to the Harvard graduate school for his Ph.D., which he was granted in 1936. Dr. Moore has been active in New York Section affairs and was Section Chairman in 1948.

Charles E. Lawall, assistant vice-president of coal properties for the Chesapeake & Ohio Railway, Huntington,

L. F. REINARTZ

C. E. LAWALL

J. F. MYERS

F. W. LIBBEY

A. C. RUBEL

W. Va., was Chairman of the Coal Div., AIME, in 1940, and, with a membership dating back to 1914, has been active in AIME affairs and a frequent contributor to technical literature. Dr. Lawall was made president of West Virginia University in 1939, having been director of its School of Mines. He had been associated with Pittsburgh Testing Laboratories, New Jersey Zinc Co., Bethlehem Steel Co., and Lehigh University.

John F. Myers, superintendent of concentration for the Tennessee Copper Co., Copperhill, Tenn., is one of those who made the organization of the Minerals Beneficiation Div., AIME, a *fait accompli* in 1948, and was its first Chairman. Mr. Myers graduated from Colorado School of Mines in 1913 and went to work for the Butte & Superior Copper Co. He was with American Zinc Co. of Tennessee for a year and New Jersey Zinc Co. for 11 years, joining Tennessee Copper in 1926 as superintendent of milling.

Fay W. Libbey, with the dept. of geology and mineral industries of the State of Oregon in Portland, made his entrance into the mining field in 1906 as night foreman for the Nipissing Mines Co., Cobalt, Ont. Two years later he was superintendent of Vulture Mines Co., Wickenburg, Ariz., going from there to the custom assay office in Phoenix, and then into mine leasing, oil field work, and consulting. He was Chairman of the Oregon Section in 1942.

Albert C. Rubel, vice-president of the Union Oil Co. of California, Los Angeles, got his B.S. from the University of Arizona in time to be assayer for Magma Copper for three months before going into the Army in 1917. After separation from the 304th Engineers, he became geologist for the Commonwealth Petroleum Co. and then the Richmond Levering Co. In 1923 he joined Union Oil Co. as a geologist, becoming a director in 1936.

1951 DIVISION CHAIRMEN NAMED

THESE are the men who have been named to head the various divisions and subdivisions of AIME in 1951. They have all had long and successful careers in industry, and all have made numerous contributions to AIME activities and literature during the years of their membership. They are to be commended for the excellent work they have done thus far, and given the fullest measure of assistance and cooperation in the tasks which lie ahead in 1951.

A. BUTTS

T. L. JOSEPH

Mineral Industry Education Division

Allison Butts, professor of electrometallurgy, Lehigh University, Bethlehem, Pa. . . . at Lehigh since 1917, as assistant, instructor, assistant professor, and associate professor . . . born in Poughkeepsie . . . A.B. Princeton, B.S. from MIT . . . with U.S. Metals Refining Co. 1913-16 . . . associate editor the *Mineral Industry*, 1920-27 and special editor for Webster's New International Dictionary, 1934 . . . textbook author, plus various other publications . . . member Institute of Metals of Great Britain, Electrochemical Society, ASM, ASEE, Sigma Xi.

Iron and Steel Division

T. L. Joseph, assistant dean, Institute of Technology, University of Minnesota, Minneapolis . . . B.A., M.A., University of Utah . . . U.S. Army in World War I . . . Bureau of Mines, 1919-36, as: metallurgical chemist, assistant metallurgist, associate metallurgist, metallurgist and supervising engineer with North Central Experiment Station . . . in 1925 became professor of metallurgy and head of metallurgical dept. at Minnesota . . . J. E. Johnson, Jr., award in 1927 . . . has written numerous articles for Bureau of Mines publications and technical magazines.

R. M. BRICK

R. J. LUND

Institute of Metals Division

R. M. Brick, director, dept. of metallurgical engineering, University of Pennsylvania . . . at Pennsylvania since 1945 . . . at Yale, 1934-45 as Sterling Research Fellow, instructor in metallurgy, and assistant professor of metallurgy . . . Met. E. from Lehigh, Ph.D. from Yale . . . a variety of papers on physical metallurgy, and textbook, *Structure and Properties of Alloys* . . . Tau Beta Pi, Sigma Xi, Alpha Chi Sigma, AFA, ASM, ASEE, SESA, Institute of Metals (London), Franklin Institute.

Mineral Economics Division

Richard J. Lund, supervisor, engineering economics, Battelle Memorial Institute, Columbus, Ohio . . . born

C. C. LONG

in Racine, Wis., 1905 . . . B.A., M.A. and Ph.D. in geology from University of Wisconsin . . . subsurface correlation work in Oklahoma and Texas oil fields . . . three years as instructor at Wisconsin . . . with the Dept. of Commerce and then the economics branch, Bureau of Mines . . . chapters in the *Minerals Yearbook* on nickel, tungsten, molybdenum, cobalt, vanadium, radium, uranium . . . special studies on scrap metals, and initiated yearly surveys on consumption of scrap iron and steel . . . edited *Mining Congress Journal* 1937-40 . . . during the war headed the miscellaneous minerals branch of WPB in Washington.

Metals Branch

Carleton C. Long, since 1937 director, research dept., St. Joseph Lead Co. of Pa., Monaca, Pa. . . . born in Boulder, Colo. . . . B.S. from University of Colorado, M.A. from Stanford, and Ph.D., Colorado . . . in 1930 was control chemist with AS&R at the Durango smelter . . . joined St. Joseph Lead in 1935 as research engineer . . . principally interested in physical and inorganic chemistry . . . publications in the *Journal of Physical Chemistry, Journal of the Optical Society of America,* and the *Photochemical Journal* (England) . . . several articles in American and British mountaineering journals describing high country exploration, first ascents, creation and codification of mountaineering data.

E. D. GARDNER

Mining Subdivision

Eugene D. Gardner, chief mining engineer, Bureau of Mines, Washington, D. C. . . . in mining for 44 years, recently chief, Bureau's oil shale mining division, Denver, Colo. . . . born West Jordan, Utah . . . B.S. and E.M., University of Utah . . . joined the Bureau in 1918 after 5 years with Apex Utah Mining Co. and 7 years geological work . . . in charge of mining division in the western states for 17 years . . . 3 years as regional engineer in Rolla, Mo., and headed oil shale division 1946-49 . . . has authored many Bureau bulletins and magazine articles . . . headed Papers and Program Committee, Mining Subdivision, in 1950.

D. M. DAVIDSON

Geology Subdivision

Donald M. Davidson, vice-president and chief geologist, E. J. Longyear Co., Minneapolis . . . worldwide exploration and development of mineral deposits . . . active in development in Northern Rhodesia copper field . . . B.A. (magna cum laude), University of Minnesota, 1925 . . . M.Sc. (Sigma Xi prize), 1926 . . . Ph.D. 1928 . . . geologist and chief geologist, Rhodesian Selection Trust, Ltd., 1928-33 . . . senior engineer, Selection Trust, Ltd., London, 1933-40 . . . chief geologist, E. J. Longyear, and chief geologist and manager of exploration, 1940-46.

Geophysics Subdivision

Sherwin F. Kelly, director and president, Sherwin F. Kelly Geophysical Services, Inc., Wilmington, Del. . . . born in New Mexico . . . B.Sc. Kansas University . . . attended Université de Paris, Musee d'Histoire Naturelle (Paris), College de France, Ecole des Mines; Toronto University . . . aviator in World War I, and with the American Commission to Negotiate Peace . . . a pioneer in introducing electrical prospecting into the U.S. . . . taught at University of Toronto, 1923-26 . . . manager, Schlumberger Electrical Prospecting Methods, 1927-30 . . . consulting geologist, geophysicist and lecturer on geology and geophysics since 1930 . . . has lectured at Missouri School of Mines, Northwestern, University of Washington, and Lafayette College . . . widely published and belongs to numerous professional groups.

S. F. KELLY

Coal Division

Carroll A. Garner, vice-president, Jeddo-Highland Coal Co. . . . born Ashland, Pa., 1889 . . . B.S. in mining, Pennsylvania State College, 1910 . . . a year with Miami Copper, and one with Inspiration Consolidated Copper . . . instructor in mining at Pennsylvania State 1912-13 . . . 5 years with Lehigh Valley Coal Co. . . . 8 years as assistant general manager at Jeddo-Highland.

C. A. GARNER

Extractive Metallurgy Division

Oliver C. Ralston, chief, metallurgical branch, Bureau of Mines, Washington . . . born Colorado Springs, Colo. . . . B.S., M.E., 1910, Colorado College . . . assayer, surveyor, and instructor in chemistry, Leadville High School . . . Bureau of Mines, Pittsburgh, 1912; Salt Lake City, 1914 . . . assistant chief metallurgist in Seattle, 1920; Berkeley, Calif., 1921 . . . chief, division of nonmetallic minerals, 1935-45; chief, metallurgical branch, since 1946 . . . patents, papers, and books on flotation concentration of ores . . . over 100 contributions to periodicals.

O. C. RALSTON

Industrial Minerals Division

A. B. Cummins, manager of minerals, asphalt and magnesia dept., Johns-Manville Corp., Manville, N. J. . . . born in Los Angeles . . . B.S., University of Chicago, 1920; Ph.D., University of California, 1926 . . . first job "producing blackberries, age 8—profits not bad" . . . research chemist, Celite Corp., 1924-25; then development engineer and research engineer . . . joined Johns-Manville as manager, Celite research, and chemical engineer, 1929 . . . consultant in nonmetallics and industrial minerals since 1932 . . . development of equipment, processes and products in processing of diatomaceous earth . . . also work on air classifications, decolorizing products, heat insulations, magnesia compounds and chemicals . . . patentee and author . . . member ACS, AIChE, ASTM, AAAS, and other groups.

A. B. CUMMINS

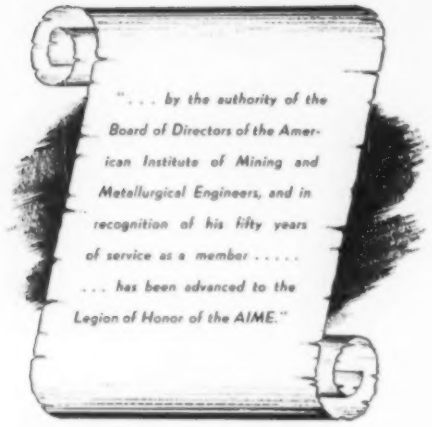
". . . by the authority of the
Board of Directors of the Amer-
ican Institute of Mining and
Metallurgical Engineers, and in
recognition of his fifty years
of service as a member . . . . .
. . . has been advanced to the
Legion of Honor of the AIME."

Twenty Five Named to Legion of Honor

THE AIME Legion of Honor rolls will be increased by twenty five at the Annual Meeting in St. Louis, when the following men will be cited for 50 years of membership in the Institute.

H. C. BOYNTON

Henry Cook Boynton . . . born at Willsborough, N. Y. on Apr. 16, 1874 . . . Harvard A.B. 1900 (Magna Cum Laude) . . . Austin teaching fellow in geology 1900-01 at Harvard, in metallurgy, 1902-03 also at Harvard . . . M.S. 1901 . . . Sc.D. 1904 . . . metallurgy and metallography instructor at Harvard . . . did practical economics work in geology and mining . . . member various national and local technical societies . . . John A. Roeblings Sons Co., Trenton, in 1906 until 1940 . . . consulting metallurgist 1947.

A. C. BRINKER

Arthur C. Brinker . . . Colorado State School of Mines, E.M. 1901 . . . Camp Bird, Ltd., Ouray, Colo. until 1910 . . . assisted in examination work of various mines . . . manager of silver-lead and gold-silver mines for London Exploration Co. from 1911 to 1921 . . . approximately eight years devoted to developing and examining properties in North and South America . . . project engineer for Gibbs & Hill, Inc., New York, from 1945 until 1948.

James Francis Brophy . . . born at Pittsburgh in 1872 . . . traveled west working at various mining jobs in 1889 . . . worked in coal and metal mines, railroad shops, and firing locomotives . . . entered Ohio State University in 1893 . . . returned to Butte as mining assistant to engineers . . . graduated from Ohio State in 1899 . . . did engineering work in eastern United States . . . several years later moved to Red Lodge, Mont. and opened coal property . . . also bought group of patented ore claims and staked other groups.

Donald C. Brown . . . graduated Marietta College, Ohio in 1884 . . . several months additional work in mineralogy and assaying . . . following graduation employed by Mexican Ore Co., El Paso, and Catorce, Mexico, 1885-87 . . . Cia Metalurgica Mexicana, San Luis Potosi, 1890; assistant general manager in 1901 . . . in 1915 first vice-president for same concern . . . spent some time in Mexico . . . returned to New York in 1925.

George A. Camphuis . . . born at Newport, Fifeshire, Scotland . . . attended Camborne School of Mines, Cornwall, England, graduated E.M., 1903 . . . employed by English mining companies in Idaho . . . several years with United Mexican Mines Assn. in Mexico . . . manager for Exploration & Mine Development Co., 1913 . . . formed company Camphuis & Rives, El Paso in 1917 doing mine examination and development work . . . several years in mining work throughout southwestern United States . . . worked for Mexican companies, 1923-27 . . . returned to United States, engineering practice in California . . . employed by Cerro Colorado (La Gloria Min.) Chihuahua, Mexico, 1932 . . . manager and consulting engineer Camphuis Engineering Co., Los Angeles, 1936.

George Leonard Collord . . . Princeton graduate 1899 . . . accepted position as chemist for Shenango Furnace Co., Sharpsville, Pa. . . . made assistant superintendent of furnaces . . . joined Clairton Steel Co., now Carnegie Steel Co., as superintendent of blast furnaces . . . general superintendent of blast furnaces, Tennessee Coal, Iron & Railroad Co., Birmingham, 1906 . . . rejoined Shenango Furnace Co. as blast furnace manager . . . made vice-president and general manager.

T. COX

Thomas Cox . . . born at St. Erth, Cornwall, England . . . attended Birbeck Institute, Bedford Park Branch of South Kensington Science and Art Dept., London . . . came to United States in 1883 . . . worked at Gloster mine, Helena, Mont., 1883-88 . . . worked for Woods Larson & Co., railroad construction . . . he remained with this company working on various sites throughout the western part of the country . . . resident managing engineer, Morning mine, Mullan, Idaho . . . he joined the Oregon Waterpower & Railway Co. as assistant engineer in 1902 . . . ensuing years worked on consulting problems, oil and petroleum development work, design and construction of industrial plants . . . during World War I served in Washington, D. C. . . . worked on construction of San Francisco-Oakland Bay Bridge . . . resigned in 1944, since retired.

John Van Nostrand Dorr . . . born in Newark, N. J. . . . worked as laboratory assistant with Thos. A. Edison in Edison's laboratory at Orange, N. J. . . . graduated from Rutgers in 1894 with B.Sc. in chemistry . . . he was engaged for a year in industrial chemical research in New York and then went west . . . for approximately

14 years worked as chemist, assayer, and research worker for various companies in South Dakota, Colorado, and Arizona . . . the Dorr Cyanide Machinery Co. was formed in 1910; in 1916 succeeded by the Dorr Co. . . . his 26 inventions and various modifications have been successfully applied both here and abroad . . . member various technical societies and awarded medals for achievements in both metallurgical and chemical professions.

J. V. N. DORR

L. EATON

Lucien Eaton . . . Harvard University 1900, A.B.; 1901, S.B.; 1902, S.M. . . . engineering dept., Cleveland Cliffs Iron Co., 1902-06 . . . joined Iron Belt & Shores Mines, Iron Belt, Wis. superintendent from 1905 to 1909 . . . worked in various mining companies . . . consultation work in Quebec, 1917 . . . went to Santo Domingo, Peru as resident director, Inca Mining & Development Co. . . . several months were spent in Russia doing consulting work, 1928 . . . connected with the U. S. Bureau of Mines for one year . . . mining engineer for consulting concerns . . . went to Nicaragua in 1937 . . . returned to United States as a consulting engineer in Massachusetts.

J. M. FITZGERALD

John M. Fitzgerald . . . born in Philadelphia, 1877 . . . entered railway service 1893, engineering dept. of the Columbus, Sandusky & Hocking Railroad . . . worked in engineering, construction, maintenance, and operating dept. of the Choctaw, Oklahoma & Guld Railroad . . . joined Virginia & Southwestern Railway as assistant general manager . . . became vice-president of Pittsburgh Terminal Railroad & Coal Co. . . . received Hon. LL.D. from University of Pittsburgh . . . was president, Davis Coal & Coke Co. . . . joined Western Maryland Railway Co. as vice-president; later made president . . . he then became associated with the Eastern Railroad Presidents Conference and is presently vice-chairman.

K. F. GORANSSON

K. F. Goransson . . . studied at the University of Lausanne, 1897-98 . . . practiced at steel work and firms building steam engines for two years in Germany and England . . . one year at Columbia University, New York, received M.A. . . . returned to Sweden in 1901 and joined Sandvik Steel Co. . . . became president in 1920 and chairman in 1929 . . . retired from presidency in 1948 and is now chairman . . . also chairman of Chamber of Commerce of Gavle.

B. Britton Gottsberger . . . born in 1874 . . . graduate of Columbia School of Mines in 1895 . . . employed as assayer for Montsenat Consolidated Mining Co., 1896 . . . joined American Mining Co. of El Oro, Mexico as engineer, 1897-99 . . . engineer with Tennessee Copper Co., 1900 . . . worked for various concerns in mining capacities . . . opened consulting office.

H. R. HANLEY

Herbert R. Hanley . . . born in Paxton, Ill. . . . attended Missouri School of Mines & Metallurgy (University of Missouri), B.S., mining engineering in 1901 . . . met. engr., 1918 . . . joined Bully Hill Copper Mining & Smelting Co. in 1901 . . . assistant superintendent in 1904 . . . made assistant manager in 1908-16 . . . became associated with U. S. Smelting Refining & Mining Co. as superintendent, electro zinc plant, 1916-19 . . . consulting engineer in San Francisco, until 1923 . . . professor of metallurgy, Missouri School of Mines 1923 to date . . . developed various industrial processes . . . authored articles on metallurgy.

Laurier Fox-Strangways Holland . . . born at London, England . . . attended Kings College, London, and School of Mining, Queen's University, Ontario, M.E., 1898 . . . worked in midwest as mining engineer, oil and petroleum geologist, and examining engineer . . . general manager, Guildford Gold Mine, 1934-35 . . . secretary and general manager, Consolidated Leases, Inc. . . . secretary and treasurer, Placerville Gold Mining Co., Placerville, Calif. . . . contributed papers to technical journals.

V. F. S. LOW

V. F. Stanley Low . . . graduated University of Melbourne, bachelor of civil engineering, 1893 . . . joined Mt. Lyell Mining & Railway Co. Ltd., Tasmania, 1894 . . . became assistant engineer in charge of mining dept. . . . one year's experience in mining and concentration work . . . general manager of Hampden Copper Mines, Cloncurry, North Queensland . . . accepted position with Girilainbone Copper Mine, New South Wales . . . worked with several mining companies in Australia . . . went to London and opened office as mining engineer . . . returned to Australia.

William T. MacDonald . . . graduated School of Mines, Columbia University, E.M., 1909 . . . worked in mines and mills in various parts of Colorado and California . . . joined Utah Copper Co. in 1911 as chemist, then metallurgist, and assistant superintendent of Magna mill, Garfield, Utah . . . transferred to Hurley, N. Mex., made assistant superintendent of mills . . . joined Ray Consolidated Copper Co., 1915, assistant superintendent of mills for five years . . . during World War I commissioned in Engineering Corps . . . in 1921 was mill superintendent for Moctezuma Copper Co., Nacozari, Sonora, Mexico . . . joined International Nickel Co., Ontario in 1929 . . . moved to La Jolla, Calif. in 1936, presently located there.

Ernest A. Manners . . . born in Posen, Germany . . . Technical School, Breslau, Germany, 1884 . . . worked in gold fields and silver mines in Australia . . . returned to Germany in 1888 . . . engaged in mining work in South Africa . . . in 1890 did exploring work in Australia . . . consulting engineer for New Zealand Mines Trust in 1898 . . . made general manager and consulting engineer for Howell Exploration Co., Ltd., 1900 . . . remained there and later went to England.

Herbert A. Megraw . . . Cornell University graduate B.S., 1898 . . . years following were spent working in mines in Mexico . . . worked on editorial staff of *Engineering & Mining Journal* for approximately five years . . . Bureau of Aircraft Production, Washington, D. C., 1918 . . . joined engineering concern in New York . . . vice-president, Crown Oil & Wax Co., Baltimore, 1922 . . . went to Seville, Spain in 1927 for several years . . . returned to Baltimore in 1936.

F. L. MORRIS

Fred L. Morris . . . born at Paris, Ill., graduated College of Mines, University of California, B.S., 1900 . . . employed in drift mines of Placer County, Calif. . . . reported on properties in Mexico . . . also employed in dredging work for Oroville Gold Dredging & Exploration Co. . . . opened consulting office in San Francisco in 1906.

Horace Moses . . . attended New Mexico Western College . . . employed 1900-09 various capacities from miner to mine foreman . . . became superintendent of mines for Chino Copper Co., Santa Rita, N. Mex., 1909-17 . . . general superintendent and general manager, Gallup American Coal Co., Gallup, N. Mex. for 20 years . . . joined Kennecott Copper Corp., Chino mines div., Santa Rita, general manager for 10 years . . . retired from active business in 1947.

H. MOSES

Arthur C. Spencer . . . studied at Case School Applied Science, Cleveland, 1889-92 . . . graduated 1902 as bachelor of science . . . student at Johns Hopkins University for one year . . . investigated coal deposits connected with Iowa Geological Survey . . . received Ph.D. in geology 1896 from Johns Hopkins University . . . appointed assistant geologist, U. S. Geological Survey, 1896 . . . geologist in 1901 with Bureau, remained until retirement.

A. C. SPENCER

Alexander N. Winchell . . . University of Minnesota, B.A., 1896; M.S., 1897; University of Paris, D.Sc., 1900 . . . professor of geology and mineralogy, Montana School of Mines, seven years . . . 1908-44 professor mineralogy and petrology, University of Wisconsin . . . resident consultant, American Cyanamid Co., 1945.

A. N. WINCHELL

Lewis E. Young . . . born in Topeka . . . graduated Pennsylvania State College, B.S., mining engineering, 1900 . . . Iowa State College, E.M., 1904 . . . University of Illinois, Ph.D., 1945 . . . University of Missouri, D.Eng., 1947 . . . instructor at Iowa State College, 1900-03 . . . four years professor of mining, Colorado School of Mines . . . consulting engineer for four years . . . 1907-13, director, Missouri School of Mines . . . special field work, Illinois Geological Survey . . . one year as professor of business administration . . . joined Union Colliery Co., St. Louis as mining engineer . . . general manager, 1922-26 . . . production vice-president, Pittsburgh Coal Co., Pittsburgh, 1927-39 . . . consulting mining engineer, Pittsburgh 1939 to date . . . author technical papers on mine mechanization and practice . . . spent a busy year in 1949 as AIME President, visiting a very large number of Local Sections . . . he was a Director in 1937, served three terms on the board, and was Vice-President from 1942 to 1945.

L. E. YOUNG

H. P. Townsend . . . born King Williams Town, Cape Colony . . . three years at Royal School of Mines, South Kensington . . . obtained associateship in 1893 . . . several years surveyor and assayer . . . general manager mining company in Rhodesia . . . employed in South Africa, 1923 . . . New Modderfontein Gold Mining Corp., Ltd., Van Ryne, Transvaal, 1940.

Charles Henry White . . . University of North Carolina, S.B., 1894 . . . Harvard University, S.B. (Magna Cum Laude), 1897; A.M., 1902 . . . instructor, assistant professor, professor of mining and metallurgy, Harvard University for 17 years . . . Captain in Ord. Dept., 1918-19 . . . consulting geologist in San Francisco for several mining companies, 1919-27 . . . several years spent abroad as consulting geologist for various concerns . . . private practice since 1938.

Dr. Compton to Address Annual Meeting Welcoming Luncheon

A. H. COMPTON

Arthur Holly Compton, Nobel-prize winning physicist who is famed for his work on the development of the atomic bomb, will be the principal speaker at the Welcoming Luncheon on Feb. 19. Dr. Compton of Washington University in St. Louis took the Nobel prize in 1927 for his discoveries concerning X-rays, and again came into prominence between 1931 and 1934 when he directed a worldwide study of cosmic rays. Later, he was assigned to the Manhattan Project, working on design of the atom bomb and the use of plutonium as an explosive agent. He started and directed development of the first atomic chain reaction, and served as chairman of the National Academy of Science Committee to evaluate the use of atomic energy. Dr. Compton is vice chairman of the U. S. National Commission for UNESCO, and was U. S. delegate to gatherings of this group in Washington and Mexico. He is now a trustee of the Institute of International Education, Inc. These facts represent only the highlights of a long and noteworthy career, and there is, unfortunately, a lack of space in which to list the numerous honors bestowed upon Dr. Compton by educational, scientific and government groups all over the world.

Student Forum at Washington University

The Careers Forum for students to be held on Thursday, Feb. 22, will meet at Washington University, and not at the University of Missouri as was claimed on P. 65 of the January issue.

Annual Meeting Committee Chairmen

H. I. YOUNG
Chmn., Gen'l Comm.

F. J. MEEK
Secy., Gen'l Comm.

N. L. SHEPARD
Chmn., St. Louis Sect.

Behind the scenes at every meeting and convention are those who have laid the groundwork for the activities. They appear calm and unruffled as the meeting opens, but behind them are months of planning, red tape cutting, and several hundred letters, telegrams and memoranda.

Pictured here are some of those men to whom is owed a vote of thanks for the top-notch planning that has gone into the AIME Annual Meeting, to be held in St. Louis, Feb. 19 to 22, 1951.

Space limitations preclude introducing each and every committee member and chairman individually—but they'll all be there in St. Louis, where you can have the pleasure of meeting them in person.

Committee chairmen whose pictures were not available include: J. D. Kerr, Banquet; L. P. Davidson, Welcoming Luncheon; E. L. Clark, Field Trips; Mrs. H. I. Young, Women's Auxiliary; C. G. Stifel, Finance.

Made your meeting reservations yet?

K. A. PHILLIPS
Chmn., Informal Dance

H. A. FRANKE
Chmn., Dinner-Smoker

C. TOLMAN
Chmn., Reception

A. B. CLEAVES
Chmn., Publicity

C. L. WILSON
Student Activities

AIME Annual Meeting Program, February 19-22, 1951

Jefferson and Statler Hotels, St. Louis

To conserve space especially because of the numerous joint sessions of two or three groups, the names of Divisions and Subdivisions are coded, as follows: MIED—Mineral Industry Education Division. MED—Mineral Economics Division. M—Mining Subdivision. G—Geology Subdivision. Geophys—Geophysics Subdivision. NM—(Nonmetallics) Industrial Minerals Division. Coal—Coal Division. MBD—Minerals Beneficiation Division. IMD—Institute of Metals Division. ISD—Iron and Steel Division. Petroleum Branch—named as such. SEG—Society of Economic Geologists.

Saturday, February 17

10 am to 5 pm—Council of Section Delegates.

Sunday, February 18

2 pm—Board of Directors.
2:30 pm—MIED.

7:00 pm—MIED.

Monday, February 19

8:30 to 8:45 am—Meeting of presiding officers and authors.

9:45 am to 12 m

Petroleum Branch—*Executive Committee.* 9:00 am to 11:45 am.
EMD—*Lead; Miscellaneous.*
IMD—*Martensite.*
ISD—*Sulphur.*
NM, G, SEG—*Clay.*
MBD—*Business Meeting.*
Coal—*Depreciation Problem.*
NM—*Canadian Industrial Minerals.*
MIED.
10 am—Metals Branch Council.

12:15 pm—Welcoming Luncheon. Speaker, Arthur Holly Compton.

2:30 pm

MED—*Foreign Minerals.*
M, G—*Geology and Mining Methods.*
Coal—*Depreciation Problem.*
NM—*Canadian Industrial Minerals.*
NM, G, SEG—*Clay.*
G, SEG—*Symposium on Ground Water.*
Petroleum Branch—*Executive Committee.*
MBD—*Materials Handling; Solid-fluid Separation.*
EMD—*Zinc; Miscellaneous.*
EMD—*Aluminum; Magnesium.*
IMD—*Martensitic Transformation.*
ISD—*Sulphur.*

Evening—Dinner-Smoker.

Tuesday, February 20

8:30 to 8:45 am—Meeting of presiding officers and authors.

9:00 am to 12 m

MED, M, G, Geophys—*Exploration Costs.*
M—*General Session.*
G, SEG—*Orebody Manifestations.*
MBD—*New Milling Equipment.*
Coal—*General Session.*
NM—*Dimension Stone.*
NM—*Clay.*
Petroleum Branch—*Production Review.* (8:30-11:00 am)
EMD—*Zinc and Lead from Slag.*
EMD—*Titanium.*
IMD—*Recrystallization.*
ISD—*Sulphur.*
10 am—Mining Branch Council
Women's Auxiliary *Annual Meeting.*
10 am—Mining Branch Council. Business Meeting.

11 am—Howe Lecture by J. R. Vilella. Statler Ballroom.

12:15 — Luncheons

Mineral Economics Division.
Mineral Industry Education Division.
Mining, Geology, Geophysics Division.
IMD—*Executive Committee.*

2 pm

NM—*Lightweight Aggregates.*
NM, M—*Mining Methods.*
MBD—*Concentration.*
G, SEG—*Orebody Manifestations.*
Coal—*General Session.*
EMD—*Zinc and Lead from Slag.*
EMD—*Titanium.*
ISD—*Sulphur.*

2:30 pm

Petroleum Branch—*Waterflooding in the Illinois Basin.*
MED—*Taxation, Tariffs, Subsidies.*
IMD—*Diffusion and Precipitation.*

4 pm—Annual Business Meeting.
4 pm—Executive Committee, Coal Division.
5 pm—Directors' Meeting *Executive.*

Evening

Metals Branch Dinner (IMD, ISD and EMD). Statler Hotel.
Petroleum Branch Dinner. Statler Hotel.
Informal Dance. Jefferson Hotel.
SEG Banquet. Jefferson Hotel.

Wednesday, February 21

8 am to 9:15 am—"Scotch Breakfast," MBD.
8:30 to 8:45 am—Meeting of presiding officers and authors.

9 am to 12 m

M—*Mining Methods.*
MBD (9:30 am)—*Crushing and Grinding; Operating Controls.*
Coal *Preparation.*
Coal, SEG—*Geology.*
NM, G, SEG—*Clay.*
NM—*General Session.*
Geophys—*General Session.*
Petroleum Branch (9:15 to 11:30)—*Drilling, Logging, Acidizing.*
ISD (9 to 10:45 am)
EMD—*Electrolytic Zinc.*
EMD—*Copper; Cobalt; Refractories.*
IMD (9 to 10:45 am)—*Phase Transformation.*
IMD (9 to 10:45 am)—*Plasticity and Mechanical Properties.*

10 am—Women's Auxiliary *Round Table.*

10:45 am—IMD *Annual Business Meeting.*

11 am—IMD *Annual Lecture by G. Borelius. Statler Ballroom.*

12:15 — Luncheons

Coal Division.
Industrial Minerals Division.
EMD Executive Committee.
Physical Chemistry of Steelmaking.
Mining and Metallurgical Society of America.

2 pm

NM, G, SEG—*Clay.*
M—*Mining Methods.*
MED, NM—*Cost Accounting in Mining.*
Coal, SEG—*Geology.*
G, SEG—*Geology General Session.*
Geophys—*General Session.*
Petroleum Branch (2:15 pm)—*Reservoir and Production Engineering.*
EMD—*Physical Chemistry.*
EMD—*Electrolytic Zinc.*
IMD—*Alloy Systems.*
IMD (2:30 pm)—*Grain Boundaries and Annealing Twins.*
ISD (2:30 pm)—*Joint Session with Southwestern OH Section.*

4:45 pm—EMD *Annual Business Meeting.*

5 pm—Executive Committee, Industrial Minerals Division.

Annual Banquet and President's Reception.

Thursday, February 22

8:30 to 8:45 am—Meeting of presiding officers and authors.

MED, NM—*Economics of Industrial Minerals.*
NM—*General Session.*
EMD—*Physical Chemistry.*
EMD, MBD—*Joint Technical Session.*
IMD—*Powder Metallurgy.*
IMD—*General Session.*
ISD—*General Session.*

12:15 — Luncheons

Mineral's Beneficiation Division.
Powder Metallurgy Committee.
ISD Executive Committee.

2 pm

MBD (2:30 pm)—*Clean-up Session.*
EMD—*Physical Chemistry.*
IMD—*Powder Metallurgy.*
Careers Forum for Students.

Friday, February 23

Field Trips.

AIME OFFICERS
Donald H. McLaughlin, President
Vice Presidents
R. W. Thomas A. B. Kinzel C. V. Millikan
C. H. Benedict Philip Kraft
Vice-President and Treasurer
Andrew Fletcher

AIME STAFF
E. H. Robie, Secretary
E. J. Kennedy, Jr., Asst. Secy. Ernest Kirkendall, Asst. Secy.
H. N. Appleton, Asst. to Secy. H. A. Maloney, Asst. Treas.
R. E. O'Brien, Western Secretary, Mining Branch
808 Newhouse Bldg., Salt Lake City

aime NEWS

Program of the Metals Branch,

American Institute of Mining and Metallurgical Engineers Annual Meeting,

Hotel Statler, St. Louis, Feb. 19 to 22, 1951.

SATURDAY, FEBRUARY 17

10:00 a.m.,

Meeting of Council of Section Delegates

SUNDAY, FEBRUARY 18

12:15 p.m.,

Luncheon and Business Meeting

Student Relations Committee

2:00 p.m.,

Board of Directors Meeting

American Institute of Mining & Metallurgical Engineers

8:00 p.m., Room 102

Program Committee Meeting

Institute of Metals Division

MONDAY, FEBRUARY 19

9:00 a.m., EMD, Ballroom Assembly South

Lead-Miscellaneous

C. A. Nelson and H. R. Bianco, Associate Chairmen

A Recently Rehabilitated Secondary Nonferrous Smelting and Refining Plant: E. R. Marble, Jr., Federated Metals Div., American Smelting & Refining Co., Newark, N. J.

Bradley Mining Co.'s New Antimony Smelter at Stibnite, Idaho: R. J. McRae, Bradley Mining Co., Stibnite, Idaho.

Vacuum Treatment of Parkes' Process Crusts on a Pilot Plant Scale: R. F. Doelling, St. Joseph Lead Co., Josephtown, Pa.

9:00 a.m., IMD, Ballroom

Martensite Transformations

M. Cohen, Chairman; B. S. Lement, Secretary

Plastic Deformation and Diffusionless Phase Changes in Crystalline Solids: L. C. Chang, T. A. Read, Columbia University, New York. JOURNAL OF METALS, January 1951.

Transformation Characteristics of a Lithium-Magnesium Alloy: C. S. Barrett, D. F. Clifton, Institute for the Study of Metals, University of Chicago, Chicago, JOURNAL OF METALS, November 1950.

Metallographic Study of the Martensite Transformation in Lithium: J. S. Bowles, Institute for the Study of Metals, University of Chicago, Chicago. JOURNAL OF METALS, January 1951.

Crystal Structures and Transformations in Indium-Thallium Solid Solutions: L. Guttman, Institute for the Study of Metals, University of Chicago, Chicago. JOURNAL OF METALS, December 1950.

Crystallography of Cubic-Tetragonal Transformation in the Indium-Thallium System: C. S. Barrett, L. Guttman, Institute for the Study of Metals, University of Chicago, Chicago. JOURNAL OF METALS, December 1950.

9:00 a.m., ISD, Daniel Boone Room

Sulphur Symposium: Oxide-Gas Equilibria; Sulphur Activity in Liquid Iron

W. O. Philbrook and John Pollock, Associate Chairmen

Thermodynamic Study of the Reaction $CaS+H_2O \rightarrow CaO+H_2S$ *and the Desulphurization of Liquid Copper:* Terkel Rosenqvist, Institute for the Study of Metals, University of Chicago.

Equilibrium Study of Sulphurous Gases with Basic Oxide Slags: L. S. Darken, B. M. Shields, U. S. Steel Co., Kearny, N. J.

Effect of Certain Elements on Sulphur Activity in Liquid Steel: C. Sherman, Latrobe Electric Steel Co., J. Chipman, Massachusetts Institute of Technology, Cambridge, Mass.

Effect of C, Si, and Mn on Sulphur Activity in Iron Saturated With Carbon: R. C. Buehl, U. S. Bureau of Mines, Pittsburgh, Pa.

10:00 a.m., Room 102

Meeting

Metals Branch Council

12:15 p.m., Gold Room, Jefferson Hotel

Welcoming Luncheon

Speaker: Arthur Holly Compton, President, Washington University

2:30 p.m., EMD, Daniel Boone Room

Aluminum-Magnesium (Simultaneous Session)

R. S. Sherwin and H. W. St. Clair, Associate Chairmen

Potential Aluminum Resources: K. K. Kershner, C. W. Funk, W. A. Calhoun, Bureau of Mines, Washington, D. C.

Recovery of Minerals from Sea Water: C. M. Shigley, Dow Chemical Co., Freeport, Texas. JOURNAL OF METALS, January 1951.

Apparatus for Determining Thickening Characteristics

of Fine Slimes: R. S. Sherwin, Jr., Reynolds Metals Co., Sheffield, Ala.

Extraction of Alumina from Haiti and Jamaica Bauxites: Dr. T. D. Tiemann, Reynolds Metals Co., Sheffield, Ala.

2:30 p.m., EMD, Ballroom Assembly South

Zinc-Miscellaneous (Simultaneous Session)

W. G. Woolf and T. H. Weldon, Associate Chairmen

Sintering Practice at Josephtown Smelter: H. K. Najarian, K. F. Peterson, R. E. Lund, St. Joseph Lead Co., Josephtown, Pa. JOURNAL OF METALS, February 1951.

Reverse Leaching of Zinc Calcine: L. P. Davidson, R. K. Carpenter, H. J. Tschirner, American Zinc Co. of Illinois, Monsanto, Ill. JOURNAL OF METALS, February 1951.

Sampling of High Grade Electrolytic Zinc and Its Statistical Evaluation: H. J. Tschirner, American Zinc Co. of Illinois, Monsanto, Ill.

Gallium: A Byproduct Metal: Dr. A. P. Thompson, H. R. Harner, Eagle-Picher Co., Joplin, Mo. JOURNAL OF METALS, February 1951.

Cyclone Collectors vs. U-Tubes for Fume Collecting System Cooling Purposes: Harry E. Hoon, Jr., Northern Blower Co., Cleveland.

2:30 p.m., IMD, Ballroom

Panel Discussion On the Martensitic Transformation

Morris Cohen, Moderator

Panel Members: P. Duwez, California Institute of Technology; J. C. Fisher, General Electric Co.; R. A. Grange, U. S. Steel Co.; L. Guttman, University of Chicago; E. S. Machlin, Massachusetts Institute of Technology; T. A. Read, Columbia University; A. R. Troiano, Case Institute of Technology; and D. M. Van Winkle, Carnegie Institute of Technology.

2:30 p.m., ISD, Missouri Room

Sulphur Symposium: Slag Metal Equilibria; Kinetics of Desulphurization

J. Marsh and D. C. Hilty, Associate Chairmen

Sulphur Equilibria in Blast Furnace Slags: Bo Kalling, Sweden, N. J. Grant, John Chipman, Massachusetts Institute of Technology, Cambridge, Mass.

Equilibrium between Blast Furnace Metal and Slag as Determined by Remelting: E. W. Filer, L. S. Darken, U. S. Steel Co., Kearny, N. J.

Effect of SiO_2 Reduction on Blast Furnace Desulphurization: N. J. Grant, John Chipman, Massachusetts Institute of Technology, Troili.

Distribution of Sulphur between Liquid Iron and Slags at Low Iron Oxide Concentration: Roberto Rocca, Milano Italy, N. J. Grant, John Chipman, Massachusetts Institute of Technology.

Effect of Si and Mn on the Mechanism of Sulphur Transfer in Blast Furnace Slags: G. Derge, Carnegie Institute of Technology, Pittsburgh, Pa.

4:30 p.m., Room 102

Membership Committee Meeting

Institute of Metals Division

TUESDAY, FEBRUARY 20

9:00 a.m., EMD, Ballroom Assembly Center

Titanium (Simultaneous Session)

E. J. Chapin and E. J. Center, Associate Chairmen

Preparation of Titanium Tetrachloride from Rutile: C. H. Gorski, U. S. Bureau of Mines, Rolla, Mo. JOURNAL OF METALS, February 1951.

Determination of Gases in Titanium: E. F. Scheffer, Titanium Div., National Lead Co., Sayreville, N. J.

SYMPOSIUM—*Spectrographic and Chemical Analysis of Titanium*

9:00 a.m., EMD, Ballroom Assembly South

Symposium (Simultaneous Session)

B. L. Sackett and R. R. McNaughton, Associate Chairmen

Removal and Recovery of Zinc and Lead from Furnace Slag

9:00 a.m., IMD, Missouri Room

Recrystallization

D. Turnbull, Chairman; B. Alexander, Secretary

Formation and Behavior of Sub-boundaries in Silicon Iron Crystals: C. G. Dunn, F. W. Daniels, General Electric Co., Pittsfield, Mass. JOURNAL OF METALS, February 1951.

Oriented Growth in Primary Recrystallization: J. J. Becker, Harvard University, Cambridge, Mass. JOURNAL OF METALS, February 1951.

Recrystallization and Grain Growth Characteristics of Zirconium: F. J. Dunkerley, F. Pledger, V. Damiano, University of Pennsylvania, Philadelphia, J. Fulton, MIT, Cambridge, Mass.

9:00 a.m., ISD, Ballroom

Sulphur Symposium: External Desulphurization in the Blast Furnace

T. L. Joseph and T. F. Plimpton, Associate Chairmen

Desulphurizing Molten Iron with Calcium Carbide: S. D. Baumer, P. M. Hulme, Air Reduction Co., New York.

Method for Using Powdered CaO to Desulphurize Hot Metal: Bo Kalling, Stora Kopparbergs Bergslags AB, Domnarvet, Sweden.

Results of Using the Kalling Process for Desulphurizing Hot Metal: Sven Fornander, Surahammars Bruks AB, Surahammar, Sweden.

Desulphurizing Pig Iron with Treated Blast Furnace Slag: B. R. Queneau, U. S. Steel Co., Chicago.

11:00 a.m., ISD, Ballroom

Howe Memorial Lecture

W. M. Peirce and H. K. Work, Associate Chairmen

Twenty-five More Years of Metallography: J. R. Vilella, U. S. Steel Co., Kearny, N. J.

12:15 p.m., Room 102

Luncheon Meeting

Executive Committee, Institute of Metals Division

2:00 p.m., EMD, Ballroom Assembly Center

Titanium (Simultaneous Session)

J. R. Long and T. W. Lippert, Associate Chairmen

Factors Influencing the Purity and Rate of Deposition of Iodide Titanium: L. C. Beale, J. M. Blocker, Jr., I. E. Campbell, Battelle Memorial Institute, Columbus, Ohio.

Arc Melting of Titanium: S. F. Radtke, R. M. Schriver, J. A. Snyder, E. I. du Pont de Nemours & Co., Pigments Div., Wilmington, Del.

SYMPOSIUM—*Melting and Casting of Titanium*

2:00 p.m., EMD, Ballroom Assembly South

Symposium (Simultaneous Session)

Removal and Recovery of Zinc and Lead from Furnace Slag (continued from morning session).

2:00 p.m., ISD, Ballroom

Sulphur Symposium: Desulphurization in the Open Hearth

H. L. Tear and Shadburn Marshall, Associate Chairmen

Making of Low Sulphur Steel from High Sulphur Raw Materials and High Sulphur Fuel by the Cold Metal Process: F. L. Robertson, C. H. Bacon, John Summers & Sons Ltd.

Application of Physico-Chemical Principles to Open Hearth Desulphurization: D. E. Babcock, Republic Steel Corp., Youngstown, Ohio.

Complete Sulphur Balance in the Open Hearth Furnace: B. M. Larsen, U. S. Steel Co., Kearny, N. J.

2:30 p.m., IMD, Missouri Room

Diffusion and Precipitation

E. A. Peretti, Secretary

Cobalt Self-diffusion—A Study of the Method of Decrease in Surface Activity: R. C. Ruder, E. I. duPont de Nemours & Co., Wilmington, Del., C. E. Birchenall, Carnegie Institute of Technology, Pittsburgh. JOURNAL OF METALS, February 1951.

Interface and Marker Movements in Diffusion in Solid Solutions of Metals: L. C. DaSilva, Instituo de Pesquisas Technologicas, São Paulo, Brazil, R. F. Mehl, Carnegie Institute of Technology, Pittsburgh. JOURNAL OF METALS, February 1951.

Effect of Ternary Additions on Age-Hardening of a Copper-Silver Alloy: H. Margolin, New York University, New York, W. R. Hibbard, Jr., Yale University, New Haven, Conn. JOURNAL OF METALS, February 1951.

Aging of Sand Casting Zinc Alloys: T. E. Leontis, C. E. Nelson, Dow Chemical Co., Midland, Mich. JOURNAL OF METALS, February 1951.

Age Hardening: L. F. Mondolfo, Illinois Institute of Technology, Chicago. JOURNAL OF METALS, February 1951.

6:00 p.m., Missouri Room Foyer

Metals Branch Cocktail Party

7:00 p.m., Missouri Room

Metals Branch Annual Dinner

Toastmaster: C. D. King, Chairman, Operating Committees, U. S. Steel Co.

Speaker: George W. Wolf, President, U. S. Steel Export Co.

Subject: *The Hole in Our Armor.*

WEDNESDAY, FEBRUARY 21

9:00 a.m., EMD, Ballroom Assembly South

Symposium (Simultaneous Session)

L. P. Davidson and W. G. Woolf, Associate Chairmen

Electrolytic Zinc

9:00 a.m., EMD, Ballroom Assembly Center

Copper-Cobalt Refractories (Simultaneous Session)

L. G. Leckie and J. C. Kinnear, Jr., Associate Chairmen

Electric Furnace Melting of Copper at Baltimore: P. R. Drummond, American Smelting & Refining Co., Baltimore.

El Paso Refinery of Phelps Dodge Refining Corp.: B. B. Kunkle, Phelps Dodge Refining Corp., El Paso, Texas.

Developments in Refractories for Metallurgical Industries: W. F. Rochow, Harbison-Walker Refractories Co., Pittsburgh.

Studies on the Metallurgy of Cobalt Production from Cupriferous Pyrite: S. Nakabe, Besshi Mining Co., Ltd., Tokio, Japan. (Presented by P. R. Drummond)

Extraction of Cobalt, Nickel, and Copper from Complex Sulphide Ore Concentrates of Southeastern Missouri: K. Kershner, H. Kenworthy, R. G. Knickerbocker, U. S. Bureau of Mines, Rolla, Mo.

9:00 a.m., IMD, Daniel Boone Room

Plasticity and Mechanical Properties (Simultaneous Session)

N. Grant, Secretary

Torsion Texture of Copper: W. A. Backofen, MIT, Cambridge, Mass. JOURNAL OF METALS, December 1950.

Effect of Ferrite Grain Structure upon Impact Properties of 0.80 Pct Carbon Spheroidite: M. Baeyertz, E. S. Bumps, Armour Research Foundation, Illinois Institute of Technology, Chicago, W. F. Craig, Jr., Climax Molybdenum Co., Chicago. JOURNAL OF METALS, December 1950.

Effect of Alloying Elements on True Stress and True Strain in Pearlitic Steel: R. H. Raring, J. A. Reinbolt, W. J. Harris, Jr., Naval Research Lab., Washington, D. C.

9:00 a.m., IMD, Ballroom

Phase Transformations (Simultaneous Session)

C. S. Barrett, Chairman; C. H. Samans, Secretary

Microscopic Observation of the Solidification of Copper-Nickel Alloy Droplets: R. E. Coch, D. Turnbull, General Electric Research Lab., Schenectady, N. Y.

Transitions in Chromium: M. E. Fine, E. S. Greiner, W. C. Ellis, Bell Telephone Labs., Inc., New York. JOURNAL OF METALS, January 1951.

Kinetics of Solid Phase Reactions in Oxide Films on Iron—The Reversible Transformation at or near 570°C: E. A. Gulbransen, R. Ruka, Westinghouse Research Labs., East Pittsburgh. JOURNAL OF METALS, December 1950.

9:00 a.m., ISD, Missouri Room

General Session

M. Tenenbaum and A. H. Sommer, Associate Chairmen

Vanadium-Oxygen Equilibrium in Liquid Iron: John Chipman, MIT, Cambridge, Mass., M. N. Dastur, H. A. Brassert & Co., New York. JOURNAL OF METALS, February 1951.

Solution Loss and the Reducing Power of Blast Furnace Gas: T. L. Joseph, University of Minnesota, Minneapolis. JOURNAL OF METALS, January 1951.

10:45 a.m., Ballroom

Annual Business Meeting

Institute of Metals Division

M. Gensamer, Chairman

11:00 a.m., IMD, Ballroom

Annual Lecture, Institute of Metals Division

D. H. McLaughlin and M. Gensamer, Associate Chairmen

Kinetics of Precipitation in Supercooled Metallic Solutions: G. Borelius, Royal Institute of Technology, Stockholm, Sweden.

12:15 p.m., Room 102

Luncheon Meeting

Executive Committee, Extractive Metallurgy Division

12:15 p.m., Room 104

Luncheon Meeting

Physical Chemistry of Steelmaking Committee, Iron and Steel Division

2:00 p.m., EMD, Ballroom Assembly South

Symposium (Simultaneous Session)

Electrolytic Zinc (continued from morning session).

Open Hearth Committee To Hold Technical Session

Iron and Steel Division members and guests are invited to attend and participate in a special program arranged by the Southwestern Section of the Open Hearth Committee. The meeting will be held on Wednesday, Feb. 21, at 2:00 p.m., in Parlor A of the Lennox Hotel. Clarence King and Gordon McMillin will be Associate Chairmen of the meeting. The program arranged is:

Problems Encountered in Pouring Rimmed Steel, covering analysis, pouring rate, nozzle size, fading of manganese, and effect of mold sections and height of pour.

Use of Special Refractories to Increase Furnace Life, covering basic brick in end and front walls, superduty silica brick, and alternate courses of basic brick in roof construction (Zebra roof).

Pit Refractories and Practice, describing special refractories used in runners, optimum ladle lining thicknesses, and nozzle, sleeve and stopper heads.

The Southwestern Section of the Open Hearth Committee will also hold its Fellowship Dinner on Wednesday, Feb. 21, at 7:00 p.m. Tickets for the dinner will be available when registering for the technical session. There is no registration fee for attending this technical session.

2:00 p.m., EMD, Ballroom

Physical Chemistry of Extractive Metallurgy (Simultaneous Session)

H. H. Kellogg and N. Arbiter, Associate Chairmen

Rate of Evaporation of Molten Metals at Reduced Pressures: H. W. St. Clair, U. S. Bureau of Mines, Washington, D. C.

Electrical Conductivity of Metals and Alloys in the Molten State: Manuel Tama, Ajax Engineering Corp., Trenton, N. J.

Nickel Carbonyl, Reaction Rates, and Equilibria: H. A. Doerner, G. S. Beaudreau, R. E. Donelson, U. S. Bureau of Mines, Albany, Ore.

Thermodynamics of Iron Silicate Slags I. Slags Saturated with Solid (γ) Iron: R. Schuhmann, Jr., P. J. Ensio, MIT, Cambridge, Mass.

2:00 p.m., IMD, Daniel Boone Room

Alloy Systems (Simultaneous Session)

M. Hansen, Chairman; M. E. Nicholson, Jr., Secretary

Solubility of Hydrogen in Molten Lead: W. R. Opie, National Lead Co., N. J. Grant, MIT, Cambridge, Mass.

Constitution of Iron-Chromium-Molybdenum Alloys: S. R. Baen, U. S. Army Field Forces, Fort Knox, Ky., Pol Duwez, California Institute of Technology, Pasadena, Calif.

Constitution of the System Gallium-Indium: J. P. Denney, General Electric Co., Schenectady, N. Y., J. H. Hamilton, Utah Engineering Experimental Station and University of Utah, J. R. Lewis, University of Utah.

Lattice Parameters of Magnesium Alloys: R. S. Busk, Dow Chemical Co., Midland, Mich. JOURNAL OF METALS, December 1950.

Alloys of Copper and Iron: C. S. Smith, Institute for the Study of Metals, University of Chicago, Chicago, E. W. Palmer, American Brass Co., Waterbury, Conn. JOURNAL OF METALS, December 1950.

2:30 p.m., IMD, Missouri Room

Grain Boundaries and Annealing Twins (Simultaneous Session)

F. J. Dunkerley, Secretary

Growth of Molybdenum Single Crystals: N. K. Chon, R. Maddin, R. B. Pond, Johns Hopkins University, Baltimore.

Intergranular Energy of Iron and Some Iron Alloys: L. H. Van Vlack, Carnegie-Illinois Steel Corp., Chicago.

Formation of Annealing Twins: J. E. Burke, General Electric Co., Schenectady, N. Y. JOURNAL OF METALS, November 1950.

Formation of Annealing Twins During Grain Growth: R. L. Fullman, J. C. Fisher, General Electric Co., Schenectady, N. Y.

Annealing Twins in Aluminum: R. L. Fullman, General Electric Co., Schenectady, N. Y.

A Postulated Mechanism for Cubic Twinning: W. C. Ellis, R. C. Treuting, Bell Telephone Labs., Inc., Murray Hill, N. J.

2:30 p.m., Room 106

Publications Committee Meeting

Institute of Metals Division,
F. N. Rhines, Chairman

4:45 p.m., Ballroom Assembly South

Annual Business Meeting, Extractive Metallurgy Division

C. C. Long, Chairman

7:00 p.m., Gold Room, Jefferson Hotel

AIME Annual Banquet and Awards

9:00 p.m., Crystal Room, Jefferson Hotel

President's Reception

10:00 p.m., Gold Room, Jefferson Hotel

Annual AIME Ball

THURSDAY, FEBRUARY 22

9:00 a.m., EMD, Daniel Boone Room

Physical Chemistry of Extractive Metallurgy (Simultaneous Session)

P. T. Stroup and L. M. Pidgeon, Associate Chairmen

Sulphur Activities in Liquid Copper Sulphides: R. Schuhmann, Jr., O. W. Moles, MIT, Cambridge, Mass.

Mechanism and Rate Controlling Factors in the Dissolution of Gold in Cyanide Solutions: H. H. Kellogg, V. Kudryk, Columbia University, New York.

Metallurgical Reactions of the Fluorides: H. H. Kellogg, Columbia University, New York. JOURNAL OF METALS, February 1951.

Solubility of Copper Minerals in Ammonia: N. Arbiter, Phelps Dodge Corp., New York.

9:00 a.m., EMD and IABD, Ballroom Assembly Center

Joint Session (Simultaneous Session)

S. F. Rovitz and B. W. Gonser, Associate Chairmen

Recovery of Vanadium from Titaniferous Magnetite: S. S. Cole, J. S. Breitenstein, Titanium Div., National Lead Co., Sayreville, N. J.

Separation of Precious Metals from Anode Slimes: R. T. Hukki, Finland Institute of Technology, Helsinki, Finland. (Presented by P. R. Drummond)

Semi-pilot Plant Investigations on Electrowinning Manganese from Chloride Electrolytes: J. H. Jacobs, P. E. Churchward, T. E. Hill, Jr., W. H. Curry, E. C.

Perkins, O. Q. Leone, U. S. Bureau of Mines, Boulder City, Nev.

Sintering Practice at Josephtown Smelter: H. K. Najarian, K. F. Peterson, R. E. Lund, St. Joseph Lead Co., Josephtown, Pa. JOURNAL OF METALS, February 1951.

9:00 a.m., IMD, Ballroom

General Session (Simultaneous Session)

J. S. Smart, Jr., Secretary

Effect of Heat Treatment on the Electrical Properties of Germanium: H. C. Theuerer, J. H. Scaff, Bell Telephone Labs, Inc., Murray Hill, N. J. JOURNAL OF METALS, January 1951.

Graphite-Rod Hairpin-Resistor Radiation Furnace for High Temperatures: W. J. Kroll, Consulting Metallurgist, W. W. Stephens, J. P. Walsted, U. S. Bureau of Mines, Albany, Ore. JOURNAL OF METALS, November 1950.

Ignition Temperature of Magnesium and Certain Magnesium Alloys: W. M. Fassel, Jr., J. R. Lewis, J. H. Hamilton, University of Utah, Salt Lake City, Utah, L. B. Gulbransen, Colorado School of Mines, Golden, Colo.

9:00 a.m., IMD, Missouri Room

Powder Metallurgy (Simultaneous Session)

L. A. Barera and R. Steinitz, Associate Chairmen

Mechanical Properties of Stainless Steel Powder: A. H. Grobe, G. A. Roberts, Vanadium Alloys Steel Co., Latrobe, Pa. JOURNAL OF METALS, February 1951.

Rates of Sintering of Copper Under a Dead Load: F. N. Rhines, Carnegie Institute of Technology, Pittsburgh, H. Cannon, Rensselaer Polytechnic Institute, Troy, N. Y.

Powder Metallurgy of Zirconium: H. H. Hausner, H. S. Kalish, R. P. Angier, Sylvania Electric Products, Inc., Bayside, L. I.

Phenomena Occurring During Sintering: B. H. Alexander, Sylvania Electric Products, Inc., Bayside, L. I.

9:00 a.m., ISD, Ballroom Assembly South

Steel Making

John Chipman and G. McMillin, Associate Chairmen

Some Observations Made on Rimming Steel Ingots: A. Hultgren, Metallurgical Professor, Tekniska Hogskolan, Valhallabagen, Stockholm, Sweden, G. Phragmen (deceased), S. Wohlfahrt, J. E. Ostberg. To be presented by M. Tenenbaum. JOURNAL OF METALS, February 1951.

Oxygen in Liquid Openhearth Steel—Oxidation During Tapping and Ladle Filling: T. E. Brower, J. W. Bain, B. M. Larsen, U. S. Steel Co., Kearny, N. J. JOURNAL OF METALS, June 1950.

Desulphurizing Action of Titanium in Steels: W. P. Fishel, W. P. Roe, J. F. Ellis, Vanderbilt University, Nashville, Tenn.

Graphical Representation of Metallurgical Equilibria: C. J. Osborn, Council for Scientific and Industrial Research, Div. of Aeronautics, Melbourne, Australia. JOURNAL OF METALS, March 1950.

12:15 p.m., Room 104

Luncheon Meeting

Powder Metallurgy Committee

12:15 p.m., Room 102

Luncheon Meeting

Executive Committee, Iron and Steel Division

2:00 p.m., EMD, Ballroom Assembly South

Physical Chemistry of Extractive Metallurgy

R. Schuhmann, Jr., and H. H. Kellogg, Associate Chairmen

Thermodynamic Properties of Silicon and Its Oxides at Elevated Temperatures: J. V. Parker, J. J. Ward, J. W. Clegg, Battelle Memorial Institute, Columbus, Ohio.

New High-Temperature Calorimeter: R. L. McKisson, L. A. Bromley, University of California, Berkeley, Calif.

Heats of Formation of Sodium-Tin Alloys: R. L. McKisson, L. A. Bromley, University of California, Berkeley, Calif.

Ion Exchange in Metallurgy: E. J. Breton, Jr., A. W. Schlechten, Missouri School of Mines, Rolla, Mo.

2:30 p.m., IMD, Missouri Room

Powder Metallurgy Seminar: Panel Discussion on Powder Metal Particles

J. J. Cordiano and L. T. Work, Associate Chairmen

What Are Metal Powder Particles: L. T. Work, Consulting Engineer, New York.

Fundamental Properties of Metal Powder: B. Kopelman, Sylvania Electric Products, Inc., Bayside, L. I.

Particle Size Measurement in the Powder Metallurgy Field: Julius Sachse, Metals Disintegrating Co., Elizabeth, N. J.

Recent Developments in Methods for Particle Size Determination: J. Shaw, SKC Research Associates, Paterson, N. J.

IMD Fall Meeting Paper Deadline

Apr. 15, 1951 is the deadline for all Institute of Metals Div. papers to be presented at the fall meeting, Oct. 15 to 17, at the Detroit-Leland Hotel, Detroit.

Chicago Section Hears Five Leading Speakers at Three Winter Meetings

An active Chicago Section launched its series of meetings this winter on Oct. 4 with a panel of three speakers on Titanium. T. W. Lippert, general manager, Titanium Metals Corp. of America, S. A. Herres, metallurgical engineer, Allegheny Ludlum Steel Corp., and C. H. Moore, assistant director of research, National Lead Co., Titanium Alloy Division, comprised the group of speakers. Each took a different aspect of titanium production, with Mr. Lippert discussing marketing activities, uses, production problems, and the future of the metal. Mr. Herres touched on technical aspects of production from sponge metal on to formed products, and Mr. Moore covered the ground from ore to sponge metal with some interesting sidelights on, and a display of, synthetic titania jewels. C. E. Swartz, Armour Research Foundation, was technical chairman at the meeting.

At the Nov. 1 meeting, the Annual Ladies Night Dinner Program was held, with Ulrich Middeldorf, chairman, department of art, University of Chicago speaking on "Use of Metals in the Arts". He noted the assistance to modern architecture that has come from use of more metal construction, and went on to discuss the use of metals in sculpture, painting, and engraving. W. E. Mahin, Armour Research Foundation, was technical director for the meeting.

Wilfred Sykes, chairman, executive committee, Inland Steel Co., spoke at the Dec. 6 gathering on "The Future of the Chicago District in the Steel Industry." He discussed steel's middle western market, and the future of the Chicago area regarding raw material supplies for the steel industry in that area. B. M. Luvezey, general superintendent, Carnegie-Illinois Steel Corp., South Works, was technical chairman for the evening.

AIME Controversial Matter Policy To Be Discussed at MED Luncheon

When AIME liberalized its policy with respect to controversial matters on June 22, 1950, the door was opened to the Board for expressing views on matters pertaining to the mineral industries that are vital to the nation in times of danger. To what extent and how AIME can help in meeting demands made on the mineral industry by the present emergency are problems of considerable concern.

At a luncheon meeting of the Minerals Economics Div., on Tuesday, Feb. 20, at the annual meeting in St. Louis, Institute officials will present their interpretations of the revised resolution, and comment on methods of taking such action as is permitted under present policies. There also will be opportunity for discussion from the floor.

AIME Receives Two Grants

Two substantial gifts were received by the AIME Board of Directors at its meeting on Nov. 15. One was a contribution of $5000 from the Cities Service Co., through the Doherty Memorial Fund, for special services to Petroleum Branch members. Authorization has been given to use income from the Doherty Fund to underwrite a volume on Petroleum Conservation, the manuscript which has just been completed by Stuart Buckley; and to offset a part of the cost of publishing Petroleum Statistics. The same amount also has been contributed in other recent years.

A gift of $2250 was made by the American Smelting & Refining Co., through the Seeley W. Mudd Memorial Fund, for the purchase of 1500 copies of the volume entitled *Metal Magic*. This will be distributed free of charge to new Junior Members of the AIME in the coming year or two.

Engineering Societies Library Issues Series of Bibliographies

The series of bibliographies on subjects of general interest, compiled by the staff of the library, have been helpful to many engineers and the complete list is now being given here for those who may not have seen earlier announcements.

ESL Bibliographies: (1) Filing Systems for Engineering Offices. 41 references. 1948. $2.00. (2) Prestressed Reinforced Concrete. 190 references. 1948. $4.00. (3) Precision Investment Casting by the Lost Wax Process. 111 references. 1949. $2.50. (4) Pallets Used in Modern Materials Handling. 114 references. 1949. $2.00. (5) Machinery Foundations; Design, Construction, Vibration Elimination. 120 references. 1950. $2.00. (6) Non-Metallic Bearings. 101 references. 1950. $2.00. (7) Domestic and Industrial Applications of Solar Heating. Approximately 150 references. 1950. $2.00. (8) Management of Construction Jobs. In preparation.

1951 Preliminary Budget Discussed

At the meeting on Dec. 20, 1950, the Executive and Finance Committees reviewed the preliminary budget of the Institute for the coming year which had previously been prepared by the Finance Committee. It was pointed out that the most difficult item to estimate at this time is advertising income, because 1951 contracts will not be in hand before February. However, indications were that advertising income could be placed at $131,500, compared with an expected $104,000 in 1950. MINING ENGINEERING is expected to yield $63,000, the JOURNAL OF METALS $45,000, and the JOURNAL OF PETROLEUM TECHNOLOGY $23,500. Total income in this preliminary budget is $496,000, and total expenses approximately $482,000. A final budget will be presented later.

Some curtailment of AIME income is likely to result from another action of the Directors at this meeting: it was voted that no more orders should be accepted for shipment of AIME publications to the USSR, Poland, Czechslovakia, or Romania. Heretofore, close to 300 annual subscriptions for Institute journals have been booked for shipment to these countries, to say nothing of numerous bound volumes.

Mexico Section Welcomes Visitors

Luncheon meetings of the newly organized Mexico Section of the AIME are held on the first Monday of each month at the American Club in Mexico City. AIME members who may be in the city at that time will be welcomed. They should get in touch with William G. Kane, Secretary-Treasurer of the new Section, whose Post Office address is Apartado 711, Mexico, D.F., and whose street address is San Juan de Letran No. 9, Desp. 805; telephone 10-27-24.

Officers of the new Mexico Section are: Chairman, Alfredo Terrazas; Vice-Chairman, Valentin Garfias; Secretary-Treasurer, William G. Kane.

ASME Dues Raised

By a vote of at least two thirds of the voting members, as provided by the bylaws, the American Society of Mechanical Engineers has voted to raise its dues by $5 effective October 1951. The new rate is $25 per year for Fellows, Associates, Members, and Junior Members over 33 years of age; $20 for Junior Members 30 to 33; and $10 for Junior Members less than 30 years of age.

Personals

ROLAND D. PARKS

WILLIAM F. CHUBB

OSCAR A. GLAESER

Roland D. Parks of M.I.T. has been appointed associate of Behre Dolbear & Co., mineral consultants, New York, N. Y. **F. Blondel** has been appointed foreign consultant in Paris and **Tadishiro Inouye** in Tokyo.

William F. Chubb has taken over the foundation chair of metallurgy at King Fouad 1st University, Giza, Egypt, and will also act as consulting metallurgist to the Ministry of War and Marine.

Oscar A. Glaeser, industrial relations engineer for U. S. Smelting Refining & Mining Co., was named assistant to the vice-president and general manager of western operations. **Byron E. Grant** was made assistant manager of western mines.

Ralph K. Gottshall has been appointed assistant to the president, Atlas Powder Co., Wilmington. He was formerly assistant general manager of the explosives dept.

S. Power Warren has temporarily discontinued his consulting work and returned to the employ of the government. He is with the evaluation branch of the production and expansion div. of the defense minerals administration, and is now located at Falls Church, Va.

Laning Dress is now employed with Roberts & Shaefer Co., Chicago, as assistant to the executive vice-president.

H. S. McQueen is now associated with the Salt Dome Production Co., Houston, as executive vice-president and chief geologist.

Donald H. McIntosh is now superintendent of the western section, research dept., American Smelting & Refining Co., Salt Lake City.

James William Linhart has accepted the position of steel roll metallurgist for the Ohio Steel Foundry Co., Lima, Ohio. He was previously research engineer for Jones & Laughlin Steel Corp., Pittsburgh.

John H. McElhinney, vice-president in charge of operations of Wheeling Steel Corp., Wheeling, W. Va., has been elected to the board of directors of the corporation.

Thomas J. Crocker has been appointed manager of Bethlehem Collieries Corp., Johnston, Pa. He had been assistant manager since 1942. **L. H. Chalfant** had been appointed assistant manager and is continuing in that capacity.

Robert Gregg has retired as president of the Tennessee Coal, Iron & Railroad Co.

Leo F. Reinartz, assistant vice-president of Armco Steel Corp., was one of five Carnegie Institute of Technology Alumni to be given an Alumnus Award of Merit for outstanding work in the iron and steel industry. These are the first such awards that have ever been given.

Jack R. Lewis has accepted a position as metallurgical engineer with the NEPA Div., Fairchild Engine & Airplane Corp., Oak Ridge, Tenn.

Morris E. Nicholson has taken a position as assistant professor at the Institute for the Study of Metals, University of Chicago. He was formerly assistant section head of the physical metallurgy section of the engineering research dept., Standard Oil Co. (Indiana), Chicago.

Michael I. Bricksin is now metallurgist for the U.S.N., industrial laboratory, naval shipyard, Mare Island, Vallejo, Calif.

Malcolm R. McGregor has joined the General Metals Corp., Oakland, Calif. as metallurgist.

Kuno Doerr, Jr., was reelected vice chairman directing the smelting div., Montana Safety Council. Mr. Doerr is manager of the East Helena plant of the American Smelting & Refining Co.

Rudolph W. Zillmann is now metallurgist for the Pittsburgh Steel Foundry Corp., Glassport, Pa. He recently completed work for a Sc.D. at M.I.T. in the field of physical metallurgy.

Richard M. Treco, previously research metallurgist, D.I.C. staff, M.I.T., is now senior metallurgist engineer for Sylvania Electric Products, Inc., metallurgical laboratories, Bayside, N. Y.

Virgil Lessels has accepted the position of metallurgist with the Chile Exploration Co. at Chuquicamata, Chile. He had been chief concentrating testing engineer for the International Smelting & Refining Co., Tooele, Utah.

Robert L. Pettibone has been appointed to the position of chief metallurgical engineer, Sintercast Corp. of America, Yonkers, N. Y. He previously held the position of research metallurgist.

Waldemar F. Dietrich, senior member of Dietrich, Morse & Associates, consulting engineers, Sacramento, has been appointed chief of the rare and precious metals branch of the Minerals Div., Bureau of Mines, U. S. Dept. of the Interior.

C. Robert Lillie has been made project engineer for the Standard Oil Co. (Indiana), materials div., engineering research dept., Chicago.

Obituaries

Arthur C. Green (Member 1921), former director and vice-president of sales, Goodman Mfg. Co., died on Oct. 31, 1950. He was born in Clarkston, Mich., in 1882 and was educated at the University of Michigan. In 1904 he graduated with the degree of B.S. In 1911 he joined the Goodman Mfg. Co., Chicago, as sales engineer and district manager. In 1930 he was appointed central district manager and in 1936 given charge of western sales and elected director of the company. He became general sales manager in 1937 and two years later was made vice-president and sales manager.

Temple W. Tutwiler (Member 1921) died on Sept. 9, 1950 after a long illness. Born at Cincinnati he attended the University of Alabama. After graduation he went to work in various steel mills. In 1909 he joined the U. S. Steel Corp., Gary and became general foreman of the blast furnaces. He went to India for the Tata Iron & Steel Co. to supervise production of steel. He remained there during World War I supplying the British Empire with rails and shells for wartime use. He was a director for Cities Service Co. and during World War II worked on the construction of a refinery, the Tutwiler Refinery, Lake Charles, La. In 1945 he was president of the Tutwiler Hotel Corp. and the Black Creek Coal & Coke Co. He was also president of the Tutwiler Investment Co.

Allen H. Woodward (Member 1900) died on Nov. 26, 1950. Mr. Woodward was born in Wheeling, W. Va., in 1876. He attended the University of the South and M.I.T., graduating in 1899. Following graduation he joined the Woodward Iron Co. as a locomotive fireman and engineer. He became superintendent of furnaces, general superintendent, and general manager. Later he was made president and chairman of the board. Other business connections included posts as director of the Wheeling Steel Corp., vice-president of the Seaboard Airline Railroad, and the Atlanta, Birmingham & Coast Line Railway.

NECROLOGY

Date Elected	Name	Date of Death
1943	Herman G. A. Cowes	October 1950
1940	Harry V. Long	Oct. 16, 1950
1941	Abraham S. Hersov	February 1949
1937	Richard Stevens Eskridge	Dec. 4, 1950
1938	Charles W. Howbert	Dec. 4, 1950
1903	George B. Rodgers	Sept. 10, 1950
1941	Charles Morgan	May 20, 1950
1911	Arthur B. Shutts	Nov. 30, 1950
1931	Bert E. Sandell	Nov. 14, 1950

Proposed for Membership

Metals Branch AIME

Total AIME membership on Nov. 30, 1950, was 17,023; in addition 4,251 Student Associates were enrolled.

ADMISSIONS COMMITTEE

Albert J. Phillips, Chairman; George B. Cortes, Lloyd C. Gibson, Ivan Given, Plato Malozemoff, R. D. Mollison, John T. Sherman, Harold K. Work. Alternates: Harry P. Croft, Fred W. Hanson, T. D. Jones, Frank A. Ayer, H. W. Hitzrot, and H. K. Masters.

Institute members are urged to review this list as soon as the issue is received and immediately to wire the Secretary's office, night message collect, if objection is offered to the admission of any applicant. Details of the objection should follow by mail. The Institute desires to extend its privileges to every person to whom it can be of service but does not desire to admit persons unless they are qualified.

In the following list C/S means change of status; R, reinstatement; M, Member; J, Junior Member; AM, Associate Member; S, Student Associate.

Arizona
Phoenix—Loftus, George M. (J) (C/S—S-J)
Superior—Cooksley, Martin C. (M) (C/S—J-M)
Tucson—Nelson, Harvey J. (J) (C/S—S-J)

California
Altadena—Kolberg, Hal L. (A)
Arcadia—Jackson, Stanfurd L. (M)
Berkeley—Johnson, Walter F. (M) (R. C/S—J-M)
Desert Center—Robertson, Donald B. (J) (C/S—S-J)
El Cerrito—Swanson, Theodore M. (A) (C/S—S-A)
Huntington Park—Nagel, Wilfred E. (J) (C/S—S-J)
Oakland—Lee, David LaV. (A). McGregor, Malcolm R. (J) (C/S—S-J)

Connecticut
Goshen—Randall, Robert W. (J) (C/S—S-J)
New Haven—Reiter, Stanley F. (J) (C/S—S-J)
Westport—Mooney, William C. III (J) (C/S—S-J)

Delaware
Wilmington—Gee, Edwin A. (M) (C/S—J-M)

Idaho
Stibnite—Beeson, Phillip A. (J) (C/S—S-J)

Illinois
Chicago—Dwight, Austin E. (A) (C/S—S-A). Myhre, Tom (M).
Elmhurst—Chernock, Warren F. (J) (C/S—S-J)
Evanston—Gault, Fred L. (J)
Glen Ellyn—Pfeifer, Herman J. (A)
LaSalle—Waszkowiak, Raymond J. (M)
Peru—Coolbaugh, William E. (J) (C/S—S-J)

Indiana
Hammond—Sumpter, Charles E. (M)
West Lafayette—Hughel, Thomas J. (M) (C/S—S-M)

Massachusetts
Woburn—Machlin, Eugene S. (J) (C/S—S-J)

Michigan
Detroit—Opinsky, Arthur J. (J) (C/S—S-J)
Midland—Fenn, Raymond W., Jr. (J) (C/S—S/J). Leontis, Thomas E. (M) (C/S—J-M)

Minnesota
Virginia—Betzler, William F., Sr. (J) (C/S—S-J)

Montana
Anaconda—VanDenburg, James F. (J)
East Helena—Pounds, Ivor, Jr. (J)
Helena—Thompson, Robert L. (M) (R.)

New Mexico
Carlsbad—Carr, Louis B. (M)

New Jersey
Chatham—Leverett, Warren H. (M) (R.)
Colonia—McCain, Kenneth B. (M)
Cranford—Towers, John, Jr. (J) (R. C/S—S-J)

Ohio
Canton—Grell, Charles W. (J) (C/S—S-J)
Cleveland—Federico, Anthony M. (J) (C/S—S-J). Michelson, John A. (A) (C/S—S-A)
Columbus—Goldhoff, Robert M. (J) (C/S—S-J)
Leetonia—Berteisen, Robert C. (A)

Oregon
Gresham—Leipper, Alexander (M)

Pennsylvania
Beaver Falls—Kirchhoff, Peter O. (J) (C/S—S-J)
Irwin—Dick, William R. (M)
Lancaster—Campbell, Kenneth E. (J)
Munhall—Thomas, Robert O. (M) (R. C/S—S-M)
Palmerton—Pocalyko, Andrew (J) (C/S—S-J)
Philadelphia—Klein, Alfred W. (J) (C/S—S-J). McGivern, James F., Jr. (J) (C/S—S-J)
Pittsburgh—Dattisman, Edwin J., Jr. (M). Dougherty, James W., Jr. (J) (C/S—S-J). Lawthers, Dean D. (J) (C/S—S-J). LeMay, Jack E. (M). Mather, Roger F. (M) (C/S—J-M)
Reading—Hagan, Earl J. (J) (C/S—S-J)
Washington—Brown, Benjamin H. (M)

Utah
Magna—Gordon, Scott E. (M)

Washington
Tacoma—Olsen, Robert P. (J)
Twisp—Broderick, Adrain J. (J) (C/S—S-J)

Wisconsin
Milwaukee—Matthews, Russell B. (M)

Australia
Mount Isa, Queensland—Anderson, Russell V. (M) (C/S—J-M)

Bolivia
Oruro—Dankowitz, Jack (M)

Canada
Ontario—Fraser, Alan R. (M). Loach, Gerald O. (M) (R. C/S—J-M)
Quebec—Watts, John A. (J)
Trail, B. C.—Matthews, Robert J. (J)

Chile
Chuquicamata—Jones, Francis E. (M)

Egypt
Bulkeley, Ramleh—Dorra, Albert (M)

Japan
Tokyo—Nakabe, Sanai (M)

Mexico
Mexico City, D.F.—Villafana, Manuel B. (M) (R.)

Spain
Madrid—Calvo, Rafael (M)

Sweden
Trollhattan—Von Hofsten, Gerlard S. (M) (C/S—S-M)

PHILIPS *Electron Microscope*

featuring

CONTINUOUSLY VARIABLE MAGNIFICATION

•

INSTANTANEOUS CONVERSION FROM MICROSCOPY TO ELECTRON DIFFRACTION TECHNIQUES

•

EXACT FOCUS DETERMINATION

•

FREE FROM EFFECTS OF HUMIDITY, DUST, ALTITUDE

•

VARIABLE ACCELERATING VOLTAGE UP TO 100 K.V.

•

SILENT OPERATION

•

EXCEPTIONAL STABILITY

•

FREE FROM NORMAL VIBRATION

•

THRU-FOCUS CONTROL

•

RESOLUTION TO THIRTY ANGSTROMS

•

LARGE DIRECT VIEWING SCREEN

The Philips Electron Microscope is a proved instrument with numerous exclusive features which give it unmatched operating characteristics.

Through the use of an intermediate lens system, magnification is continuously variable from 1,000 to 60,000 diameters.

Electron diffraction patterns can be derived from selected specific areas of the field by simple and instantaneous conversion from microscopy to electron diffraction techniques—without need for re-evacuation, change of pole shoes, specimen transferral or other inconveniences.

Full descriptive data and detailed specifications are available without obligation. You are further invited to visit our application laboratories to see the Electron Microscope in use on your problems—your samples.

The Philips Electron Microscope is completely contained in a desk type housing with access panels on all sides, facilitating inspection of all internal components.

NORTH AMERICAN PHILIPS COMPANY INC. Norelco

1891 PHILIPS DIAMOND JUBILEE 1951
SIXTY YEARS OF SCIENTIFIC ACHIEVEMENT

NORTH AMERICAN PHILIPS COMPANY, INC.

RESEARCH and CONTROL INSTRUMENTS DIVISION ★ DEPT. 16-2, 750 S. FULTON AVENUE, MT. VERNON, N. Y.

IN CANADA: Philips Industries Ltd., 1203 Philips Square, Montreal ★ EXPORT REPRESENTATIVE: Philips Export Corporation, 750 South Fulton Avenue, Mt. Vernon, N. Y.

STOKES HIGH VACUUM EQUIPMENT... for every requirement of vacuum processing

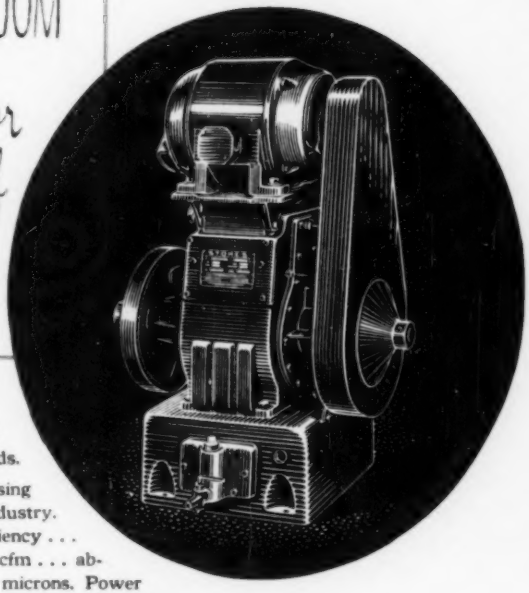

Modern design of Stokes vacuum equipment develops from the continuing contact of Stokes Engineers with processors in many fields.

Stokes Microvac Pumps — basic to vacuum processing — are designed for the broadest requirements of industry. They have high volumetric and mechanical efficiency . . . capacities of 15 to 500 cfm . . . absolute pressures to 10 microns. Power consumption is low. Compact design with top-mounted motor requires minimum floor space.

There are but four moving parts including the high speed, full-opening exhaust valve of corrosion-resistant Teflon. Lubrication is completely automatic, without packing, stuffing-boxes or grease fittings. Wear is kept to a minimum, and long trouble-free service assured. Parts are precision-finished, standard and interchangeable.

Stokes is the only manufacturer of equipment for complete vacuum systems, including Microvac mechanical pumps, oil diffusion pumps, McLeod Gages and Vacuum Valves.

Send for Catalog 700, "Stokes Microvac Pumps for High Vacuum", now a standard reference work on High Vacuum; containing charts, graphs, diagrams, schematics, typical problems, tables, formulas, constants, conversion factors.

Consult with Stokes on the application of vacuum to vacuum sintering, melting, de-gassing, heat treating, inert gas purging, vacuum metallizing, and to other applications in which vacuum deserves exploration.

STOKES MAKES

Plastics Molding Presses,
Industrial Tabletting
and Powder Metal Presses,
Pharmaceutical Equipment,
Vacuum Processing Equipment,
High Vacuum Pumps and Gages,
Special Machinery

STOKES

F. J. STOKES MACHINE COMPANY, 5916 TABOR ROAD, PHILADELPHIA 20, PA.